

Copyright
by

Mohammad Ali Farhadinia
2008

The Dissertation Committee for Mohammad Ali Farhadinia certifies that this is the approved version of the following dissertation:

**Development and Implementation of a Multi-dimensional Reservoir
Souring Module in a Chemical Flooding Simulator (UTCHEM)**

Committee:

Steven L. Bryant, Co-Supervisor

Kamy Sepehrnoori, Co-Supervisor

Mojdeh Delshad

Quoc P. Nguyen

Howard M. Liljestrand

**Development and Implementation of a Multi-dimensional
Reservoir Souring Module in a Chemical
Flooding Simulator (UTCHEM)**

by

Mohammad Ali Farhadinia, B.S.; M.S.

Dissertation

Presented to the Faculty of the Graduate School of
The University of Texas at Austin
in Partial Fulfillment
of the requirements
for the degree of

Doctor of Philosophy

**The University of Texas at Austin
December 2008**

Dedication

To my family for their love and support

Acknowledgments

I would like to express my deepest gratitude to my supervisor professors, Dr. Steven Bryant and Dr. Kamy Sepehrnoori for their guidance, advice and patience. I admire the way they treated the problems and their support during this work.

I need to extend my appreciation to Dr. Mojdeh Delshad for her help and guidelines in using UTCHEM. She almost served as co-supervisor in my dissertation.

I would like to express my appreciation to my committee members Dr. Quoc Nguyen and Dr. Howard Liljestrang for their time and effort.

This acknowledgment will be incomplete without the invaluable contribution of my friends and family members: notably, late father for nurture, mother for nature, my wife for patience, my son for his love.

I greatly acknowledge financial support from National Iranian Oil Company toward my PhD program.

**Development and Implementation of a Multi-dimensional Reservoir Souring
Module in a Chemical Flooding Simulator (UTCHEM)**

Mohammad Ali Farhadinia, PhD.
The University of Texas at Austin, 2008

Supervisors:
Dr. S. L. Bryant
Dr. K. Sepehrnoori

Reservoir souring is an after-production phenomenon in the reservoirs which are subjected to water injection. Souring can affect the properties of reservoir rocks, production facilities, and the environment. Due to the severity of the problem, during the last two decades several companies have tried to develop souring models to predict the timing of the onset of souring. Thus, the reservoir souring prediction is a relatively new subject in the reservoir engineering. Study of the published models on the reservoir souring prediction shows that there are many implications between the simulated results and field data. These implications basically arise from the capability of the models to include some effective parameters in generation and transportation of hydrogen sulfide in the reservoir. Until now, there was no comprehensive simulator to predict the reservoir souring at the variable conditions in field application. In this study, we introduce a new model which has more abilities than previous models in generation and transportation of H₂S in reservoirs for the purpose of field applications.

Today, the consensus is that sulfate reducing bacteria (SRB) are mainly responsible for hydrogen sulfide (H₂S) production in the seawater-injected reservoirs.

Basically, reservoir souring is the result of a biological reaction between sulfate from injected seawater and volatile fatty acids in formation water. Once hydrogen sulfide is generated, it may interact with rock surfaces and/or partitions between oil and water phases. With this knowledge of the generation and behavior of hydrogen sulfide in porous media, the reservoir souring model was developed. The degree of exactness and reliability of the model depends on its abilities to include the important parameters that affect the generation and transportation of the hydrogen sulfide in the reservoirs.

This work introduces a new three-dimensional model for the prediction of the hydrogen sulfide onset in seawater-injected reservoirs. The developed model was implemented in The University of Texas at Austin chemical flooding simulator, UTCHEM.

The process of reservoir souring and the souring models have been identified by published papers. There are three different conceptual models. The first published reservoir souring model was a mixing model assuming that there is a mixing zone between the injection and formation water due to seawater injection. In the mixing zone, the sulfate in the injected seawater will react with volatile fatty acids in formation water in the presence of planktonic SRB and it will generate hydrogen sulfide. The produced hydrogen sulfide interacts with rock surfaces and partitions between oil and water phases. In this model, the SRB move with the mixing zone. The next published model was a biofilm model. Unlike the mixing model, the SRB in biofilm model are sessile bacteria, which are attached to the rock surfaces near the injection well. Sessile SRB are not moving with the bulk flow, and it is assumed the necessary conditions for the growth of bacteria are provided only in the biofilm region formed in the vicinity of the injected

well. The third published model for the prediction of the reservoir souring was Thermal Viability Shell (TVS). The TVS model was based on the experimental results correlating temperature, pressure, and reduced sulfate at reservoir conditions. This model assumed that when injecting low temperature seawater to the high temperature reservoir a region with suitable temperature for the growth of SRB would develop. The production of hydrogen sulfide would take place only in TVS. The produced H_2S and SRB move with TVS (not the injection front) from injector to the producer.

In order to use UTCHEM for reservoir souring prediction, the biodegradation module was modified to account for the generation and transport of hydrogen sulfide. The biodegradation module of the simulator was used to simulate the biogenic production of H_2S . The transport of this component was formulated by using the tracer option, which has the capability of including the retardation factor due to the adsorption and partitioning.

The solution procedure is IMPES where first pressure equation is solved implicitly. Then, the species concentration equations are solved explicitly followed by the solution of temperature equation. After solving the temperature equation, the biological reactions for H_2S generation are solved. The system of ordinary differential equations, which describes the reaction rate for each species, is solved in each time-step for every gridblock.

Table of Content

List of Tables	XII
List of Figures	XV
Chapter 1	
Introduction	1
1.1 Reservoir Souring	1
1.2 Research Objectives	4
1.3 Review of Chapters	4
Chapter 2	
Literature review	6
2.1 Basic Knowledge Needed in the Study of Reservoir Souring	8
2.1.1 Hydrogen Sulfide	8
2.1.2 Biochemistry	8
2.1.3 Sulfate Reducing Bacteria	9
2.1.4 Geochemistry	9
2.2 Mechanisms of Reservoir Souring	10
2.2.1 Microbial Sulfate ion (SO_4^{2-}) or Sulfur Reduction	10
2.2.1.1 Classification of SRB According to Temperature Optima	11
2.2.2 Inorganic Souring	13
2.3 Transport of H_2S in Porous Media	13
2.4 Critical Review of Reservoir Souring Prediction Models	14
2.4.1 Existing Reservoir Souring Models	15
2.4.1.1 Kuparuk River Field Model	15
2.4.1.1.1 Proposed Souring Mechanism	16
2.4.1.1.2 Historical Hydrogen Sulfide Production	16
2.4.1.1.3 Cultivated SRB Colonies	17
2.4.1.1.4 Isotopic Analysis	17
2.4.1.1.5 Lack of Plausible Alternative Mechanisms	18
2.4.1.1.6 Modeling Approach and Assumptions	18
2.4.1.2 Mixing Model	19
2.4.1.3 Biofilm Model	21
2.4.1.4 Thermal Viability Shell Model (TVS)	23
2.4.1.5 Algorithm Based Model	26
2.4.2 In-house Models and Simulators	27
2.4.2.1 BPOPE Model	27
2.4.2.2 Seto et al. Model	28
2.4.2.3 Kuijvenhoven et al. Model	29
2.4.2.4 Amy et al. Model	29
2.5 Comparison of the Existing Souring Models and In-house Simulator.	30
2.6 Application and Implication of the Existing Reservoir Souring Models.	32

2.6.1 Effect of Sweep Efficiencies on Prediction of Reservoir Souring	35
2.6.2 Effects of Temperature and Concentration, Reservoir Characteristics and Conditions on Reservoir Souring Prediction .	38
Chapter 3	
Problem Statement	39
3.1 Overview	39
3.2 Modeling and Simulation of the Reservoir Souring Process	41
3.2.1 Biological Reactions Produce Hydrogen Sulfide	41
3.2.2 Retardation Slows the Hydrogen Sulfide Migration	42
3.3 Model Development	42
Chapter 4	
Review of UTCHEM Simulator	44
4.1 Mass and Energy Balances	44
4.1.1 Mass Conservation Equations	44
4.1.2 Energy Conservation Equations	47
4.1.3 Pressure Equation	47
4.2 Biodegradation Reaction	48
4.2.1 Mathematical Model Formulation	49
4.3 Simplification of the General Mass Balance Equation for the Reservoir Souring Process in a Typical Seawater Injected Reservoir	50
4.3.1 Biological Reactions	52
4.3.2 Adsorption	52
Chapter 5	
Model Development	54
5.1 Introduction	54
5.2 Conceptual Model of Souring	58
5.3 Stoichiometry of the Reactions	56
5.4 Partitioning	57
5.5 Adsorption	58
5.6 Material and Energy Balances	59
5.7 Simulation of the Reservoir Souring in UTCHEM	59
5.8 Advantages of Developed Model versus Previous Models	59
5.9 Summary of the Developed Model	61
Chapter 6	
Application of UTCHEM in Reservoir Souring Process	63
6.1 Introduction	64
6.2 Data Required for Reservoir Souring Models	64
6.2.1 Parameters for the Biological Reactions	64

6.2.2 Parameters for Partitioning and Adsorption on Rock Surfaces.	70
6.2.3 Water Chemistry	71
6.2.4 Adsorption of H ₂ S by Residual Oil	73
6.2.5 Scavenging of H ₂ S	74
6.3 Factors that Control Activity of Sulfate Reducing Bacteria in Reservoirs During Water Injection	76
6.3.1 Nutrient Factors	76
6.3.1.1 Carbon/Energy	76
6.3.1.2 Nitrogen	76
6.3.1.3 Electron Acceptors	76
6.3.1.4 Inorganic Salts	77
6.3.2 Physical Constraint	77
6.3.2.1 Temperature	77
6.3.2.2 Pressure	77
6.3.2.3 pH	77
6.3.2.4 Redox Potential	77
6.3.2.5 Salinity	78
6.3.2.6 Permeability	78
6.4 Switch Between Reservoir Souring Models	78
6.4.1 Mixing Model	78
6.4.2 Biofilm Model	79
6.4.3 TVS Model	79
6.4.4 UTCHEM Souring Model.....	80
6.5 Simulation of the Reservoir Souring Prediction.....	81
6.6 Reproduction of the Published Models by UTCHEM Model	86
6.7 Investigation of the Effective Parameters on Reservoir Souring Prediction	90
6.7.1 Propagation of Temperature Profile in the Seawater Injected Reservoir	91
6.7.1.1 Analytical and Numerical Solutions of Heat Transfer in the Seawater Injected Reservoirs	91
6.7.1.2 Vertical Distribution of Temperature Profile in the Reservoirs	104
6.7.2 Effect of Dispersivity of the Media on Concentration Profiles	112
6.7.3 Effects of Layering of the Reservoir on the Profile of Hydrogen Sulfide	117
6.7.3.1 Two and Three Layer Reservoirs	117
6.7.3.2 Effect of Vertical Grid Refinement on the Predicted Results.....	119
6.8 Investigation of the Chemical and Physical Constraints on Reservoir Souring	129
6.9 Overall View on the Limiting Constraints in the Reservoir	135
6.10 Summary of Chapter 6	141
Chapter 7	
Field Application of the Developed Model and Simulator	143

7.1 Introduction	144
7.2 Response Surface Methodology and Experimental Design	144
7.2.1 Fitted Model Examination	145
7.3 Field Application of the Developed Model and Simulator	150
7.3.1 Application of the Simulator for a Multi-layered Reservoir .	151
7.3.2 Application of the Simulator for a Multi-layered and Multi-well Reservoir	160
7.3.3 Effects of Grid Refinement on the Reservoir Souring Predictions in Field Case Studies.....	171
Chapter 8	
Summary, Conclusions, and Recommendations for Future Works	173
8.1 Summary	173
8.2 Conclusions	174
8.3 Recommendations for Future Works	176
Appendix A	178
Appendix B	210
Appendix C	247
Appendix D	250
Appendix E	251
Appendix F	252
Nomenclature	270
References	273
VITA	280

List of Tables

Table 2.1: Comparison of the existing reservoir souring prediction models	31
Table 2.2: Comparison of in-house reservoir souring prediction simulators ...	32
Table 3.1: Activation range of the different SRB types	41
Table 5.1: Comparison of the reservoir souring models	60
Table 6.1: Analysis of produced water (after Cochrane et al., 1988)	72
Table 6.2: Henry's law constants for H ₂ S in crude oil and formation water, mmHg/ppmv H ₂ S, (after Eden et al., 1993)	73
Table 6.3: Partition coefficient for H ₂ S between crude oil and formation water, ppmw H ₂ S in oil/ppmw H ₂ S in water, (After Eden et al., 1993)	73
Table 6.4: Retardation factors corresponding to laboratory measurements of scavenging capacity of H ₂ S with reservoir rock (after Sunde et al., 1991).....	75
Table 6.5: Initial and injected concentration data (mg/l)	83
Table 6.6: Reservoir conditions (for 1D and layered cases) and characteristics (1D cases)	97
Table 6.7: Injected seawater properties	97
Table 6.8: Variation of thermal properties of rock and fluids in the reservoir ...	101
Table 6.9: Thermal properties of rock and fluids in the reservoir	101
Table 6.10: Variation of the thermal properties of rock and fluids in the reservoir .	106
Table 6.11: Kinetics and transport properties of six different simulations	115
Table 6.12: Reservoir characteristics for example 2Lmix5	118
Table 6.13: Reservoir characteristics for example 2Lmix6	118
Table 6.14: Reservoir characteristics for example 3Lmix7	118
Table 6.15: Reservoir characteristics for example 3Lmix8	118
Table 6.16: Reservoir characteristics for example 2Lmix5-refin1	119
Table 6.17: Reservoir characteristics for example 2Lmix5-refin1	119

Table 7.1: Parameters used for experimental design study	145
Table 7.2a: Reservoir characteristics	151
Table 7.2b: Reservoir conditions	151
Table 7.2c: Reservoir conditions (continued)	151
Table 7.2d: Reservoir data for energy balance equation	152
Table 7.2e: Reservoir simulation data	152
Table 7.3a: Reservoir characteristics	160
Table 7.3b: Reservoir conditions	160
Table 7.3c: Reservoir conditions (continued)	160
Table 7.3d: Reservoir data for energy balance equation	160
Table 7.3e: Reservoir simulation data	160
Table C1: Reservoir conditions and characteristics	247
Table C2: Injected seawater properties	247
Table C3: Retardation factor used in the model	247
Table C4: Biological species used in UTCHEM model	247
Table C5: Flow parameters	248
Table C6: Data on bacterial reaction kinetics	248
Table C7: Initial concentrate ion data	248
Table C8: Reservoir characteristics data	248
Table C9: SRB/Nutrients data	248
Table D1: Reservoir characteristics and data	250
Table D2: Reservoir characteristics and data (continued)	250
Table D3: Well constraints	250

Table D4: Thermal properties of rock and fluid in the reservoir	250
Table E1: The run number, parameters, and responses used in experimental design	251

List of Figures

Figure 2.1: Classification of SRB growth rate according to the temperature optima	12
Figure 2.2: Observation of hydrogen sulfide in production wells in Kuparuk field (after Frazer and Boiling, 1991)	17
Figure 2.3: Kuparuk river field's forecasting model (after Frazer and Boiling, 1991)	18
Figure 2.4: Mixing model (after Ligthelm et al., 2001)	20
Figure 2.5: Biofilm model (after Sunde et al., 1993)	22
Figure 2.6: S-shape biogenic reduction of sulfate (after Eden et al., 1993)	24
Figure 2.7: TVS model (after Eden et al., 1993)	25
Figure 2.8: Mixing model reservoir souring prediction (after Sunde et al., 1993) .	34
Figure 2.9: Biofilm model reservoir souring prediction (after Sunde et al., 1993).	34
Figure 2.10: Cross section of a stratified reservoir with no gravity effect	36
Figure 2.11: Typical H ₂ S history observed at a production well with different models	36
Figure 2.12: Schematic illustration of areal sweep efficiency in a reservoir	37
Figure 3.1: Schematic illustration of oil field reservoir souring	40
Figure 3.2: Simplified view of concentrations and temperature distributions during water flooding	41
Figure 3.3: Development of a comprehensive reservoir souring model	43
Figure 5.1: Conceptual model of souring process in UTCHEM	56
Figure 6.1.a: Water and oil cut versus pore volume for primary results case	84

Figure 6.1.b: Water and oil cut versus time for primary results case	84
Figure 6.2: Total concentration of components in production well (mg/l) for primary results case	85
Figure 6.3a: Tracer concentration (mg/l) after 75 days of seawater injection for primary results case	85
Figure 6.3b: H ₂ S concentration (mg/l) after 75 days of seawater injection for primary results case	86
Figure 6.4: Comparison of the mixing model prediction of H ₂ S in aqueous phase (mg/l) via the UTCHEM simulator and with the reproduced results (after Ligthelm et al., 1991)	89
Figure 6.5: Comparison of biofilm model prediction of H ₂ S in aqueous phase (mg/l) via the UTCHEM simulator and with the reproduced results (after Sunde et al., 1993)	89
Figure 6.6: The TVS model of prediction of H ₂ S in aqueous phase (mg/l) via the UTCHEM simulator	90
Figure 6.7: Temperature distribution in the reservoir, no heat transfer to overburden/underburden (numerical dispersion = 13ft)	96
Figure 6.8: Temperature distributions in the reservoir with heat transfer to overburden/underburden (numerical dispersion = 13ft)	96
Figure 6.9: Temperature and concentration distribution in the reservoir, no heat transfer to o/underburden, variable longitudinal dispersivity= 13-28 ft (after 100 days)	98
Figure 6.10: Temperature and concentration distribution in the reservoir, no heat transfer to overburden/underburden, variable longitudinal dispersivity= 13-28 ft (after 300 days)	98
Figure 6.11: Temperature and concentration distribution in the reservoir, no heat transfer to overburden/underburden, variable longitudinal dispersivity= 13-28 ft (after 1000 days)	99
Figure 6.12: Tracer and temperature profiles in a reservoir for the case of no heat transfer to overburden/underburden with variable reservoir thermal conductivity (2000 days)	102
Figure 6.13: Tracer and temperature profiles in a reservoir for the case of no heat transfer to overburden/underburden with variable flowing phase heat capacity (2000 days)	102

Figure 6.14: Tracer and temperature profiles in a reservoir for the case of no heat transfer to overburden/underburden with variable rock heat capacity (2000 days)	103
Figure 6.15: Tracer and temperature profiles in a reservoir for the case of no heat transfer to overburden/underburden with variable rock and flowing phase heat capacity (2000 days)	103
Figure 6.16: Tracer and temperature profiles in a reservoir for the case of no heat transfer to overburden/underburden with variable Darcy's velocity (2000 days)	104
Figure 6.17: Temperature (°F) distribution in a layered (3 layers) reservoir after 1000 days (case A1)	107
Figure 6.18: Temperature (°F) distribution in a layered (3 layers) reservoir after 1000 days (case A2)	107
Figure 6.19: Temperature (°F) distribution in a layered (3 layers) reservoir after 1000 days (case A3)	108
Figure 6.20: Temperature (°F) distribution in a layered (3 layers) reservoir after 1000 days (case B1)	108
Figure 6.21: Temperature (°F) distribution in a layered (3 layers) reservoir after 1000 days (case B2)	109
Figure 6.22: Temperature (°F) distribution in a layered (3 layers) reservoir after 1000 days (case B3)	109
Figure 6.23: Temperature (°F) distribution in a layered (3 layers) reservoir after 1000 days (case C1)	110
Figure 6.24: Temperature (°F) distribution in a layered (3 layers) reservoir after 1000 days (case C2)	110
Figure 6.25: Temperature (°F) distribution in a layered (3 layers) reservoir after 1000 days (case C3)	111
Figure 6.26: Tracer concentration (mg/l) in the reservoir	111
Figure 6.27: Temperature (°F) distribution in a layered (8layers) reservoir after 1000 days	112
Figure 6.28: Comparing of produced H ₂ S for case C in table 6.12 (Bacterial doubling time is one day, $\mu_{\max} = 0.693/\text{day}$)	116

Figure 6.29: Comparing of produced H ₂ S for case D in table 6.12 (Bacterial doubling time is one day, $\mu_{\max} = 0.693/\text{day}$)	116
Figure 6.30: Produced hydrogen sulfide concentration (mg/l) in a 2 layered reservoir, no physical dispersion (Thermophilic SRB, doubling time is one day, $\mu_{\max} = 0.693/\text{day}$)	120
Figure 6.31: Nonreacting tracer concentration (mg/l) in the producer for a 2 layered reservoir, no physical dispersion	121
Figure 6.32: Tracer concentration in 2 layered reservoir without physical dispersion	121
Figure 6.33: Produced hydrogen sulfide concentration (mg/l) in a 2 layered reservoir, with 10 ft of physical dispersion (Thermophilic SRB, doubling time is one day, $\mu_{\max} = 0.693/\text{day}$)	122
Figure 6.34: Nonreacting tracer concentration in the producer (mg/l) for a 2 layered reservoir, with 10 ft of physical dispersion	122
Figure 6.35: Tracer concentration in 2 layered reservoir with 10 ft of physical dispersion	123
Figure 6.36: Produced hydrogen sulfide concentration (mg/l) in a 3 layered reservoir, no physical dispersion (Thermophilic SRB, doubling time is one day, $\mu_{\max} = 0.693/\text{day}$)	123
Figure 6.37: Nonreacting tracer concentration (mg/l) in the producer for a 3 layered reservoir, no physical dispersion	124
Figure 6.38: Produced hydrogen sulfide concentration (mg/l) in a 3 layered reservoir, with 10 ft of physical dispersion (Thermophilic SRB, doubling time is one day, $\mu_{\max} = 0.693/\text{day}$)	124
Figure 6.39: Nonreacting tracer concentration in the producer (mg/l) for a 3 layered reservoir, with 10 ft of physical dispersion	125
Figure 6.40: Temperature profile in different layers after 1000 days (2 layers, no heat transfer to o/under burden)	125
Figure 6.41: Temperature profile in different layers after 1000 days of seawater injection (3 layers, no heat transfer to o/under burden)	126
Figure 6.42: H ₂ S concentration in the producer after vertical refinement, no physical dispersion (Thermophilic SRB, doubling time is one day, $\mu_{\max} = 0.693/\text{day}$)	126

Figure 6.43: Nonreacting tracer concentration in the producer for the case of vertical refinement, no physical dispersion	127
Figure 6.44: H ₂ S concentration in the producer after vertical refinement, with physical dispersion (Thermophilic SRB, doubling time is one day, $\mu_{\max} = 0.693/\text{day}$)	127
Figure 6.45: Nonreacting tracer concentration in the producer for the case of vertical refinement, with 10 ft of physical dispersion	128
Figure 6.46: Temperature profile(1000 days after water injection) in different layers after grid refinement in vertical direction (no heat transfer to overburden/underburden)	128
Figure 6.47: Temperature profile along the reservoir at different injected pore volumes	130
Figure 6.48: Produced H ₂ S (mg/l in aqueous phase) vs. pore volume injected seawater for different SRB types	131
Figure 6.49: Effects of nutrient concentration on the produced H ₂ S concentration (mg/l, aqueous phase) for the thermophilic-SRB	132
Figure 6.50: The effects of retardation factor on the H ₂ S concentration profile in the producer (biological reactions are attribute to thermophilic-SRB)..	133
Figure 6.51: Effect of pore velocity on the produced H ₂ S in terms of injected pore volume (case study reservoir with thermophilic SRB)	134
Figure 6.52: Effect of pore velocity on the produced H ₂ S in terms of injected time, month, (Case study reservoir with thermophilic SRB)	135
Figure 6.53: Concentration of hydrogen sulfide at different time in the reservoir.	137
Figure 6.54: Concentration of all spices in aqueous phase after 200 days of injection	137
Figure 6.55: Concentration of all spices in aqueous phase after 200 days of injection	138
Figure 6.56: Concentration of all spices in aqueous phase after 500 days of injection	138
Figure 6.57: Concentration of all spices in aqueous phase after 500 days of injection	139

Figure 6.58: Concentration of all spices in aqueous phase after 1000 days of injection	139
Figure 6.59: Concentration of all spices in aqueous phase after 1000 days of injection	140
Figure 6.60: Delay in the temperature front with respect to the injection front at different time	140
Figure 6.61: Concentration of all spices in aqueous phase in the production well.	141
Figure 7.1: Normal probabilities of residuals	146
Figure 7.2: Effects of nutrients and temperature on the produced hydrogen sulfide	147
Figure 7.3: Effects of adsorption and partitioning on the produced hydrogen sulfide	147
Figure 7.4: Effects of temperature and partitioning on the produced hydrogen sulfide	148
Figure 7.5: Effects of nutrients and partitioning on the produced hydrogen sulfide	149
Figure 7.6: Effects of temperature and adsorption on the produced hydrogen sulfide	149
Figure 7.7: Effects of nutrients and adsorption on the produced hydrogen sulfide	150
Figure 7.8: Profile of water tracer after 3 months of sea water injection.....	154
Figure 7.9: Profile of water tracer after 1 year of sea water injection	154
Figure 7.10: Profile of water tracer after 2 years of sea water injection	155
Figure 7.11: Profile of hydrogen sulfide after 2 years of sea water injection	155
Figure 7.12: Profile of nitrate after 2 years of sea water injection	156
Figure 7.13: Profile of phosphate after 2 years of sea water injection	156
Figure 7.14: Profile of SRB after 2 years of sea water injection	157
Figure 7.15: Temperature advancement after 3 months of sea water injection....	157

Figure 7.16: Temperature advancement after 1 year of sea water injection	158
Figure 7.17: Temperature advancement after 2 years of sea water injection	158
Figure 7.18: Water break through vs. pore volume injected	159
Figure 7.19: History of the produced hydrogen sulfide and other species involved in biological reactions	159
Figure 7.20: Location of the injection and production wells in field case 2.....	162
Figure 7.21: History of the produced hydrogen sulfide in well 1, 2, 4 and 5.....	163
Figure 7.22: History of the produced hydrogen sulfide in well 7, 10, 12 and 13...	163
Figure 7.23: Tracer distribution after 1 year of water injection	165
Figure 7.24: Tracer distribution after 2 years of water injection	165
Figure 7.25: Tracer distribution after 3 years of water injection	166
Figure 7.26: Temperature distribution after 1 year of water injection	166
Figure 7.27: Temperature distribution after 2 years of water injection	167
Figure 7.28: Temperature distribution after 3 years of water injection	167
Figure 7.29: Hydrogen sulfide distribution after 2 years of water injection.....	168
Figure 7.30: Nitrate distribution after 2 years of water injection	168
Figure 7.31: Nitrate distribution after 2 years of water injection.....	169
Figure 7.32: SRB distribution after 2 years of water injection.....	169
Figure 7.33: Sulfate distribution after 2 years of water injection.....	170
Figure 7.34: Acetate distribution after 2 years of water injection.....	170
Figure 7.35 History of the produced hydrogen sulfide in wells 1, 2, 4, and 5.....	172
Figure 7.36 History of the produced hydrogen sulfide in wells 7, 10, 12, and 13...	172

Chapter 1

Introduction

1.1 Reservoir Souring

Reservoir souring is a process in which a previously sweet (no H₂S) oilfield starts to produce fluids (oil, gas, water) which contain H₂S. The term also refers to increasing H₂S concentrations in produced fluids from their initial level. Anecdotal and published accounts in the petroleum industry show that reservoir souring occurs frequently. This is particularly true when seawater is injected into a reservoir for the purpose of increased oil recovery. After some period of time, on the order of months or years after seawater injection starts, many operators observe significant production of H₂S. British Petroleum (BP) reported that 70% of seawater flooded reservoirs have soured (Al-Rasheedi et al., 1999).

Industrial problems associated with H₂S production are the increase of corrosivity of produced fluids, plugging of the formation, legal issues regarding safety, and health risks and liabilities (Mali et al., 2003; Tuttle, 1990). It is costly and difficult to address these problems after a field development plan is already in place. Moreover, hydrogen sulfide production increases the sulfur content of the crude oil which decreases its value and increases refining costs. Estimated losses in the oil industry in the United States stemming from souring are 1 to 2 billion USD per year (Mueller and Nielsen, 1996).

The subject of reservoir souring prediction is relatively new. According to the latest research, souring can result from organic and inorganic sources (Cochrane et al., 1988; Cavallaro and Martinez, 2005). In reservoir conditions, the organic source is mainly responsible for hydrogen sulfide production. In this case a biological reaction between an electron acceptor (sulfate from injection water) and substrates (volatile organic acids in formation water) in the presence of SRB (sulfate reducing bacteria) results in hydrogen sulfide, SRB, and CO₂ (Muller and Nielsen, 1996).

During last two decades, several companies such as Shell (Ligthelm et al., 1991) and Statoil (Sunde and Thorstenson, 1993; Tyrie and Ljosland, 1993) developed their own models and simulators (Frazer and Bolling, 1991; Amy and Eilen, 2000) to predict the onset of the reservoir souring. Comparing the oil-field data with the simulated results shows that in many cases these results are not consistent. Where, the history of the predicted results does not match with the observed field data. To match the field data with the predicted results, some unlikely assumed circumstances were used. These discrepancies basically result from their proposed models which are not able to include many important parameters and conditions which may differ from one reservoir to

another (Maxwell and Spark, 2005). In the next chapter, we discuss the basis and assumptions of the published models and the features which are need to be added for a more comprehensive model.

To date, there is no comprehensive simulator to predict reservoir souring. As we discuss in detail (Chapter 2), the published simulators are mostly limited to certain fields and there are many limitations in their applications. These limitations prevent them from being used in as a general simulator in different reservoirs with various conditions and characteristics. Being able to estimate the likelihood and timing of the onset of H₂S production would permit more realistic assessments of project economics. A predictive model would also enable operators to make more accurate decisions on remedial actions to prevent souring or to mitigate its impact. Therefore, predicting the process of reservoir souring on a field scale would be of significant value.

The first step in the development of a reservoir souring prediction model is investigation of the possible mechanisms of hydrogen sulfide production in a reservoir. When the source of hydrogen sulfide is determined, a knowledge of the transport of fluids in porous media is necessary to simulate the movement of hydrogen sulfide from injection to production wells. The transport of water and oil phases can be explained by hydraulic conductivity of the porous media. The transport of an active component like hydrogen sulfide is more complex. In this case, the interaction with rock surfaces and partitioning between phases retard the movement of hydrogen sulfide with respect to the bulk flow. This delay in the arrival of an active component is expressed in term of retardation factor.

When hydrogen sulfide is produced in a reservoir, no matter which kind of sources it has, it can react with iron containing component of the rock (e.g., siderite). Furthermore, depending on the pressure and temperature H₂S partitions between oil and water phases. The combined effects of partitioning and adsorption cause the hydrogen sulfide to show a delay in its arrival to the production well with respect to the front of injected seawater. The adsorption capacity and the partitioning factor determine the retardation factor which determines the delay in display of the hydrogen sulfide.

1.2 Research Objectives

The ultimate goal of this research is to develop a simulator to predict the onset of reservoir souring more accurately and reliably. Our starting point is the further development of current UTCHEM (UTCHEM Technical Documentation, 2000) capabilities for the prediction of the onset of reservoir souring.

The objectives that we expect to achieve during this research are stated below:

1. Critical review of existing reservoir souring models
2. Development of a comprehensive reservoir souring model
3. Field scale application to investigate H₂S production and transportation

1.3 Review of Chapters

Chapter 2 provides a complete literature review of the history of reservoir souring, published models and in-house simulators for the prediction of reservoir souring in seawater injected reservoirs. Chapter 3 explains the problem statement and gives an overview of the parameters which control the reservoir souring. A review of the

UTCHEM simulator regarding the general mass, energy balances and biodegradation equations which are needed for reservoir souring is given in Chapter 4. Chapter 5 explains the steps for the model development. A full discussion of the application of UTCHEM in investigation of the parameters which affect the reservoir souring is given in Chapter 6. In chapter 6, the effects of available nutrients on biological reactions, contribution of temperature propagation, dispersivity of the media, and type of SRB on the predicted result of reservoir souring are described. In Chapter 7, first we apply the experimental design approach to investigate the effective parameters in production and transportation of hydrogen sulfide in porous media. Then, we show the capability of the developed model and simulator in the prediction of reservoir souring in field case by introducing two complicated field applications. Finally, Chapter 8 summarizes the results and future work.

Chapter 2

Literature Review

The phenomenon of souring is the increase in amount of hydrogen sulfide (H_2S) per unit mass of total fluid produced from a reservoir. A well which produces H_2S is said to be sour, in contrast to a sweet well, which does not produce H_2S . However, small gas phase concentrations of H_2S , up to around 3 parts per million by volume (ppmv), is typically beneficial in its effects on oil well and process equipment. The baseline for being sour is usually referred to around 3 ppmv and not zero. This concentration measurement is usually conducted at standard temperature of $0^\circ C$ and pressure of 1 atmosphere in the gas phase relative to a partition from an aqueous phase at/or less than pH of 5 (Eden et al., 1993; Kalpakci et al., 1995).

Based on our current information, souring occurs in a reservoir during a period of several months to several years after seawater injection to increase oil recovery (Dinning and Arctander, 2005). Due to unwanted effects of souring on the environment, facilities,

legal issues regarding safety, health risks and an increase in sulfur content of crude oil, several companies have modeled the process of reservoir souring in order to predict its onset.

In the summer of 1987, the multi-sponsored £ 1/3 MUK oilfield reservoir souring program, which took three years, was launched. This program investigated both microbiological (biogenic) and non-microbiological souring mechanisms (Eden et al., 1993). The first attempt to model the reservoir souring process goes back to 1991 when Ligthelm et al. (1991) proposed a mixing model in which a chemical reactor model including scavenging of H₂S with iron-containing minerals and oil/water partitioning effect (i.e. dissolution of H₂S in the residual oil phase) was considered. This was followed by the biofilm model, which is based on biological reaction model including the bacterial growth rate in the vicinity of an injection well, introduced by Statoil in 1993 (Sunde and Thorstenson, 1993).

Eden, et al. (1993) developed an alternative biogenic souring model that included the temperature and pressure effects on bacterial activity. This model is known as dynamic thermal viability shell (TVS). The model assumes that the generation of H₂S depends on the establishment of a stable thermal viability shell which is the portion of the water-flooded reservoir where temperature and pressure are within the range suitable for the sulfate reducing bacteria (SRB) activities (Platenkamp, 1985). Modeling of the reservoir souring in the fractured reservoirs has been described with algorithm based models by Burger in 2005, as explained in the following sections.

2.1 Basic Knowledge Needed in Study of Reservoir Souring

As explained below, a preliminary knowledge on biochemistry is necessary to calculate the generation of hydrogen sulfide in the reservoir. On the other hand, geochemistry helps to understand the interaction of the formation water composition on the biogenic production of hydrogen sulfide in the reservoir.

2.1.1 Hydrogen Sulfide

Among many hydrogen sulfides, including polysulfides and hydrosulfides, hydrogen sulfide (H_2S) is the most common. The natural sources of hydrogen sulfide are coal, natural gas, oil, volcanic gases, sulfur springs and lakes. In natural sources, hydrogen sulfide is nearly always present with other sulfur compounds. In a number of industrial operations, hydrogen sulfide is a byproduct or waste material. In industry, whenever sulfur or certain sulfur compounds contact with organic materials, hydrogen sulfide could be formed (Hydrogen Sulfide, University Park Press, Baltimore, 1979). The interaction of hydrogen sulfide with rock surfaces and partitioning between oil and water phases are discussed in Section 6.4.2.

2.1.2 Biochemistry

As we will explain in the following sections, a knowledge of the biochemistry is essential in the simulation of reservoir souring. Biochemistry is the science of chemical

reactions that are brought about by living organisms. The biological reactions are controlled by living species, bacteria. Bacteria need nutrients and trace elements to survive. These reactions follow the Van't Hoff rule of a doubling rate of reaction for 10°C increase in temperature in a restricted temperature range. The classification of biological reactions, the behavior of the enzymes in activation of reactions, and engineering design for specific purposes are found in related references (Sawyer et al., 1978).

2.1.3 Sulfate Reducing Bacteria (SRB)

The sulfate reducing bacteria (SRB) are a specific group of bacteria which are able to use sulfate as the final electron acceptor in their respiration mechanism. Detailed study of the identification, metabolisms, cell characteristics, and interactions with living species are given for the biological point of view (Barton, 1995). For the reservoir engineering point of view, we need to use the results of research which show their classification according to reservoir conditions and variables. The effective parameters on the SRB activities which are essential in the simulation of reservoir souring are explained in the related sections.

2.1.4 Geochemistry

Geochemistry deals with the chemical processes which distribute and change elements in the solid earth, its oceans, and the atmosphere as a function of time. In the reservoir, the formation water is a complex solution of different elements. The composition of the water and interaction of different species change the properties of the

media. The properties of the media affect the chemical and biological reaction progress. In simulation of reservoir souring, a knowledge of the interaction of chemistry of the reservoir is needed to get reliable results (Walter, 2005; Zou Habio, 2007; Larry, 2002; Drever, 1982).

2.2 Mechanisms of Reservoir Souring

Hydrogen sulfide in a reservoir could be from any of the following sources: geological sources, geochemical sources and biological sources. Geological sources of hydrogen sulfide date back to the ancient geological process of reservoir formation. The potential geochemical and biological processes are explained in the following sections.

2.2.1 Microbial Sulfate Ion (SO_4^{2-}) or Sulfur Reduction

It is well known that sulfate reducing bacteria (SRB) when growing on oxygen containing substrates similar to the short chain volatile acids, such as formic, acetic, propionic and butyric, lactic acid, phenols and benzoates are capable of reducing of SO_4^{2-} to H_2S . Volatile fatty acids exist in many oilfield-produced waters and may be a predominant factor in the production of hydrogen sulfide in reservoirs during seawater injection for oil recovery. There are three main groups of SRB. Each group's optimal growth rate are at different temperatures. Mesophiles, which grow optimally at 35°C , thermophiles at 55°C and hyperthermophiles 85°C . Since the temperature of a reservoir changes during injection of seawater, the growth rate of bacteria will change (Eden et al., 1993).

2.2.2 Classification of SRB According to Temperature Optima

Sulfate reducing bacteria (SRB) are anaerobic and can be isolated in low numbers from many sources. The sources of SRB are many natural soils, sediments, and water. The energy for the SRB growth is obtained by oxidation of organic substrates. SRB use sulfate as the external electron acceptor. As a result, the sulfate is reduced to the sulfide. The biological reaction of SRB in the reservoir is impacted by the temperature of the media. The temperature of the reservoir ranges between the injected water temperature (5-20°C) to the formation temperature (40-100°C).

The mechanisms of SRB growth and survival under different conditions have been studied extensively. Figure 2.1 shows the growth rate versus temperature for the three groups of SRB, mesophiles, thermophiles, and hyperthermophiles. According to Figure 2.1, each SRB group has a lower limit, upper limit and maximum temperature in which the biological reactions happen.

Early studies indicate that mesophilic SRB (m-SRB) exist in sour oil and water in production facilities within shallow reservoirs. Mesophilic SRB which belong to the genus *Desulfovibrio*, grow optimally at temperatures 20-40°C. These isolates will not grow at temperature above 45°C. The detectable number of m-SRB in seawater is very low, typically below 10 organisms per milliliter (Okabe et al., 1992; Leu et al., 1999; Sunde et al., 1992).

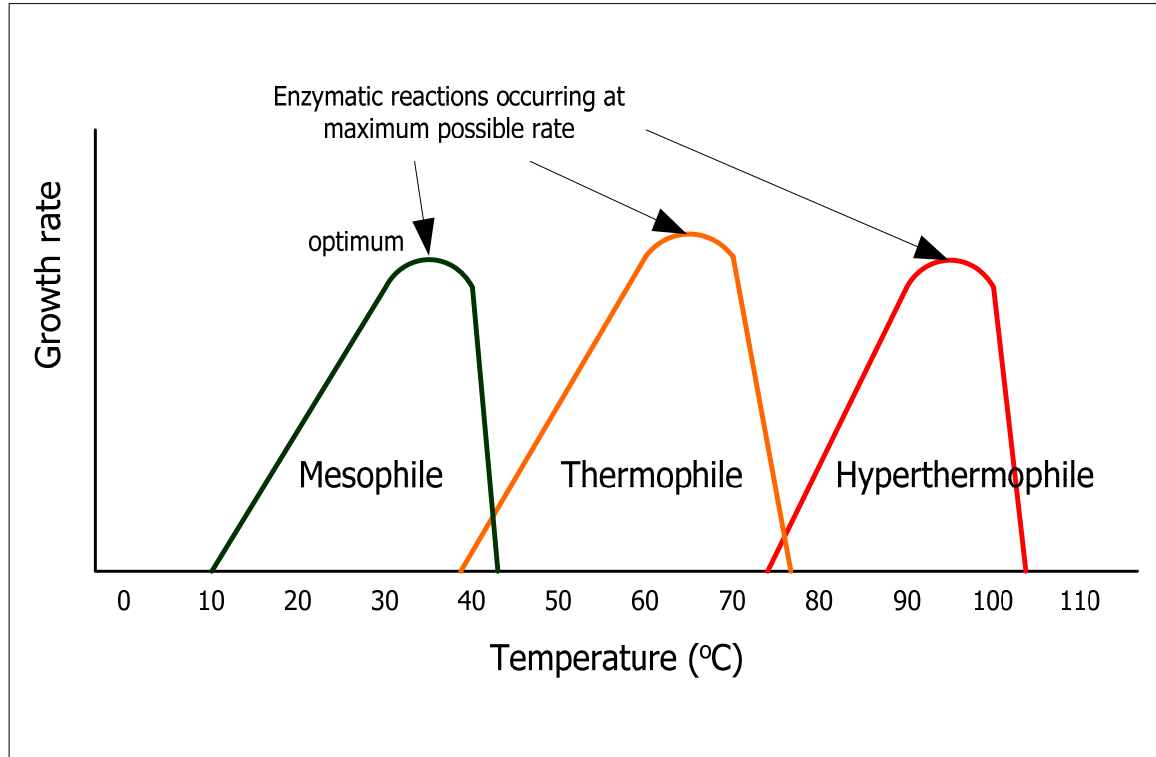


Figure 2.1 Classification of SRB growth rate according to the temperature optima

Recent studies reveal the presence of thermophilic SRB (t-SRB) in the open seawater near oil production and hot produced waters in the North Sea oil fields. Thermophilic SRB are able to grow at temperatures of 40-80°C. Thus, they are recognized as an important hydrogen sulfide source in oil reservoirs and production facilities. Temperatures around 100°C were previously considered too high to support SRB activity in reservoir souring. But, extreme thermophiles and hyperthermophilic archaea and bacteria have been identified in different oil fields such as Thistle offshore production platform, Prudhoe Bay, Endicott, and Kuparuk. This identification indicates that it is more likely for these isolates to be widely distributed in hot seawater injected oil fields. These isolates can grow at high temperatures of 80-113°C and reduce sulfur compounds while utilizing some components of crude oil (like acetic acid, propionic acid, and butyric acid) in their anaerobic metabolism (Sunde et al., 1992, Eden et al., 1993).

2.2.3 Inorganic souring

The following five different mechanisms can be distinguished for the inorganic production of H₂S:

- (a) thermochemical reduction of sulfate from injected seawater
- (b) maturation of organic matters which contain sulfur
- (c) dissolution of minerals which contain sulfide, such as pyrrhotite in acid water
- (d) FeS₂ (pyrite or marcasite) reduction which followed by (c)
- (e) conversion of sulfite which is used as an oxygen scavenger in injection water

From these inorganic H₂S production mechanisms, mechanisms (b), (c) and (d) may have a role in low-level indigenous H₂S in reservoir fluids. Mechanism (a) can relate the H₂S formation with injection seawater, but at temperatures prevalent at reservoir it could not be a possible source (Khatib and Salantro, 1997; Marsland et al., 1989).

2.3 Transport of H₂S in Porous Media

In general, several transport properties of the formation determine the migration of H₂S and water through a reservoir (Chen et al., 1994, Chang et al., 1991, Sarkar et al., 1994). The flow of water in porous media is described by hydraulic conductivity while the movement of H₂S dissolved in the water is described by the retardation factor. The retardation factor of H₂S represents all of the interactions with the stationary oil phase and the solid surfaces of the porous media (Wanner et al., 1995; Wilson, 1996; Seto and Believeau, 2000). These interactions include reaction of H₂S with iron-containing minerals and forming pyrite or pyrrhotite. Consequently, these interactions retard the

migration of H₂S relative to the water and delay its arrival downstream. This delay affects the H₂S concentration profile within a reservoir and the forecast of reservoir souring onset (Zhang et al., 1992; Wick et al., 2001).

2.4 Critical Review of Reservoir Souring Prediction Models

Reservoir souring is the process of increasing of the hydrogen sulfide concentration in the produced fluids from a reservoir which is subjected to seawater injection. Usually, the increase of hydrogen sulfide concentration is observed after one pore volume and most often after several pore volumes of sea water injection. Due to the unwanted effects of reservoir souring on the facilities and environment, it would be of significant value to we predict its onset in advance. During last two decades several companies have tried to investigate the sources of hydrogen sulfide production in the reservoirs. Following the investigation, they tried to develop the models which can predict the timing of the onset of the reservoir souring in the reservoirs. All publications and anecdotes certify that biological activities of SRB are mainly responsible for the souring of reservoir after injection of sea water. With this in mind, several companies have developed their own models and simulated the reservoir souring process to predict the onset of souring for the purposes of mitigation and prohibition of its effects.

Generally, all reservoir souring models are compromised of two steps: first, the mechanisms of hydrogen sulfide generation and second, transportation of produced H₂S from injector(s) to producer(s). There is an agreement between all existing models about the generation of H₂S. In these models, SRB are mainly responsible for the souring, but their abilities to include the important parameters in the biogenic reactions are different.

For the second step, transport of H₂S in the porous media, different models have different approach. Some of them consider adsorption on the rock surfaces and partitioning between oil and water phases and others do not. In the following sections, we investigate the mechanisms of reservoir souring process in the reservoirs. Consequently, we describe the existing reservoir souring prediction models in detail regarding their theoretical basis of their developments and their advantages and disadvantages.

2.4.1 Existing Reservoir Souring Models

2.4.1.1 Kuparuk River Field Model

The Kuparuk river field is the second largest producing oil field in the United States. This field is located approximately 40 miles west of the Prudhoe Bay field, on the north slope of Alaska. The Kuparuk reservoir is located 6,200ft sub-sea and is sandstone. The initial production started in December 1981 under a solution gas drive mechanism. Injection of water from shallow cretaceous water source wells and Beaufort sea water started in January 1983 and November 1985, respectively. In 1991, the combination of waterflood and water-alternating immiscible gas injection were the recovery mechanism in the majority of the field. Production from Kuparuk field was initially sweet. Detection of H₂S from a single well was reported in April 1986. In 1991, 130 wells (about 37% of all producers) produce hydrogen sulfide in detectable levels. Figure 2.2 shows the increasing level of H₂S in Kuparuk field (Frazer et al., 1991).

2.4.1.1.1 Proposed Souring Mechanism

It is believed that the SRB is the main cause of souring in the Kuparuk reservoir. The supporting evidences are: 1) historical hydrogen sulfide production, 2) cultivated SRB colonies, 3) isotopic analysis (Frazer et al., 1991).

2.4.1.1.2 Historical Hydrogen Sulfide Production

The historical production of H₂S supports the microbiological mechanism. The SRB growth requirements include: 1) carbon (from organic acids or alcohols), 2) nitrogen, 3) phosphorus, 4) iron, and, 5) sulfur (sulfate and sulfite ions). The Kuparuk formation water and Cretaceous water, used as initial water support, have a lack of sulfate or sulfite ions, whereas, injected seawater is rich in sulfate ions. The lack of sulfate prior to seawater injection should greatly restrict the SRB activities. This is compatible with the observed souring trend. The field was sweet with no detectable H₂S with Cretaceous water breakthrough. However, after seawater injection, hydrogen sulfide was detected. The history of observed hydrogen sulfide in production wells is reflected in Figure 2.2 (Frazer et al., 1991).

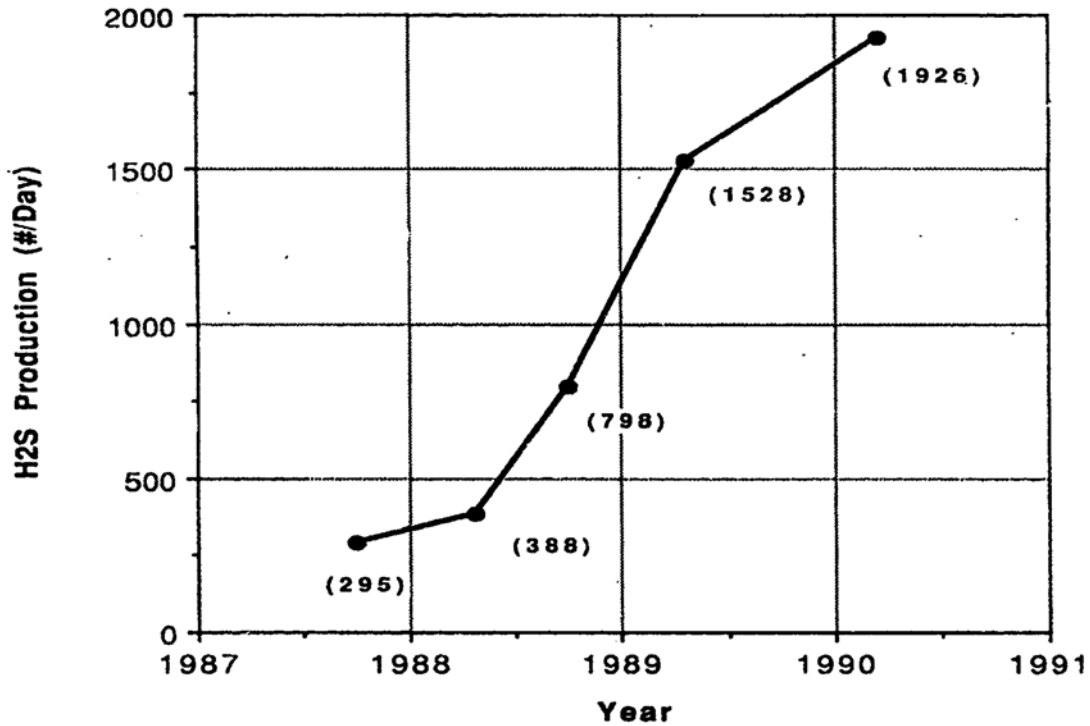


Figure 2.2 Observation of hydrogen sulfide in production wells in Kuparuk field (after Frazer and Boiling, 1991)

2.4.1.1.3 Cultivated SRB Colonies

Bacterial counts have shown the SRB concentration in injected water reached 10^8 per milliliter. Although the biocide treatments are periodically performed in surface facilities, SRB colonies have been grown from reinjected water streams (Frazer et al., 1991).

2.4.1.1.4 Isotopic Analysis

The isotopic signatures of the sulfur in produced fluid (ratios of ^{34}S to ^{32}S) support the microbiological souring mechanism (Frazer et al., 1991).

2.4.1.1.5 Modeling Approach and Assumptions

Frazer and Boiling (1991) developed a hydrogen sulfide forecasting technique for the Kuparuk river field. A brief explanation of the process streams is given in Figure 2.3. At the production facilities, water, oil, and gas are separated. The H_2S , which is produced in the reservoir, is transported to the wellbores by produced water. The produced formation gas and water are reinjected into the reservoir. Seawater is injected as make-up water for pressure support. Additionally, the lift gas is supplied to the wells via a gas lift system. The mixed-produced fluids and lift gas are compressed and separated in production facilities and distributed via a tie-line to the wells.

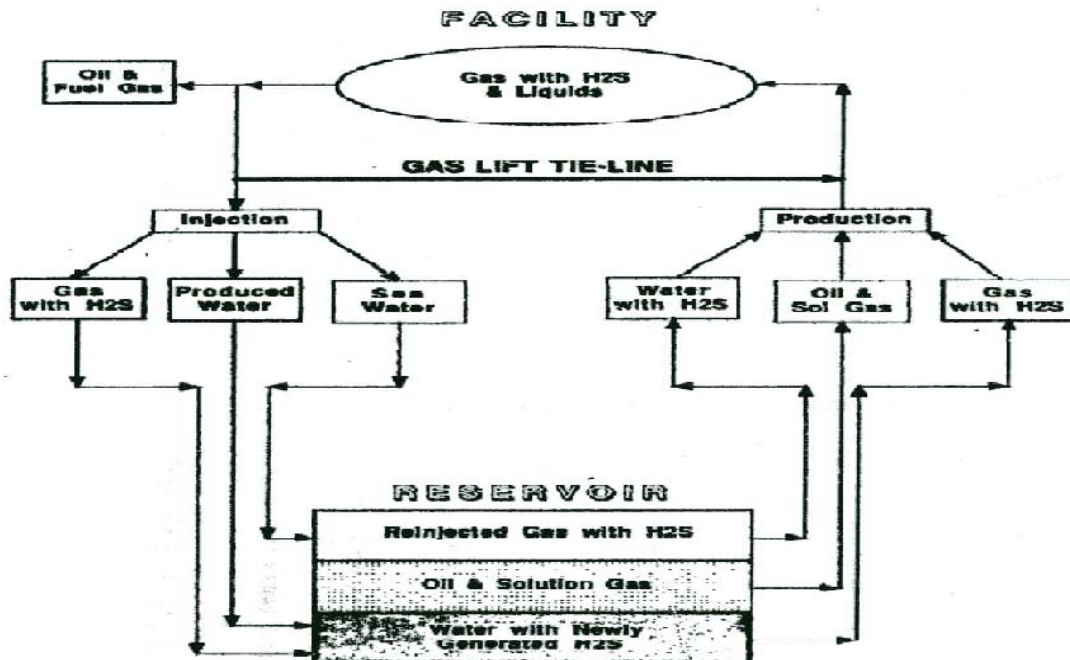


Figure 2.3 Kuparuk river field's forecasting model (after Frazer and Boiling, 1991)

The technique which is used for the modeling of the reservoir souring is to divide the reservoir to three separate continuous stirred tank reactors (CSTRs). One CSTR is considered for reinjected gas, one for oil and solution gas, and one treats the water. Actual injected and produced streams for each phase are the input of the H₂S prediction model for the history-matching purposes. The model assumes a first order biogenic reaction for production of H₂S, which is governed by sulfate concentrations in injection water. In this model, an average sulfate conversion factor of 2%, which is determined by history-matching, is applied to forecast the souring onset (Frazer et al., 1991).

2.4.1.2 Mixing Model

Ligthelm et al. (1991) introduced an analytical model based on biological generation of hydrogen sulfide in an oil reservoir. In this model, it is assumed that formation water is displaced with injection water with constant velocity in one-dimensional porous medium. Due to diffusion and dispersion, a mixing zone will develop between injected and formation water. In this mixing zone, both fatty acid from formation water and sulfate from injected water (and nutrient) for growing of planktonic SRB (free cells) are present and H₂S will be generated. Furthermore, in this model one mole of H₂S is produced from the reaction between one mole of fatty acid and one mole of sulfate under constant temperature and pressure in dilute solutions. Figure 2.4 shows a schematic profile of the concentration changes as assumed in the model.

When there is no reaction, the concentration profiles are described by error function and the developed mixing zone length is of the order $4\sqrt{(Dt)}$ where D is dispersion coefficient and t is the time scale of displacement process. In case of bacterial

reactions, these concentration profiles need to be corrected for the reactions' time-constant τ_b which is inversely proportional to the number of bacteria. The number of bacteria is assumed to be sufficient to make τ_b small compared to the time-scale t of the displacement process.

With this consideration the mixing zone ΔX around any location of X_a is

$$\Delta X = 2\sqrt{(D\tau_b)} \quad (2.1)$$

According to Figure 2.4 the cumulative H_2S produced per unit cross-sectional area in the aqueous phase within the 1D porous medium is proportional to the length of the mixing zone.

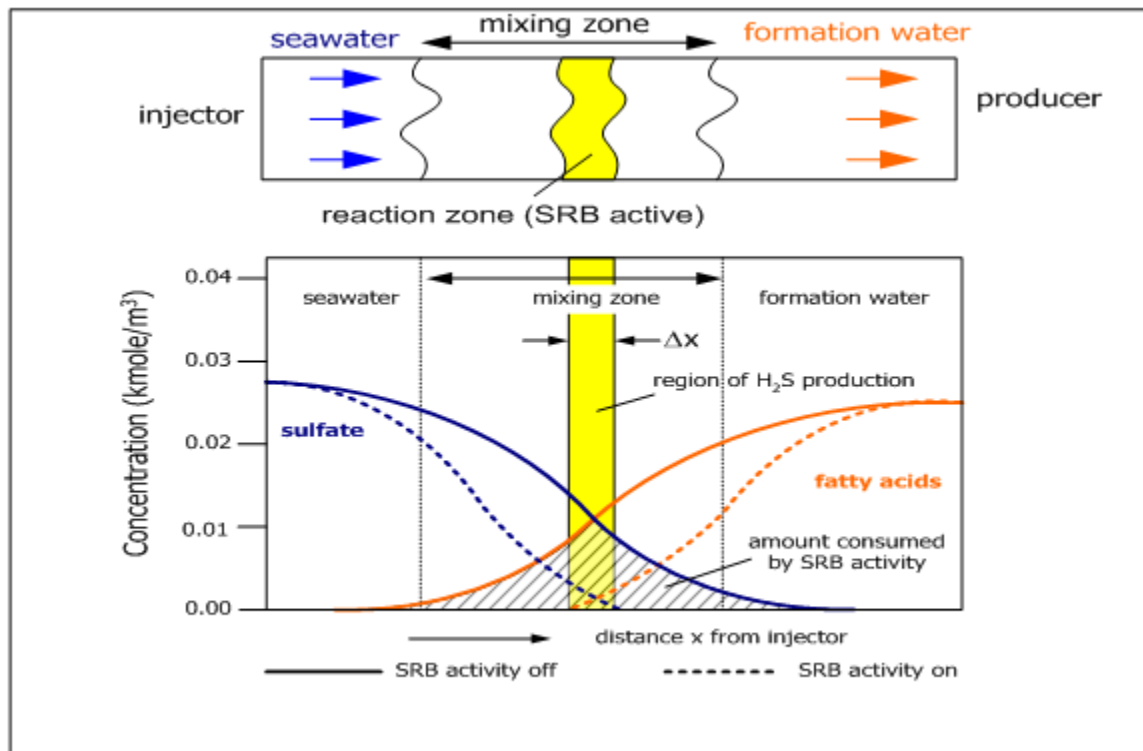


Figure 2.4 Mixing model (after Ligthelm et al., 2001)

$$P = C\sqrt{(Dt)} \quad (kmole / m^2) \quad (2.2)$$

where C is a constant which depends on the initial compositions of sea water and formation water. The total H_2S produced per unit time per unit cross sectional area of aqueous phase bearing pore volume is given by

$$R_H^w \Delta X = \frac{dP}{dt} = \frac{C\sqrt{D}}{2\sqrt{t}} \quad (kmole / m^2 .s) \quad (2.3)$$

And the strength of the H_2S source term

$$R_H^w = \left[\frac{C}{4\sqrt{\tau_b}} \right] \frac{1}{\sqrt{t}} \quad (kmole / m^3 .s) \quad (2.4)$$

The H_2S source moves with the same velocity as water phase and has a constant width ΔX .

In the mixing model, the SRB-generated H_2S is carried along with the water phase. H_2S dissolves in residual oil phase or is scavenged by iron containing minerals. The partitioning of H_2S between flowing water and stagnant oil will retard its arrival relative to water phase. Scavenging of H_2S will lower its concentration and strongly affect the retardation (Ligthelm et al., 1991).

2.4.1.3 Biofilm Model

The biofilm model was developed by Sunde, et al. in 1993. In this model, it is assumed that sessile bacteria which attach to the rock surface near the injection well are the main cause of souring. In other words, in the vicinity of the well there is a biofilm where all nutrients and conditions for the growth of SRB are provided and H_2S is produced only in this region (Figure 2.5).

The biofilm model is a one-dimensional model which is developed based on conservation equations. This model considers bacterial growth rate and includes the

effects of nutrients, water mixing, transport and adsorption of H₂S in the reservoir. The biogenic reaction equation, which is used in this model, includes a mathematical relationship between the initial rate of SRB reaction, the substrate concentration and characteristics of the enzyme. The bacteria growth rate is described by Michaelis-Menten rate expression for enzyme as follows:

$$\mu = \mu_{\max} \left(\frac{C_s}{K_s + C_s} \right) \quad (2.5)$$

In this equation μ , μ_{\max} , C_s , and K_s are specific and maximum growth rate (1/day), substrate concentration, and half-saturation constant of the substrate.

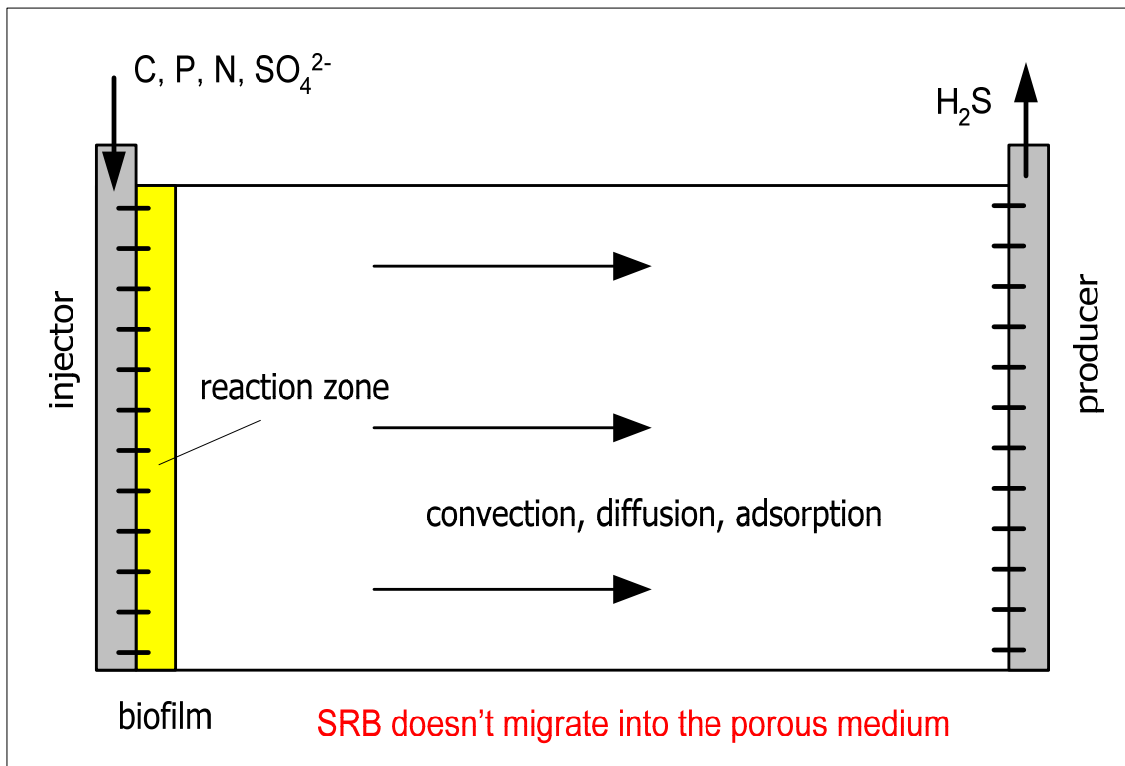


Figure 2.5 Biofilm model (after Sunde et al., 1993)

The constants μ_{\max} and K_s are determined in laboratory with experiments.

In Equation 2.5, two extreme cases can be distinguished. When $C_s \gg K_s$ it represents a zero order reaction, $\mu = \mu_{\max}$, and for the case $C_s \ll K_s$ it shows a first order reaction,

$$\mu = \mu_{\max} \left(\frac{C_s}{K_s} \right) \quad (2.6)$$

When the electron acceptor and nutrient are the limiting reactants, Equation 2.5 is expressed by the following equation:

$$\mu = \mu_{\max} \left(\frac{C_s}{K_s + C_s} \right) \left(\frac{C_A}{K_A + C_A} \right) \left(\frac{C_p}{K_p + C_p} \right) \quad (2.7)$$

where, C_A , C_p represent the concentration of electron acceptor and nutrient and K_A , K_p are their corresponding half saturations.

Although this model considers the effects of concentrations of different species on growth rate of SRB, it does not regard the effects of pressure, temperature and other physical constraints such as salinity and pH on the bacterial growth rate (Sunde et al., 1993).

2.4.1.4 Thermal Viability Shell Model (TVS)

TVS is another reservoir souring prediction model which was developed by Eden, et al. (1992). This model is based on an empirical relation that describes the mesophilic bacteria activities in aqueous environment at North Sea conditions. Experimental data show the consumption of sulfate follows a classic ‘‘S-curve’’ over time for a particular bacteria. The curve lies between lower limit temperature, $T_L=20^\circ\text{C}$ and upper limit temperature, $T_U=50^\circ\text{C}$. This S-curve can be approximated with a trilinear model as

illustrated in Figure 2.6. The slope of the middle line in this trilinear approximation is calculated with statistical techniques. The slope, β , is a function of P in atmosphere and T in $^{\circ}\text{C}$ as defined in the following equation:

$$\beta = 0.6134P - 10.67T_0 - 0.07048PT_0 + 1.476T_0^2 + 0.001015PT_0^2 - 0.0249T_0^3 \quad (2.8)$$

where $\frac{T_0 - 20}{50 - 20} = \frac{T - T_L}{T_U - T_L}$

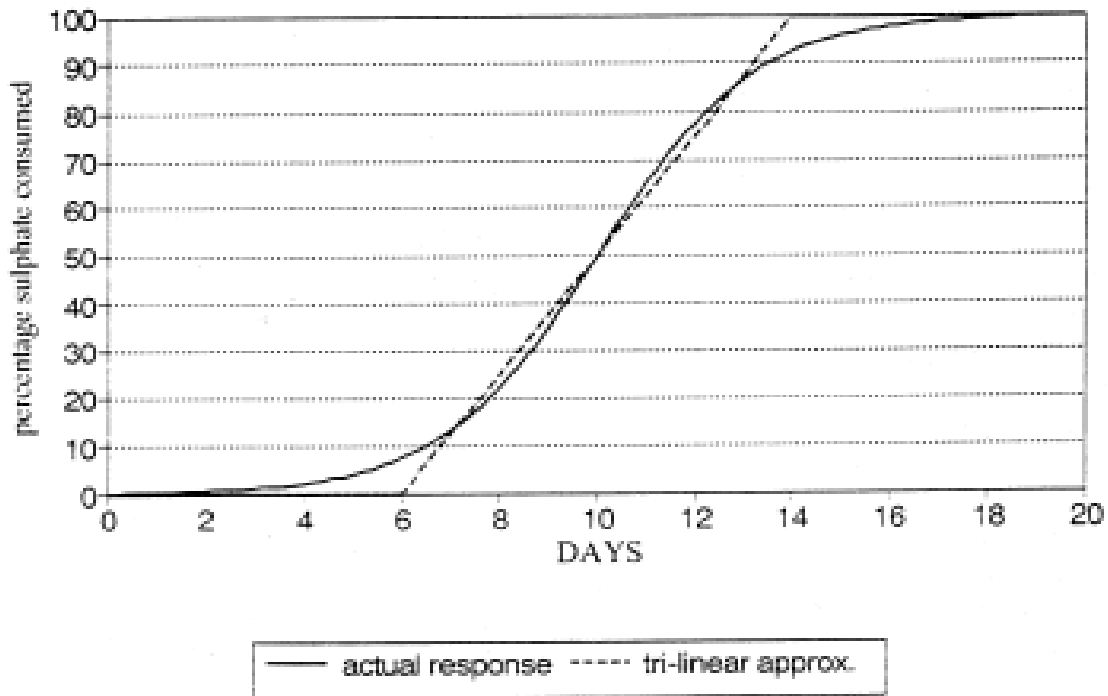


Figure 2.6 S-shape biogenic reduction of sulfate (after Eden et al., 1993)

The β must be set to zero whenever the pressure is so large as to give a negative β or whenever T lies outside the region between T_L and T_U . In this formulation, β , T_L , and T_U stand for the rate of sulfate consumption, lower limit temperature, and upper limit

temperature, respectively. In order to use this model, the pressure and temperature along the reservoir from injector to producer need to be calculated. In the original version of the model, the pressure distribution is assumed a quadratic decay from injector to producer while temperature distribution is based on the method developed by Platenkamp (1985).

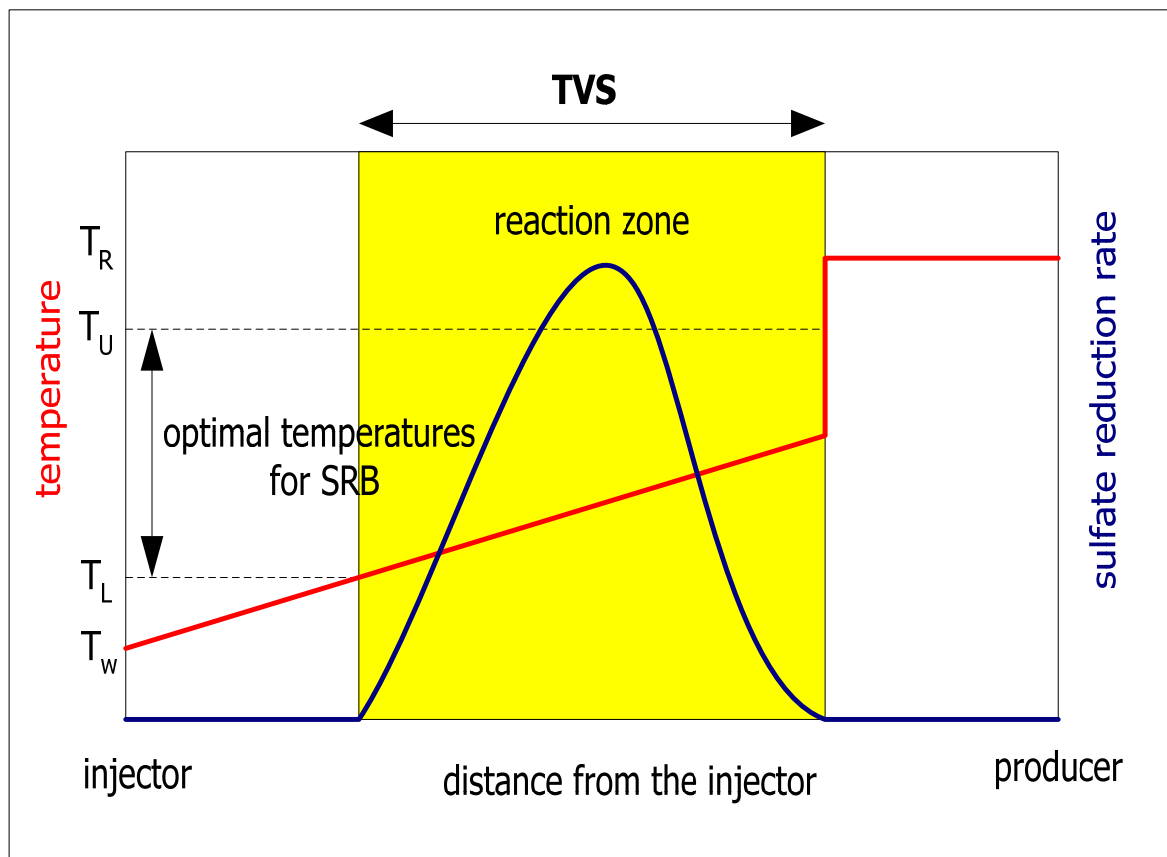


Figure 2.7 TVS model (after Eden et al., 1993)

Inserting calculated temperature and pressure in Equation (2.8) gives the rate of sulfate consumption as a function of time. With the substitution the amount of sulfate consumed per liter by bacterial activity in produced water at any time will be

$$S = \int \beta dt \quad (2.9)$$

In this model the retardation of produced H₂S with respect to water breakthrough in production well is explained by the lag of TVS with respect to injection water front. In Figure 2.7, T_R is reservoir temperature and T_W is the seawater temperature. Actually, in this model the nutrient limiting effect is not considered. Moreover, the partitioning of H₂S into stagnant oil phase and adsorption of H₂S with reservoir rock are not included in TVS model (Eden et al., 1993).

2.4.1.5 Algorithm-Based Models for Prediction of Souring in Fractured Reservoirs

Burger et al. (2004), described a model to predict the reservoir souring in fractured reservoirs. In this model, the reservoir is divided into equal-sized volume elements. These elements have specified porosity and are filled with oil and connate water. In the first step, water flows from the injector to the first element. A volume of water displaces equal volume of hydrocarbon which represents the imbibition of water to the matrix. It is assumed that the imbibition process is complete during the time frame of simulation step. In the next step, a volume of water which is equal to the initial injected water flows to the second element. As a result, some water flows into the matrix and mixes with formation water and displaces an equal volume of this mixture back to the fracture. This sequence is repeated for each time-step until the fluids arrive to the producer.

It is assumed that all of the bacterial reactions take place in the fractures and because of low porosity, bacteria do not enter the matrix. It is also assumed that a portion of the total sulfide produced outside of matrix area is transported to the matrix with the

water flow and a part of this is partitioned between the water and oil, which exist in the matrix. This process continues for each time-step between fracture and matrix (Burger et al., 2005).

2.4.2 In-house Models and Simulators

Several companies developed techniques for prediction of reservoir souring in their own field. For example BP's general purpose reservoir simulator, BPOPE (Alrashedi et al., 1999), Seto and Beliveau (2000) who worked on Caroline field; and Kuijvenhoven et al. (2005) who used an in-house simulator for the reservoir souring mitigation in Bonga field. Furthermore, Amy and Eilen (2000) simulate the reservoir souring under produced water reinjection (PWRI).

2.4.2.1 BPOPE Model

British Petroleum (BP) has used its own general purpose reservoir simulator, BPOPE, to assess the potential of reservoir souring resulting from water injection. The BPOPE simulator is a black oil model that can include the transport of the specific components of each phase in the reservoir as adsorbing or reacting tracers. The simulator also has rock mechanics capability to simulate the thermally induced fracturing.

The forecasting of the hydrogen sulfide production in this model consists of three main processes:

- i) generation,
- ii) transport, and
- iii) natural scavenging.

The generation of hydrogen sulfide in the BPOPE model is based on Arrhenius-type (temperature dependent) reaction between sulfate ions and a generic nutrient. The reaction is assumed to take place in all grid-blocks containing sulfate and nutrient. The result of reaction is the generation of hydrogen sulfide.

For the transportation part, it is assumed that sulfate, nutrient, and hydrogen sulfide are components in the water phase while moving through the reservoir. The model can handle the partitioning of the hydrogen sulfide between phases. The interaction of H₂S with reservoir rock and other phases is considered as a single adsorption process. It is assumed that the adsorption follows Langmuir adsorption isotherm. The history-matching of the results of reservoir souring was used to find a realistic generation rates and parameters of natural scavenging.

2.4.2.2 Seto et al. Model

Seto et al. (2000) presented a mechanism for reservoir souring which is based on the evolution of acid gas from sour aqueous phases in the reservoir. In this mechanism the physical principles of Henry's law govern the solubility of hydrogen sulfide in water. The generation of H₂S in this model is attributed to the sulfate reducing bacteria (SRB). Using material balance analysis and reservoir simulation, the reservoir souring in the Caroline field was studied. The simulation showed that the liberation of hydrogen sulfide from aqueous phase as pressure declines is a novel mechanism for an already soured reservoir.

2.4.2.3 Kuijvenhoven et al. Model

Kuijvenhoven et al. (2005) worked on the Bonga field located in the deep waters of the Nigerian coast. In this field, water is injected extensively for the purpose of pressure support to effectively recover the hydrocarbons. To forecast the reservoir souring in Bonga field, they adapted their in-house reservoir simulator to implement their proposed model. In their model they assumed a combination of mixing and biofilm model.

2.4.2.4 Amy et al. Model

Amy et al., 2000, worked on the process of PWRI hydrogen sulfide forecasting. They used the Sawyer and McCarthy model (1978) to evaluate the initial potential of hydrogen sulfide formation. The Sawyer and McCarthy model is a method based on the biological reaction in which sulfate is the electron acceptor and acetic acid is carbon source. Using this model, it is possible to determine the limiting nutrients. Determining the limiting nutrient for the bacterial growth depends on the water quality compositions, reservoir conditions, the amount of the mixture of produced and seawater.

2.5 Comparison of the Existing Souring Models and In-house Simulators

The following table (Table 2.1) compares the existing reservoir souring models with regards to their biological aspects, dimensionality and transport capabilities. The comparison of the existing models shows that they have some similarities and differences in terms of hydrogen sulfide generation and transportation. These models assume that some kind of SRB is responsible for the generation of hydrogen sulfide and in case of

transport of H_2S , all of them are one-dimensional. The main difference among these models in the case of H_2S generation are their biological capabilities and assumed reaction zones. While there are two extremes between biofilm and mixing zone, wherein the biofilm model the biological species are attached to the rock surface in the vicinity of injection well, and in the mixing model bacteria move with mixing zone. Another aspect of these models is their prediction of the delay in observed H_2S after water breakthrough. In the mixing model, the delay in H_2S observation is explained by oil/water partitioning and adsorption, while in the biofilm model it is explained by only adsorption. In general, the mixing model and biofilm models predict the onset of souring differently. In the mixing model a sharp increase in H_2S is observed and then the peak vanishes (Figure 2.8). While in the biofilm model, after observation of souring, the concentration of H_2S will increase linearly with pore volume injected (Figure 2.9).

As discussed in Chapter 6, after injection of cold seawater to the hot reservoir, due to the heat capacity of the reservoir rock, the temperature propagation has a lag with respect to injection front. The explanation of the delay in H_2S arrival in TVS model is the delay between TVS and injection front. On the other hand, the algorithm-based models describe the delay of arrival of hydrogen sulfide in term of partitioning between phases.

Table 2.2 compares some aspects of in-house reservoir souring simulators. The in-house simulators were design to simulate the process of souring in some specific fields. They have a weak theoretical basis regarding the production and transportation of H_2S in the reservoirs. In other words, these simulators were calibrated for the specific conditions which may differ from one reservoir to another, thus, their results cannot be extended to different conditions.

Table 2.1 Comparison of the existing reservoir souring prediction models

Reservoir souring prediction models		Kuparuk River field	Mixing	Biofilm	TVS	Algorithm-based
Generation of H₂S	SRB type	No preference	Planktonic (free cells)	Sessile (attached cells)	Mesophiles	Sessile (attached cells)
	Biological model	First order reaction	Empirical Time constant	Michaelis-Menten	Empirical rate fitting	Michaelis-Menten
	Reaction zone	Injection Stream	Mixing Zone	Biofilm near injector	TVS	Outside matrix area
	SRB movement	No preference	With mixing zone	Attached to biofilm	Move with TVS	In fractured area
	Temp.	No	No	No	Yes	Yes
	Press.	No	No	No	Yes	No
	Nutrient	No	No	Yes	No	No
H₂S Transport	Dim.	1D	1D	1D	1D	1D
	O/W partition	No	Yes	No	No	Yes
	Ads.	No	Yes	Yes	No	No

Table 2.2 Comparison of in-house reservoir souring prediction simulators

In-house reservoir souring simulators		BPOPE	Amy and Eilen	Seto and Beliveau	Kuijvenhoven et al.
Applied field		North Kuwait	Draugen	Caroline	Bonga
Mechanisms of H ₂ S Generation		Arrhenius- type reaction	Sawyer and McCarthy H ₂ S Generation	Change of H ₂ S Solubility in water with pressure	Mixing and Biofilm model
Transport of H ₂ S	Dim.	--	--	--	---
	O/W partition	Yes	No	Yes	Yes
	Ads.	Yes	No	No	Yes

2.6 Applications and Implications of the Existing Reservoir Souring Models

In previous sections, we discussed the importance of reservoir souring phenomenon and investigated the theoretical basis of the existing reservoir souring prediction models. A knowledge of the timing of the onset of reservoir souring will help operators to devise the methods which prevent the souring and mitigate its consequences. A detail investigation of these models shows that their theoretical basis have some differences and their prediction of the onset of souring will be different. Different

reservoirs have various flow paths which provide distinct residence times and adsorption capacity. Furthermore, the variation in temperature and pressure in the porous media is inevitable and a comprehensive model needs to include these parameters (Okabe and Characklis, 1992; Maxwell and Spark, 2005).

Figures 2.8 and 2.9 show that mixing and biofilm models predict the onset of souring in completely different ways. Comparison of the actual field data show that the onset of souring in some reservoirs can be explained with biofilm model and some other with mixing model (Sunde and Thorstenson, 1993). Experimental data shows that SRB have the characteristics of both sessile and planktonic bacteria and for the permeabilities greater than 100 milli-Darcy they can pass through the porous media (Sunde and Thorstenson, 1992). Hence, these models need to be modified to include both kinds of bacteria which give the models the characteristics of biofilm and mixing models. On the other hand, H_2S is an active component, it reacts with rock surfaces and partitions between oil and water phases. Any predictive model needs to have the capability to include these two phenomena. A comprehensive souring model should have the capability to consider the effects of physical constrains such as temperature, pressure, pH, salinity, geochemical parameters on biological reactions which are responsible for reservoir souring.

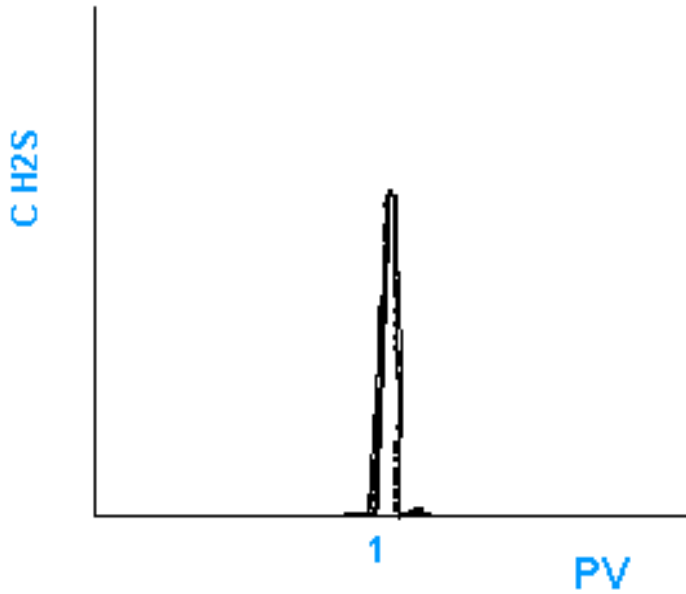


Figure 2.8 Mixing model reservoir souring prediction (after Sunde et al., 1993)

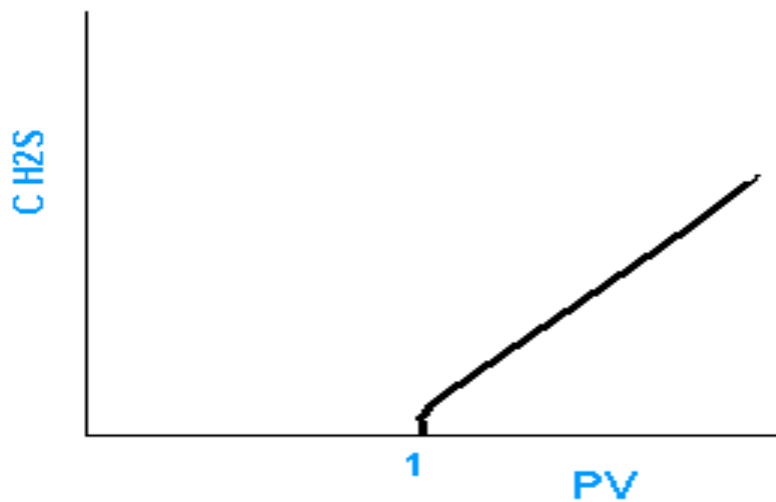


Figure 2.9 Biofilm model reservoir souring prediction (after Sunde et al., 1993)

Another requirement of a comprehensive model is the capability to include the reservoir characteristics such as layering and heterogeneity. For long time injection of seawater, the permeability and porosity alteration also need to be included in the model.

In real reservoirs there is not one-dimensional flow. Comprehensive models must be multi-dimensional and take in to account the generation, partitioning, and adsorption of hydrogen sulfide in different paths.

2.6.1 Effect of Sweep Efficiencies on Prediction of Reservoir Souring

In the following, we discuss the effects of vertical and areal sweep efficiencies on the predicted results of the reservoir souring models. Figure 2.10 illustrates a reservoir with non-communicating layers. From the basic principle of reservoir engineering we know that the displacement of formation water by injection water take place in heterogeneous horizontal layers. With our assumption there is no transmissibility in vertical direction. The concentration of the observed hydrogen sulfide in the producer can be explained by the following equation:

$$C_T = \frac{(kh)_1}{\sum kh} C_1 + \frac{(kh)_2}{\sum kh} C_2 + \dots + \frac{(kh)_N}{\sum kh} C_N \quad (2.10)$$

In this equation, k, h and C are the permeability, height, and the concentration of hydrogen sulfide resulted from each layer when observed in production well, respectively. Figure 2.11 shows a typical history of the expected concentration of hydrogen sulfide with the mixing and biofilm models in a layered reservoir.

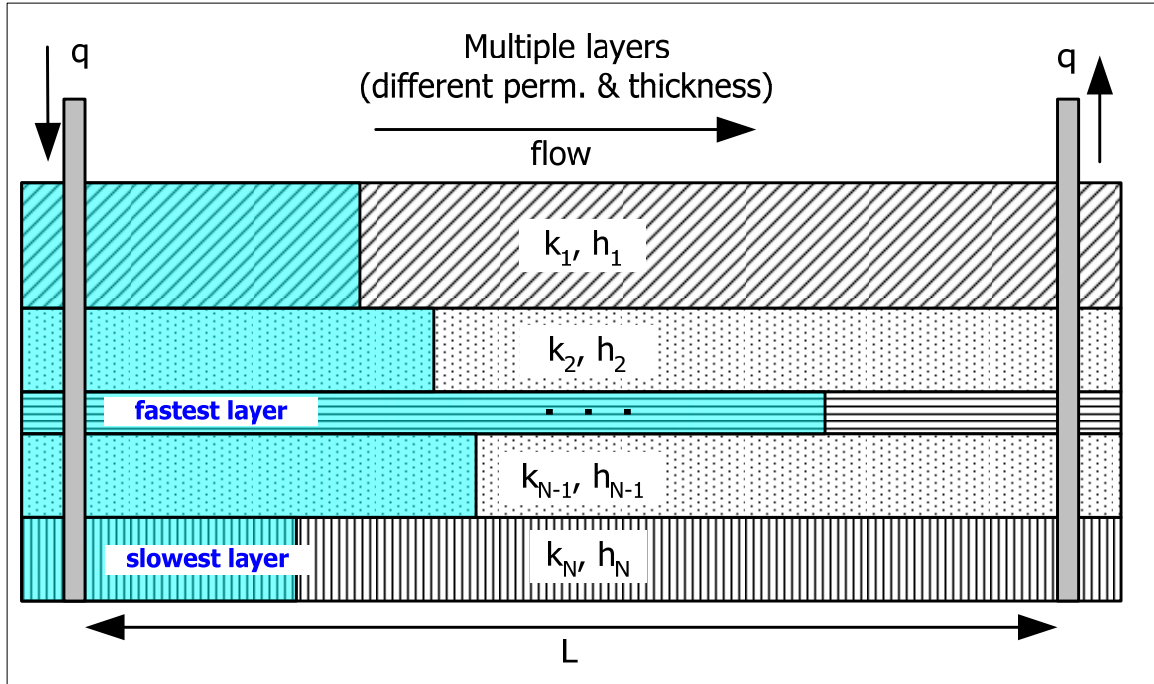


Figure 2.10 Cross section of a stratified reservoir with no vertical communication (after Furui and Bryant, 2005)

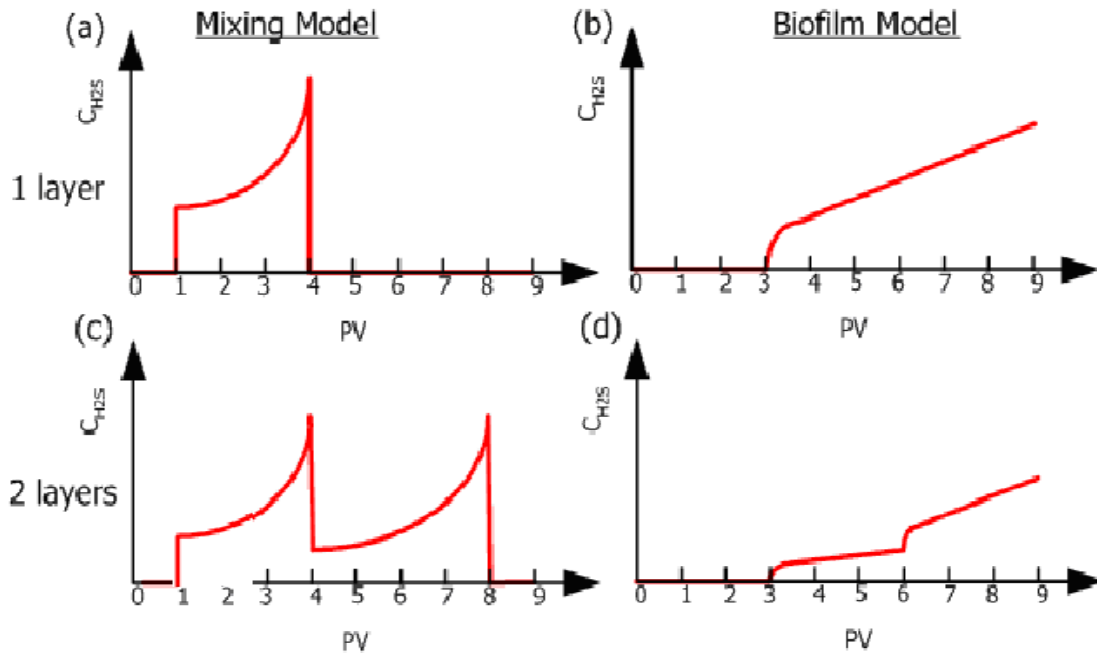


Figure 2.11 Typical H₂S history observed at a production well with mixing and biofilm models in a layered reservoir (after Furui and Bryant, 2005)

In addition to the vertical sweep efficiency, the areal sweep efficiency in the reservoir will affect the forecast of H₂S concentration in the producing well. As illustrated in Figure 2.12, the actual flow path from injector to the producer is more likely radial rather than linear. The shortest streamline will breakthrough first. Consequently, there will be an early breakthrough for water and early observation of souring. Different streamlines provide different residence time for the production of H₂S and also its adsorption on rock surfaces. The observed concentration of H₂S in the produced water will depend on the residence time if the necessary conditions for the SRB activities are provided. Later we will discuss in detail the concentration profile of biogenic hydrogen sulfide generation in the porous media.

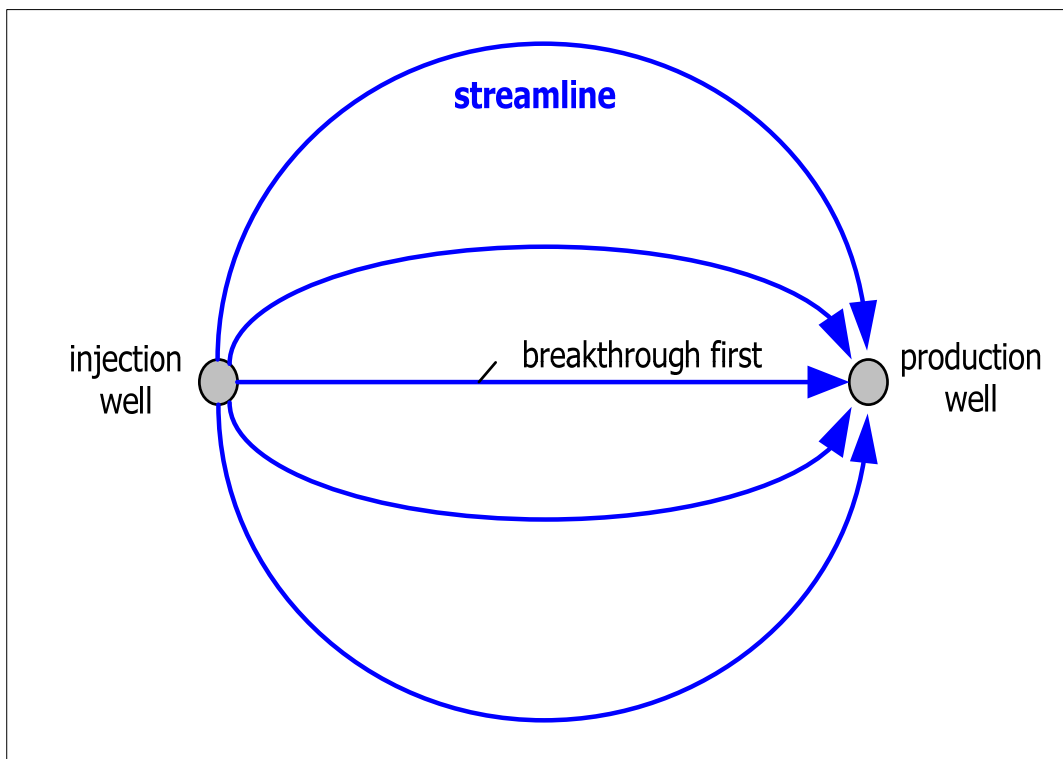


Figure 2.12 Schematic illustration of areal sweep efficiency in a reservoir (after Furui and Bryant, 2005)

2.6.2 Effects of Temperature and Concentration, Reservoir Characteristics and Conditions on the Reservoir Souring Prediction

The effects of temperature profile on reservoir souring prediction have been included in our model which is introduced in Chapter 5. Other models are not able to consider the temperature effects on the reservoir souring. Due to the importance of the temperature propagation in reservoirs, this phenomenon is discussed in detail in Chapter 6. The effects of the available nutrients, retardation factors, and reservoir characteristics and conditions on the process of reservoir souring are also discussed in Chapter 6.

Chapter 3

Problem Statement

3.1 Overview

As we discussed in the previous chapters, reservoir souring is the process of production of hydrogen sulfide in a sea water injected reservoir. Using the knowledge of the mechanisms of generation and transportation of hydrogen sulfide in the reservoir, several reservoir souring models have been developed. The degree of exactness and reliability of these models depend on their capabilities to mimic the essential parameters which determine the generation and transportation of the hydrogen sulfide in the porous media.

Figure 3.1 shows the whole process of reservoir souring. While injecting cold sea water which contains sulfate, nitrate, phosphate, and SRB to the hot formation which provides organic acids, in the presence of SRB, sulfate reacts with organic acids to produce hydrogen sulfide. The produced hydrogen sulfide interacts with rock surfaces and partitions between oil and water phases. The expected concentrations and temperature profiles are shown in Figure 3.2. The temperature distribution ranges from

seawater (T_w) to the reservoir (T_{res}) temperatures. The activities of SRB, which are responsible for souring, depend on the temperature distribution. At low temperatures mesophiles, at high temperatures thermophiles (The dominant SRB type) or hyperthermophiles are activated and the biological reaction between sulfate and organic acids will initiate. Table 3.1 shows the range of activation of the discussed SRB (Sunde et al., 1992; Cord et al., 1987).

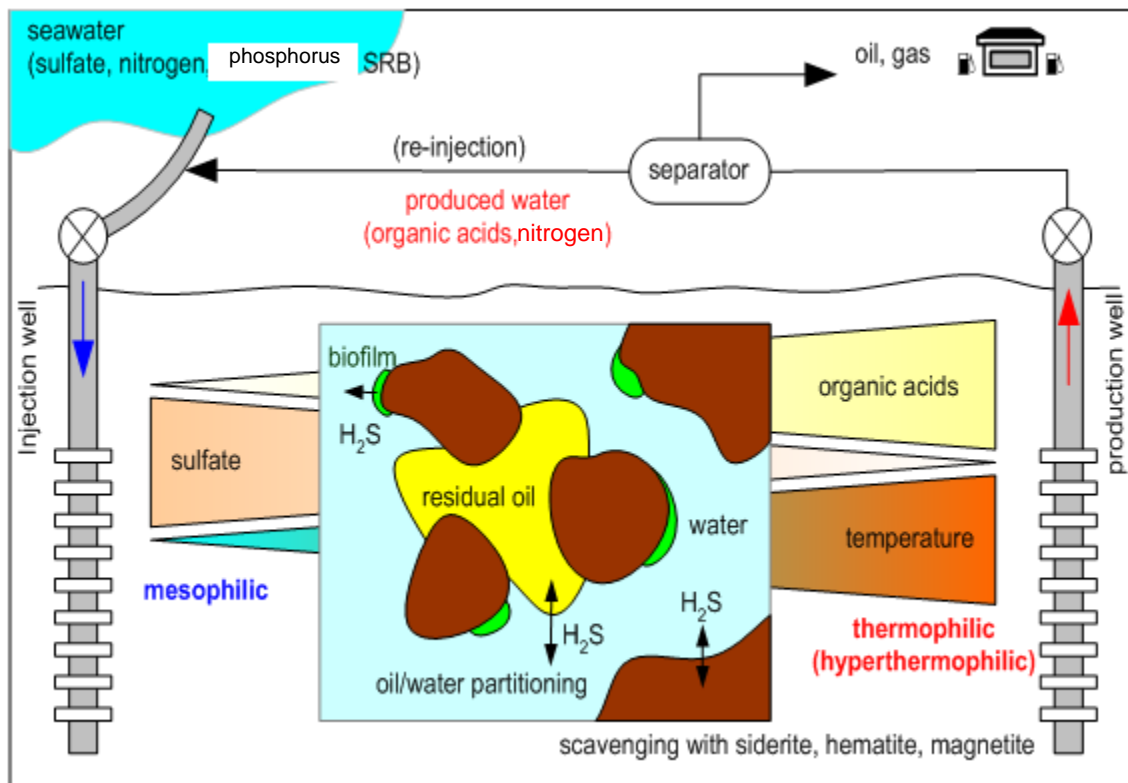


Figure 3.1 Schematic illustration of oil field reservoir souring (Furui and Bryant, 2004)

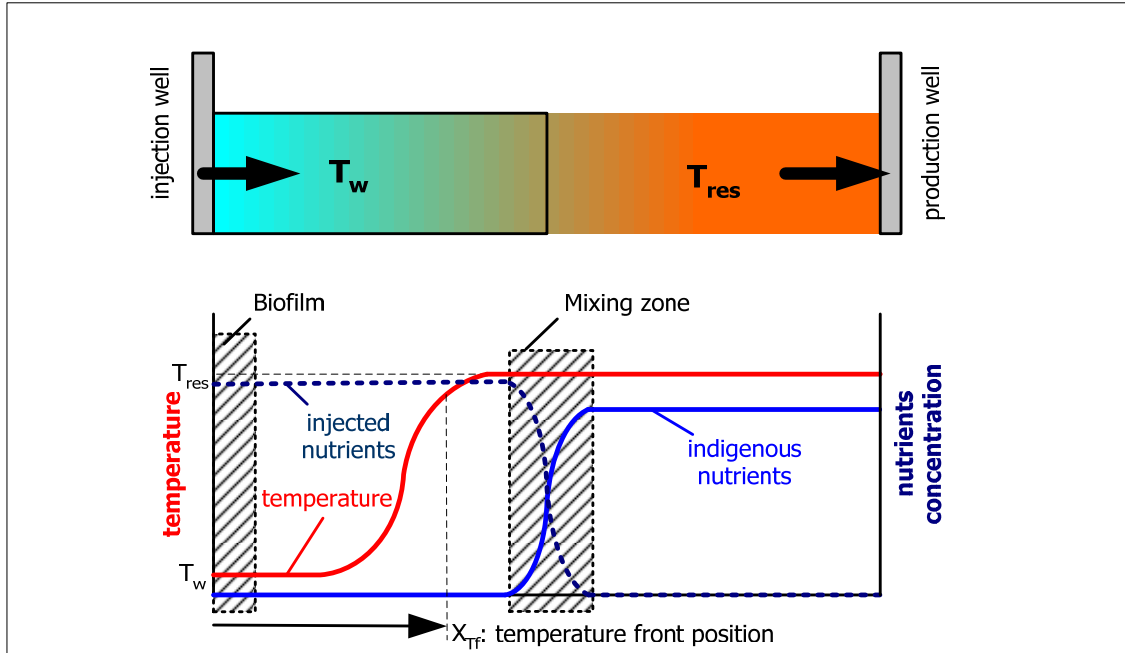


Figure 3.2 Simplified view of concentrations and temperature distributions during water flooding (Furui and Bryant, 2004)

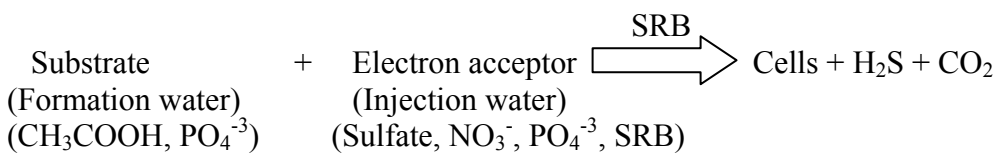
Table 3.1 Activation range of the different SRB types (after Okabe et al., 1992; Leu et al., 1999; Sunde et al., 1992)

SRB Types	Lower limit of activation (°F)	Maximum growth rate Temperature (°F)	Upper limit of activation (°F)
Mesophilic	50	95	109
Thermophilic	100	145	170
Hyper thermophilic	163	203	219

3.2 Modeling and Simulation of the Reservoir Souring Process

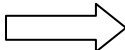
Modeling and simulation of the reservoir souring can be summarized in two processes as shown below:

3.2.1 Biological Reactions Produce Hydrogen Sulfide



In this reaction the organic acid in formation water is provided by residual oil.

3.2.2 Retardation Slows the Hydrogen Sulfide Migration

Partitioning and Interaction with rock surfaces  Delay in observed souring

A comprehensive predictive model should have the capabilities to describe the mechanisms of generation and transportation of hydrogen sulfide under different reservoir conditions and characteristics.

3.3 Model Development

In order to develop a comprehensive model, several steps were followed, as shown in Figure 3.3. First, we studied the reservoir souring in detail regarding the generation and transportation of hydrogen sulfide in porous media. Then, we performed a critical review of the published models on reservoir souring. The evaluation of the capabilities of the published models in simulation of the generation and transportation of hydrogen sulfide in porous media, were the key points which lead us to a more comprehensive model. With this knowledge, we introduced a new model which has more capabilities in simulating the generation and transportation of hydrogen sulfide in porous media.

Model Development

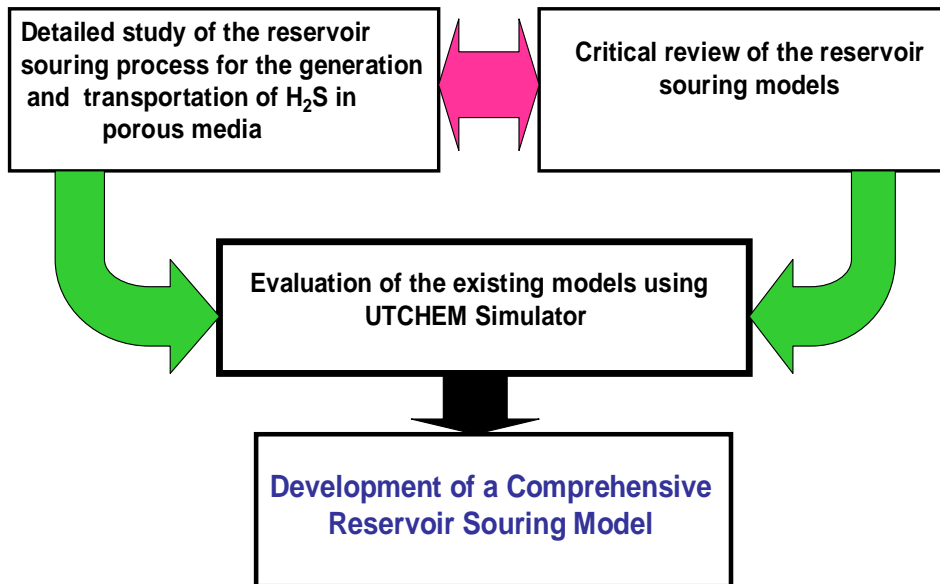


Figure 3.3 Development of a comprehensive reservoir souring model

Chapter 4

Review of UTCHEM Simulator for the purpose of reservoir souring prediction

UTCHEM is a multicomponent, multiphase, and 3-dimensional finite difference simulator. UTCHEM was originally developed at The University of Texas at Austin to simulate the enhanced oil recovery processes which use surfactants and polymers. In the development of this simulator, advanced concepts in higher order numerical accuracy were used (UTCHEM technical documentation, 2000).

4.1 Mass and Energy Balances

In this section, the model formulation for a typical water injection is described. The balance equations in terms of injection of water, biological production of hydrogen sulfide, partition of hydrogen sulfide between oil and water phases and adsorption of hydrogen sulfide by rock surfaces are presented in this section.

4.1.1 Mass Conservation Equations

The assumptions imposed in developing the flow equations are: local thermodynamic equilibrium, immobile solid phases, slightly compressible rock and fluids, Fickian dispersion, ideal mixing, and Darcy's law for the flow in porous media.

Equations 4.1-4.21 below are reproduced from the UTCHEM technical manual (Delshad, Pope and Sepehrnoori 1995; UTCHEM technical manual, 2000).

The continuity of mass in terms of overall volume of component κ per unit pore volume (\tilde{C}_κ) and the above assumptions lead us to the following equation:

$$\frac{\partial}{\partial t} (\phi \tilde{C}_\kappa \rho_\kappa) + \bar{\nabla} \cdot \left[\sum_{\ell=1}^{n_p} \rho_\kappa (C_{\kappa\ell} \bar{u}_\ell - \bar{D}_{\kappa\ell}) \right] = R_\kappa \quad (4.1)$$

where the overall volume of component κ per unit pore volume is the sum of over all phases which include the adsorbed phases:

$$\tilde{C}_\kappa = \left(1 - \sum_{\kappa=1}^{n_{cv}} \hat{C}_\kappa \right) \sum_{\ell=1}^{n_p} S_\ell C_{\kappa\ell} + \hat{C}_\kappa \quad \text{for } \kappa = 1, \dots, n_{cv} \quad (4.2)$$

n_{cv} is the total number of volume-occupying components such as water, oil, surfactant and air. n_p is the number of phases; \hat{C}_κ is the adsorbed concentration of species κ , ρ_κ is the density of pure component κ at a reference pressure P_R relative to its density at reference pressure P_{R_0} , $\rho_{\kappa 0}$ is the density of pure component κ at a reference pressure P_{R_0} .

We propose ideal mixing and small and constant compressibility C_κ^0 .

$$\rho_\kappa = \rho_{\kappa 0} (1 + C_\kappa^0 (P_R - P_{R_0})) \quad (4.3)$$

The assumed form of Fickian dispersive flux is:

$$\bar{D}_{\kappa\ell, x} = \phi S_\ell \bar{K}_{\kappa\ell} \bar{\nabla} C_{\kappa\ell} \quad (4.4)$$

The dispersion tensor $\bar{K}_{\kappa\ell}$ which includes molecular diffusion ($D_{\kappa\ell}$) are calculated by the following equation:

$$\vec{\bar{K}}_{\kappa\ell ij} \equiv \frac{D_{\kappa\ell}}{\tau} \delta_{ij} + \frac{\alpha_{T\ell}}{\phi S_{\ell}} \frac{|\vec{u}_{\ell}|}{|\vec{u}_{\ell}|} \delta_{ij} + \frac{(\alpha_{L\ell} - \alpha_{T\ell})}{\phi S_{\ell}} \frac{u_{\ell i} u_{\ell j}}{|\vec{u}_{\ell}|} \quad (4.5)$$

where $\alpha_{L\ell}$ and $\alpha_{T\ell}$ are longitudinal and transverse dispersivities of phase ℓ ; τ is the tortuosity factor; $u_{\ell i}$ and $u_{\ell j}$ are the components of Darcy flux of phase ℓ in direction i and j ; δ_{ij} is the Kronecker delta function. The magnitude of vector flux for each phase is calculated as

$$|\vec{u}_{\ell}| = \sqrt{(u_{x\ell})^2 + (u_{y\ell})^2 + (u_{z\ell})^2} \quad (4.6)$$

where the phase flux from Darcy's law is

$$\vec{u}_{\ell} = -\frac{k_{r\ell} \vec{\bar{k}}}{\mu_{\ell}} (\vec{\nabla} P_{\ell} - \gamma_{\ell} \vec{\nabla} h) \quad (4.7)$$

$\vec{\bar{k}}$ is the intrinsic permeability tensor and h is the vertical depth. Relative permeability $k_{r\ell}$, viscosity μ_{ℓ} , and specific weight γ_{ℓ} for phase ℓ are defined in the following.

The source term R_{κ} is a combination of all rate terms which can be expressed as:

$$R_{\kappa} = \phi \sum_{\ell=1}^{n_p} S_{\ell} r_{\kappa} + (1-\phi) r_{\kappa S} + Q_{\kappa} \quad (4.8)$$

where Q_{κ} is the injection/production rate for component κ per bulk volume; $r_{\kappa\ell}$ and $r_{\kappa S}$ are the reaction rates for component κ in phase ℓ and solid phases respectively.

For fluxes in y and z directions the analogous equations are applied.

4.1.2 Energy Conservation Equation

In the derivation of the energy balance equation, we assume that energy is only a function of temperature and energy flux in the aquifer or reservoir occurs by advection and conduction. With these assumptions the energy balance equation can be written as follows:

$$\frac{\partial}{\partial t} \left[(1-\phi)\rho_s C_{vs} + \phi \sum_{\ell=1}^{n_p} \rho_{\ell} S_{\ell} C_{v\ell} \right] T + \bar{\nabla} \cdot \left(\sum_{\ell=1}^{n_p} \rho_{\ell} C_{p\ell} \bar{u}_{\ell} T - \lambda_T \bar{\nabla} \cdot T \right) = q_H - Q_L \quad (4.9)$$

In this equation, T is the reservoir temperature; C_{vs} and $C_{v\ell}$ are the rock and phase ℓ heat capacities at constant volume; $C_{p\ell}$ is the phase ℓ heat capacity at constant pressure; and λ_T is the thermal conductivity. q_H is the enthalpy source term per bulk volume. Q_L , the heat loss to overburden and underburden formations, is computed using the Vinsome and Westerveld (1980) heat loss method.

4.1.3 Pressure Equation

The pressure equation is obtained by substituting Darcy's law for the phase flux terms and summing the mass balance equations over all volume-occupying components.

Using the definition of capillary pressure and noting that $\sum_{\kappa=1}^{n_{cv}} C_{\kappa\ell} = 1$, the pressure equation

in terms of the reference phase pressure (phase1) is

$$\phi C_t \frac{\partial P_1}{\partial t} + \bar{\nabla} \cdot \bar{k} \cdot \lambda_{rTC} \bar{\nabla} P_1 =$$

$$-\bar{\nabla} \cdot \sum_{\ell=1}^{n_p} \bar{k} \cdot \lambda_{r\ell c} \bar{\nabla} h + \bar{\nabla} \cdot \sum_{\ell=1}^{n_p} \bar{k} \lambda_{r\ell c} \bar{\nabla} P_{c\ell 1} + \sum_{\kappa=1}^{n_{cv}} Q_{\kappa} \quad (4.10)$$

where, $\lambda_{r\ell c} = \frac{k_{r\ell}}{\mu_{\ell}} \sum_{\kappa=1}^{n_{cv}} \rho_{\kappa} C_{\kappa\ell}$ and $\lambda_{rTC} = \sum_{\ell=1}^{n_p} \lambda_{r\ell c}$.

C_t , the total compressibility is the volume-weighted sum of the rock or soil matrix (C_r)

and component (C_{κ}°) compressibilities:

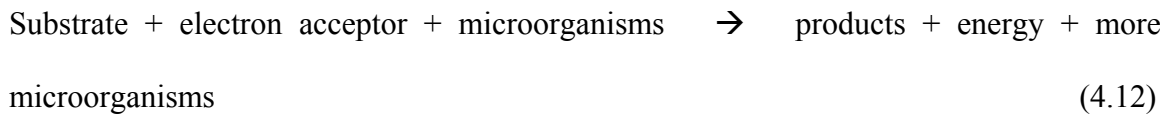
$$C_t = C_r + \sum_{\kappa=1}^{n_{cv}} C_{\kappa}^{\circ} \tilde{C}_{\kappa} \quad (4.11)$$

where,

$$\phi = \phi_R \left[1 + C_r (P_R - P_{R0}) \right]$$

4.2. Biodegradation Reactions

A biodegradation reaction is an oxidation-reduction reaction between electron acceptor and a substrate (electron donor). This reaction is happen in the presence of a microorganism's enzymes. A typical biodegradation reaction is considered as the following equation:



4.2.1 Mathematical Model Formulation

The UTCHEM biological model (the conceptual model is provided in Figure 5.1) was developed based on the following assumptions:

the UTCHEM model utilizes the Molz et al. (1986) model to accommodate an unlimited number of biological reactions among the species. Substrate can be biodegraded by either free-floating or attached microorganisms at different rates. The biodegradation equations are solved separately from the flow system. Where, in each gridblock, in each time-step after calculation of concentrations, the following six simultaneous ordinary differential equations are solved in a separate subroutine.

The following equations illustrate the UTCHEM biological model (de Blanc, 1996; UTCHEM technical manual) when they are simplified to apply to a system of a single substrate, electron acceptor and biological species:

$$\frac{dS}{dt} = -\frac{\beta\kappa\bar{X}}{m_c}(S - \bar{S}) - \frac{\mu_{\max}X}{Y}\left(\frac{S}{K_S+S}\right)\left(\frac{A}{K_A+A}\right) - K_{\text{abio}}S \quad (4.13)$$

where in the right hand side of this reaction, the first term is reaction of substrate in attached biomass, the second term is the reaction of substrate in free cells, and the third term considers the possible abiotic reaction of consumption of substrate.

$$\frac{d\bar{S}}{dt} = \frac{\beta\kappa}{V_c}(S - \bar{S}) - \frac{\mu_{\max}\rho X}{Y}\left(\frac{\bar{S}}{K_S+\bar{S}}\right)\left(\frac{\bar{A}}{K_A+\bar{A}}\right) - K_{\text{abio}}\bar{S} \quad (4.14)$$

$$\frac{dA}{dt} = -\frac{\beta\kappa\bar{X}}{m_c}(A - \bar{A}) - \frac{\mu_{\max}XE}{Y}\left(\frac{S}{K_S+S}\right)\left(\frac{A}{K_A+A}\right) \quad (4.15)$$

$$\frac{d\bar{A}}{dt} = -\frac{\beta\kappa}{V_c}(A - \bar{A}) - \frac{\mu_{\max}\rho_X E}{Y} \left(\frac{\bar{S}}{K_S + \bar{S}} \right) \left(\frac{\bar{A}}{K_A + \bar{A}} \right) \quad (4.16)$$

$$\frac{dX}{dt} = \mu_{\max} X \left(\frac{S}{K_S + S} \right) \left(\frac{A}{K_A + A} \right) - bX \quad (4.17)$$

$$\frac{d\bar{X}}{dt} = \mu_{\max} \bar{X} \left(\frac{\bar{S}}{K_S + \bar{S}} \right) \left(\frac{\bar{A}}{K_A + \bar{A}} \right) - b\bar{X} \quad (4.18)$$

4.3 Simplification of the General Mass Balance Equation for the Reservoir Souring Process in a Typical Seawater Injected Reservoir

Regarding the general mass balance Equation 4.1, we can determine the number of components, phases and other parameters which are essential in the souring phenomenon as follows:

κ = species; 1= water, 2= oil, 3-8 reserved for chemical flooding, 9= hydrogen sulfide 10= acetate, 11= sulfate, 12= SRB, 13= carbon dioxide, 14= nitrate, 15= phosphate

n_p = number of phases; 1= water, 2=oleic, 3=stagnant

n_{CV} = volume occupying species ; 1=water, 2=oil

\bar{u}_l = Darcy flux of phase ℓ , Lt^{-1}

$C_{\kappa\ell}$ = concentration of species κ in phase ℓ , $\frac{L^3}{L^3}$; $\kappa=1$ to 15; $\ell=1,2$

$\bar{D}_{\kappa\ell}$ = Dispersion flux of species κ in phase ℓ ; $\kappa=1$ to 15; $\ell=1,2$

R_κ = total source/sink species κ , $mL^{-3}t^{-1}$, $\kappa=1$ to 15

In reservoir souring, we need to consider injection, production, partitioning and adsorption of the engaged components. Particularly, we must consider the partition of H_2S between oil and water phases and also adsorption of H_2S on rock surface.

s_ℓ = saturation of phase ℓ , L^3/L^3 PV, $\ell = 1, 2$

\hat{C}_κ = adsorption concentration of species κ , L^3/L^3 PV; in our case H_2S .

ρ_κ = density of species κ at P_R relative to its density at 1 atm, m/L^3

$r_{\kappa\ell}$ = reaction rate for species κ in phase ℓ , $mL^{-3}t^{-1}$

In this case: Biological reactions of:

sulfate in water phase,

carbon source in water phase,

nitrate in water phase,

phosphate in water phase

$r_{\kappa S}$ = reaction rate for species κ in solid phase, $mL^{-3}t^{-1}$;

In this case adsorption of H_2S on rock surface

Q_κ = source/sink for species κ per bulk volume, L^3t^{-1}/L^3

In this case :

Injection of water, sulfate, phosphate, nitrate and bacteria

Production of water, sulfate, phosphate, nitrate, bacteria, and H_2S

4.3.1 Biological Reactions

If we ignore the external mass transport from bulk flow to the rock surfaces (this means that there is no resistance for the species to move from bulk flow to the attached cells) the system of six equations (Equations 4.12- 4.17) will reduce to Equation 4.17. As a result the attached and free cells behave similar to each other and a single equation each for loss of the substrate and electron acceptor is needed:

$$\frac{dS}{dt} = -\frac{\mu_{\max}X}{Y} \left(\frac{S}{K_S+S} \right) \left(\frac{A}{K_A+A} \right) - K_{\text{abio}}S \quad (4.19)$$

$$\frac{dA}{dt} = -\frac{\mu_{\max}XE}{Y} \left(\frac{S}{K_S+S} \right) \left(\frac{A}{K_A+A} \right) \quad (4.20)$$

where X is the concentration of biomass and all other concentrations are aqueous phase concentrations (de Blanc 1996, UTCHEM technical manual, 2000).

When nutrients such as nitrogen and phosphorous limit the reaction, the substrate utilization is modified to the following equation:

$$r_S = \frac{dS}{dt} = -\frac{\mu_{\max}X}{Y} \left(\frac{S}{K_S+S} \right) \left(\frac{A}{K_A+A} \right) \left(\frac{N}{K_N+N} \right) \quad (4.21)$$

r_S = rate of substrate utilization ($ML^{-3}T^{-1}$)

N = concentration of a limiting nutrient (ML^{-3})

K_N = limiting nutrient half saturation coefficient concentration (ML^{-3})

4.3.2 Adsorption

In UTCHEM, the adsorption capacity of a component on the formation rock surface is defined as grams of the adsorbed component to the gram of rock (a_T). D_s , the

retardation factor parameter, is the ratio of the average concentration of the adsorbed component to its concentration in the flowing phase, as expressed in Equation 4.21:

$$D_s = \frac{\bar{C}_T}{C_{T\ell}} = \frac{(1 - \phi)\rho_r a_T}{\phi\rho_\ell C_{T\ell}} \quad (4.22)$$

The retardation due to adsorption is formulated as follows (UTCHEM Technical documentation, 2000):

$$RET=1+ D_s .$$

\bar{C}_T = average adsorbed concentration, $C_{T\ell}$ = flowing concentration in phase ℓ ,
 a_T = microgram adsorbed/gram rock, ρ_ℓ = density of flowing phase, ML^{-3} , ρ_r = rock density,
 ML^{-3} , ϕ = porosity.

Chapter 5

Model Development

This chapter introduces a multi-dimensional module for the prediction of the hydrogen sulfide onset in seawater-injected reservoirs. The developed module was implemented in The University of Texas at Austin chemical flooding simulator, UTCHEM. The results of the developed model and simulator for predicting the reservoir souring in seawater-injected reservoirs are provided in the next chapter.

5.1 Introduction

In order to use UTCHEM for reservoir souring prediction, some parts of the code related to the biological option were modified (Appendix B). As described previously, with these modifications the basic concepts of the souring process regarding the generation and transportation of the hydrogen sulfide can be expressed with UTCHEM. The BIO option of the simulator was used to simulate the biogenic production of H₂S. The transport of this component was formulated by using the tracer option, which has the capability of including the retardation factor. In UTCHEM, retardation is due to the adsorption and/or partitioning behaviors of components while moving in porous media

(UTCHEM Technical documentation, 2000). In the following sections, we introduce the step of model development, conceptual model of souring in UTCHEM, and a comparison of the advantages of the developed model with the previous models.

5.2 Conceptual Model of Souring

Figure 5.1 represents the conceptual model of the biodegradation process, which is used in UTCHEM. In the developed simulator, substrate concentrations can change in each gridblock. SRB can attach to the rock surfaces (biofilm). They can also remain in aqueous phase. Thus, we accounted for both attached (sessile) and free-floating (planktonic) bacteria reactions. The temperature ranges from seawater (injected fluid) to reservoir temperature. The pressure also changes between injectors and producers. In Figure 5.2, S represents substrate molecules in the bulk liquid that must diffuse across a stagnant liquid layer to become available to attached biomass (biofilm and sessile bacteria). The subscript f refers to intra-biomass concentration.

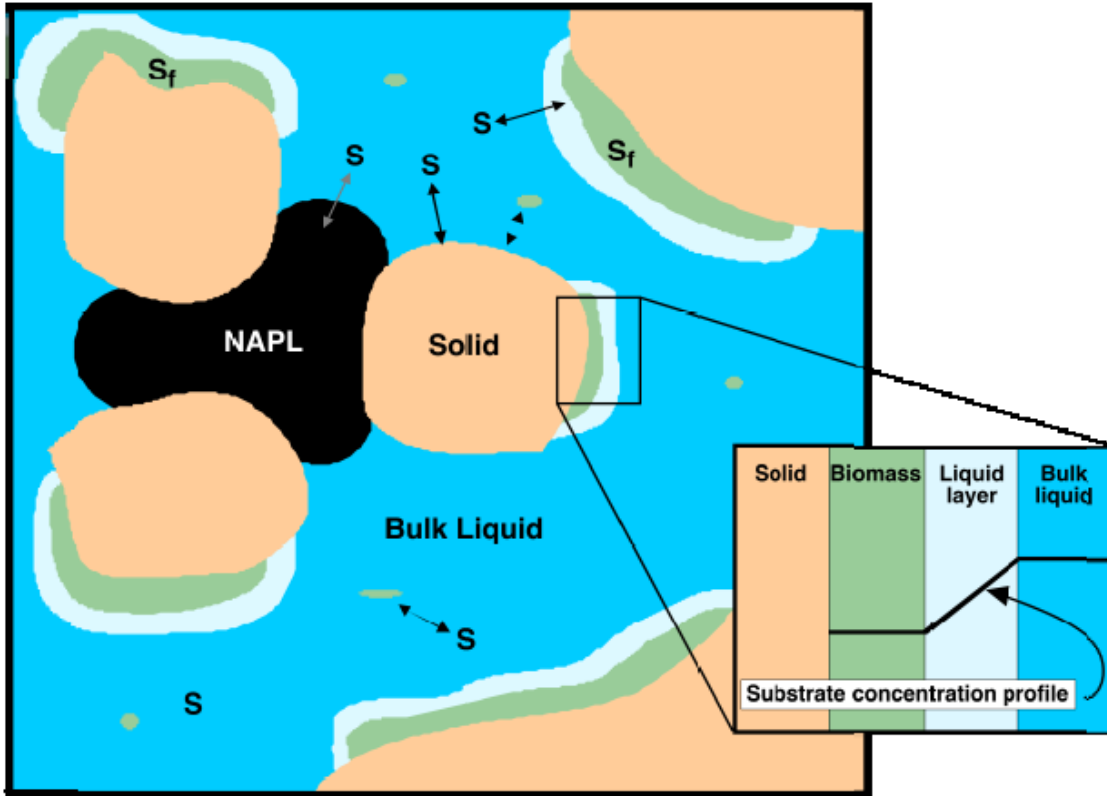


Figure 5.1 Conceptual model of souring process in UTCHEM

In order to investigate the temperature effect on the biological reactions, it is assumed that in each gridblock the reactions would occur only if the temperature in that gridblock was in the range suitable for the growth of the specific biological species.

The multi-dimensional reservoir souring simulator has the capability to include the heterogeneity and changes in the concentrations and temperatures within the reservoir. Furthermore, the partitioning and adsorption of H_2S while moving in the reservoir is also included.

5.3 Stoichiometry of the Reactions

The bio-reaction of hydrogen sulfate generation is identified as



The growth of SRB for the generation of biomass depends on carbon (C), nitrogen (N) and phosphorus (P). It also needs energy, which is provided from carbon (C) and sulfate (SO₄) sources. In this reaction, it is assumed that approximately 90% of C is consumed for respiration and the remaining 10% moves to the biomass structure. In the biomass structure, it is assumed that the mass ratio of C, N and P are 82%, 14%, and 4%, respectively (Sunde et al., 1993).

For organic carbon, there is a range of volatile fatty acids present in formation brine. The species with maximum availability (over 80%) is acetate, with a molecular weight of 60 g/g-mole (Eden et al., 1993).

5.4 Partitioning

Partitioning of a component between two phases is modeled using a K-factor approach, which asserts that the ratio of component concentrations in the two phases is constant. There are two definitions for the partitioning of components between phases. The first definition is the molar concentration (mole/L³) of a component in oil phase divided by its molar concentration to water phase ($K_H^{ow} (molar) = \frac{C_{T,Oil}}{C_{T,Water}}$). The second definition is the ratio of the mass concentration (mass/L³) of the component in oil phase to that in water phase ($K(mass) = \frac{C_{T,Oil}}{C_{T,Water}}$).

For the first definition, the retardation factor due to partitioning is defined using the following equation:

$$A_1 = 1 + K_H^{ow} \frac{\rho_o M_w S_o}{\rho_w M_o S_w} \quad (5.2)$$

The second definition, used in UTCHEM, is expressed as follows:

$$A_2 = 1 + \frac{C_{T_2}}{C_{T_1}} \quad (5.3)$$

where,

A_1, A_2 = retardation factor, ρ_o = density of oil, ML^{-3} , ρ_w = density of water, ML^{-3} , M_w = molecular weight of water, M_o = molecular weight of oil, S_o = oil saturation, S_w = water saturation, $C_{T\ell}$ = flowing concentration in phase ℓ .

For H_2S , the partitioning constant (K or K_H^{ow}) is a function of temperature but only depends weakly on pressure (Ligthelm et al., 1991; Eden et al., 1993).

5.5 Adsorption

The capacity of adsorption of a component in the reservoir rock is defined as grams of the adsorbed component to the gram of rock (α_T) which depends on the reservoir rock and the concentration of the component present. D_s , the retardation factor parameter, is the ratio of the average concentration of the adsorbed component to its concentration in the flowing phase, as expressed in Equation 5.4:

$$D_s = \frac{\bar{C}_T}{C_{T\ell}} = \frac{(1 - \phi)\rho_r a_T}{\phi \rho_\ell C_{T\ell}} \quad (5.4)$$

The retardation due to adsorption is formulated as follows:

$$RET = 1 + D_s \quad (5.5)$$

where,

\bar{C}_T = average adsorbed concentration, $C_{T\ell}$ = flowing concentration in phase ℓ , a_T = microgram/gram rock, ρ_ℓ = density of flowing phase, ML^{-3} , ρ_r = rock density, ML^{-3} , ϕ = porosity.

The factor D_s is dependent upon the temperature, and also depends strongly on the capacity of the rock to adsorb the hydrogen sulfide. The retardation factor due to adsorption can range into the thousands due to different rock compositions (Ligthelm, et al., 1991; UTCHEM Technical documentation, 2000).

5.6 Material and Energy Balances

The governing equations of overall mass and energy balance, as stated in the UTCHEM Technical Manual (2000), are given in Chapter 4. The model uses the same general material balance approach with appropriate biological reaction for the generation term.

5.7 Simulation of the Reservoir Souring in UTCHEM

In the simulation process, UTCHEM first solves implicitly for pressure distribution. Then the concentration profiles are solved explicitly. After solving the energy balance equations, the biological reactions which generate H₂S are handled. The system of ordinary differential equations, which describes the reaction rate for each species, is solved in each time-step for every gridblock. In fact, the reaction term in general mass balance equation is replaced by the biological reaction which adjust the new concentration for reacting species.

In the following sections, we describe the souring process and behavior of hydrogen sulfide in the porous media, the simulator options, and our approach toward the simulation process.

5.8 Advantages of Developed Model versus Previous Models

The theoretical basis of the published reservoir souring model was explained in the previous chapters. Table 5.1 summarizes the capability of the different reservoir souring models in generation and transportation of hydrogen sulfide. This table indicates

Table 5.1 Comparison of the reservoir souring models

Reservoir souring prediction models		Frazer, et al., 1991	Mixing	Biofilm	TVS	UTCHEM Model
Generation of H ₂ S	SRB type	No preference	Planktonic (free cells)	Sessile (attached cells)	Mesophiles	Sessile And Planktonic SRB
	Biological model	First order reaction	Empirical Time constant	Michaelis-Menten	Empirical rate fitting	Molz et al.
	Reaction zone	Injection Stream	Mixing Zone	Biofilm near injector	TVS	Mixing and attached zones
	SRB movement	No preference	With mixing zone	Attached to biofilm	Move with TVS	Can move with mixing zone or attached to rock surfaces
	Temp.	No	No	No	Yes	Yes
	Press.	No	No	No	Yes	Yes
	Nutrient	No	No	Yes	No	Yes
H ₂ S Transport	Dim.	1D	1D	1D	1D	3D
	O/W partition	No	Yes	No	No	Yes
	Ads.	No	Yes	Yes	No	Yes

that the developed model is more comprehensive and has more ability to include the effective parameters which may change in simulation of reservoirs. First of all regarding the transportation terms, the developed model and simulator is 3D, while the previous models were 1D. The developed model has the ability to consider the partitioning between phases and adsorption on rock surfaces, while some of the previous could not. In generation term, the SRB are very sensitive to the temperature and the available nutrients. Besides, the SRB can attach to the rock surfaces or move with the bulk flow. As previously shown, the developed model has the ability to include the effect of

temperature and nutrients on the growth of bacteria, furthermore, the bacteria can attach or float in the media. These specifications indicate that the developed model is more comprehensive and realistic prediction of the reservoir souring in real fields.

5.9 Summary of the Developed Model

In biogenic production of hydrogen sulfide, the kind of SRB, the temperature profile in the reservoir, and nutrient concentrations are the most important parameters. In the process of seawater-injection, usually the concentration of sulfate and temperature of seawater remains constant. Also, the initial concentration of acetate in formation water is assumed constant. Thus, for the specific kind of SRB, the available nutrients and reservoir temperature determine the magnitude of produced hydrogen sulfide. This means that the higher nutrient concentrations result in higher production of hydrogen sulfide. The effect of temperature profile in the reservoir depends on the SRB type. If the temperature profile remains in the range which is suitable for the growth of bacteria, its effect would be minimal, otherwise the generation of hydrogen sulfide will reduce.

The transportation of hydrogen sulfide depends on the retardation factor. The retardation factor consists of the partitioning and adsorption of hydrogen sulfide in the reservoir. The partitioning of hydrogen sulfide between oil and water phases is a weak function of the pressure and depends on the temperature. At reservoir conditions we may assume that partition coefficient remains constant. On the other hand, the adsorption capacity of the reservoir rocks may change a lot for different reservoir. Consequently, the retardation factor for different reservoirs may change if the adsorption capacities are changing. The effect of high retardation factor is lowering the observed peak in the

concentration of hydrogen sulfide and more delay of the arrival of hydrogen sulfide, with respect to water breakthrough.

The simulator with the reservoir souring module provides the ability to predict the onset of reservoir souring. We are able to simulate various reservoirs under a variety of conditions and properties, and investigate the effects of various parameters on the prediction results. The developed multi-dimensional simulator has the capability to include all pertinent parameters which are essential in construction of a mechanistic model. The theoretical basis of the UTCHEM model regarding the generation and transportation of H₂S has been reviewed with other authors. With all of the variables in a single simulator, the UTCHEM model has the ability to predict the onset of the reservoir souring.

Chapter 6

Application of UTCHEM to Reservoir Souring Process

In this chapter, we discuss data required for the reservoir souring process and investigate the effects of parameters on the predicted results. Then, a study of the temperature profile and injection front regarding the assumptions on the mechanisms of heat transfer in the reservoirs is presented. The effects of physical dispersion and heterogeneity of the reservoir on the developed profiles of temperature and concentrations are also investigated. The combined effects of temperature and SRB types on the prediction results of souring are discussed. The effects of chemical parameters such as available nutrients and biological species on the generation of H₂S are fully discussed. Additionally, the effects of retardation due to adsorption and partitioning on the hydrogen sulfide transportation in the reservoir are investigated. To complete our study of the application of UTCHEM, the results of published models for the reservoir souring are reproduced in a separate section. Finally, a comparison between reservoir souring models is given to demonstrate the unique capabilities of our model and simulator.

6.1 Introduction

In the previous chapters, we identified the basic chemical, physical and biological phenomena that must be considered in a predictive model of reservoir souring. In this section, the data required for these models including the parameters for biological reactions, water chemistry, partitioning of hydrogen sulfide between oil and water phases, and scavenging of hydrogen sulfide by rock surfaces are described.

6.2 Data Required for Reservoir Souring Models

In this section, the input parameters required for the reservoir souring models are discussed. These data include the parameters which are needed in simulation of generation and transportation of hydrogen sulfide in porous media. The kinetics constants and the stoichiometry of the biogenic reactions and the compositions of the injection and formation waters are needed for the generation term. Additionally, oil/water partitioning coefficient and adsorption of H₂S on reservoir rock are required to describe the transportation term. Since the generation and transportation terms are sensitive to the reservoir conditions, the pressure and temperature distributions from injector to the producer should be known to describe the whole process of souring.

6.2.1 Parameters for the Biological Reactions

To simulate the biological reactions in UTCHEM, first we must set IBIO=1. Then, the sixth input section is required for introducing concentrations, reaction kinetics, and properties related to chemical and biological species. The biodegradation section is read by a separate subroutine called BIOREAD, which is in the standard UTCHEM

format. UTCHEM user's guide and UTCHEM technical documentation give more details on this option.

In order to run a sample case the following parameters should be introduced in the UTCHEM input file.

DENBLK

DENBLK- density of rock

Units:g/cm³.

CMIN, EPSBIO, IBTIM, BVOLMAX

CMIN- Minimum concentrations of substrate and electron acceptor which are engaged in the reactions.

This parameter is used for two purposes. First, if concentrations of all substrates and electron acceptors in a gridblock are below CMIN, biodegradation reactions are assumed negligible at that gridblock and are not modeled. Second, when the concentration of all substrates and electron acceptors fall below CMIN during solution of the biodegradation reaction expressions, further biodegradation reactions are assumed to be negligible and program execution returns to the main program. The unit of CMIN is mg/l.

EPSBIO- Convergence tolerance for solution of the biodegradation equations.

Values of 10^{-4} to 10^{-6} are recommended, although larger values can also result in accurate simulation.

IBTIM- Flag indicating type of time step control for solution of biodegradation equations.

Possible values:

- 0- No time-step control, biodegradation equations are solved at every transport time-step
- 1- Manual time-step control, biodegradation time-step is specified by user
- 2- Automatic time-step control, biodegradation time-step is controlled by UTCHEM based on an acceptable error specified by the user

BVOLMX- Maximum biomass volume (% porespace)

NBC, NMET, IBKIN, IBPP, IBTEM (new flag), TLOB, TMXB, TUPB

NBC- Total number of chemical and biological species that are considered in biodegradation reactions, including oil components, surfactants, products generated by abiotic and biodegradation reactions, nutrients required for biological growth, electron acceptors, and biological species.

NMET- Number of substrate/electron acceptors/biological species metabolic combinations. Include combinations of biodegrading products/electron acceptor/biological species for each product that also biodegrades.

IBKIN- Flag specifying the type of biodegradation kinetics.

Possible values:

- 0- No reactions, biodegradation parameters are read, but biodegradation equations are never solved (useful for restart runs)

- 1- Monod kinetics with external mass transfer resistance (differentiates between attached and free cells)
- 2- Monod kinetics with no external mass transfer resistance
- 3- Instantaneous kinetics (stoichiometric stiochimetric reactions)
- 4- Monod kinetics with automatic control of external mass transfer resistance

IBPP- Flag indicating whether porosity and permeability are affected by biomass growth.

Possible values:

- 0- Porosity and permeability are not affected by biomass growth
- 1- Porosity and permeability are affected by biomass growth

IBTEM- Flag indicating whether or not the temperature dependency of the biological reactions are considered (The IENG, energy balance flag should set on)

Possible values:

- 0- The effect of temperature is not considered on the biological reactions
- 1- The effect of temperature is considered on the biological reactions

TLOB- Lower limit of temperature for activation of biological reaction

TMXB- Temperature of the maximum growth rate for biological reaction

TUPB- Upper limit temperature for biological reaction

The developed code can adjust easily to include several types of SRB with different temperature limits simultaneously.

IMTVAR

IMTVAR- Flag indicating type of mass transfer control.

Possible values:

1. Mass transfer between bulk flow and attached cells is considered in each gridblock at each time step if Damkohler number is greater than the user specified value.
2. Mass transfer between bulk flow and attached cells is considered in each gridblock in each time-step only if the effectiveness factor is less than the user specified value.

The effectiveness factor is the ratio of the rate of reaction when mass transfer is included in biodegradation kinetics to the rate of reaction in the absence of mass transfer.

DAMX

DAMX- Value of Damkohler number used to control mass transfer in biodegradation calculations, recommended value, 0.1

EFMIN

EFMIN- Value of effectiveness factor used to control mass transfer in biodegradation calculations, recommended value, greater than 0.95

**KC(I), DENBIO(I), RCOL(I), TCOL(I), COLNUM(I), ENDOG(I), ENDOGB(I),
CBI(I), CBIOMN(I), ADSBIO(I), for I=1,NBS**

One line is required for each biological species

KC(I)- Index of the biological species

DENBIO(I)- density of attached biological species I (biofilm density), in g cells/cm³
biomass

RCOL(I)- Radius of an attached microcolony of biological species I, cm

TCOL(I)- Thickness of a single attached microcolony of biological species I, cm

CONUM(I)- Number of bacterial cells per microcolony of biological species I,
cells/colony

ENDOG(I)- Endogenous decay coefficient of unattached cells of biological species I,
1/days

ENDOGB(I)- Endogenous decay coefficient of attached cells of biological species I,
1/days

CBI(I)- Number of attached bacterial cells of biological species I per gram of rock,
cells/gram of solids

CBIOMN(I)- Lower limit of number of attached bacterial cells of biological species I,
cells/gram of solid

ADSBIO(I)-Biomass partitioning coefficient,
(mass of attached microorganisms)/(mass of unattached microorganisms)

This flag is used for the initial distribution of the biological species when the ratio determines the partitioning between bulk flow and rock surfaces. The IBKIN flag determine whether the attached or free cells behave differently.

ISUB(I), IEA(I), IBS(I), BRMAX(I), BRMAXB(I), YXS(I), AKS(I), AKA(I), FEA(I),
for I=1, NMET

ISUB(I)- Substrate index for metabolic combination I

IEA(I)- Electron acceptor index for metabolic combination I

IBS(I)- Biological species index for metabolic combination I

BRMAX(I)- Maximum specific growth rate of unattached microorganisms for metabolic combination I, 1/days

This parameter is the μ_{\max} in Equation 4.19

BRMAXB(I)- Maximum specific growth rate of attached microorganisms for metabolic combination I, 1/day

YXS(I)- Yield coefficient for metabolic combination I, biomass produced per mass of substrate biodegraded

This parameter is the Y in Equation 4.19

AKS(I)- Substrate half-saturation coefficient for metabolic combination I, mg/l

This parameter is the K_S in biodegradation equations.

AKA(I)- Electron acceptor half-saturation coefficient for metabolic combination I, mg/l

This parameter is the K_A in biodegradation equations.

FEA(I)- Electron acceptor utilization coefficient,

mass of electron acceptor consumed per mass of substrate biodegraded.

This parameter is the E in biodegradation equations.

For the products, inhibitors and limiting nutrients this sequence will be repeated.

6.2.2 Parameters for Partitioning and Adsorption on Rock Surfaces

In UTCHEM input file, the parameters for adsorption and partitioning are included in the tracer option. The tracer option is located at the end of fourth section of input file.

We activate the tracer option (NTW flag) and then introduce the partitioning and adsorption as follows:

TK(I) - Tracer partition coefficient for Ith water/oil tracer at initial chloride concentration and reference temperature. A value of 0.0 indicates a water or gas nonpartitioning tracer and a value of -1.0 indicates a nonpartitioning oil tracer.
Units: fraction

In the simulation process, we input 3 for the partitioning coefficient.

TKS(I) - Parameter for calculating water/oil tracer partition coefficient for Ith tracer as a function of salinity. Units: (meq/ml)⁻¹

In the simulation process, we input 0 for the salinity effect on partitioning coefficient.

TKT(I) - Parameter for calculating tracer partitioning coefficient for Ith tracer as a function of reservoir temperature. Units: (°F)⁻¹ (IUNIT=0) or (°C)⁻¹ (IUNIT=1)

In the simulation process, we input 0 for the temperature effect on partitioning coefficient.

RDC(I) - Radioactive decay coefficient for Ith tracer. A value of 0.0 indicates a non-radioactive tracer. Units: 1/days

In the simulation process, we input 0 for the radio active decay.

RET(I) - Tracer adsorption parameter (adsorbed concentration/flowing concentration). A value of 0.0 indicates no retardation. Units: dimensionless

In the simulation process, we input variable adsorption parameter.

6.2.3 Water Chemistry

Chemical compositions of injected and formation waters determine the generation of hydrogen sulfide by SRB. Particularly, concentrations of sulfate and organic acids, as well as the available nutrients are very important in microbial H₂S production. In the simulation of reservoir souring, sulfate and organic acids are considered to be provided by seawater and formation water, respectively. Seawater typically contains 2,800 mg/l of sulfate (Herbert et al., 1985).

Studies have shown that most SRB-genera preferentially degrade certain organic acids such as lactate, acetate, butyrate, and propionate (Kleikemper et al., 2002). Organic acids tend to dissolve in aqueous phase when pH is greater than 5. This condition is normally expected in an oil reservoir where the large majority of the organic acids (more than 85%) will be dissolved in the aqueous phase.

Analysis of production waters from different locations throughout the world has revealed that the presence of the short chain fatty acids is very widespread. The level of organic carbon in many formation waters changes between at least 100 mg/l carbon and as high as 1300 mg/l carbon. Table 6.1 reflects the typical concentrations of the organic acids in the water cut from the Ninian reservoir production waters (Cochrane et al., 1988).

Table 6.1 Analysis of produced water (after Cochrane et al., 1988)

Well	Acetate (mg/l)	Propionate (mg/l)	Butyrate (mg/l)
P.1	64	12	6
P.4	95	10	9
P.5	185	25	4
P.7	149	36	9
P.11	722	180	45
P.12	505	142	34
P.13	287	46	15
P.14	681	179	45
P.15	571	73	29
P.16	251	44	27
Mean	351	75	22
Range	64-722	10-180	4-45

The nutrients that must be specified are the phosphate (set to 0.06 ppm in seawater and 0.3 ppm in formation brine in their simulations), nitrate (set to 0.6 ppm nitrate in seawater) (Lightelm et al., 1991; Sunde et al., 1993).

6.2.4 Absorption of H₂S by Residual Oil

Several investigators have described the solubility and partial pressures of H₂S in the production fluids. Generally, H₂S is more soluble in organic compounds than in water and aqueous salt solutions. Eden et al. (1993) reported the H₂S partitioning coefficients between crude oil and produced water at different temperatures. The results of calculation of Henry's law constants for H₂S are presented in Table 6.2.

Table 6.2 Henry's law constants for H₂S in crude oil and formation water, mmHg/ppmv H₂S, (after Eden et al., 1993)

Temperature (deg. C)	50	60	70	80
K _o	453	503	549	592
K _w	13.8	15.7	17.0	17.7

The partitioning coefficient of H₂S between oil and water phases (K_{ow}) is defined by

$$K_{ow} = \frac{C_o}{C_w} = \frac{K_w}{K_o} \quad (6.1)$$

where C_o and C_w stands for H₂S concentrations in oil and water phases. Table 6.3 shows the calculated partitioning coefficient of H₂S at different temperatures.

Table 6.3 Partition coefficient for H₂S between crude oil and formation water, ppmw H₂S in oil/ ppmw H₂S in water, (after Eden et al., 1993)

Temperature (deg. C)	20	50	60	70	80	100
K _{ow}	4.1	3.0	3.1	3.1	3.0	3.2

As reflected in the Tables 6.2 and 6.3, although the values of K_o and K_w depend greatly on temperature, the values of K_{ow} almost remain constant with temperature (i.e., average value 3.1). In our simulation, we assigned a value of 3 for partitioning coefficient.

6.2.5 Scavenging of H₂S

Another contribution to the transport of H₂S is its interaction with the existing minerals in the reservoir rock. Scavenging and absorption both delay the arrival of hydrogen sulfide with respect to water breakthrough. These two mechanisms cannot be distinguished by measurements of delay at a production well.

Many iron-containing minerals are able to react with H₂S in the porous media. These minerals could be siderite (FeCO₃), hematite (Fe₂O₃), and magnetite (Fe₃O₄) (Ligthelm et al., 1991). These minerals can react with H₂S to produce pyrrhotite (FeS) and pyrite (FeS₂) according to the following reactions:



These reactions take place on the rock surfaces, hence this interaction is commonly modeled as an adsorption process. The adsorption capacity of the minerals depends on the temperature, pressure, and pH of the solution. Sunde et al. (1993) reported the scavenging capacity of H₂S using crushed and oxidized rock samples (Table 6.4).

Table 6.4 Retardation factors corresponding to laboratory measurements of scavenging capacity of H₂S with reservoir rock (after Sunde et al., 1991)

Reservoir	Scavenging capacity		Equivalent partitioning coefficient	Retardation factor
	mg/g solid (Sunde et al.)	ppm, aqueous phase basis		
A	0.014	82	8.2	9.2
A	0.35	2042	204.2	205.2
A	19.6	114333	11433.3	11434.3
B	0.005	29	2.9	3.9
B	0.01	58	5.8	6.8
C	0.55	3208	320.8	321.8
C	1.95	11375	1137.5	1138.5

In the calculation of retardation factors in Table 6.4, it is assumed that the formation porosity is 30%, and aqueous concentration of H₂S is 10 ppm. There is a large difference between the adsorption capacities of the samples even within cores obtained from the same reservoir. Additionally, rocks in the reservoir have much less effective contact surface than a crushed sample. The given values in Table 6.4 over-estimate the actual scavenging capacity of the reservoir rock. Thus, these data provide little guidance as to what may be the appropriate values for the field application. The scavenging of H₂S by reservoir rock under reservoir conditions is not well documented. This implies that considerable uncertainty exists in predictions of the arrival time of H₂S at a production well. Therefore, further investigations are required to calibrate the models for more accurate prediction results.

6.3 Factors that Control Activity of Sulfate Reducing Bacteria in Reservoirs During Water Injection

In order to explain the reservoir souring phenomena, it is necessary to know the nutritional requirements and the physico-chemical environments that can be developed during the process of water injection.

6.3.1 Nutritional Factors

6.3.1.1 Carbon/ Energy

Lactate has been widely used as the carbon/energy source for the isolation of SRB. In addition, SRB can utilize pyruvate and malate. Some other SRB genera can utilize short-chain fatty acids like acetate, propionate and n-butyrate or long-chain acids up to palmitate. Furthermore, they are able to utilize simple alcohols and glycerol (all materials in Sections 6.3.1.1-6.3.2.6 are from Herbert et al., 1992).

6.3.1.2 Nitrogen

Basically, ammonium salts, nitrate, hydroxylamine and possibly some amino acids can provide the nitrogen source for the growth of SRB. In our simulation we consider nitrate as a source of nitrogen.

6.3.1.3 Electron Acceptors

Even though sulfate is considered the available electron acceptor, it, along with thiosulfate, and bisulphate can be utilized by SRB. In some cases, nitrate can provide an alternative electron acceptor and results in the production of ammonia instead of sulfide.

6.3.1.4 Inorganic Salts

Phosphate is the inorganic salt that is needed for the growth of SRB as well as other bacteria. In particular, SRB requires higher iron (25 milli molar) than is usually needed for other bacterial species. In our simulation, we assume that inorganic salts are not limiting of SRB growth.

6.3.2 Physical Constraints

6.3.2.1 Temperature

In Chapters 2 and 3 the effect of temperature on the activation of different type of SRB was discussed.

6.3.2.2 Pressure

Although SRB isolated from seawater function at pressure up to 600 bar, its metabolism (i.e. shape, amount of sulfide produced) will be affected at pressures as low as 200 bar. In our simulations, because of the lack of data, we neglected the effect of pressure on SRB activities.

6.3.2.3 pH

The suitable pH for activity of SRB range from 6 to 9. In reservoir conditions normally this range of pH is satisfied.

6.3.2.4 Redox Potential

A reduction-oxidation potential of Eh (-100 mv or less) which is measured with respect to the standard hydrogen electrode (Eh) is required for the function of SRB. In

simulation of reservoir souring, it is assumed that the redox potential is sufficient for activation of SRB.

6.3.2.5 Salinity

A salinity of below 10% which is expressed as NaCl provides the environment for the growth of SRB. In a seawater injected reservoir this range of salinity is usually provided.

6.3.2.6 Permeability

The various genera of SRB differ in shape and size. Generally, their dimensions are of the order of 5 micro meter long and up to 1 micro meter in diameter. Accordingly, SRB can pass through porous media if permeability is greater than 100 md or trapped in pore throat for lower permeabilities.

6.4 Switch Between Souring Models

6.4.1 Mixing Model

UTCHEM has the capability to simulate the process of reservoir souring according to mixing model. Mixing model of reservoir souring can be simulated by UTCHEM if we set the following parameters:

ADSBIO(I)=0

This means that all the existing microorganisms just remain as unattached cells (free cells) and move with the mixing zone between injected and formation water.

The produced H₂S can partition between water and oil phases and can adsorb on rock surfaces. Thus, we assign partitioning coefficient, TK(I), and adsorption parameters, TKS(I), TKT(I), RDC(I), and RET(I) where:

TK = 3.0, TKS=0, TKT=0, RDC=0, and RET= variable.

One important parameter in input file of UTCHEM which is used to simulate the reservoir souring process is IBKIN.

IBKIN has five different options as explained in the previous section.

For the case of mixing models, because it is assumed that reactions occur only in mixing zone the IBKIN=1,2 and 4 which are base on mass transfer coefficient between attached and unattached phase show the same results. To save the simulation time without completing many unnecessary calculations, it is better that in mixing model set IBKIN=2.

The sample INPUT file is given in the Appendix A.

6.4.2 Biofilm Model

In order to simulate the process of reservoir souring with biofilm using UTCHEM, we must change the codes to consider the reaction zones and other assumptions, which are included in the biofilm model. Basically, the reaction zone is restricted to the vicinity of injection well. In the simulation process, the biological reactions are limited to the first gridblock near the injection well. The sample INPUT file for biofilm model is given in Appendix A.

6.4.3 TVS Model

UTCHEM can simulate the temperature viability shell (TVS) model. TVS model is a correlation between temperature, pressure and the concentration of produced H₂S. It

is possible to introduce the desirable correlation in UTCHEM and solve for the H₂S concentrations. This correlation only needs the temperature and pressure distributions in the reservoir. The lag in the observed souring is explained by the lag of temperature front with respect to the injection front.

6.4.4 UTCHEM Souring Model

In order to simulate the reservoir souring by UTCHEM model, the new flags and parameters should be included in the INPUT file. These parameters as described above are:

IBTEM, TLOB, TMXB, TUPB

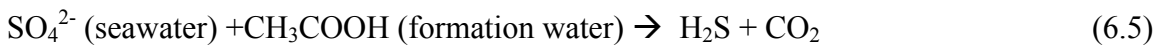
The flag IBTEM can be assigned 0 or 1. The value zero means that temperature effect on SRB growth is ignored. When we put IBTEM equal to 1, it means we want to include the temperature effect on SRB growth and consequently we should assign values for TLOB, TMXB and TUPB. Depending on the kind of SRB, TLOB is the lower limit of temperature of activation. TMXB is the temperature that SRB has the maximum growth rate and TUPB is the maximum temperature at which the SRB can continue its activation.

Our model includes the nutrient effects, partitioning between phases and adsorption on rock surfaces. These parameters also must be introduced to the INPUT file for the reservoir souring simulation. The sample INPUT file for the developed model is given in the Appendix A.

6.5 Simulation of the Reservoir Souring Prediction

A case study which shows the capabilities of UTCHEM in simulation of biological production of H₂S in a typical seawater injected reservoir is described in this section. The data required for the process include the definition of each species, biological input parameters, reaction kinetics for produced species, nutrient required, substrates and electron acceptors, and initial and injected concentrations of species are explained in the Appendix C (Sunde and Thorstenson, 1993).

UTCHEM simulation results which resemble those obtained using the existing souring predictive models are given. Consequently, the gaps that should be filled in order to develop a more comprehensive souring model are also investigated. In order to have an understanding of the souring problem, a simple case which resembles what actually may occur in a reservoir is simulated. The proposed biological reaction in the presence of planktonic SRB (from seawater) is



In this reaction, NO₃⁻ and PO₄³⁻ have the role of nutrients and limit SRB growth and consequently the H₂S production. The produced H₂S reacts with rock surfaces and partitions between oil and water phases (Sunde, et al., 1993).

A 2-dimensional case was set up (1300ft×82ft×27ft) with 26 gridblocks in the x direction and 8 vertical layers and uniform permeability and porosity of 700 md and 0.33, respectively. The reservoir is initially saturated with oil at connate water saturation of 0.147. The injection well is located in the first gridblock and the production well with a constant pressure of 3771 psi is located in the last gridblock. Both wells are completed across the entire reservoir thickness. Seawater was injected at a constant rate of 2000 ft³/day. The reservoir properties and conditions, chemical and biological species kinetics

constant and concentration of species, which are used in the simulation, are given in Tables 6.5. Additionally, it is assumed that the SRB activities are independent of temperature similar to mixing model.

Figures 6.1a and 6.1b show that water breakthrough occur at about 0.56 pore volumes (about 200 days) after injection of seawater. Figure 6.2 indicates that the maximum concentrations of H₂S and SO₄ occurred shortly after the water breakthrough. In Figure 6.2, we can see the maximum concentration of CH₃COOH, CO₂, SRB, H₂S and SO₄ occur at 0.7, 0.7, 0.7, 1.5 and 0.7 pore volumes, respectively. Due to the retardation, the maximum concentration of hydrogen sulfide occur after water breakthrough.

Figures 6.3a and 6.3b show tracer and H₂S concentration profiles in the reservoir after 90 days of injection water. Comparing the profile of tracer (Figure 6.3a) with the profile of H₂S show that the hydrogen sulfide has a delay with respect to injection front, which depends reflects the retardation effect.

Table 6.5 Initial and injected concentration data (mg/l) (after Ligthelm et al., 1991)

SRB in seawater	0.0001
SO ₄ in seawater	2700.0
POC (particulate Org. C) in seawater	0.01
NO ₃ in seawater	0.6
PO ₄ in seawater	0.06
CH ₃ COOH in formation water	1000.0
PO ₄ in formation water	0.3
SRB/Nutrient data:	
SRB Bacterial growth rate(doubling/day)	1
K _C Acetate half saturation constant (mg/l)	0.01
K _N Nitrate half saturation constant (mg/l)	0.001
K _P Phosphate half saturation constant (mg/l)	0.0001
K _{SO4} Sulfate half saturation constant (mg/l)	0.01

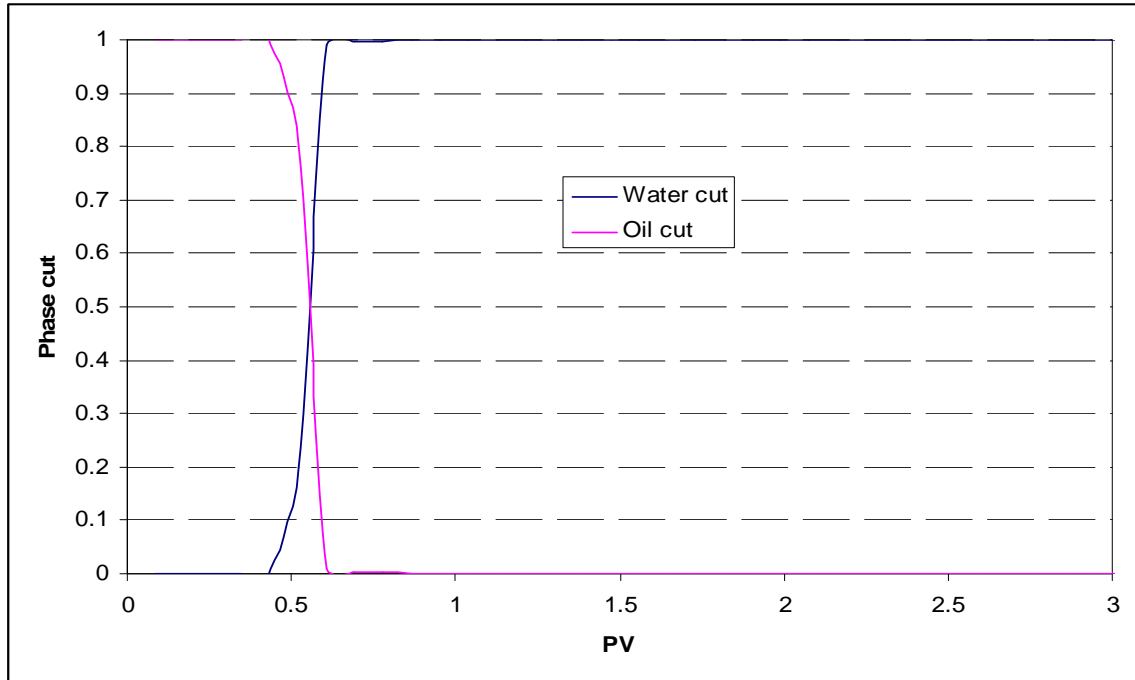


Figure 6.1.a Water and oil cut versus pore volume

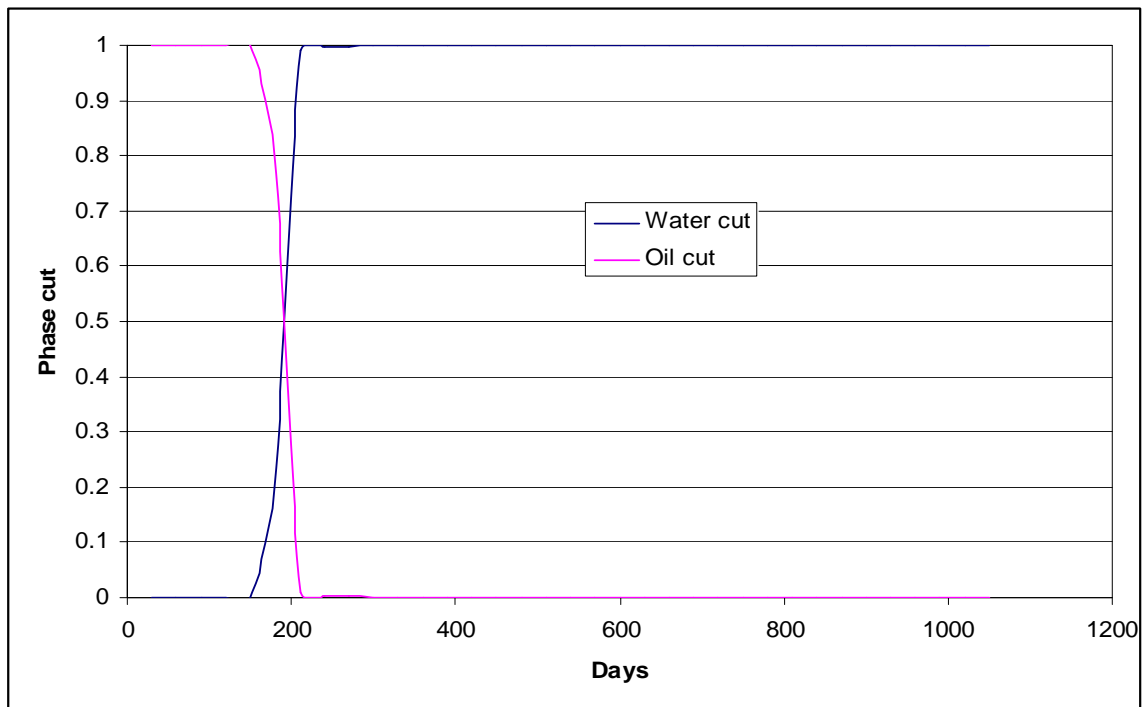


Figure 6.1.b Water and oil cut versus time

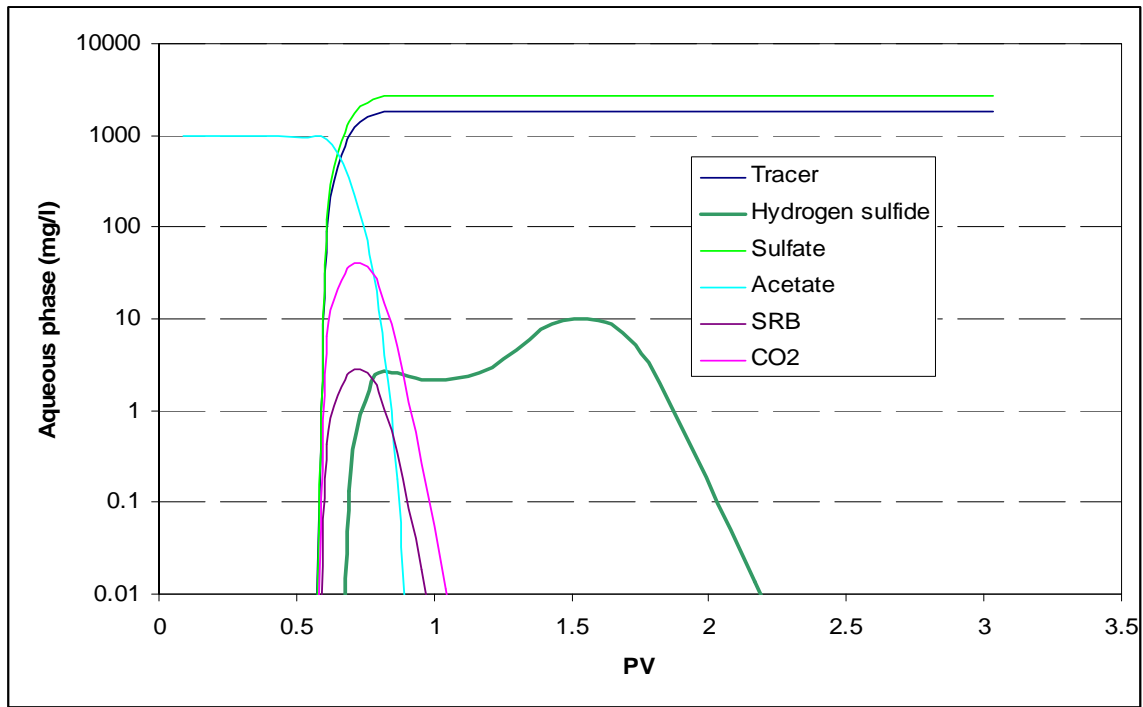


Figure 6.2 Total concentration of components in production well (mg/l) for primary results case

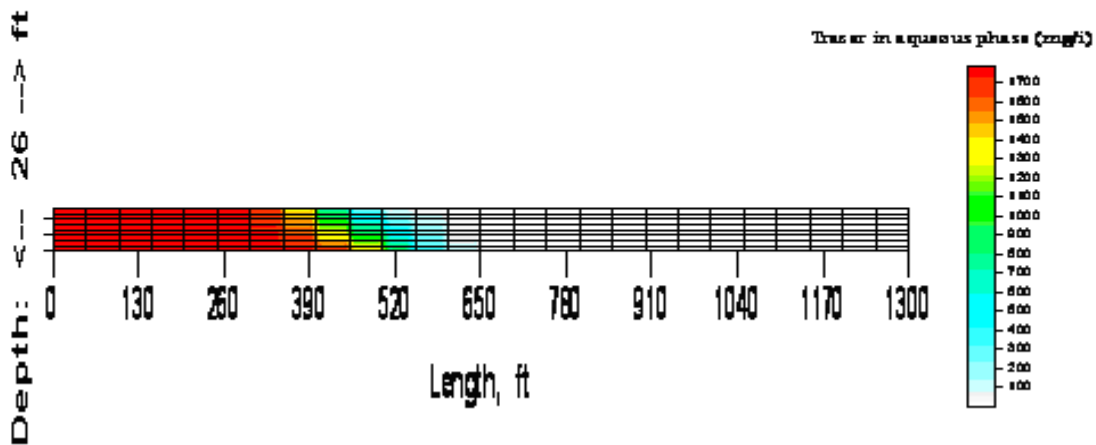


Figure 6.3a Tracer concentration (mg/l) after 90 days of seawater injection

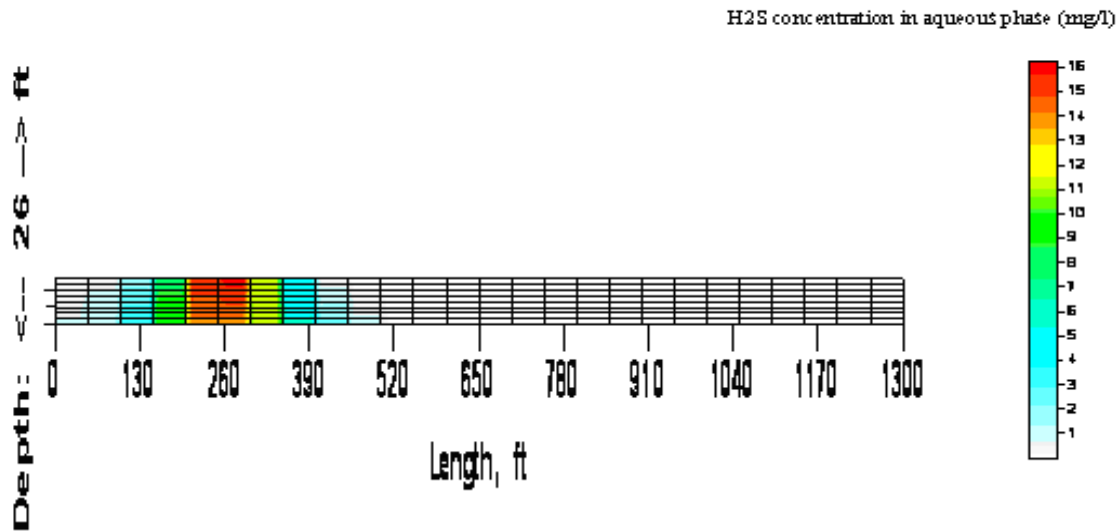


Figure 6.3b H₂S concentration (mg/l) after 90 days of seawater injection

6.6 Reproduction of the Published Models by UTCHEM Model

UTCHEM provides the ability to evaluate the existing reservoir souring prediction models. We are able to simulate the reservoirs with different conditions and properties and investigate the effects of these changes on the prediction results. Any reservoir souring prediction model must have the ability to explain the processes of generation and transportation of hydrogen sulfate in a real situation.

The theoretical basis of the mixing and biofilm models regarding the location of the biological reactions is completely different. This gives two distinct profiles for the prediction results, Figures 2-11a and b. However, the reservoir souring behavior for some reservoirs can be explained with the mixing and others with the biofilm models. TVS model correlates between the reduced sulfate and temperature and pressure of the

reservoir at specified laboratory experiments. It assumes a constant sulfate concentration in injected seawater and specified temperature range. In TVS model, the temperature and pressure changes determine the extent of the observed souring. The TVS model assumes the changes in the reservoir temperature, and the pressure provides a suitable environment in which the SRB reduces the sulfate in the seawater to H₂S. In the field case, the physical constraints and concentrations change, and we cannot rely on a correlation which resulted from the experimental data in specified conditions.

Investigation of these models, with the use of UTCHEM, shows that each model has various deficiencies in the generation and transportation of hydrogen sulfate. First, these models are one-dimensional and there is no one-dimensional flow in a real reservoir. Different flow paths provide different times for the biological generation and adsorption of H₂S. The biological species moves with a bulk flow when the permeability of the medium is over 100 md (Sunde et al., 1993). Thus, the assumption of a biofilm attached to the rock surfaces is not true for all of the reservoir layers. Biological reactions are sensitive to the physical constraints and chemical species present in the reservoirs. Assumption of a rate independent of these constraints is too far from a real situation. In addition, the adsorption capacity and the partitioning of H₂S can also change with variation of physical and chemical constraints. The growth of bacteria results in a reduction of the permeability of the medium, and for a long term injection process, this effect needs to be included in the soured reservoirs.

To the best of our knowledge, there is no published comprehensive model and simulator which can evaluate the important parameters essential to reservoir souring (Maxwell et al., 2005). Thus, this study illustrates the importance of the UTCHEM model, which has

more abilities in the generating and transporting hydrogen sulfate in seawater injected non-homogen reservoirs (see Table 5.1).

Figure 6.4 shows the results of the original mixing model (Ligthelm et al., 1991) and the simulation results of UTCHEM. There is a good agreement with the published results. A minor difference between the results is the numerical dispersion and the lack of published data on the fluid flow properties. The result of the reproduction of the biofilm model (Sunde et al., 1993) via UTCHEM, is given in Figure 6.5. Although the published data for the reservoir characteristics and initial concentrations are not complete, UTCHEM can simulate the basic concepts of biofilm model.

The published result on TVS model is confined on a correlation between temperature, pressure, and the reduced sulfate. Unfortunately, there is no result in the published paper (Eden et al., 1993) to show the reservoir characteristics and conditions. In our study, we applied the concept of TVS on the simulation process. The results which are reflected in Figure 6.6 show that applying the concept of TVS when introducing two different types of SRB, the predicted results are totally distinct.

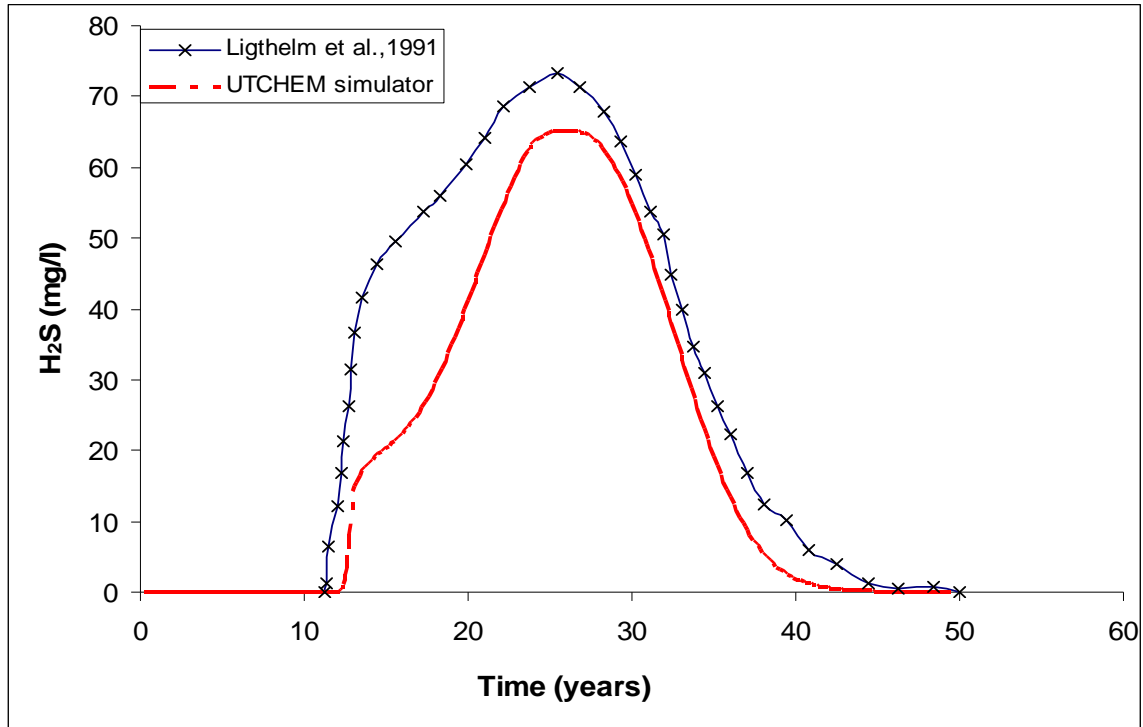


Figure 6.4 Comparison of the mixing model prediction of H₂S in aqueous phase (mg/l) via the UTCHEM simulator and with the reproduced results (Ligthelm et al., 1991)

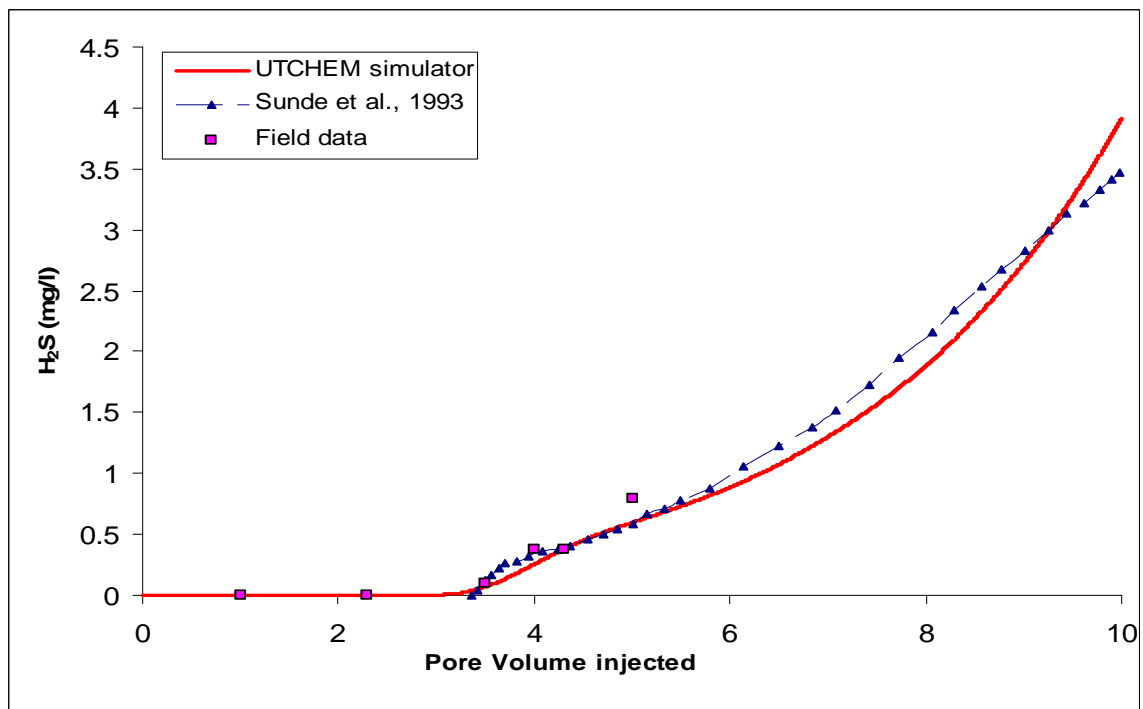


Figure 6.5 Comparison of biofilm model prediction of H₂S in aqueous phase (mg/l) via the UTCHEM simulator and with the reproduced results (Sunde et al., 1993)

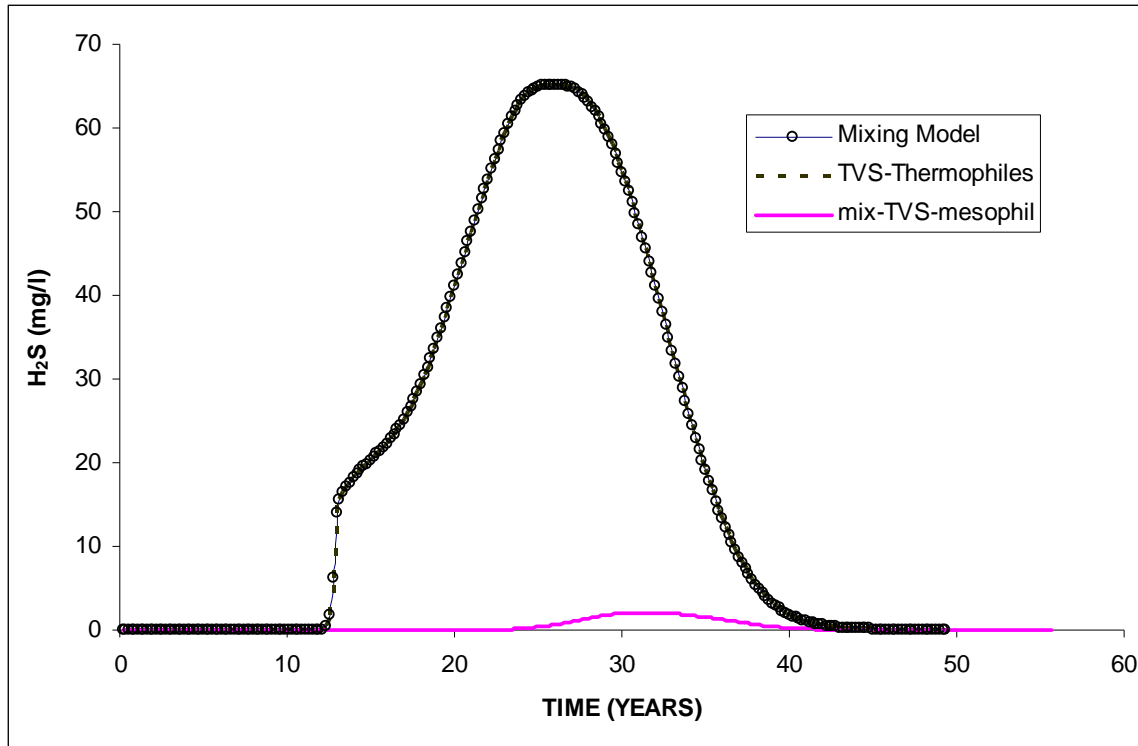


Figure 6.6 The TVS model of prediction of H₂S in aqueous phase (mg/l) via the UTCHEM simulator

6.7 Investigation of the Effective Parameters on Reservoir Souring Prediction

In order to investigate the effects of reservoir characteristics and conditions on the reservoir souring, several artificial cases have been designed. In biogenic generation of hydrogen sulfide, the temperature distribution has an important role. A detailed study of the temperature propagation in sea water injected reservoir is given in the following sections.

To investigate the effects of longitudinal dispersivity and type of SRB on the produced H₂S, different cases have been simulated. These simulations are based on our model which combines the assumptions of mixing, TVS and biofilm models in transportation of species and also considers the combined effects of these models in biological generation of hydrogen sulfide. The effects of heterogeneity of the reservoir on

the process of souring are investigated. The effect of grid refinement in vertical direction is provided in several case studies.

6.7.1 Propagation of Temperature Profile in the Seawater Injected Reservoir

6.7.1.1 Analytical and Numerical solution of Heat Transfer in the Seawater Injected Reservoirs

In order to understand the behavior of different SRB types in the reservoir, it is important to investigate the propagation of the temperature front in the seawater injected reservoirs. In general, there are two approaches for the solution of heat transfer phenomena in porous media. These solutions could be analytical or numerical. The analytical solution has less application because it is limited to the one dimensional fluid flow in the porous media. The numerical solution which is based on the general energy balance equation is used for multi-dimensional solutions. It is important to know that even fluid flow is one dimensional the heat transfer mechanism is two dimensional. This behavior arises from the fact that in heat transfer phenomena usually the heat conduction in direction of flow is negligible with respect to heat convection while in direction perpendicular to flow, there is only heat conduction.

The analytical solution of heat transfer in a typical reservoir has been developed by Lauwerier, 1995. In the following sections, first we show our analytical solution for heat transfer in a one-dimensional and single phase flow. Then, we explain the temperature propagation in seawater injected reservoirs as modeled in UTCHEM and investigate the pertinent parameters which may affect the temperature profile.

The analytical solution of temperature distribution is the solution of the following formulation (the formulation which is used in UTCHEM is given in Chapter 4) which results from general energy balance equation and applying Gauss's divergence theory to change the integration on surface to the integration in volume.

$$\frac{\partial}{\partial t}((1-\phi)\rho_s C_s + \phi(1-S_{or})\rho_w C_w + \phi S_{or}\rho_o C_o)T + \vec{\nabla} \cdot (\rho_w C_w u T - \lambda_T \vec{\nabla} T) = 0 \quad (6.6)$$

where it is assumed no heat transfer to over/under burden, no heat sour/sink, 1D, and one phase flow.

Further simplifying the above equation will give:

$$((1-\phi)\rho_s C_s + \phi(1-S_{or})\rho_w C_w + \phi S_{or}\rho_o C_o) \frac{\partial T}{\partial t} + u \rho_w C_w \frac{\partial T}{\partial x} - \lambda_T \frac{\partial^2 T}{\partial x^2} = 0 \quad (6.7)$$

where ρ_s , ρ_w , ρ_o , C_s , C_w , C_o , λ_T , and u are the density of the reservoir rock, density of water, density of oil, specific heat of the reservoir rock, specific heat of water, specific heat of oil, thermal conductivity of the reservoir (oil and sand), and Darcy velocity respectively. The solution of Equation (6.7) is based on the following assumptions on initial and boundary conditions:

$$T(x,0) = T_{res}$$

$$T(0,t) = T_w$$

$$\lim_{x \rightarrow \infty} T(x,t) = T_{res}$$

Equation 6.8 is the dimensionless form of the governing heat transfer in the reservoir:

$$\frac{\partial T_D}{\partial x_D} + \frac{\partial T_D}{\partial t_D} - \frac{1}{N_{pe}} \frac{\partial^2 T_D}{\partial x_D^2} = 0 \quad (6.8)$$

$$T_D(x_D,0) = 0$$

$$T_D(0,t_D) = 1$$

$$\lim_{x_D \rightarrow \infty} T_D(x_D,t_D) = 0$$

The dimensionless variables are:

$$T_D = \frac{T - T_{res}}{T_w - T_{res}}$$

$$x_D = x / L$$

$$t_D = \frac{\rho_w c_w}{((1 - \phi)\rho_s C_s + \phi(1 - S_{or})\rho_w C_w + \phi S_{or}\rho_s C_s)} \frac{ut}{L}$$

and Peclet's number, which is the ratio of heat transport by convection to heat transport by conduction, is defined by

$$N_{pe} = \frac{\rho_w c_w uL}{\lambda_T}$$

The solution of the Equation (6.8) has the famous form of error function in which the magnitude of Peclet's number determines the sharpness of the temperature front. Where the smaller Peclet's number cause the temperature front to be tilted.

When assuming Buckley leveret displacement by injecting fluid, the retardation of thermal front with respect to the injected front is expressed in the following formula (Lake, 1989)

$$v_{HW} = \frac{u_1}{\phi} \frac{1}{1 + D_{HW}} \quad (6.9)$$

$$\text{where, } D_{HW} = \left(\frac{1 - \phi}{\phi}\right) \frac{M_{TS}}{M_{T1}}$$

For the case of incompressible flow the heat fronts propagate slower than tracer fronts that would have velocity $\frac{u_1}{\phi}$. This slower propagation occurs because the heat capacity of solids and injection phase as included in Equation (6.9).

M_{TS} volumetric heat capacity of solids

M_{T1} volumetric heat capacity of phase 1

u_1 velocity of phase 1
 v_{HW} velocity of cold front

For our case study the calculated retardation factor is:

$$D_{HW} = \left(\frac{1-\phi}{\phi} \right) \frac{M_{TS}}{M_{T1}} \rightarrow = \frac{1-0.3}{0.3} \frac{0.2117 \times 165.43}{1.000454 \times 64.2} = 1.27$$

$$v_{HW} = \frac{u_1}{\phi} \frac{1}{1+D_{HW}} = \frac{u_1}{\phi} \frac{1}{1+1.27} = \frac{u_1}{\phi} \frac{1}{2.27}$$

This means that temperature front has a retardation of 2.27 with respect to injection front. This formulation is derived for the case of no heat transfer to overburden and underburden. As shown below, the result is approximately consistent with UTCHEM.

The numerical solution of heat transfer which is implemented in UTCHEM is based on the general energy balance equation (UTCHEM's technical manual, 2000). In contrast to the analytical solution, in the numerical solution the heat transfer to the overburden and underburden can be included. Later on we will see that the heat transfer to the over/underburden can change the temperature profile and has a big effect on the temperature propagation.

The overall energy balance equation in UTCHEM is given by Equation (4.9).

Each term in this equation is defined in the nomenclature section.

In the case study, we assumed a reservoir initially at temperature 160°F subjected to water flooding. The temperature of injected water is assumed 60°F. The reservoir characteristics and conditions are given in Tables 6.5-6.7.

Using energy balance option, the following parameters need to be input for each reservoir:

DENS = Reservoir density

CRTC = Reservoir thermal conductivity
 CVSPR = Reservoir rock heat capacity
 CVSPL(L)= Phase l heat capacity
 IHLOS = flag indicating if the heat loss calculation to overburden and underburden rock is considered or not.
 IANAL = Flag indicating if the temperature profile is calculated from analytical solution (only 1 D).
 TCONO = Thermal conductivity of overburden rock.
 DENO = Density of overburden rock.
 CVSPO = Heat capacity of overburden rock.
 TCONU = Thermal conductivity of underburden rock.
 DENU = Density of underburden rock.
 CVSPU = Heat capacity of underburden rock.

These flags, as used in the INPUT file, are introduced below:

```

CC
CC INITIAL TEMPERATURE
*--- TEMPI (F)
    160.0
CC
CC ROCK DENSITY, CONDUCTIVITY, HEAT CAPACITY
*---- DENS      CRTC   CVSPR   CVSPL(1) CVSPL(2) CVSPL(3)
    165.43      40.001  0.2117   1.000454  0.5000227  1.000454
CC
CC HEAT LOSS FLAG, ANALYTICAL SOLUTION
*---- IHLOS   IANAL
    1         0
CC
CC OVERBURDEN AND UNDERBURDEN ROCK THERMAL PROPERTIES
*--- TCONO   DENO   CVSPO   TCONU   DENU   CVSPU
    35.      165.43  0.2117  35.     165.43  0.2117
  
```

The above quantities are in English units.

Comparison of Figure 6.7 with Figure 6.8 shows that including the heat transfer to over/underburden changes the heat front profile both qualitatively and quantitatively. Thus, in case of heat transfer to overburden and underburden the S shape temperature

front approaches a linear behavior while the temperature at the injection side at any time remains constant.

As we discussed before, the delay in the temperature front for the case of no heat transfer to over/underburden can be calculated with Equation 6.9.

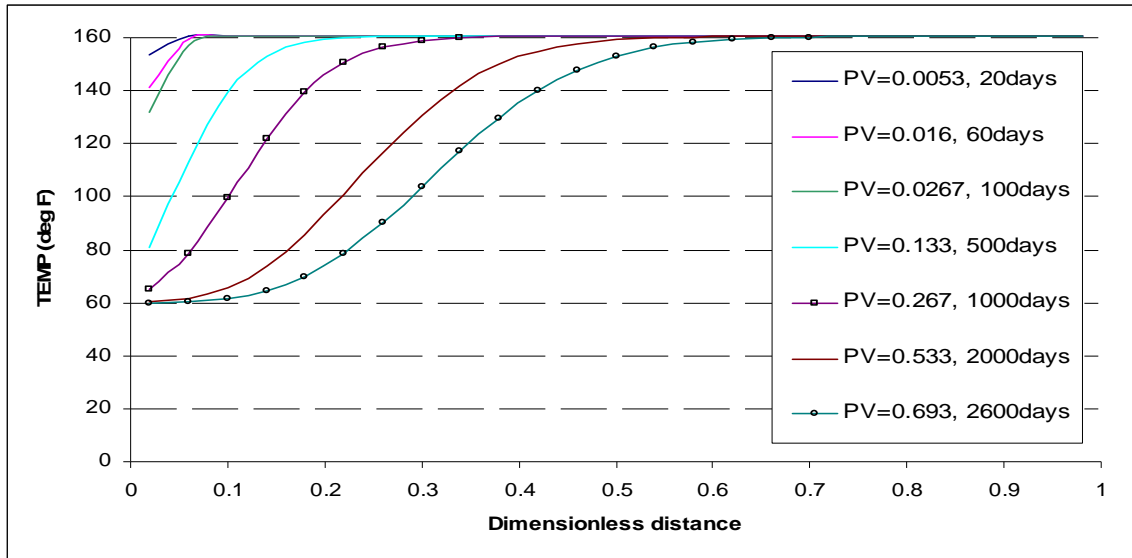


Figure 6.7 Temperature distribution in the reservoir, no heat transfer to overburden/underburden (numerical dispersion = 13ft)

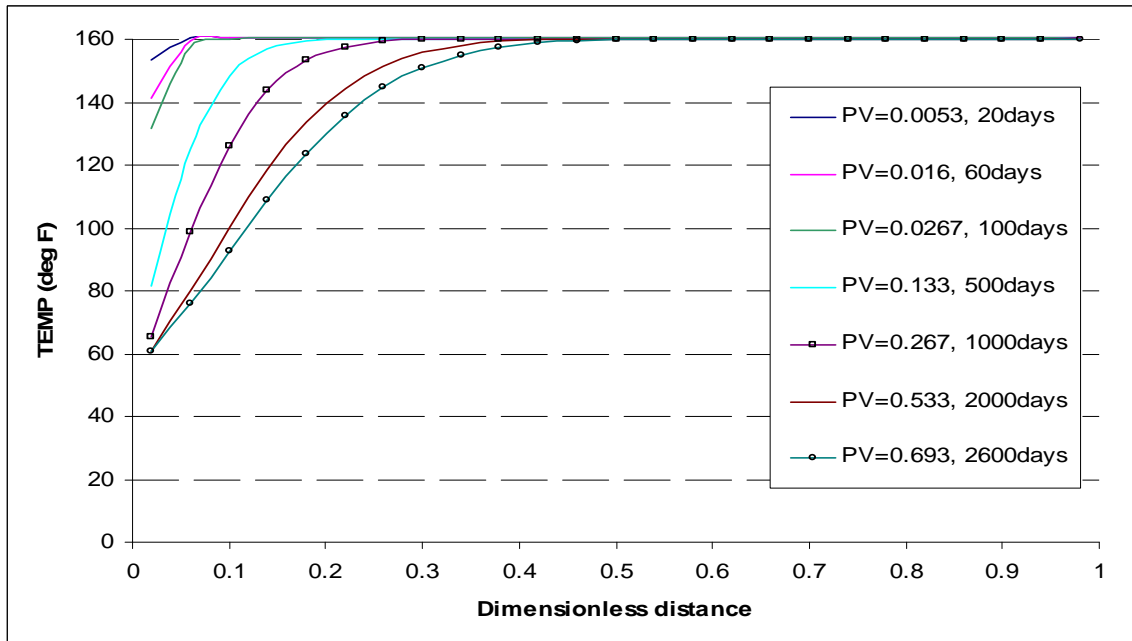


Figure 6.8 Temperature distribution in the reservoir with heat transfer to overburden/underburden (numerical dispersion = 13ft)

Table 6.6 Reservoir conditions (for 1D and layered cases) and characteristics (1D case)

Case	T(°F)	P (psi)	ϕ (%)	$\Delta X, \Delta Y, \Delta Z$ (ft)	α_l, α_v (ft)	$K_{x,y,z}$ (mDarcy)	L (ft)	S_{or}	S_{wt}	S_{wi}
A	160	3771	30	100*25, 100, 50	0, 0	300	2500	0.28	0.147	0.72
B	160	3771	30	100*25, 100, 50	0, 0	300	2500	0.28	0.147	0.72
C	160	3771	30	100*25, 100, 50	0, 0	300	2500	0.28	0.147	0.72
D	160	3771	30	100*25, 100, 50	0, 0	300	2500	0.28	0.147	0.72

Table 6.7 Injected seawater properties

Case study	SRB type	SRB (mg/l)	Sulfate (mg/l)	Seawater (ft ³ /day)
A-D	Thermophiles	0.001	2700	1000

Figures 6.9, 6.10 and 6.11 show the temperature distribution in the same reservoir at different times and variable physical dispersivity (13-28 ft) while there is no heat transfer to over/underburden. In the same graphs, a nonreacting tracer which moves with injection front is sketched to show the delay in temperature front with respect to injection front. The temperature fronts are not affected by the physical dispersion while the concentration fronts are affected.

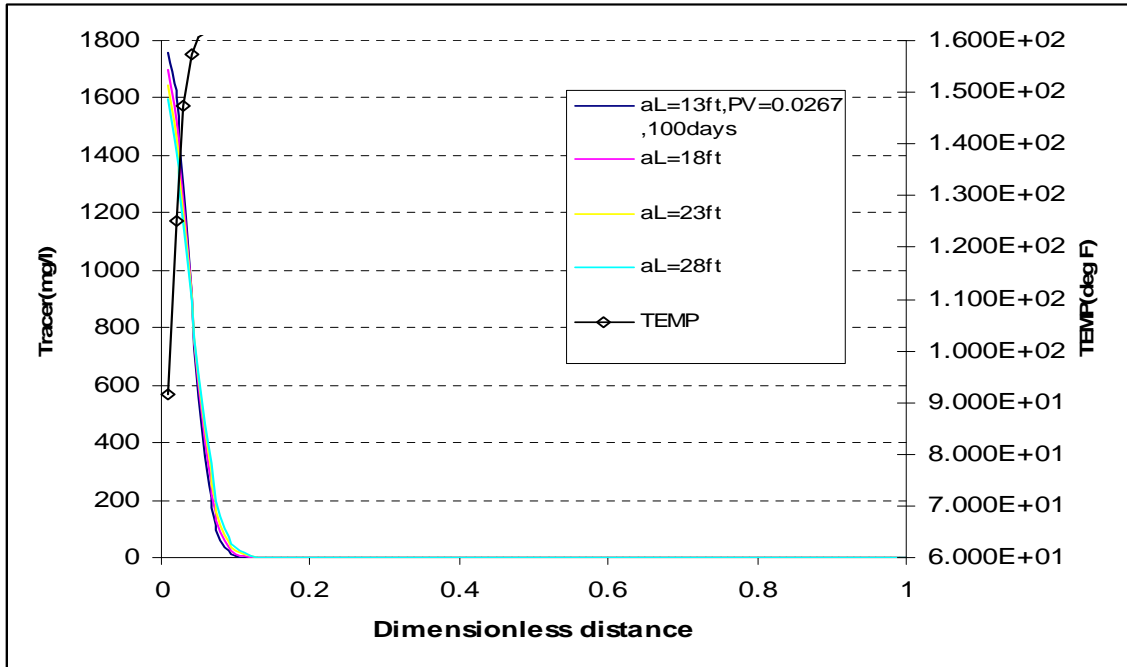


Figure 6.9 Temperature and concentration distribution in the reservoir, no heat transfer to over/underburden, variable longitudinal dispersivity= 13-28 ft (after 100 days)

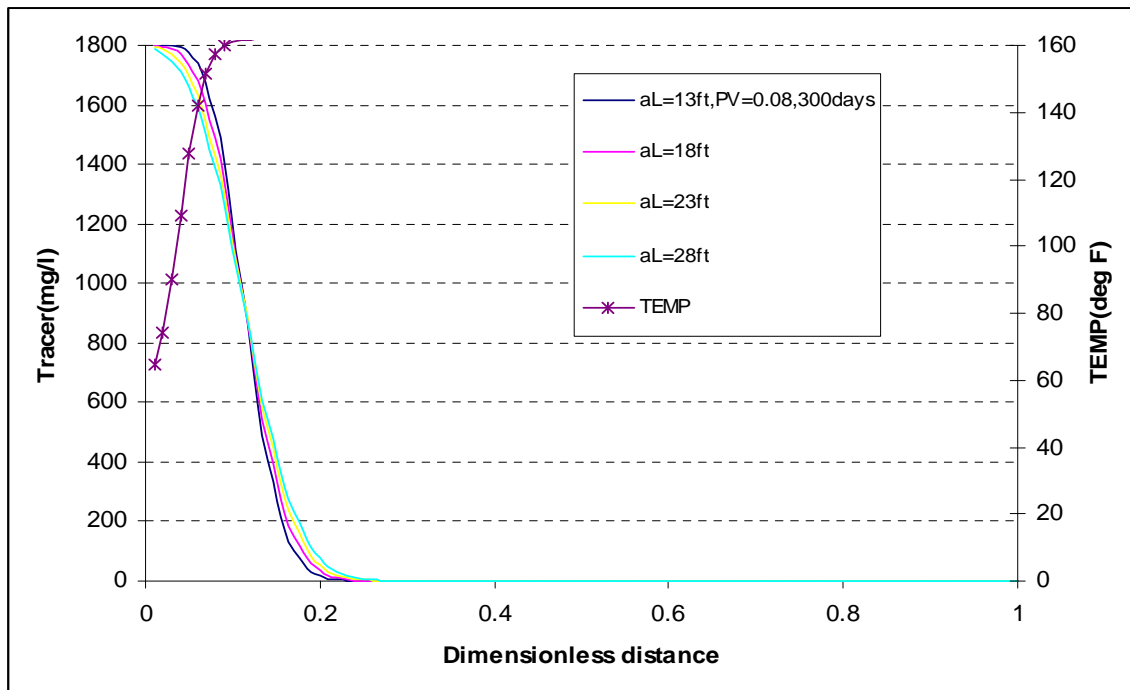


Figure 6.10 Temperature and concentration distribution in the reservoir, no heat transfer to overburden/underburden, variable longitudinal dispersivity = 13-28 ft (after 300 days)

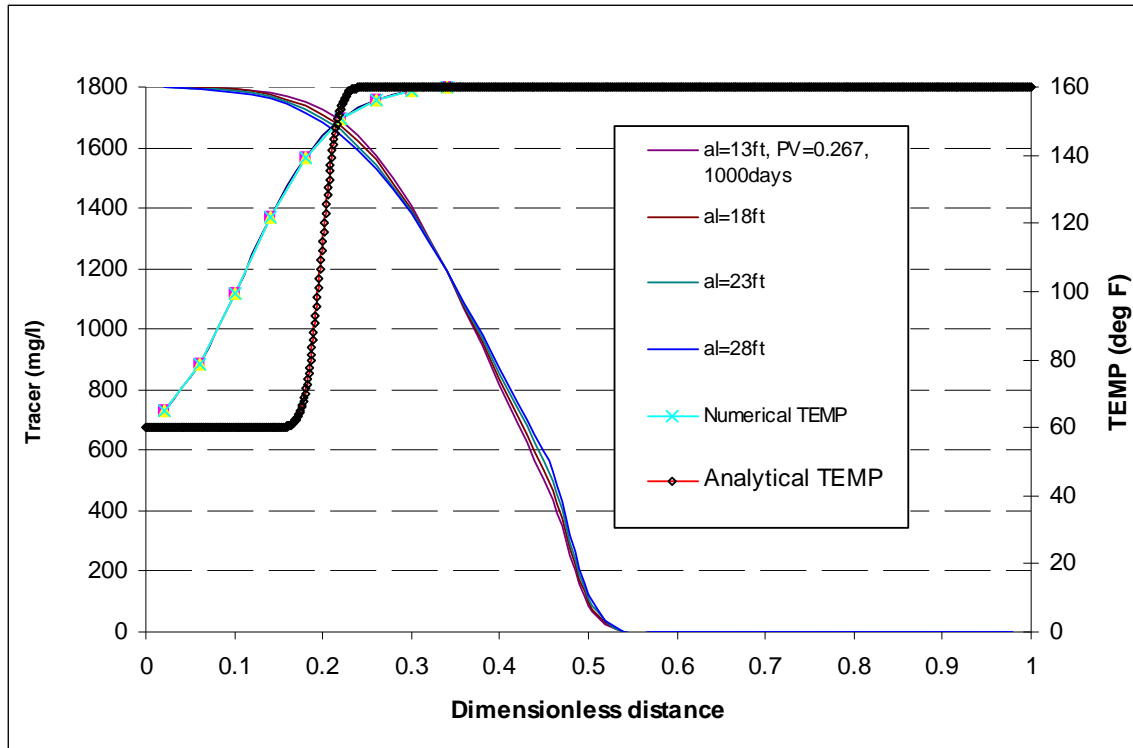


Figure 6.11 Temperature and concentration distribution in the reservoir, no heat transfer to overburden/underburden, variable longitudinal dispersivity= 13-28 ft (after 1000 days)

Several cases were studied to investigate the effects of pertinent parameters on the propagation of temperature front in water injected reservoirs. The reservoir characteristics and initial conditions are given in Tables 6.5, 6.6, and 6.7. Parameters related to heat capacity of the rock and flowing phase, density of the rock and thermal conductivity of the reservoir for each case are provided in Table 6.8 and 6.9.

As indicated in Figure 6.12 and Table 6.8 (con-0.5ref, con-ref, con-2ref), for the case of no heat transfer to over/underburden, changing the thermal conductivity of the reservoir does not affect the temperature distribution in the reservoir. In calculation of the heat transfer in the reservoir, the heat conduction in the direction of flow is negligible compared to convection.

Three cases were simulated to investigate the effect of heat capacity of the flowing phase on the temperature propagation in the reservoir, (Table 6.8, cvspl-ref, cvspl-0.5ref, and cvspl-2ref). Figure 6.13 shows that decreasing of the heat capacity of the flowing phase will retard the temperature front with respect to injection front (Tracer profile). This behavior is expected (Equation 6.9), where decreasing heat capacity of the flowing phase will increase the retardation factor of heat front. On the other hand, Figure 6.14 shows that increasing heat capacity of the rock (Table 6.8, cases cvspr-ref, cvspr-0.5ref, and cvspr-2ref) has the same effect as decreasing heat capacity of the flowing phase. Equation (6.9) shows that increasing heat capacity of the rock and decreasing heat capacity of the flowing phase will increase the retardation of heat with respect to injection front. Hence, for the discussed cases the retardation factors are calculated with the same procedure as discussed above while for the reference cases (Table 6.8, cvspl-ref and cvspr-ref) is equal to 2.27, for cases (cvspl-0.5ref and cvspr-2ref) equal to 3.54, and for cases (cvspl-2ref and cvspr-0.5ref) equal to 1.63.

In DHW-ref, DHW-0.5ref, and DHW-2ref simulations (Table 6.8), as reflected in Figure 6.15, simultaneous changes of heat capacity of rock and flowing phase while their ratios remains constant, does not affect the temperature front with the reference case. We expect the curves to be overlapped because the calculated retardation factors are the same as 2.27.

Changing the Darcy's velocity will change the total convected heat, as shown in Figure 6.16, decreasing of the velocity results in slower heat propagation (Table 6.8, cases T(Tr)-u-0.5ref, T(Tr)-u-ref, and T(Tr)-u-2ref).

Table 6.8 Variation of thermal properties of rock and fluids in the reservoir (abbreviations are given below)

Case	A	B	C	D	E	U
con-0.5ref	165.43	20	0.2117	1	0.5	0.2
con-ref	165.43	40	0.2117	1	0.5	0.2
con-2ref	165.43	80	0.2117	1	0.5	0.2
cvspl-ref	165.43	40	0.2117	0.5	0.5	0.2
cvspl-ref	165.43	40	0.2117	1.0	0.5	0.2
cvspl-ref	165.43	40	0.2117	2.0	0.5	0.2
cvspr-ref	165.43	40	0.10585	1.0	0.5	0.2
cvspr-ref	165.43	40	0.2117	1.0	0.5	0.2
cvspr-ref	165.43	40	0.4234	1.0	0.5	0.2
DHW-0.5ref	165.43	40	0.10585	0.5	0.5	0.2
DHW-ref	165.43	40	0.2117	1.0	0.5	0.2
DHW-2ref	165.43	40	0.4234	2.0	0.5	0.2
T(Tr)-u-0.5ref	165.43	40	0.2117	1	0.5	0.1
T(Tr)-u-ref	165.43	40	0.2117	1	0.5	0.2
T(Tr)-u-2ref	165.43	40	0.2117	1	0.5	0.4

A= DENS = Reservoir density (lb/ft³)

B= CRTC = Reservoir thermal conductivity (Btu (day-ft-°F)-1)

C= CVSPR = Reservoir rock heat capacity (Btu (lb-°F)-1)

D, E, CVSPL(1,2)= Phase (water, oil) heat capacity (Btu (lb-°F)-1)

U= Darcy velocity, ft/day

Table 6.9 Thermal properties of rock and fluids in the reservoir (abbreviations are given below)

DENSE	CRTC	CVSPR	CVSPL(1)	CVSPL(2)	CVSPL(3)
165.43	40	0.2117	1	0.5	1
TCONO	DENO	CVSPO	TCONU	DENDU	CVSPU
35	165.43	0.2117	35	165.43	0.2117

DENSE = Reservoir density (lb/ft³)

CRTC = Reservoir thermal conductivity (Btu (day-ft-°F)-1)

CVSPR = Reservoir rock heat capacity (Btu (lb-°F)-1)

CVSPL(L)= Phase L heat capacity (Btu (lb-°F)-1)

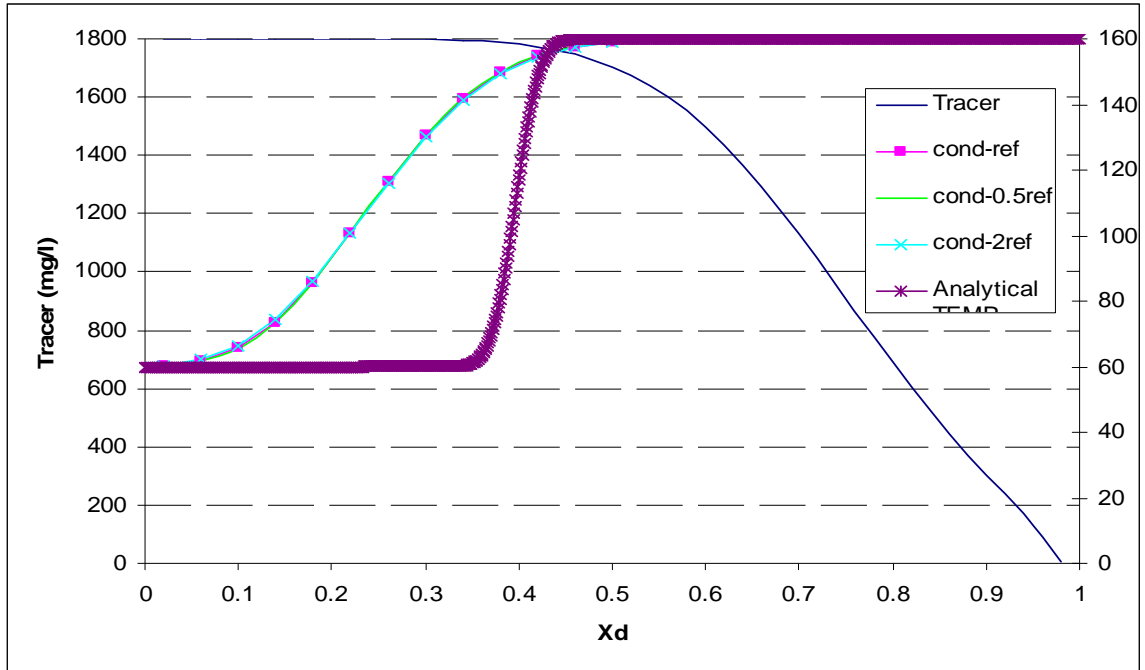


Figure 6.12 Tracer and temperature profiles in a reservoir for the case of no heat transfer to overburden/underburden with variable reservoir thermal conductivity (2000 days)

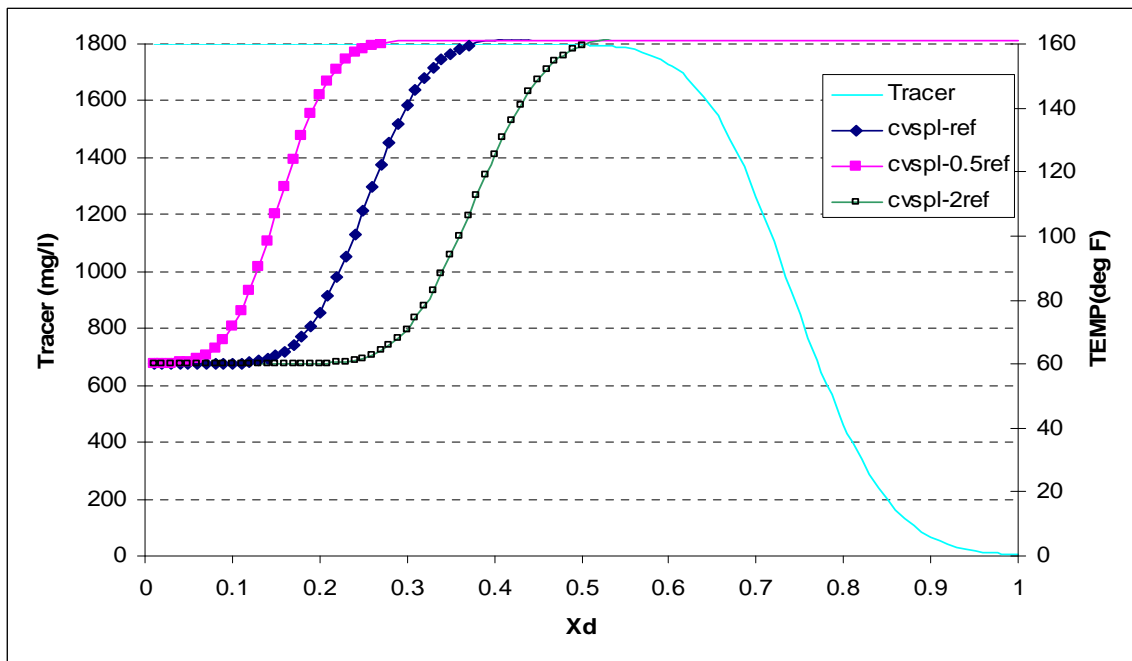


Figure 6.13 Tracer and temperature profiles in a reservoir for the case of no heat transfer to overburden/underburden with variable flowing phase heat capacity (2000 days)

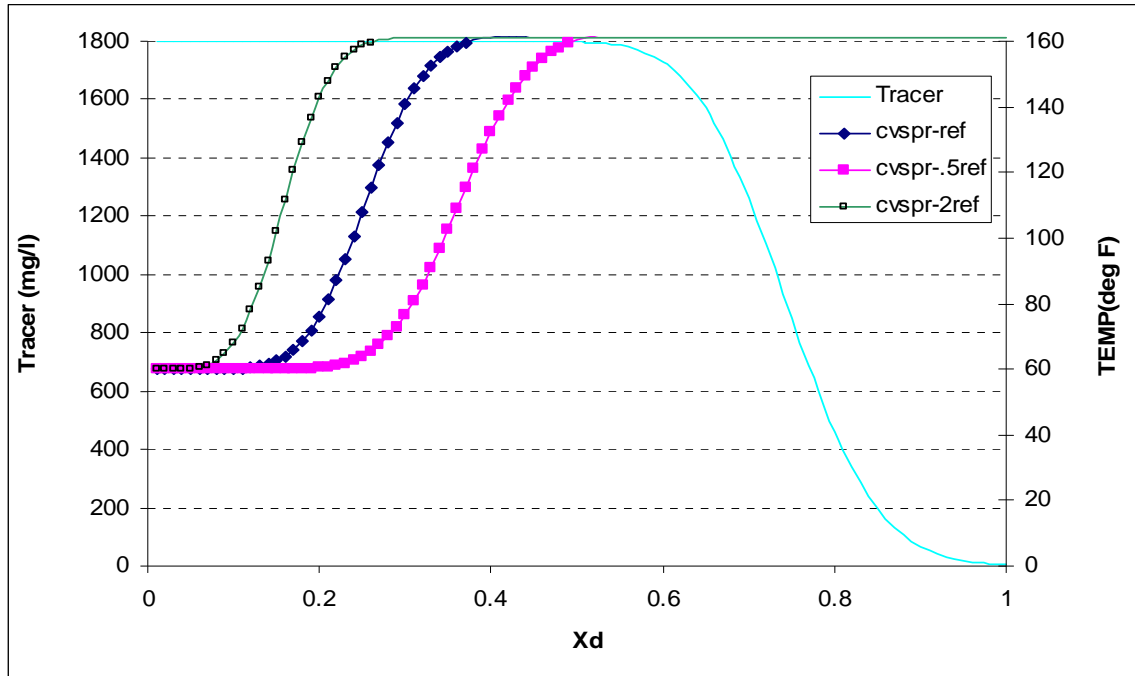


Figure 6.14 Tracer and temperature profiles in a reservoir for the case of no heat transfer to overburden/underburden with variable rock heat capacity (2000 days)

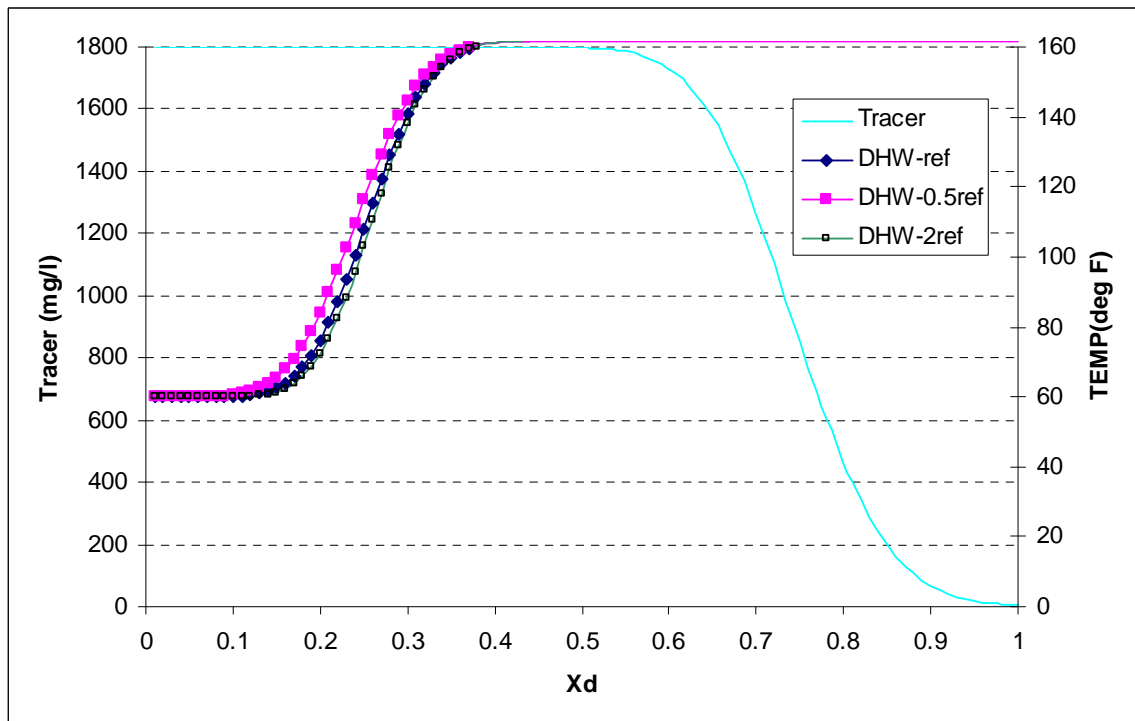


Figure 6.15 Tracer and temperature profiles in a reservoir for the case of no heat transfer to overburden/underburden with variable rock and flowing phase heat capacity (2000 days)

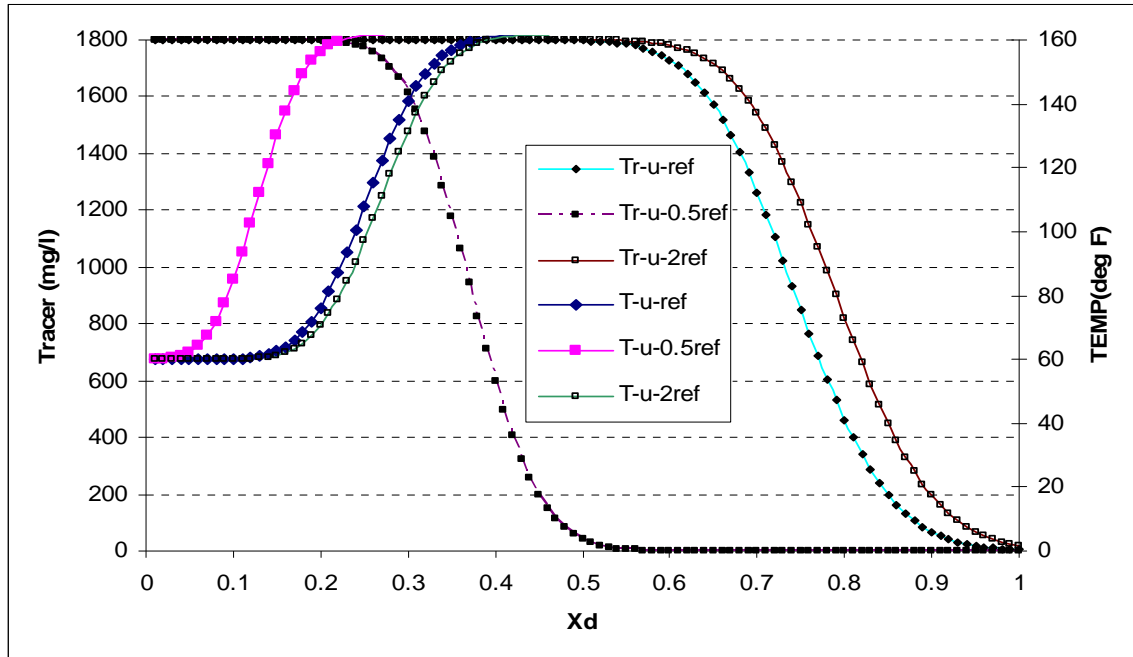


Figure 6.16 Tracer and temperature profiles in a reservoir for the case of no heat transfer to overburden/underburden with variable Darcy's velocity (2000 days)

6.7.1.2 Vertical Distribution of Temperature Profile in the Reservoirs

Convection and conduction are two prevailing mechanisms of heat transfer in the reservoir. In derivation of the general energy balance equation, usually the heat transfer in the direction of flow is considered only convection while in the direction perpendicular to the flow it is assumed just conduction. Although variations of pertinent parameters can change the lag in the temperature front with respect to injection front, increasing of thermal conductivity of the media (rock and oil) will give a more sharp temperature distribution in layered reservoirs. For a 1D reservoir, when there is no heat transfer to overburden/underburden, the thermal conductivity does not have any effect on temperature distribution if the reservoir is thin. The following study shows how, at certain conditions for the layered reservoir, we can approach a vertical equilibrium in temperature distribution. For these simulations, reservoir characteristics and conditions

are defined in Tables 6.6 and 6.14, while, the parameters related to heat transfer in the reservoir for each case are given in Table 6.10 and 6.11.

Figures 6.17, 6.18, and 6.19 show cases in which there is no heat transfer to overburden/underburden. Considering Figure 6.17 (Table 6.10, case A1) as a reference, increasing of the thermal conductivity of the reservoir (Figure 6.19, Table 6.10, case A2) results in more homogenous vertical distribution of temperature while decreasing of thermal conductivity (Figure 6.18, Table 6.10, case A2) has the inverse effect.

In another set of simulations, we include heat transfer to overburden/underburden, cases B1, B2, B3 (Table 6.10). Comparing Figures 6.20, 6.21, and 6.22 with Figures 6.17, 6.18, and 6.19, respectively, will give two results. First, including heat transfer to overburden/underburden will result in more lag in the observed temperature front, and second, more homogeneity in the vertical temperature distribution. The effect of simultaneous heat transfer to overburden/underburden and increasing of the thermal conductivity of the reservoir results in more sharpness in vertical temperature distribution (comparing Figure 6.22 with 6.17).

The other set of simulations (Table 6.10, cases C1, C2, and C3) which their results are reflected in Figures 6.23-6.25, show that for a reservoir with constant thermal conductivity, increasing the rate of heat transfer to overburden/underburden will results in more lag in temperature front and also more homogeneous vertical temperature distribution.

Further investigation of the temperature distribution are given in Figures 6.26 and 6.27. These figures illustrate that in the case of an 8-layer reservoir with stochastic permeability and porosity distributions (the reservoir characteristics are given in

Appendix D). We can conclude when vertical equilibrium in flow is approached we also approach vertical equilibrium in temperature distribution.

Table 6.10 Variation of the thermal properties of rock and fluids in the reservoir (abbreviations are given below)

Case	A	B	C	D	E	F	G	H	I	J	K
A1(REF)	165.43	40	0.2117	1	0.5	0	0	0	0	0	0
A2	165.43	20	0.2117	1	0.5	0	0	0	0	0	0
A3	165.43	80	0.2117	1	0.5	0	0	0	0	0	0
B1(REF)	165.43	40	0.2117	1	0.5	35	165.43	0.2117	35	165.43	0.2117
B2	165.43	20	0.2117	1	0.5	35	165.43	0.2117	35	165.43	0.2117
B3	165.43	80	0.2117	1	0.5	35	165.43	0.2117	35	165.43	0.2117
C1(REF)	165.43	40	0.2117	1	0.5	17.5	165.43	0.2117	35	165.43	0.2117
C2	165.43	40	0.2117	1	0.5	35	165.43	0.2117	17.5	165.43	0.2117
C3	165.43	40	0.2117	1	0.5	70	165.43	0.2117	70	165.43	0.2117

A= DENS = Reservoir density (lb/ft³)

B= CRTC = Reservoir thermal conductivity (Btu (day-ft-°F)-1)

C= CVSPR = Reservoir rock heat capacity (Btu (lb-°F)-1)

D, E, CVSPL(1,2)= Phase (water, oil) heat capacity (Btu (lb-°F)-1)

F= TCONO = Thermal conductivity of overburden rock (Btu (day-ft-°F)-1)

G= DENO = Density of overburden rock (lb/ft³)

H= CVSPO = Heat capacity of overburden rock (Btu (lb-°F)-1)

I= TCONU = Thermal conductivity of underburden rock (Btu (day-ft-°F)-1)

J= DENU = Density of underburden rock (lb/ft³)

K= CVSPU = Heat capacity of underburden rock (Btu (lb-°F)-1)

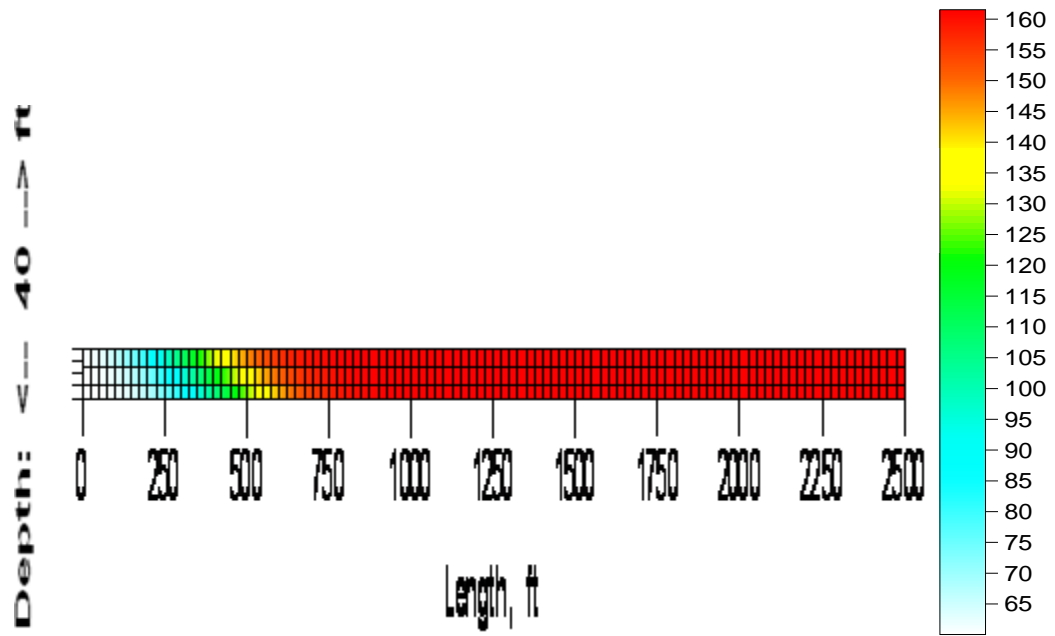


Figure 6.17 Temperature ($^{\circ}\text{F}$) distribution in a layered (3 layers) reservoir after 1000 days (case A1)

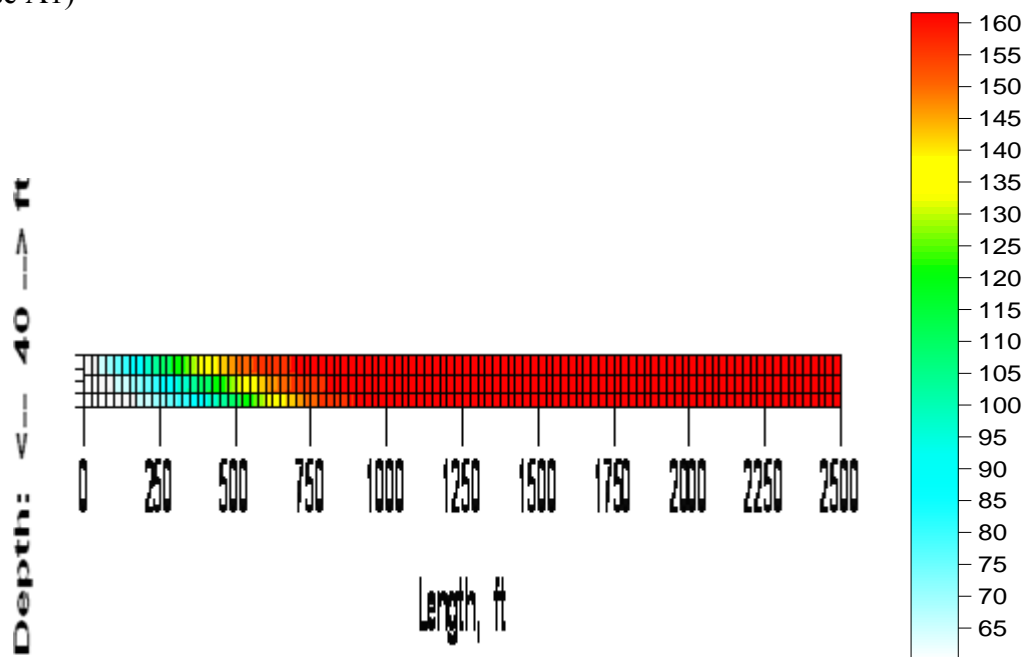


Figure 6.18 Temperature ($^{\circ}\text{F}$) distribution in a layered (3 layers) reservoir after 1000 days (case A2)

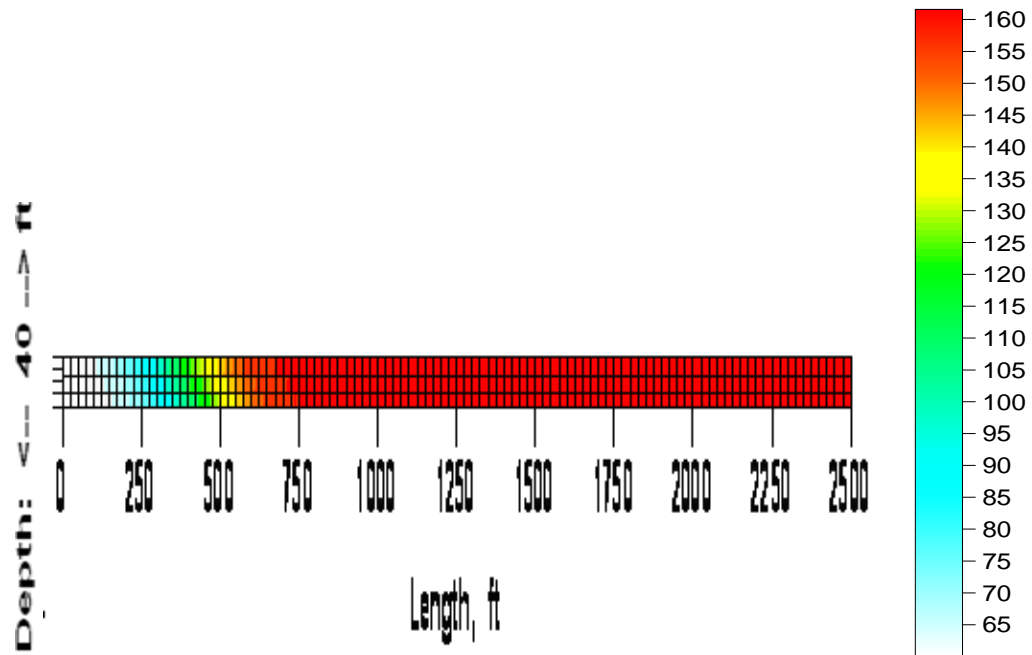


Figure 6.19 Temperature ($^{\circ}\text{F}$) distribution in a layered (3 layers) reservoir after 1000 days (case A3)

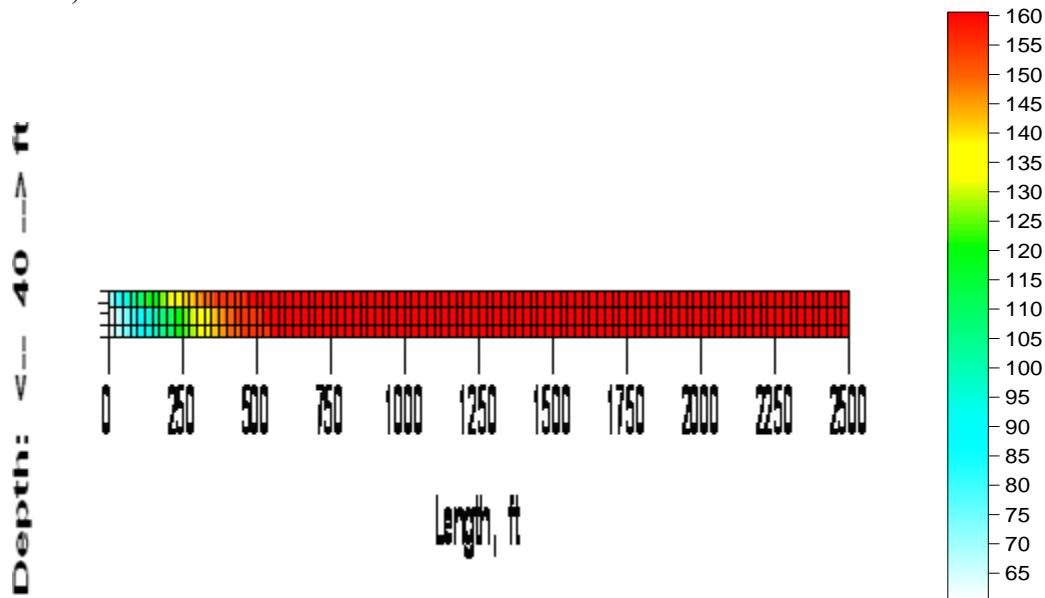


Figure 6.20 Temperature ($^{\circ}\text{F}$) distribution in a layered (3 layers) reservoir after 1000 days (case B1)

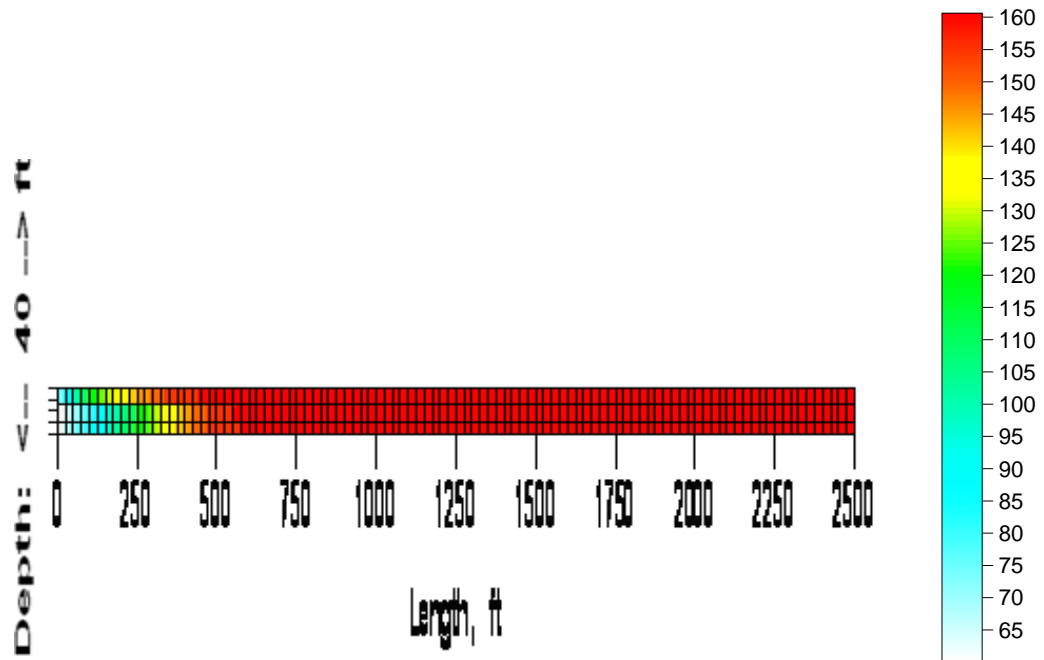


Figure 6.21 Temperature ($^{\circ}\text{F}$) distribution in a layered (3 layers) reservoir after 1000 days (case B2)

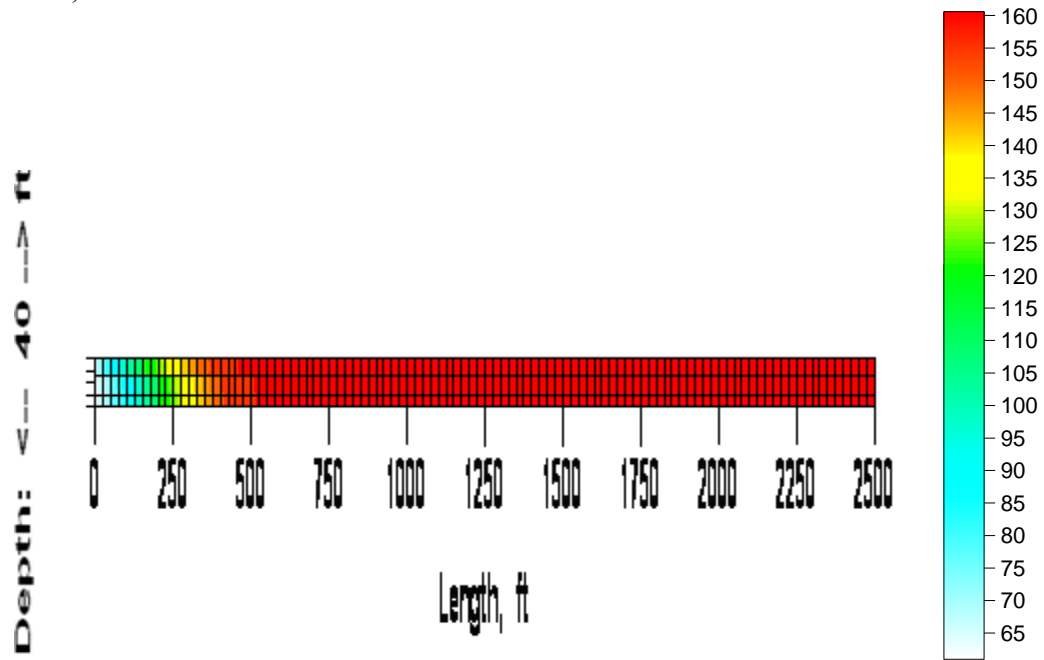


Figure 6.22 Temperature ($^{\circ}\text{F}$) distribution in a layered (3 layers) reservoir after 1000 days (case B3)

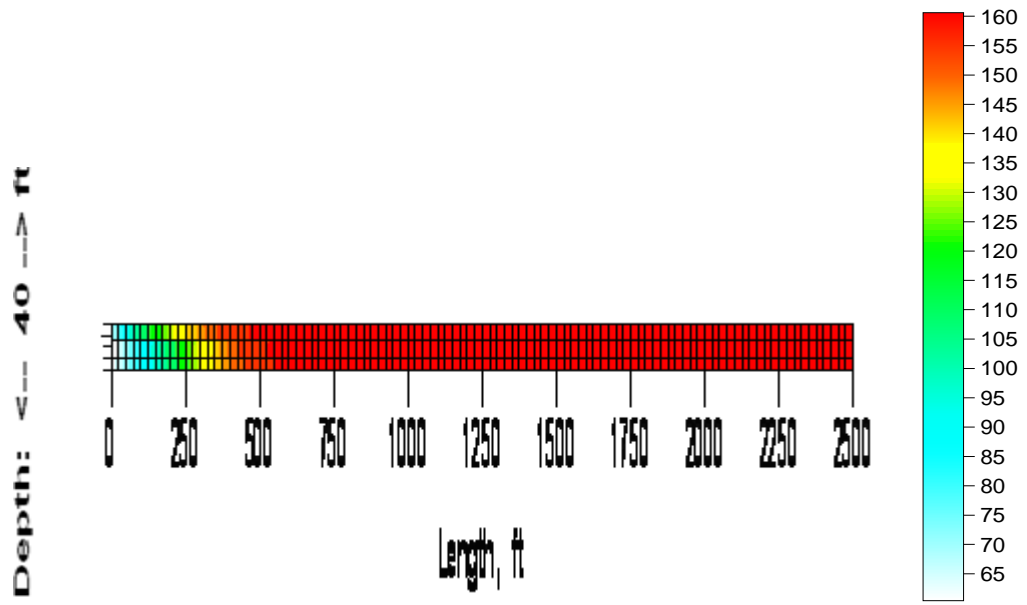


Figure 6.23 Temperature ($^{\circ}\text{F}$) distribution in a layered (3 layers) reservoir after 1000 days (case C1)

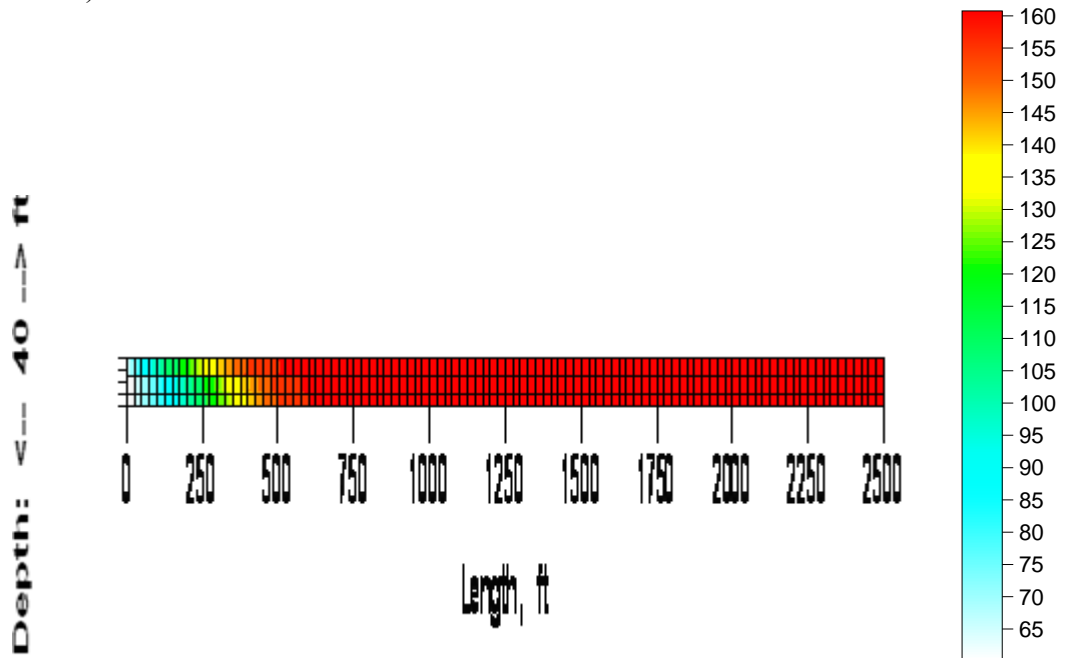


Figure 6.24 Temperature ($^{\circ}\text{F}$) distribution in a layered (3 layers) reservoir after 1000 days (case C2)

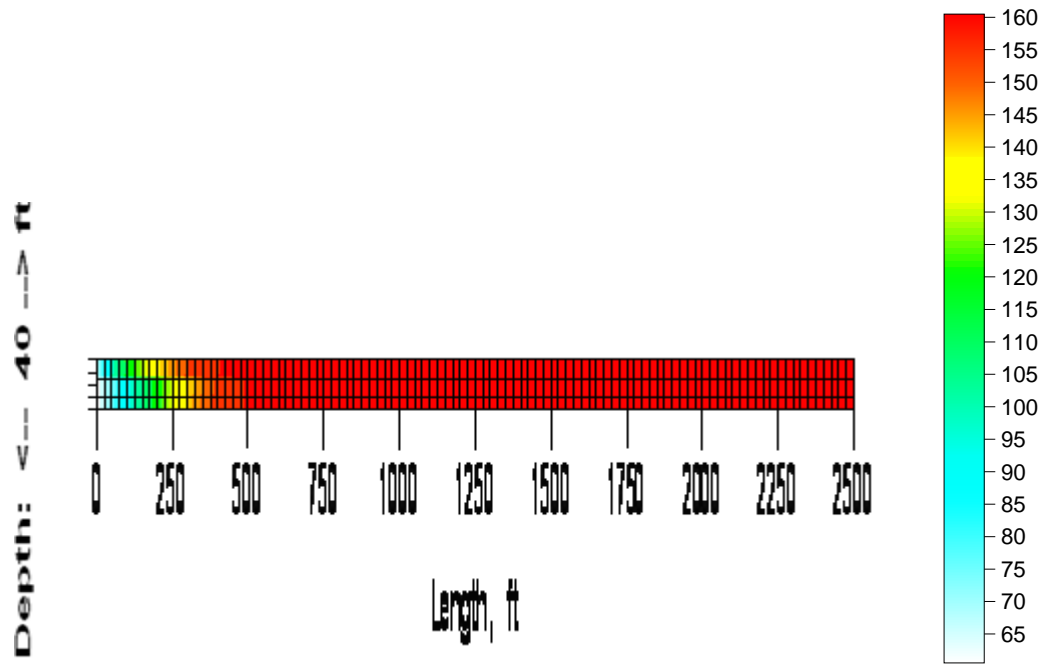


Figure 6.25 Temperature ($^{\circ}\text{F}$) distribution in a layered (3 layers) reservoir after 1000 days (case C3)

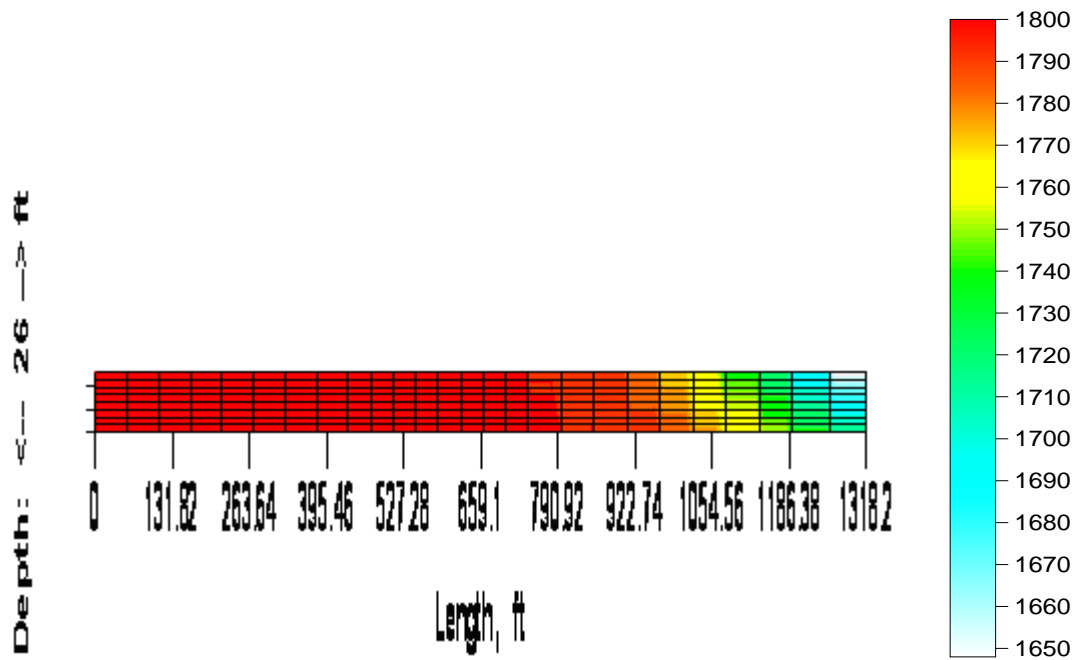


Figure 6.26 Tracer concentration (mg/l) in the reservoir after 1000 days

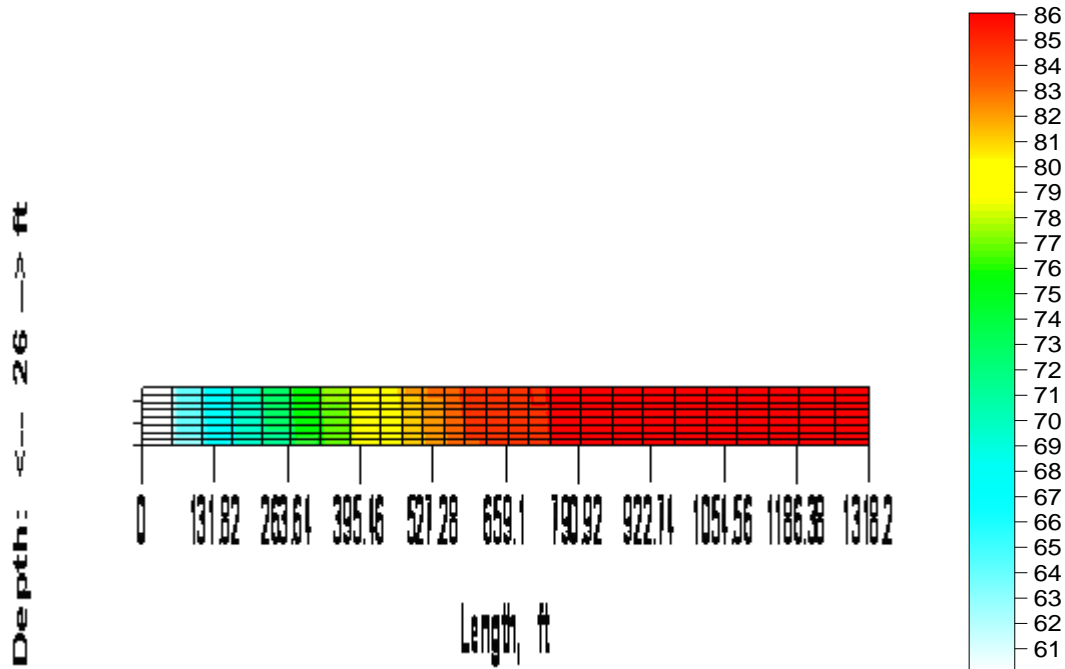


Figure 6.27 Temperature ($^{\circ}\text{F}$) distribution in a layered (8-layers) reservoir after 1000 days

6.7.2 Effect of Dispersivity of the Media on Concentration Profiles

In the previous section, we showed that the effect of dispersivity on the concentration profiles is to broaden the distribution of a reference tracer in the porous media. We also investigated the effects of the heat transfer to the over/underburden on the propagation of temperature in the reservoirs. Several cases were considered and the results were reflected in respective figures.

Here, we will show the effects of the essential parameters on the reservoir souring prediction. As in case C in Table 6.11 and Figure 6.28, the effect of overall dispersivity (the sum of the physical and numerical dispersion) on the produced H_2S for the thermophilic SRB (Table 3.1) is to increase the band of production slightly and its effect on the peak of H_2S concentration is not too much. Figure 6.28 indicates that changing the dispersivity of the media from 13 ft to 28 ft, will increase the hydrogen sulfide production

band from 0.55-1.0 PV to 0.45-1.2 PV. This observation can be attributed to the effect of dispersion, which extends the length of mixing zone, and consequently, provide a larger range available for the production of hydrogen sulfide. Later, we will show that the maximum peak in the H₂S concentration depends on the available nutrients while other parameters are considered constant.

From the basic concepts of flow in porous media, we know that the length of mixing zone for a 1D flow is $\Delta x = 3.625\sqrt{v\alpha_L t}$, where, v , α_L and t are interstitial velocity, longitudinal dispersion, and time, respectively. Since reactions take place, the band of production of H₂S is not directly proportional to the length of mixing zone, but increases with the mixing zone. The peak of H₂S concentration at fixed temperature is determined by the available nutrients which have been investigated in the following.

On the other hand, the dispersivity affects both the peak (from 1.8 to 6.5 mg/l in aqueous phase in production well) and the band of the produced H₂S by mesophiles (Case D in Table 6.11 and Table 3.1, as illustrated in Figure 6.29). Figure 6.29 shows that the variation of the overall dispersivity of the media from 13 ft to 28 ft, will change the maximum concentration of produced H₂S from 1.8 to 6.5 mg/l, and the band of production from 0.58-0.95 PV to 0.45-1.2 PV. This behavior can also be attributed to the dispersion. The smaller dispersion causes the mixing zone of activation of mesophiles (Table 3.1) to be shortened and hydrogen sulfide will be produced in a smaller range of temperature (with respect to the thermophiles, Table 3.1). The produced hydrogen sulfide will distribute in the reservoir with time and the observed peak of H₂S will decrease. Due to the reaction there is no direct quantitative relation between observed band and longitudinal dispersivity.

Referring to our previous results, in the case of a larger mixing zone (larger dispersivity cause greater distribution of species) there is more opportunity for the biological reactions to take place and more H₂S will produce. Thus, production of hydrogen sulfide resulting from mesophiles is limited by the temperature distribution in the reservoir. For this case, we expect the biological reactions to happen in a region which is near to the cold head rather than the entire reservoir. On the other hand, for the thermophiles we expect a larger region for the production of H₂S, as long as the limiting species (nitrate and phosphate) are available, the reaction will take place. In our study, the biological reaction will not happen in the entire reservoir and after consumption of nutrient in the mixing zone, there is no generation of H₂S.

The Damkohler's number (N_{Da}) in Table 6.11 shows the ratio of reaction rate to bulk fluid rate ($N_{Da} = \frac{\phi KL}{Ua}$, where ϕ is porosity of the media, K reaction rate constant (time^{-1}), L the media length (L), and Ua is the Darcy velocity in (L/time)). As indicated in Table 6.11, the higher Damkohler's number results in greater maximum in the peak of observed H₂S in the producer (in calculation of Damkohler's number for the biological reactions we assumed that maximum growth rate has the same role as the kinetics constant for the first order chemical reactions).

The Peclet's number (N_{Pe}) in Table 6.11, is the ratio of heat transport by convection to heat transport by conduction, is defined by $N_{Pe} = \frac{\rho_w c_w u L}{\lambda_T}$. Where, ρ_w , c_w , u , L , and λ_T are water density, water heat capacity, Darcy velocity, media length, and media thermal conductivity, respectively. In these simulations (Table 6.11), we used a constant Peclet's number for heat transport. Both Damkohler's and Peclet's numbers are well defined for

1D flow. For multi-dimensional flow there is no straightforward procedure to calculate them.

Table 6.11 Kinetics and transport properties of six different simulations

u(ft/day)	SRB type	μ_{\max} (1/day)	N_{Da}	Disp. αL(ft)	N_{Pe} (Heat)	Max. H₂S(mg/l) In producer
Case A						
0.95	Thermophile	0.693	1823	0	1111.5	37
0.95	Thermophile	0.0462	121	0	1111.5	37
0.95	Thermophile	0.0231	61	0	1111.5	37
0.95	Thermophile	0.0139	35	0	1111.5	37
0.95	Thermophile	0.00693	18	0	1111.5	37
0.95	Thermophile	0.00139	3.7	0	1111.5	0.032
0.95	Thermophile	0.000693	1.8	0	1111.5	0.0048
Case B						
0.95	Mesophile	0.693	1823	0	1111.5	1.8
0.95	Mesophile	0.0462	121	0	1111.5	0.11
0.95	Mesophile	0.0231	61	0	1111.5	0.014
0.95	Mesophile	0.0138	35	0	1111.5	0.0025
0.95	Mesophile	0.00693	18	0	1111.5	0.0007
0.95	Mesophile	0.00138	3.7	0	1111.5	0.009
0.95	Mesophile	0.000693	1.8	0	1111.5	0.000045
Case C						
0.95	Thermophile	0.693	1823	13	1111.5	37
0.95	Thermophile	0.693	1823	18	1111.5	37
0.95	Thermophile	0.693	1823	23	1111.5	37
0.95	Thermophile	0.693	1823	28	1111.5	37
Continued						
Case D						
0.95	Mesophile	0.693	1823	13	1111.5	1.8
0.95	Mesophile	0.0462	1823	18	1111.5	3.8
0.95	Mesophile	0.0231	1823	23	1111.5	5.4
0.95	Mesophile	0.0138	1823	28	1111.5	6.6

Case A: Grid Block=100×25ft, SRB=Thermophile, physical dispersivity=0.0

Case B: Grid Block=100×25ft, SRB=Mesophile, physical dispersivity=0.0 ft

Case C: Grid Block=100×25ft, SRB=Thermophile, physical dispersivity=0.0-15 ft

Case D: Grid Block=100×25ft, SRB=Mesophile, physical dispersivity=0.0-15 ft

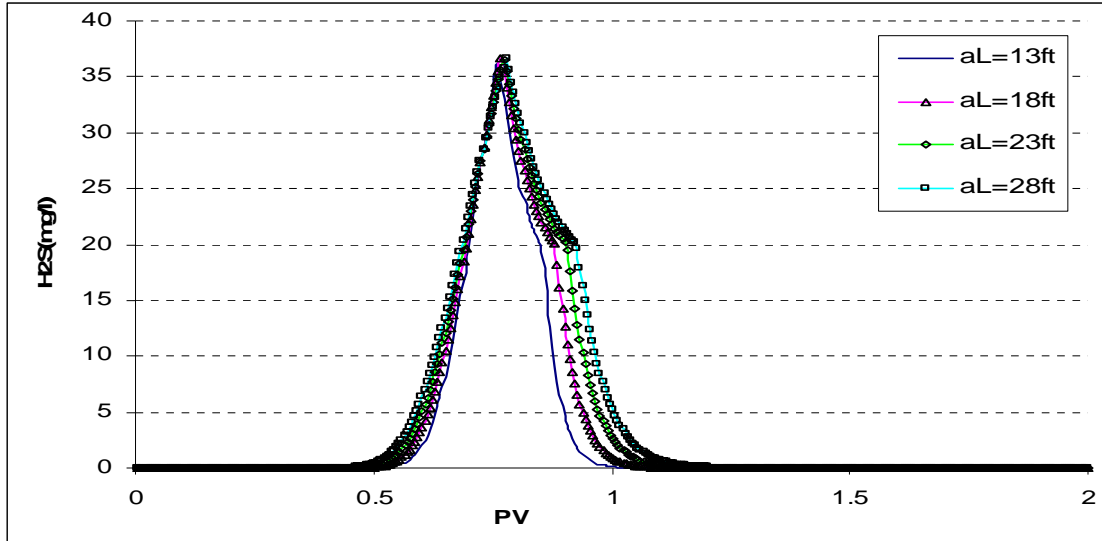


Figure 6.28 Comparison of produced H₂S for case C in Table 6.12 (Bacterial doubling time is one day, $\mu_{\max} = 0.693/\text{day}$)

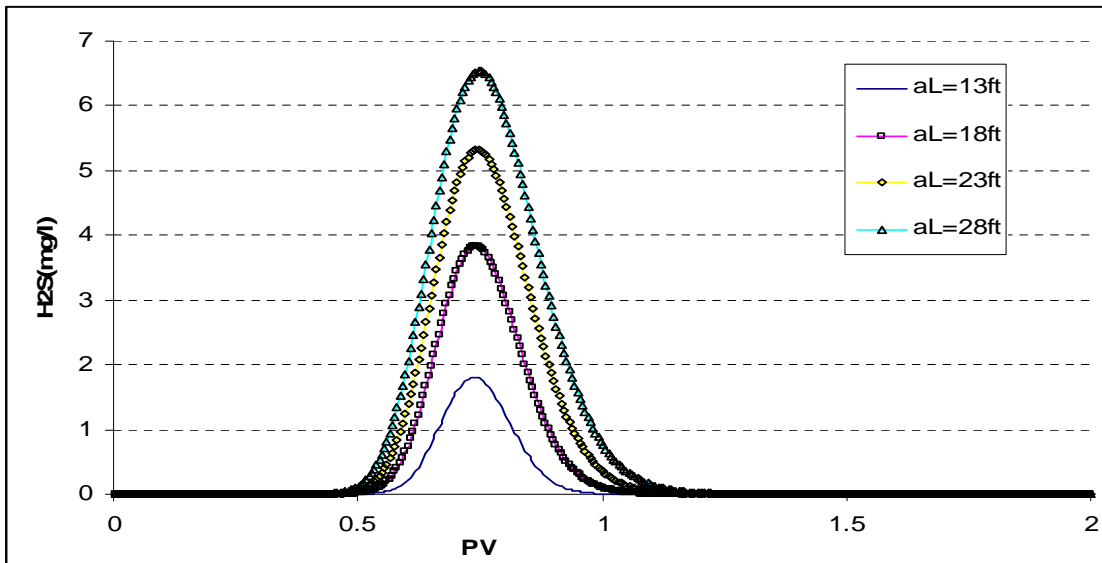


Figure 6.29 Comparison of produced H₂S for case D in Table 6.12 (Bacterial doubling time is one day, $\mu_{\max} = 0.693/\text{day}$)

6.7.3 Effects of Layering on the Hydrogen Sulfide Profile

In this section, cases show the effects of heterogeneity on the profile of the produced hydrogen sulfide. With these results, the behavior of reservoir souring under vertical equilibrium in the reservoirs is explained.

6.7.3.1 Two and Three Layer Reservoirs

In order to investigate the effects of layering on the profile of produced H₂S, four different cases have been run:

Cases 2Lmix5 and 2Lmix6 (Grids (ft); $\Delta X = 100*25$, $\Delta Y = 1*100$, $\Delta Z = 2*25$) are identical except for the dispersivity as indicated in Tables 6.12 and 6.13. All properties related to initial conditions and biological options are reflected in Tables 6.5 and 6.7. The SRB types also are thermophiles (Table 3.1) with maximum rate constant of 0.693/day.

Table 6.12 Reservoir characteristics for example 2Lmix5

2Lmix5	Kx(md)	Ky(md)	Kz(md)	α_l (ft)	α_v (ft)	ϕ	Thickness(ft)
Layer1(L1)	100	100	100	0	0	0.15	25
Layer2(L2)	400	400	400	0	0	0.35	25

Table 6.13 Reservoir characteristics for example 2Lmix6

2Lmix6	Kx(md)	Ky(md)	Kz(md)	α_l (ft)	α_v (ft)	ϕ	Thickness(ft)
Layer1(L1)	100	100	100	10	1	0.15	25
Layer2(L2)	400	400	400	10	1	0.35	25

Cases 3Lmix7 and 3Lmix8 are 3 layers example (Grids (ft); $\Delta X = 100*25$, $\Delta Y = 1*100$, $\Delta Z = 2*15,10$) which are identical except for the dispersivity, as indicated in Tables 6.14 and 6.15. All properties related to initial conditions and biological option are reflected in Tables 6.5 and 6.7. The SRB types also are thermophiles (Table 3.1) with maximum rate constant of 0.693/day.

Table 6.14 Reservoir characteristics for example 3Lmix7

3Lmix7	Kx(md)	Ky(md)	Kz(md)	α_l (ft)	α_v (ft)	ϕ	Thickness(ft)
Layer1(L1)	100	100	100	0	0	0.15	15
Layer2(L2)	400	400	400	0	0	0.35	15
Layer3(L3)	700	700	700	0	0	0.2	10

Table 6.15 Reservoir characteristics for example 3Lmix8

3Lmix8	Kx(md)	Ky(md)	Kz(md)	α_l (ft)	α_v (ft)	ϕ	Thickness(ft)
Layer1(L1)	100	100	100	10	1	0.15	15
Layer2(L2)	400	400	400	10	1	0.35	15
Layer3(L3)	700	700	700	10	1	0.2	10

Figure 6.30 shows the results of produced H₂S in a 2-layered reservoir (Case 2Lmix5) without physical dispersion, the corresponding tracer is also shown in Figure 6.31 and 6.32. Figures 6.33, 6.34, and 6.35 show that including the physical dispersion (case 2Lmix6) changes the behavior of a 2-layered, as we expect two different peaks, to the behavior of a 1D reservoir with only one observed peak. This phenomenon is the well known behavior of Taylor's dispersion (Lake and Hirasaki, 1981; Fanchi, 1983; Liu et al., 1993 and 1994; Mahadevan, 2003), in which the combined effects of the transverse profile of longitudinal velocity and transverse diffusion on a solvent slowly flowing through a tube will manifest themselves as a longitudinal diffusion phenomenon. In other words, at the condition of vertical equilibrium the behavior of multi-layered reservoir will be similar to that of a single layered. Tables 6.12 and 6.13 show that in these two cases (2Lmix5 and 2Lmix6) only changing the dispersivity has changed the observed profiles (Figure 6.28 compared to Figure 6.33) from two peaks to one peak. Figure 6.35 shows the concentrations of a tracer in 2 layers approach to each other in comparison to Figure 6.32 (without physical dispersion) which shows two distinct layers.

Figures 6.36 and 6.37 also show the profile of H₂S and a tracer in a 3-layered reservoir (case 3Lmix7, Table 6.14). Including the physical dispersion changes the profile in a

manner in which it resembles the behavior of 1D, as illustrated in Figures 6.36 and 6.39 (case 2Lmix8, Table 6.15). This phenomenon in which the behavior of 2 and 3 layers reservoir approaches to the 1D reservoir can be extended to multi-layered reservoirs.

The temperature profiles of the 2 and 3 layered cases are shown in Figures 6.40 and 6.41, respectively. In these cases, there is no heat transfer to overburden/underburden. The thermal front will propagate with different speed in each layer. Basically, this observation is the result of the injection front profiles in each layer which depends on the mobility ratio of that layer. Thus, in the faster layer the temperature front also moves faster.

6.7.3.2 Effect of Vertical Grid Refinement on the Predicted Results

Cases 2Lmix5-refin1 and 2Lmix5-refin2 (Grids (ft); $\Delta X = 20 \times 50$, $\Delta Y = 1 \times 100$, $\Delta Z = 10 \times 5$) are identical except for the dispersivity as indicated in Tables 6.16 and 6.17. All properties related to initial conditions and biological option are reflected in Tables 6.5 and 6.7.

Table 6.16 Reservoir characteristics for example 2Lmix5-refin1

2Lmix5-Refin1	Kx(md)	Ky(md)	Kz(md)	α_l (ft)	α_v (ft)	ϕ	Thickness (ft)
Layer1(L1)	100	100	100	0	0	0.15	5×5
Layer2(L2)	400	400	400	0	0	0.35	5×5

Table 6.17 Reservoir characteristics for example 2Lmix5-refin1

2Lmix5-Refin2	Kx(md)	Ky(md)	Kz(md)	α_l (ft)	α_v (ft)	ϕ	Thickness(ft)
Layer1(L1)	100	100	100	10	1	0.15	5×5
Layer2(L2)	400	400	400	10	1	0.35	5×5

Comparing Figure 6.30 with Figure 6.42 shows that for these cases refinement in vertical direction changes the results of the maximum observed concentration in H₂S

from 1.6mg/l to 1.4 mg/l. Although this observation is not a big change, looking at the temperature profiles (Figure 6.40 with Figure 6.46) shows the refinement in vertical direction gives more accurate results for temperature profile. Thus, for large reservoir the vertical grid refinement is necessary to get more accurate prediction of reservoir souring. On the other hand, vertical grid refinement while including physical dispersion for this case does not change the results of the observed peak in the produced H₂S concentrations (Figure 6.33 and Figure 6.44).

Comparing Figure 6.40 with Figure 6.46, confirms that the more pronounced result of vertical grid refinement is on the temperature profile. Increasing the number of subgrids in vertical direction will result in the more precise temperature distribution. In fact, for large reservoirs the vertical refinement is necessary to get more accurate results for the prediction of reservoir souring.

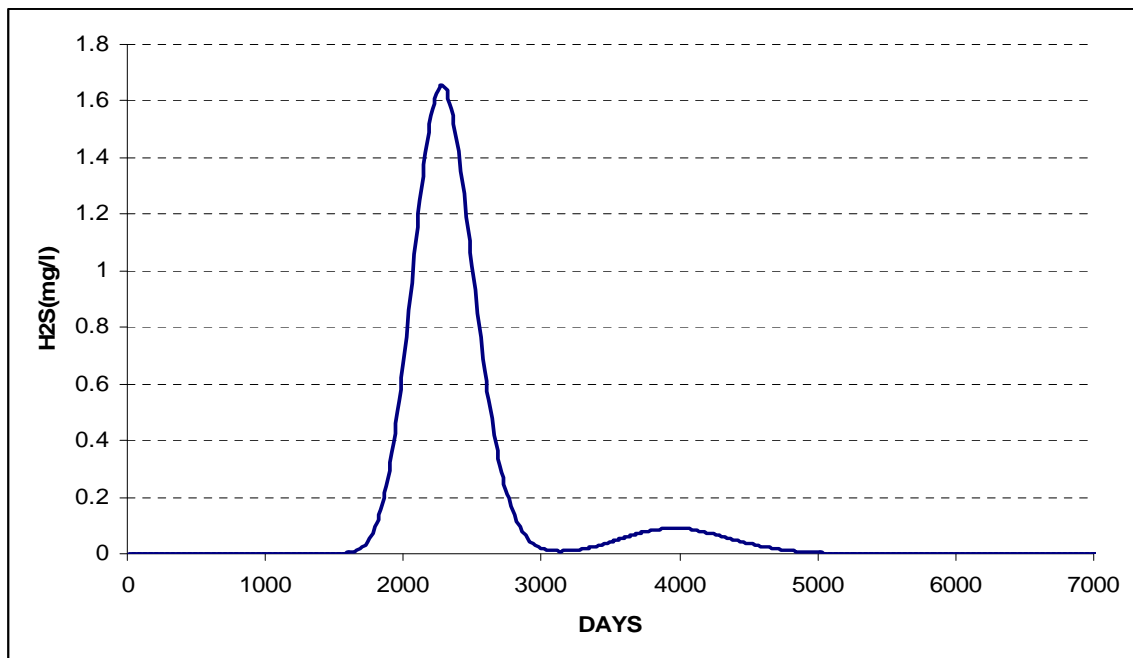


Figure 6.30 Produced hydrogen sulfide concentration (mg/l) in a 2-layered reservoir, no physical dispersion (Thermophilic SRB, doubling time is one day, $\mu_{\max} = 0.693/\text{day}$)

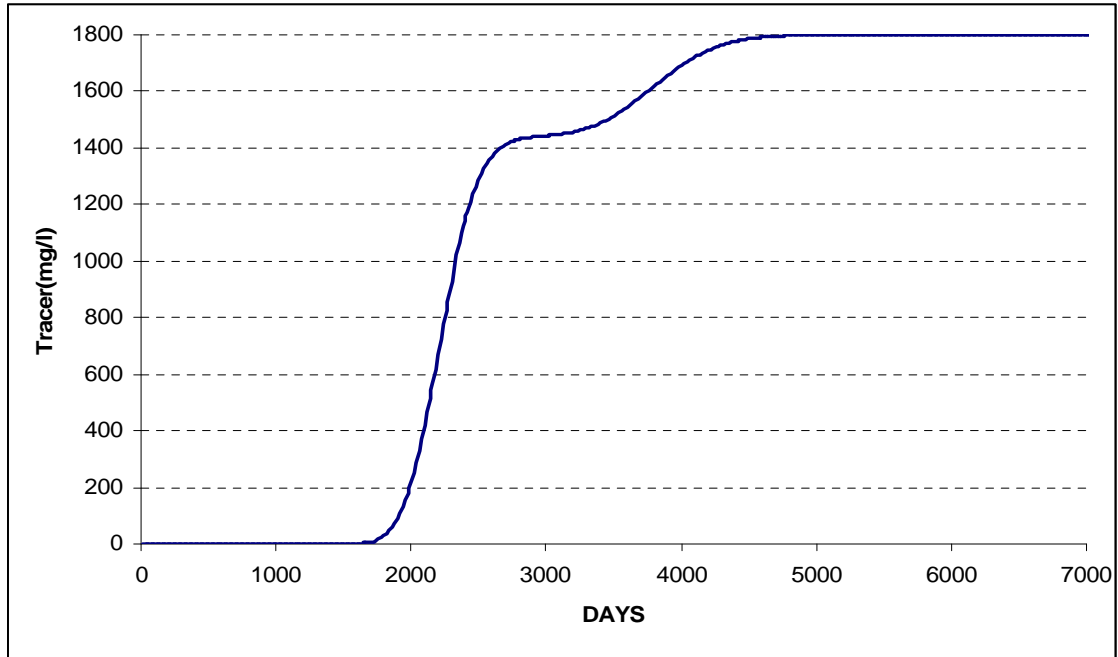


Figure 6.31 Nonreacting tracer concentration (mg/l) in the producer for a 2-layered reservoir, no physical dispersion

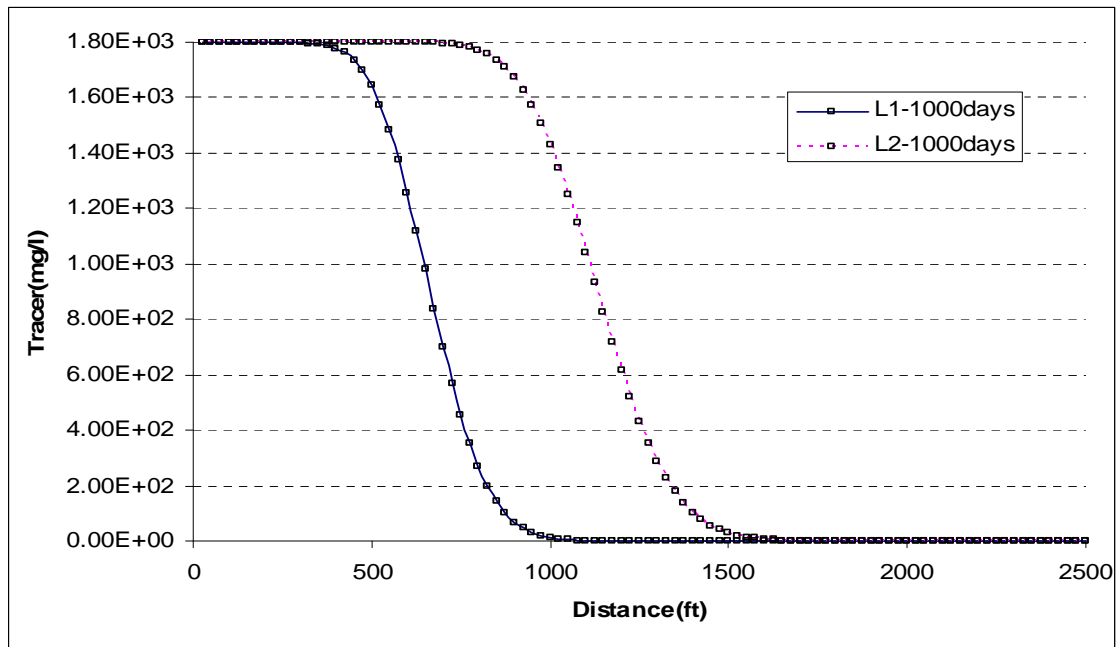


Figure 6.32 Tracer concentration in 2 layered reservoir without physical dispersion

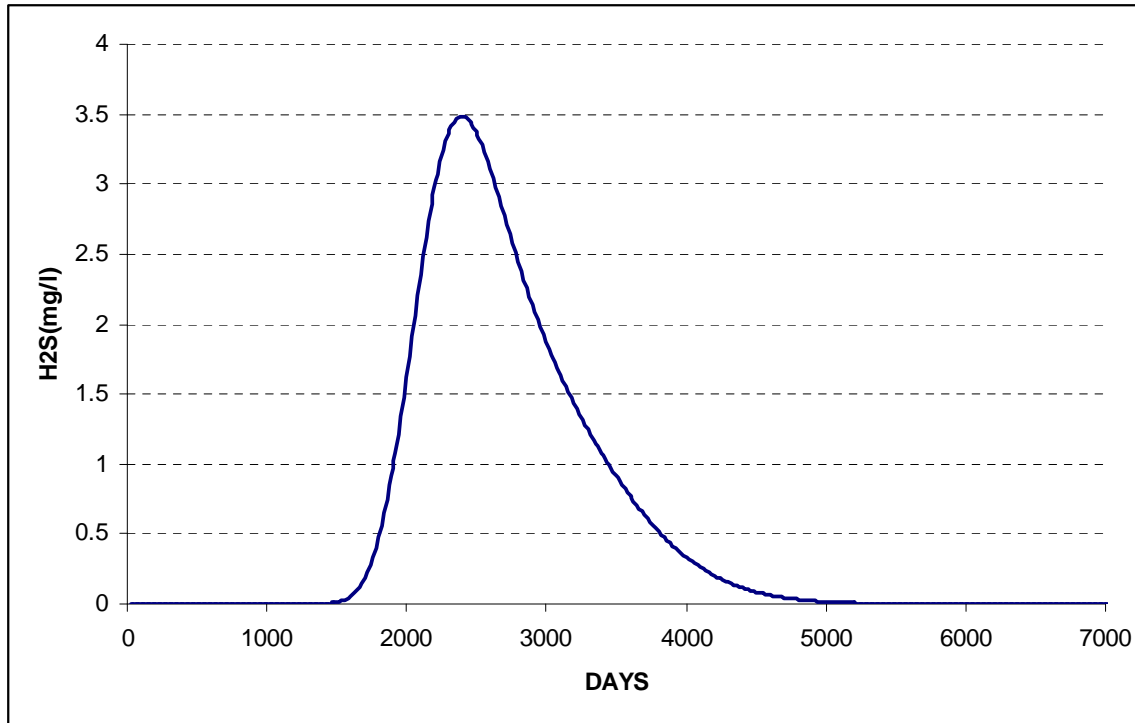


Figure 6.33 Produced hydrogen sulfide concentration (mg/l) in a 2 layered reservoir, with 10 ft of physical dispersion (thermophilic SRB, doubling time is one day, $\mu_{\max} = 0.693/\text{day}$)

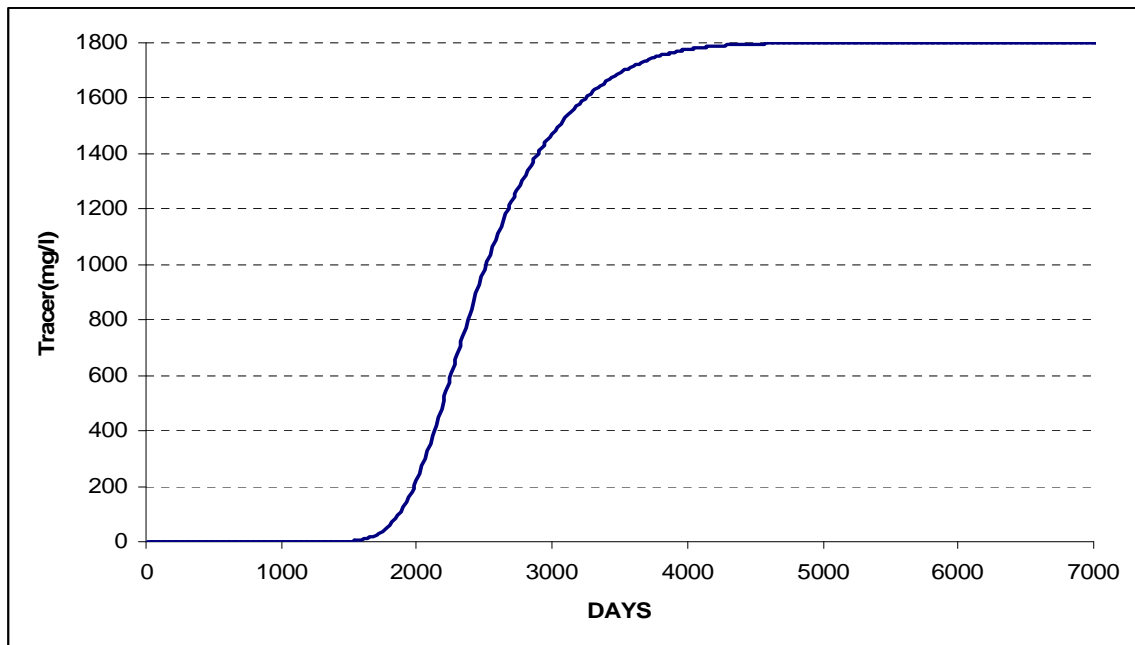


Figure 6.34 Nonreacting tracer concentrations in the producer (mg/l) for a 2-layered reservoir, with 10 ft of physical dispersion

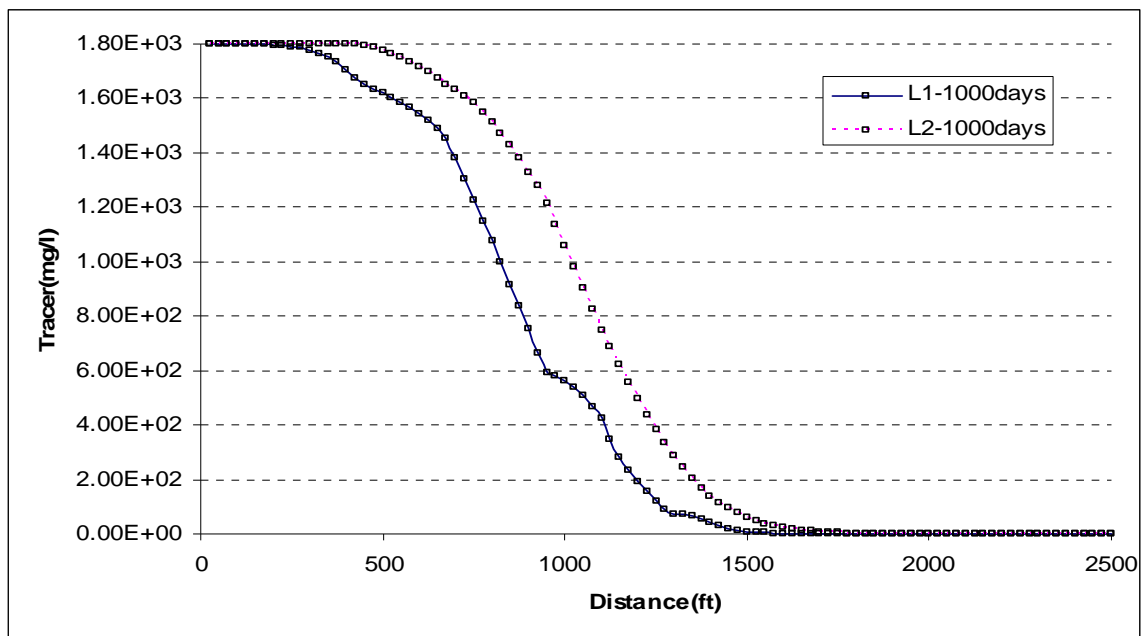


Figure 6.35 Tracer concentrations in 2-layered reservoir with 10 ft of physical dispersion

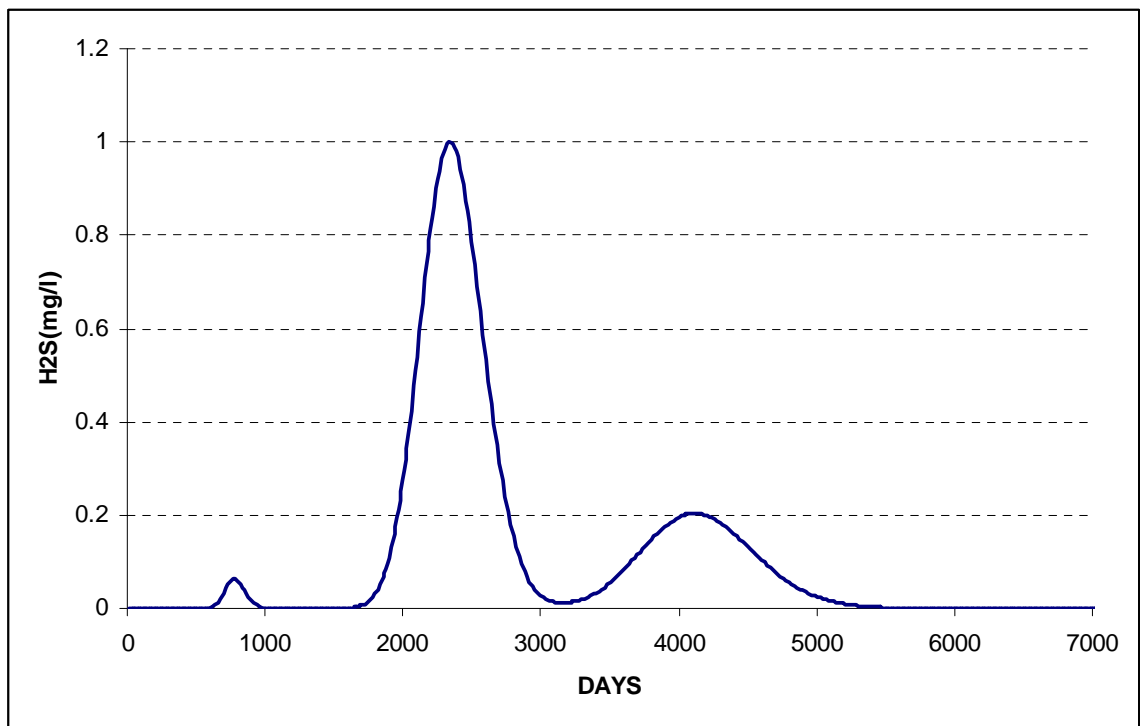


Figure 6.36 Produced hydrogen sulfide concentration (mg/l) in a 3-layered reservoir, no physical dispersion (Thermophilic SRB, doubling time is one day, $\mu_{\max} = 0.693/\text{day}$)

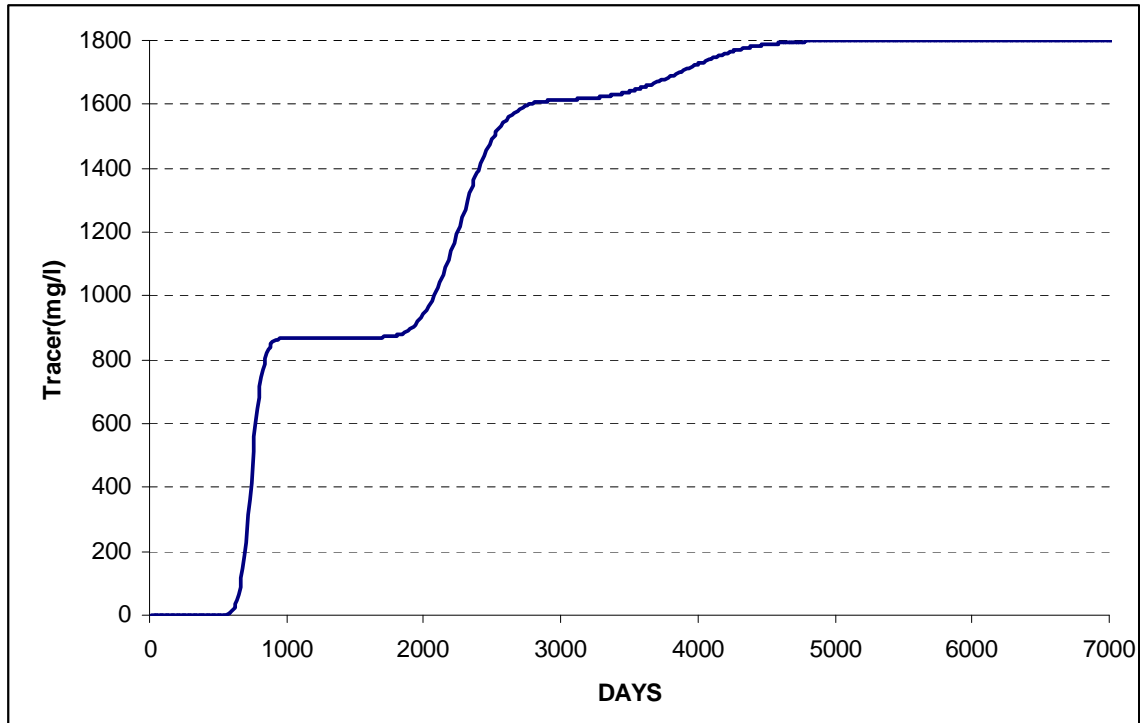


Figure 6.37 Nonreacting tracer concentration (mg/l) in the producer for a 3-layered reservoir, no physical dispersion

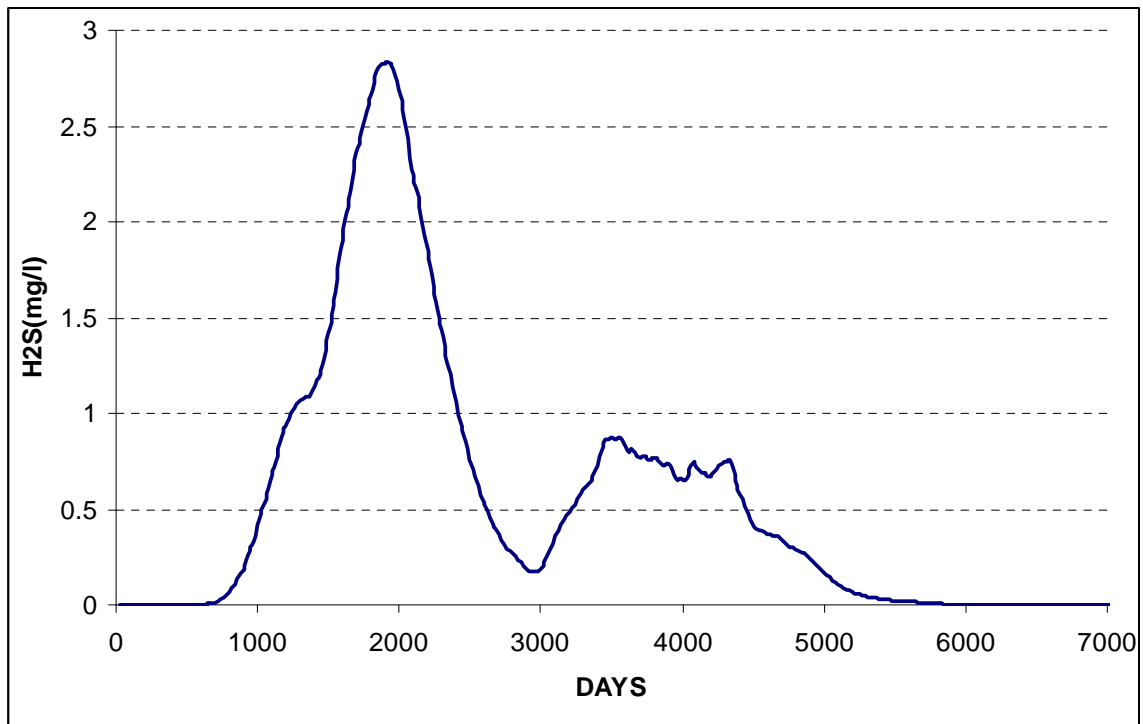


Figure 6.38 Produced hydrogen sulfide concentration (mg/l) in a 3-layered reservoir, with 10 ft of physical dispersion (Thermophilic SRB, doubling time is one day, $\mu_{\max} = 0.693/\text{day}$)

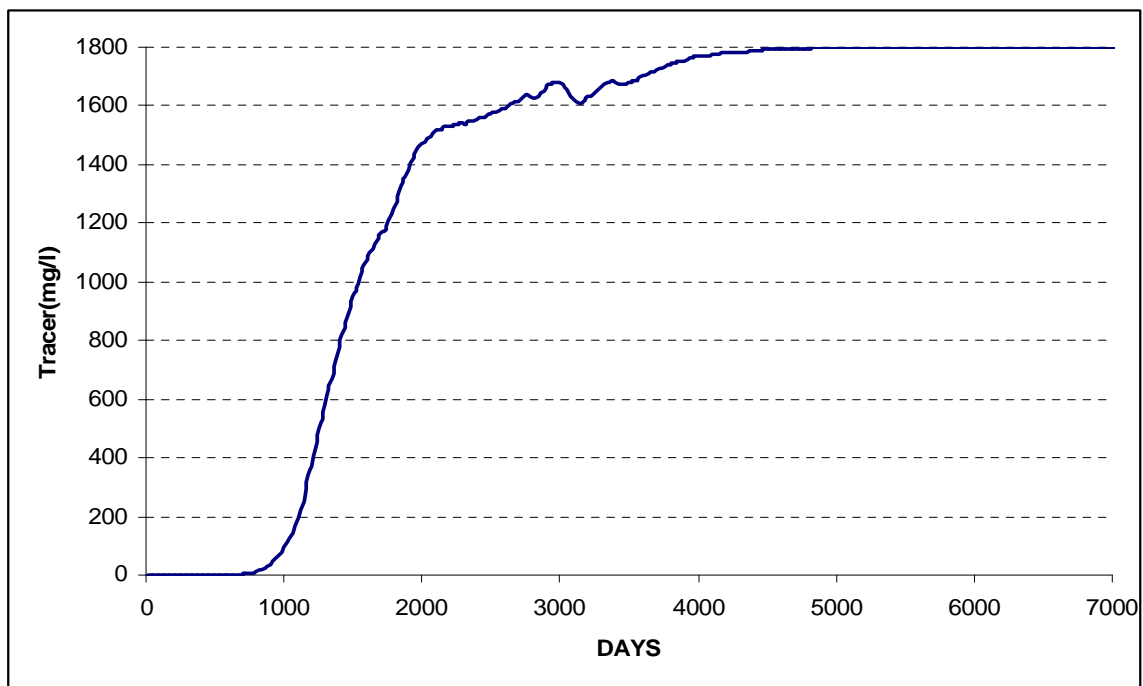


Figure 6.39 Nonreacting tracer concentration in the producer (mg/l) for a 3-layered reservoir, with 10 ft of physical dispersion

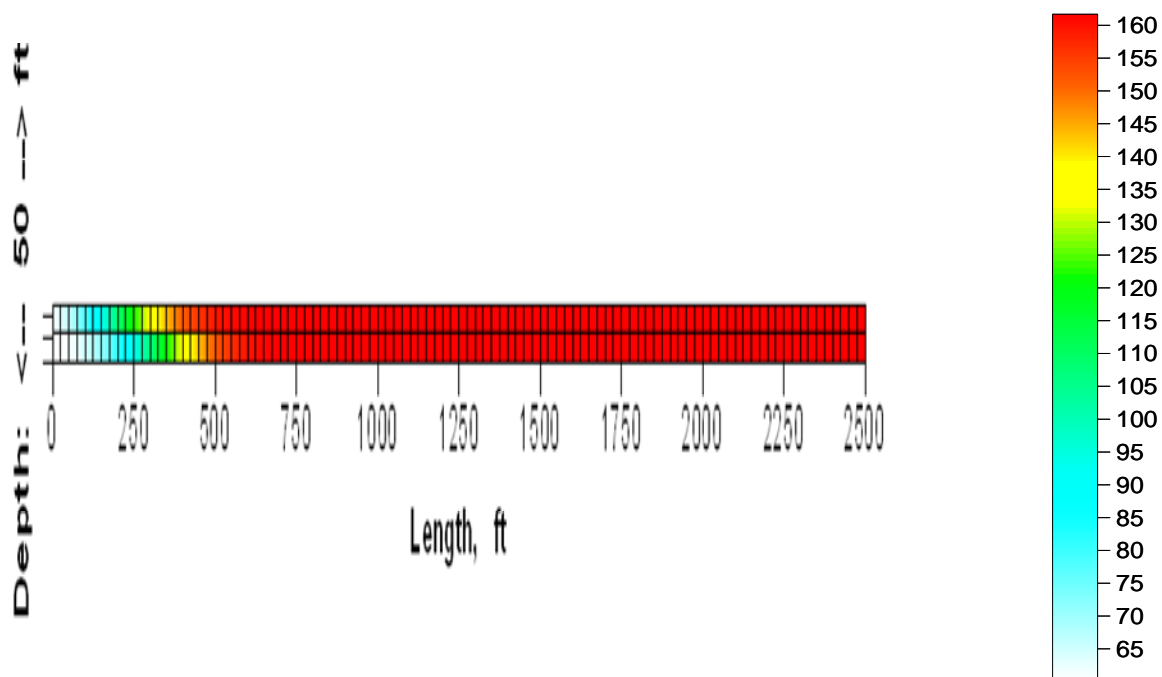


Figure 6.40 Temperature profile in different layers after 1000 days (2 layers, no heat transfer to over/under burden)

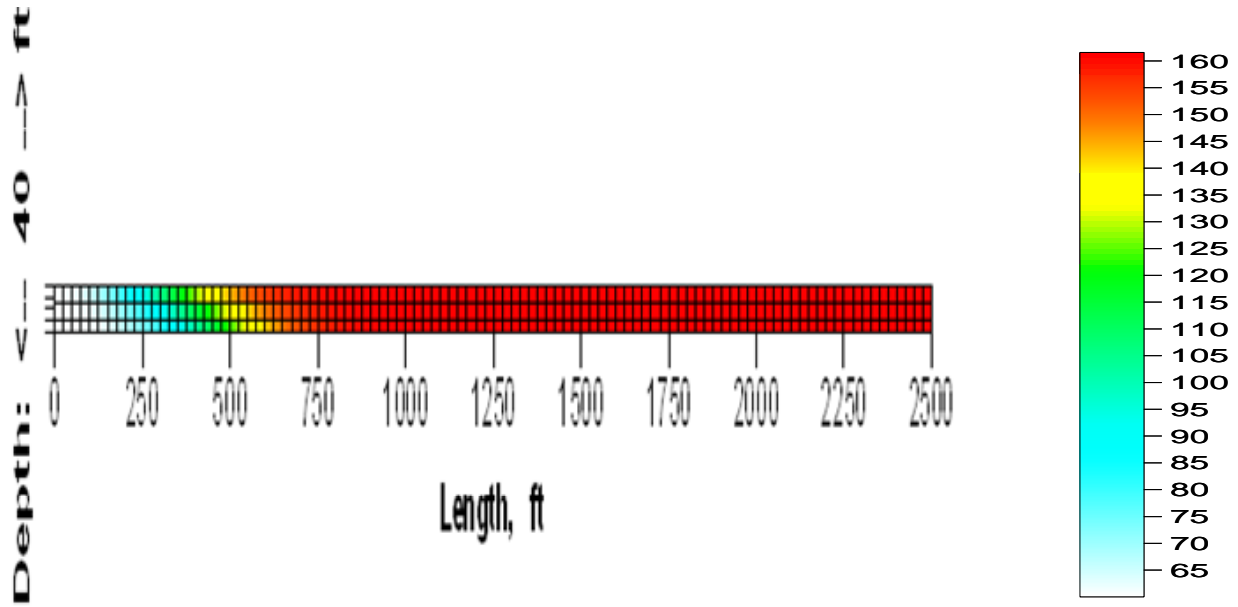


Figure 6.41 Temperature profile in different layers after 1000 days of seawater injection (3-layers, no heat transfer to over/under burden)

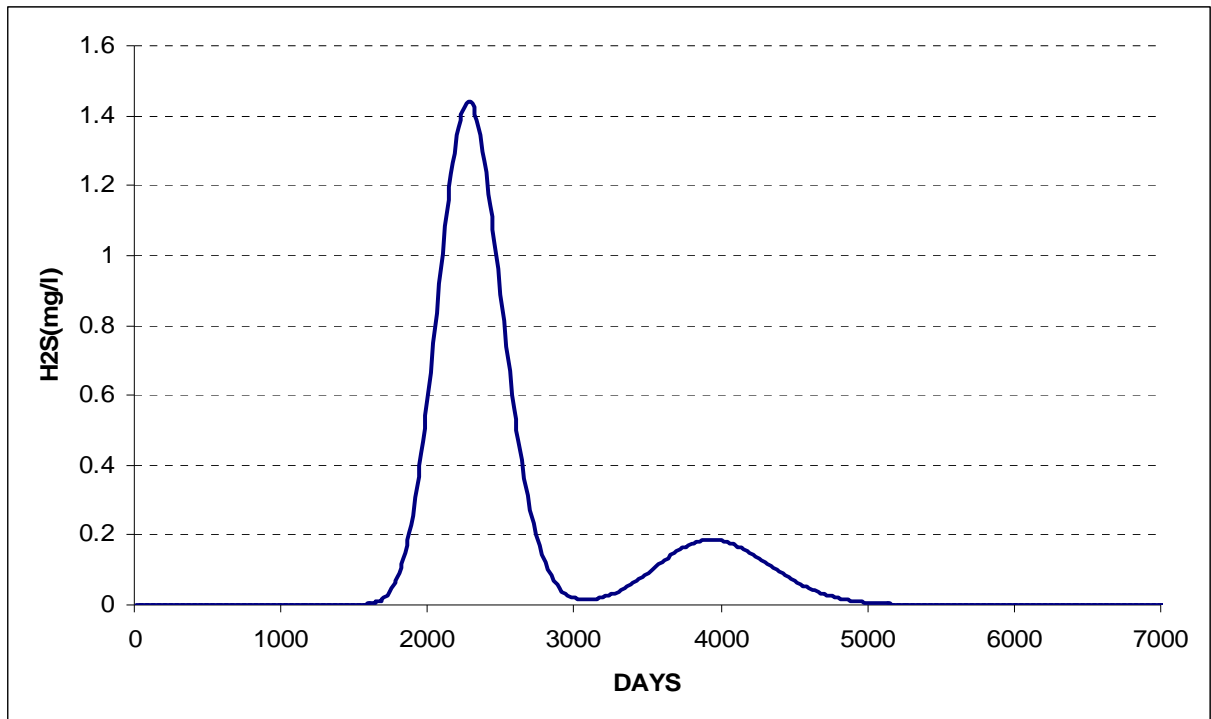


Figure 6.42 H₂S concentration in the producer after vertical refinement, no physical dispersion (thermophilic SRB, doubling time is one day, $\mu_{\max} = 0.693/\text{day}$)

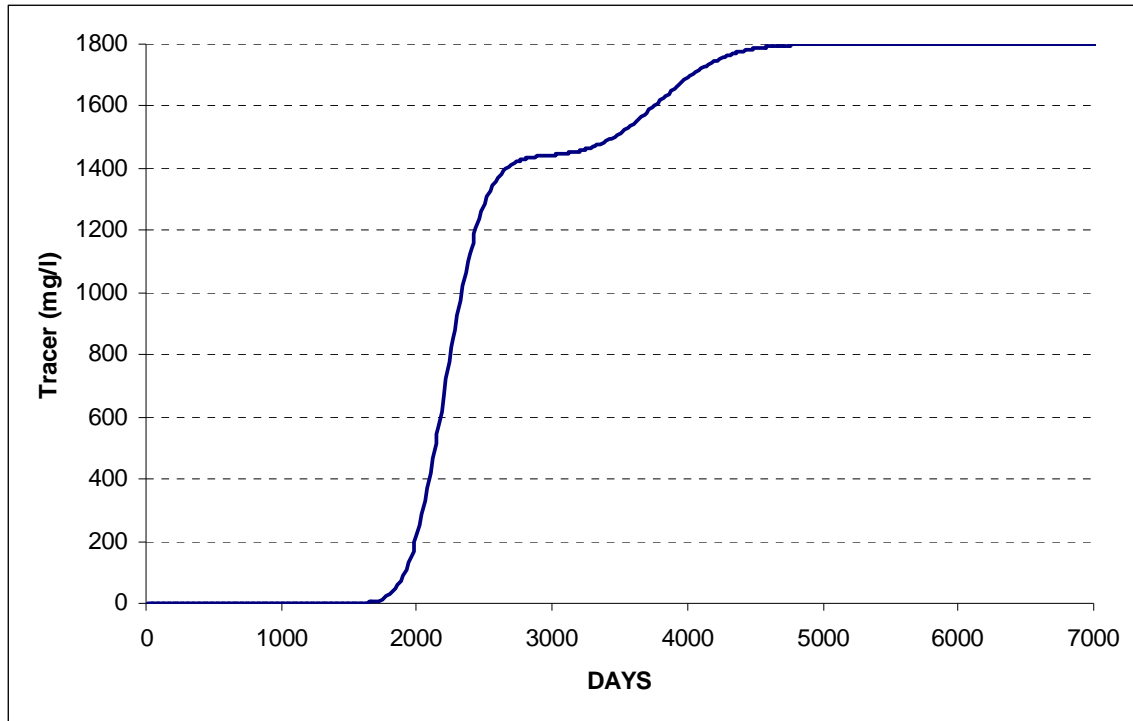


Figure 6.43 Nonreacting tracer concentration in the producer for the case of vertical refinement, no physical dispersion

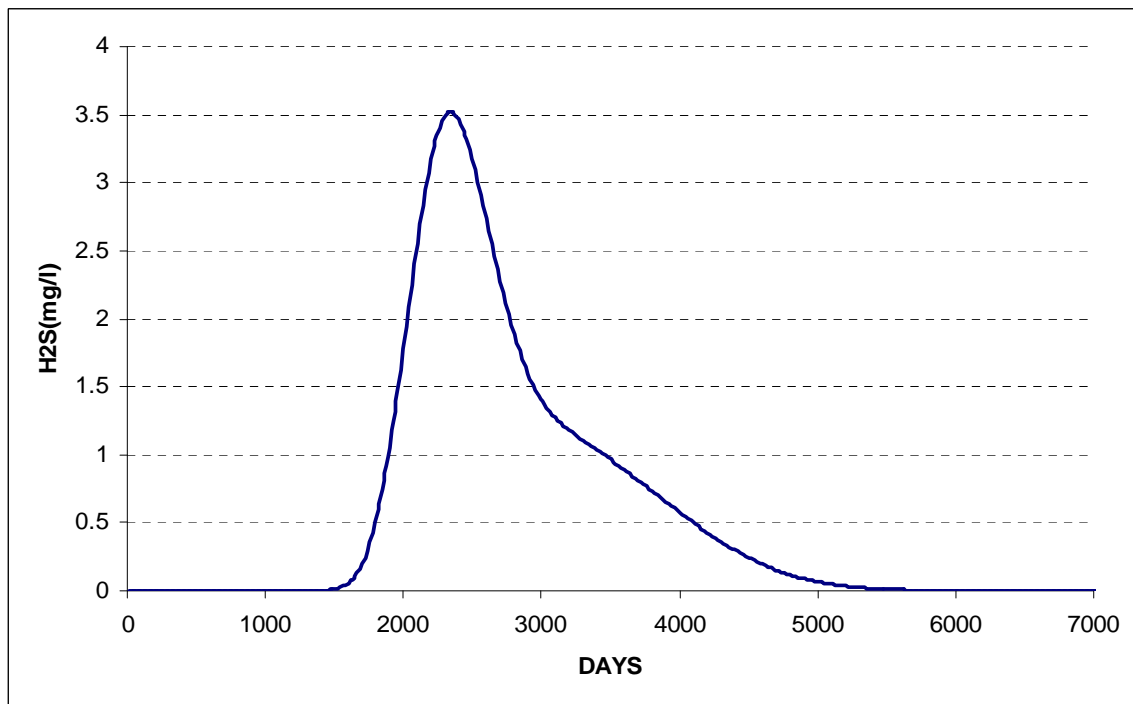


Figure 6.44 H₂S concentration in the producer after vertical refinement, with physical dispersion (Thermophilic SRB, doubling time is one day, $\mu_{\max} = 0.693/\text{day}$)

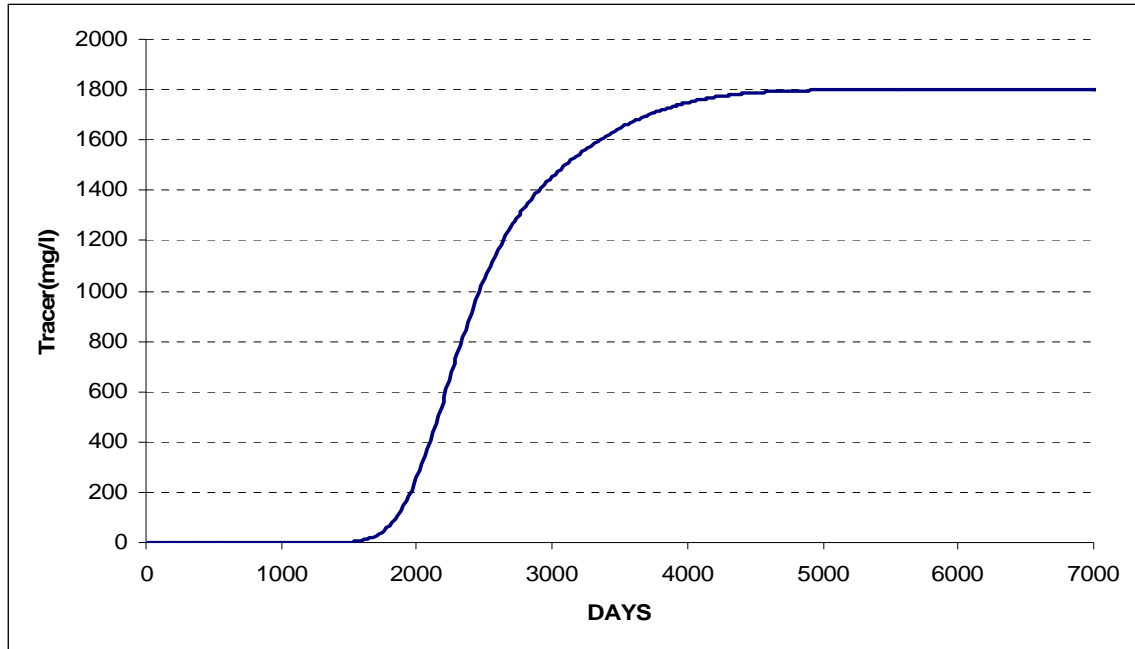


Figure 6.45 Nonreacting tracer concentration in the producer for the case of vertical refinement, with 10 ft of physical dispersion

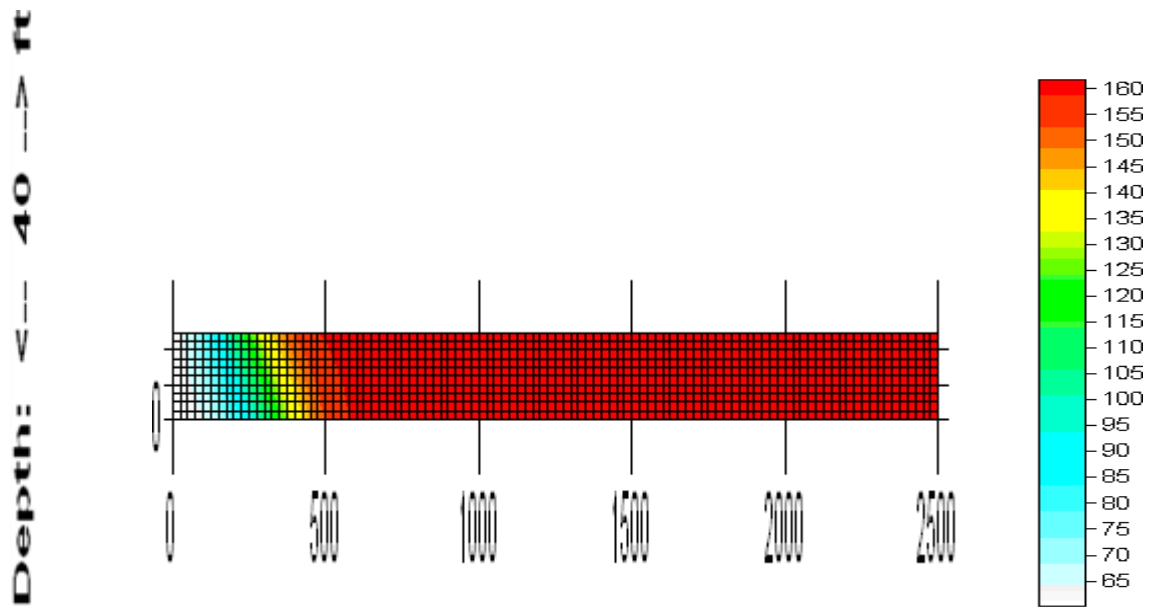


Figure 6.46 Temperature profile(1000 days after water injection) in different layers after grid refinement in vertical direction (no heat transfer to o/under burden)

6.8 Investigation of the Chemical and Physical Constraints on Reservoir Souring

The biological reactions are sensitive to the physical constraints and chemical species present in the reservoir. Thus, the assumption of a rate independent of these constraints is too far from reality (Okabe and Characklis, 1992; Chang et al., 1991; Al-Humaidan et al., 1999; Lappin et al., 1994; Reis et al., 1992). In addition, the adsorption capacity of rocks and the partitioning of H₂S can change when physical and chemical constraints change. Depending upon the type of SRB introduced to the reservoir, and the temperature of the injected water into the reservoir, different hydrogen sulfide concentrations profiles will be observed. The results of simulation of reservoir souring using the UTCHEM model under variable conditions are provided in this section. These results will give a guideline to the extreme conditions to determine the soured and not soured reservoirs.

In order to investigate the process of reservoir souring, a 1D reservoir with 26 gridblocks is studied. It is assumed that the permeability is high enough (e.g., 200 md) to allow the sulfur reducing bacteria (SRB) to move along the reservoir within the mixing zone (Sunde et al., 1993). Figure 6.47 shows the variation in temperature after injecting seawater at a temperature of 60°F to the reservoir, whose initial temperature was 160°F. The cold zone propagates with the pore volume injected seawater and has a delay with respect to the injected seawater front. This delay results from the heat capacity of the reservoir rocks and the heat transfer to overburden and underburden. In this case, the water breakthrough is about 0.6 PV when the temperature front is almost at 1,500 ft from the injector. This means that the temperature front moves at a speed of almost one third of the injected water.

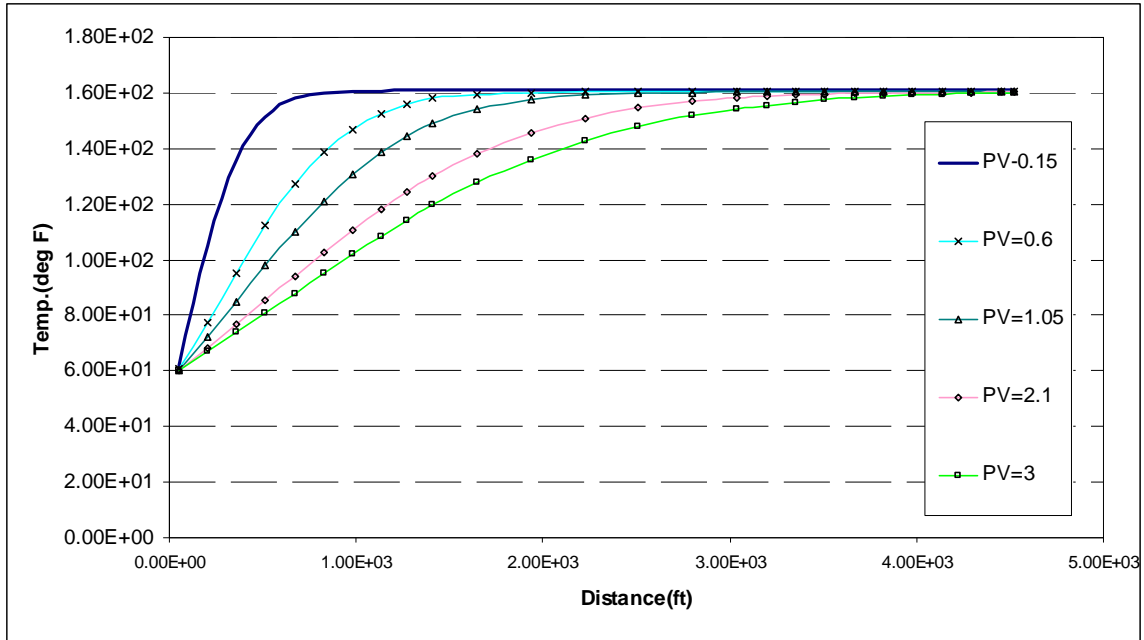


Figure 6.47 Temperature profile along the reservoir at different injected pore volumes

Figure 6.48 shows how different SRB types yield concentrations of hydrogen sulfide at the production well while applying the mixing model. For a reservoir initially at 160°F injecting seawater at a temperature 60°F, the thermophiles generate at around 12 milligram per liter (mg/l) H₂S, while mesophiles produce about 2 milligram per liter (mg/l) H₂S. For this range of temperature, hyperthermophiles are not active.

Due to the temperature profile (Figure 6.48), smaller portions of the reservoir exist in the temperature range suitable for mesophilic SRB activities. This means that when the mixing zone leaves the suitable temperature zone, no more H₂S is produced. Thus, due to dispersion, the concentration of H₂S in the mixing zone will decrease as the injected front moves to the producer.

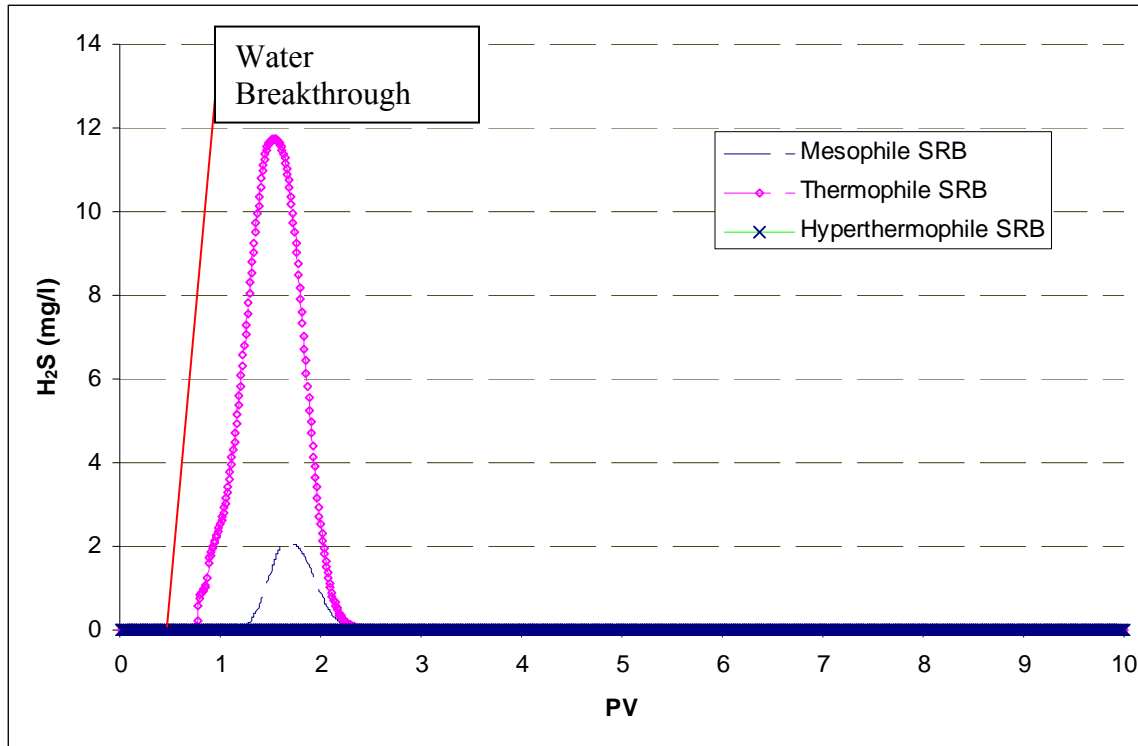


Figure 6.48 Produced H₂S (mg/l in aqueous phase) vs. pore volume injected seawater for different SRB types

Figure 6.49 shows the effects of nutrients concentrations on souring by thermophilic-SRB. These results indicate that, while increasing nutrient concentrations, the observed peak in the produced H₂S will increase. According to Figure 6.49, a ten-fold increase of the nutrients concentrations causes the maximum concentration in the H₂S change from about 11 mg/l to about 55 mg/l. Consequently, a ten-fold decrease in nutrients concentrations decreases the observed peak in the H₂S concentration from 11 mg/l to about 2 mg/l.

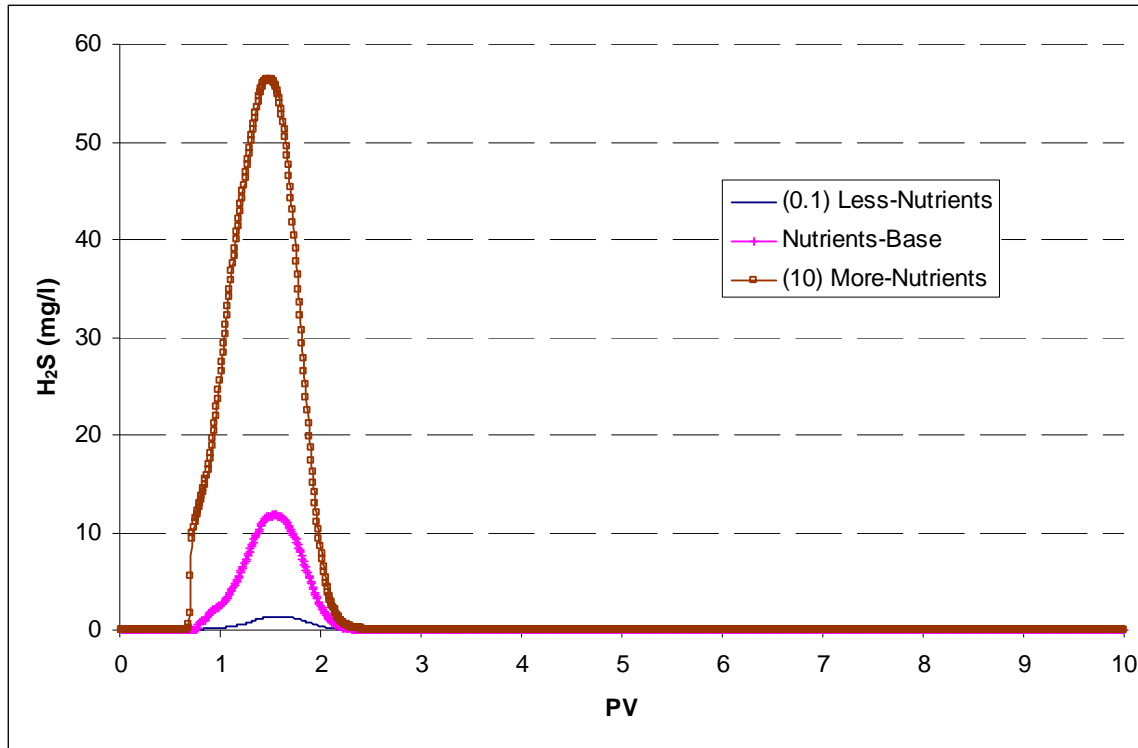


Figure 6.49 Effects of nutrient concentration on the produced H_2S concentration (mg/l, aqueous phase) for the thermophilic-SRB

Another essential parameter, which affects the delay and peak of the observed souring in a seawater injected reservoir, is the retardation factor. Figure 6.50 illustrates the effects of retardation on the H_2S concentration profile in the producer, while assuming thermophilic-SRB generated hydrogen sulfide. Obviously, increasing the retardation factor from zero to 20 will increase the delay in the observed H_2S and, consequently, a decrease in the peak of the H_2S concentration in the aqueous phase. These variations in the hydrogen sulfide concentrations reflect the fact that the higher retardation factor increases the capacity of H_2S in residual oil and, consequently, decrease the observed peak of H_2S in produced fluids. The accumulated H_2S will partition to the flowing phase while the mixing zone leaves the producer.

The onset of reservoir souring depends on the delay in the observed H₂S with respect to the water breakthrough.

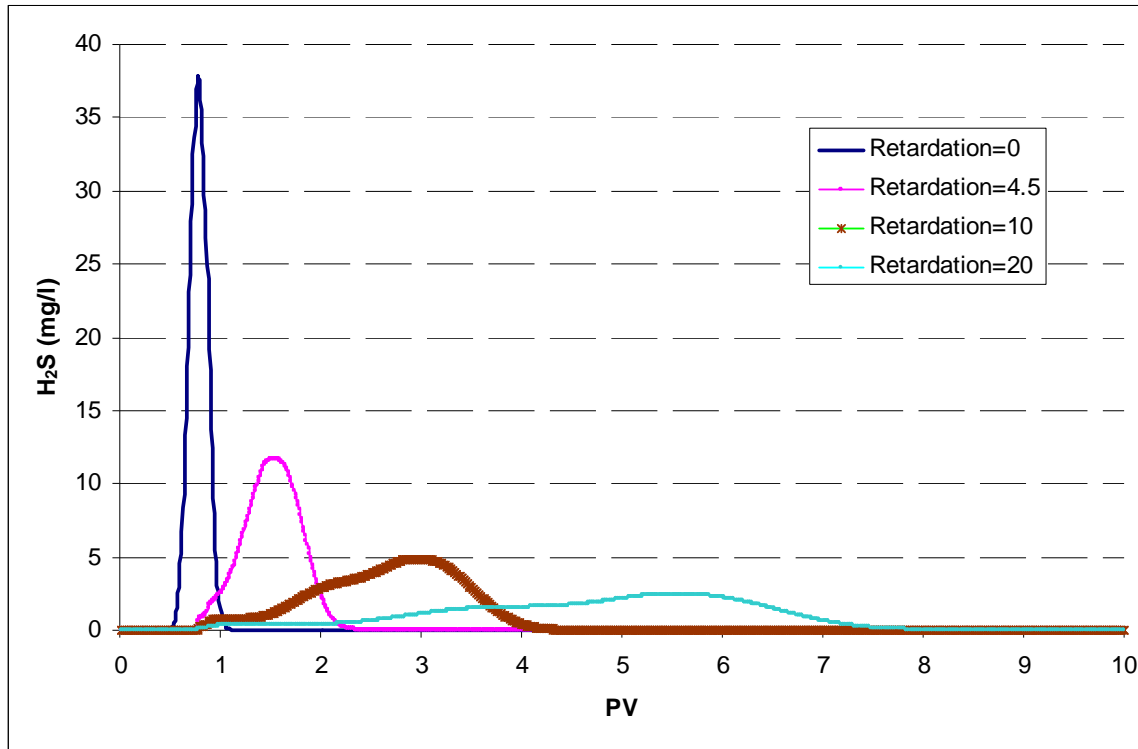


Figure 6.50 The effects of retardation factor on the H₂S concentration profile in the producer (biological reactions are attribute to thermophilic-SRB)

In the process of reservoir souring, the injection rate has an important effect on the profile in terms of the timing of the onset of souring. As reflected in Figure 6.52, the time of observed souring will increase as the injection rate decreases. In this case, when injecting at rate of 1 ft/day, 0.5 ft/day and 0.1 ft/day, the maximum observed peak in the H₂S concentrations will happen at 350 months, 750 months and above 2000 months, respectively. Although some of these timings are above the life of the reservoirs, they give an understanding of the injection rate and observed souring. On the other hand, as indicated in Figure 6.51, the injection rate does not affect the H₂S profile in terms of pore

volume injected. As explained in the previous section, the peak of hydrogen sulfide concentration depends on the available nutrients and temperature ranges. For a large reservoir, the reaction rate is not affecting the peak in hydrogen sulfide concentration and after it reaches its maximum it stays constant. This behavior is explained in the next section.

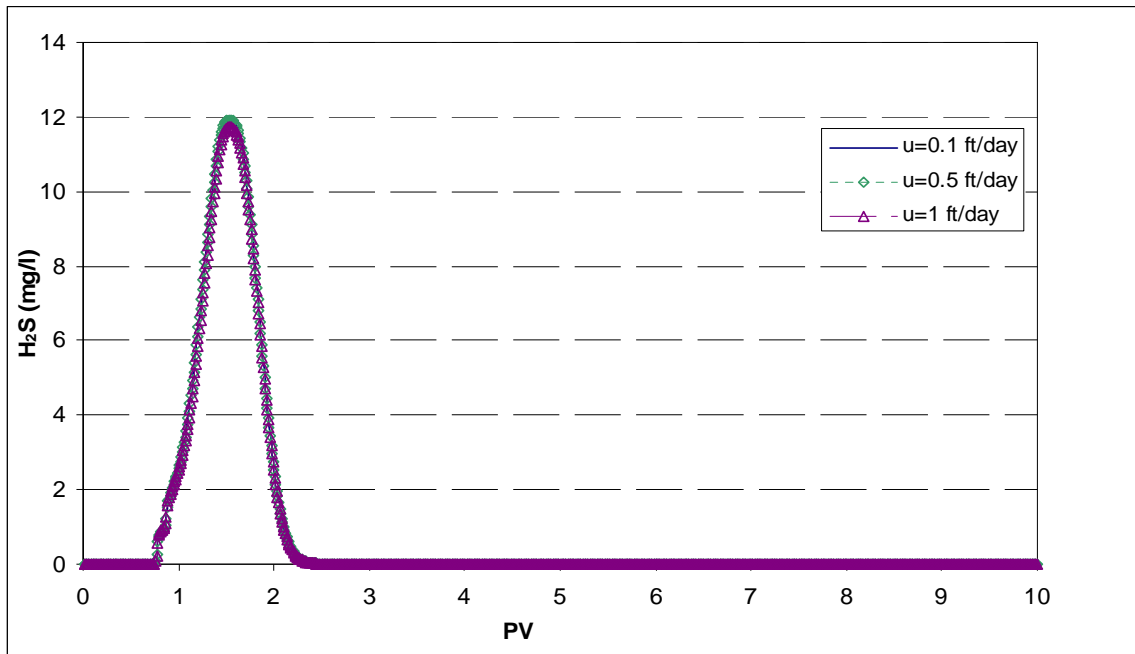


Figure 6.51 Effect of interstitial velocity on the produced H₂S in terms of injected pore volume (case study reservoir with thermophilic SRB)

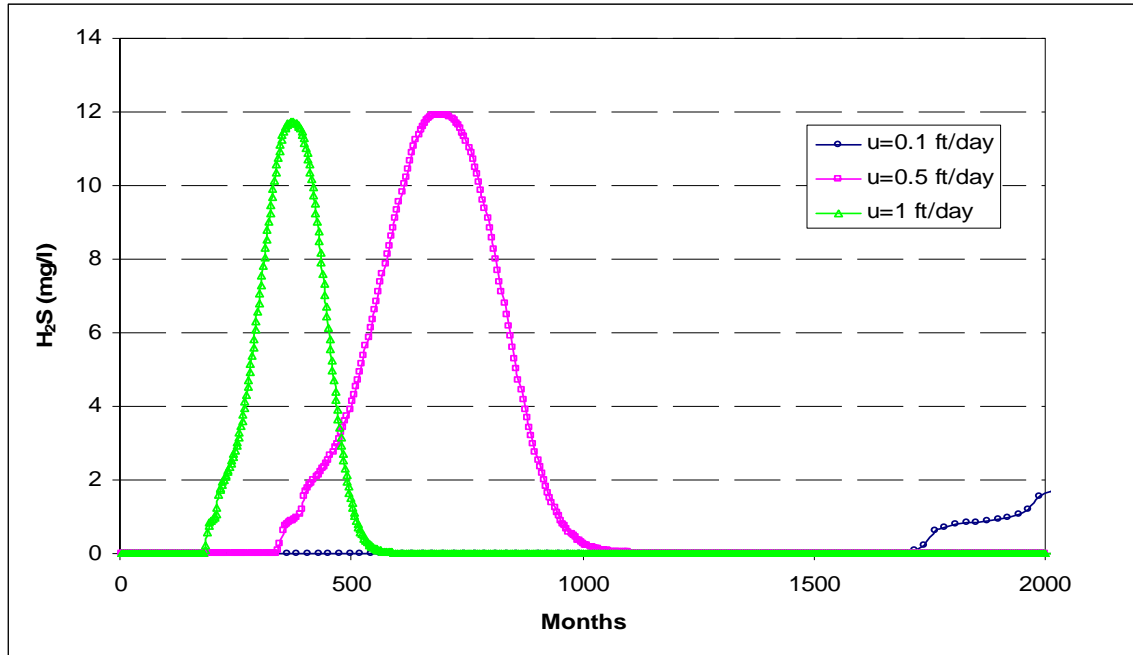


Figure 6.52 Effect of interstitial velocity on the produced H₂S in terms of injected time, month, (Case study reservoir with thermophilic SRB)

6.9 Overall View on the Limiting Constraints in the Reservoir Souring

This section contains an overall view of the reservoir souring process in a seawater injected reservoir. This investigation will help to control or mitigate the production of hydrogen sulfide in a seawater injected reservoir.

Figure 6.53 illustrates the concentration profile of hydrogen sulfide at different times after injection the reservoir. After 400 days of injection, the peak in the production of hydrogen sulfide levels off. Consequently, as a result of dispersion, the produced H₂S in the initial peak will decrease.

To have a better understanding of the process, the concentrations of all species which are engaged in the biogenic reaction are shown in Figures 6.54, 6.56, and 6.58 for 200 days, 500 days, and 1000 days after injection, respectively. Figures 6.55, 6.57, and 6.59 are given to focus on the variation of the concentration of the species. Figure 6.55

shows that after 200 days of injection seawater, in the mixing zone (between concentration profiles of SO_4^- and CH_3COOH) there are enough concentrations of each species and the biogenic reaction will continue. On the other hand, Figure 6.57 indicates that after 500 days of injecting seawater, in the mixing zone (between concentration profiles of SO_4^- and CH_3COOH) there is at least one essential nutrient (NO_3^-) missing. The missing nutrient causes the biogenic reaction to stop. This means that after 500 days there is no more generation of H_2S . Figure 6.59 illustrates the profiles of concentrations also reveals the same observation in which nutrient is missing in the mixing zone. The two significant differences between Figures 6.57 and 6.59 are distinguishable. The increasing delay between hydrogen sulfide concentration profile and mixing zone (because of retardation factor) and the more spread because of dispersion.

Figure 6.60 shows the temperature front with respect to injection front corresponding to the simulation at different times. Figure 6.60 shows that after 200 days of injection, the temperature will not be a constraint for the thermophilic SRB. Thus, for this case study, the limiting species (nutrients) control the generation of hydrogen sulfide. The final observation of these set of simulation is reflected in Figure 6.61. This figure is the whole result of the prediction of the souring in the reservoir. The hydrogen sulfide has a delay in the water breakthrough (after sulfate profile). This delay is the result of retardation.

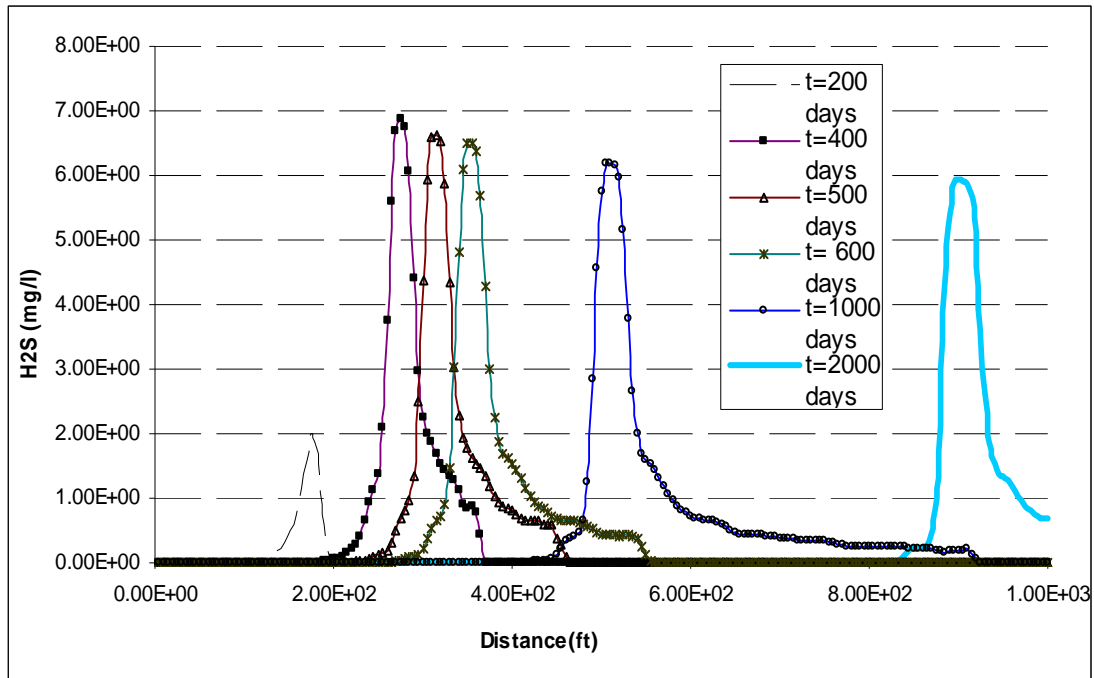


Figure 6.53 Concentration of hydrogen sulfide at different time in the reservoir

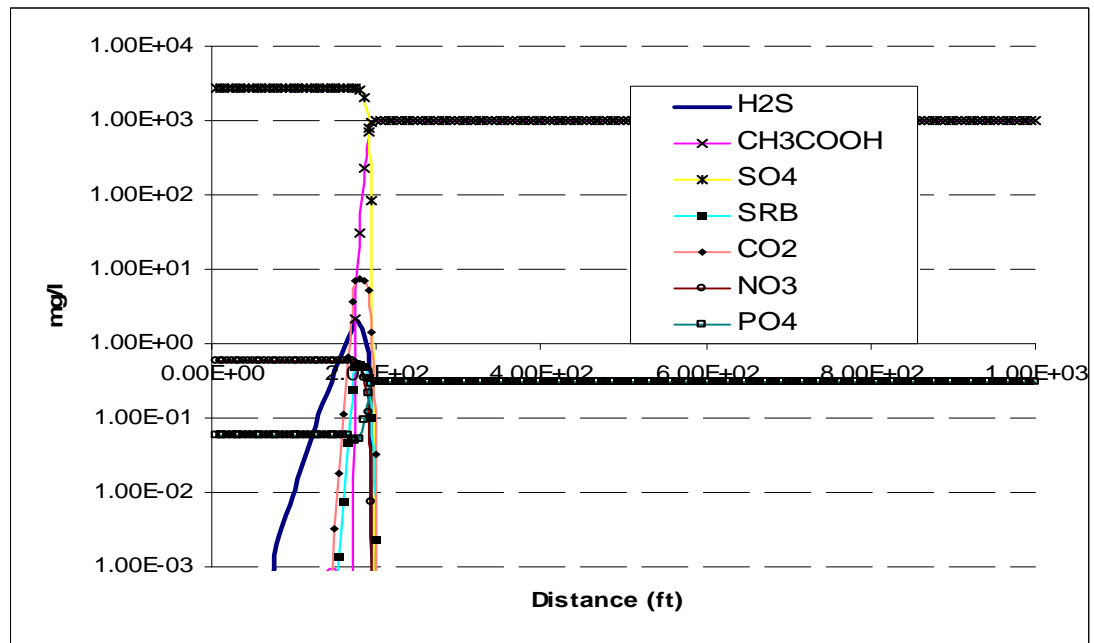


Figure 6.54 Concentration of all species in aqueous phase after 200 days of injection

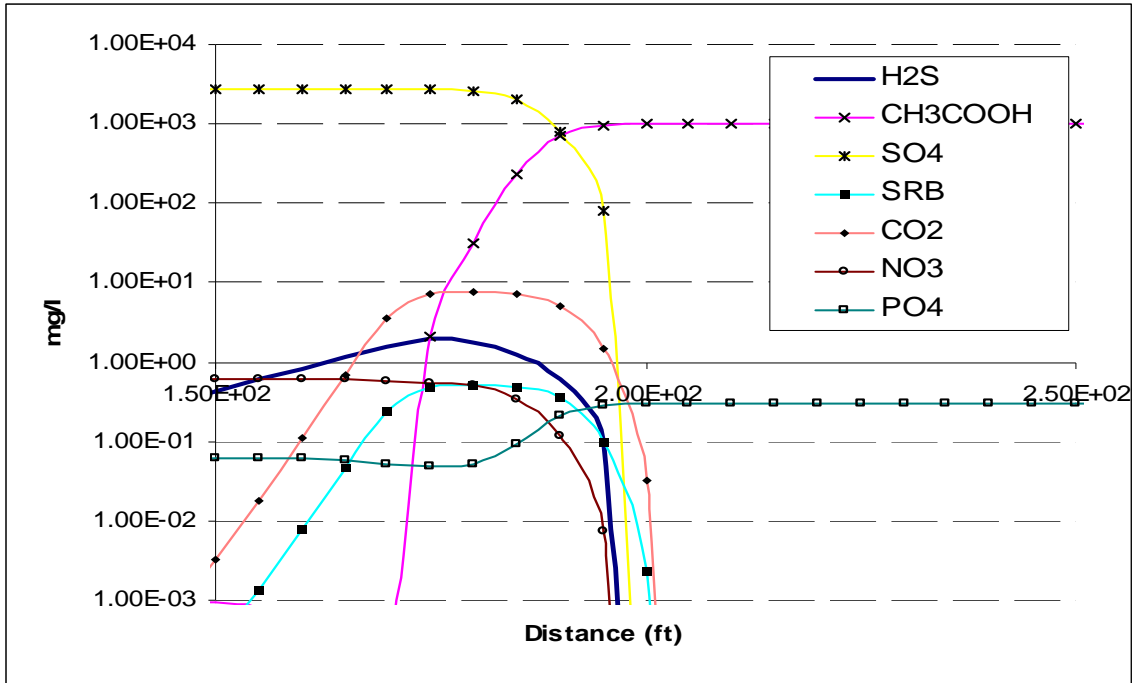


Figure 6.55 Concentration of all species in aqueous phase after 200 days of injection

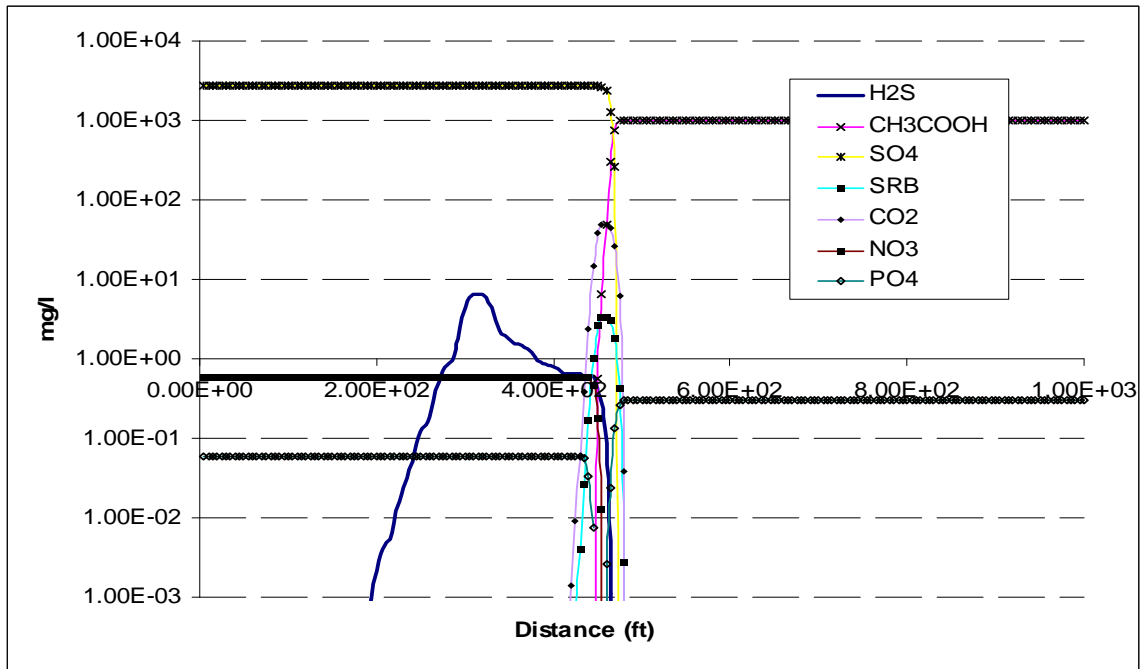


Figure 6.56 Concentration of all species in aqueous phase after 500 days of injection

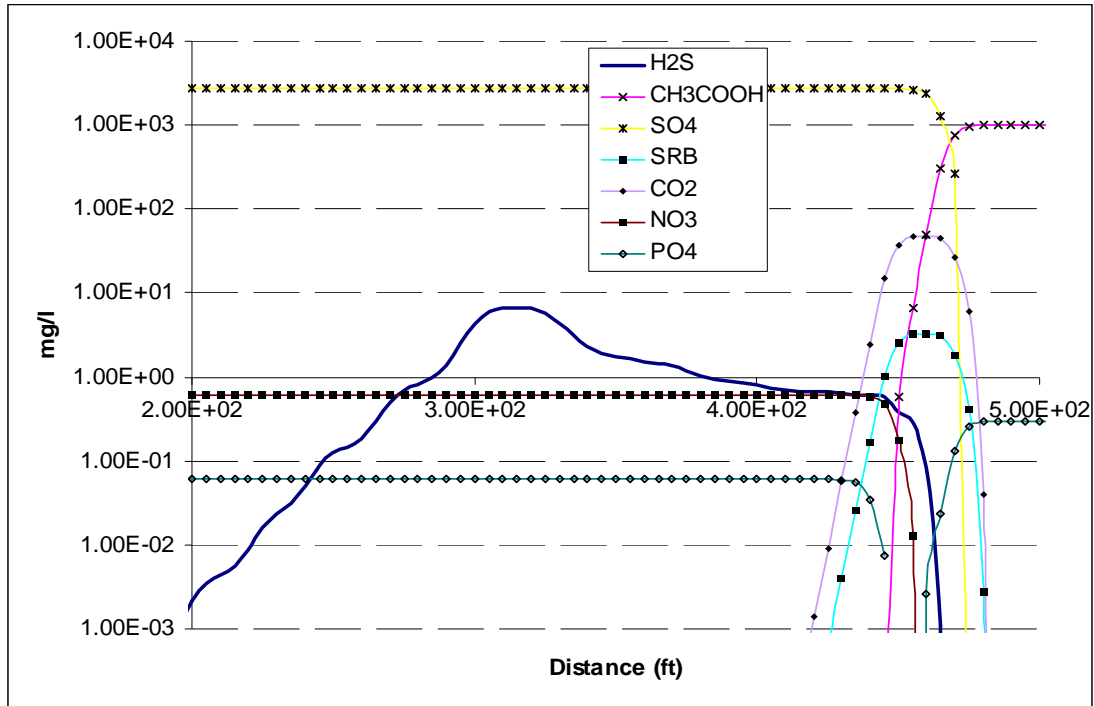


Figure 6.57 Concentration of all species in aqueous phase after 500 days of injection

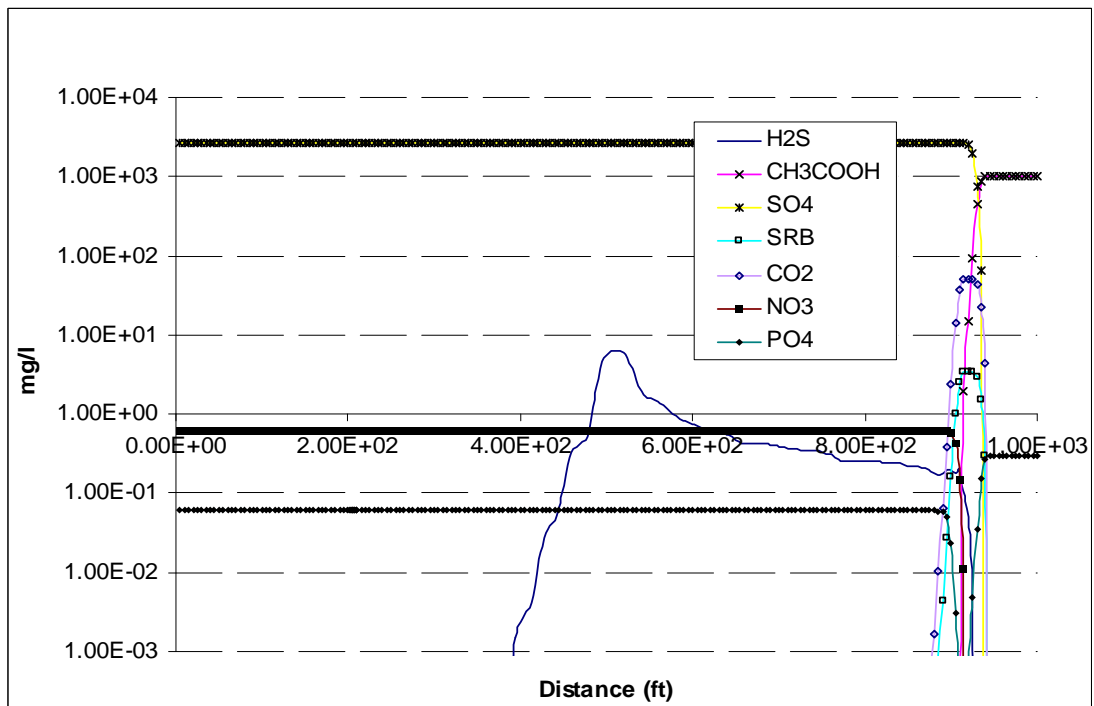


Figure 6.58 Concentration of all species in aqueous phase after 1000 days of injection

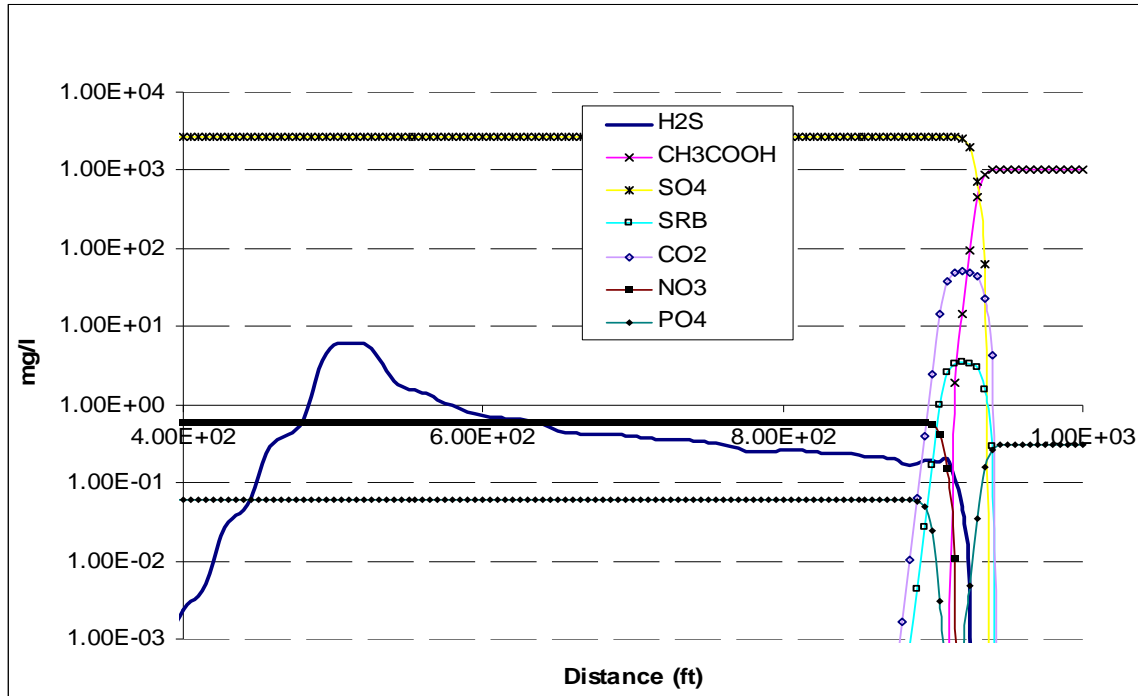


Figure 6.59 Concentration of all species in aqueous phase after 1000 days of injection

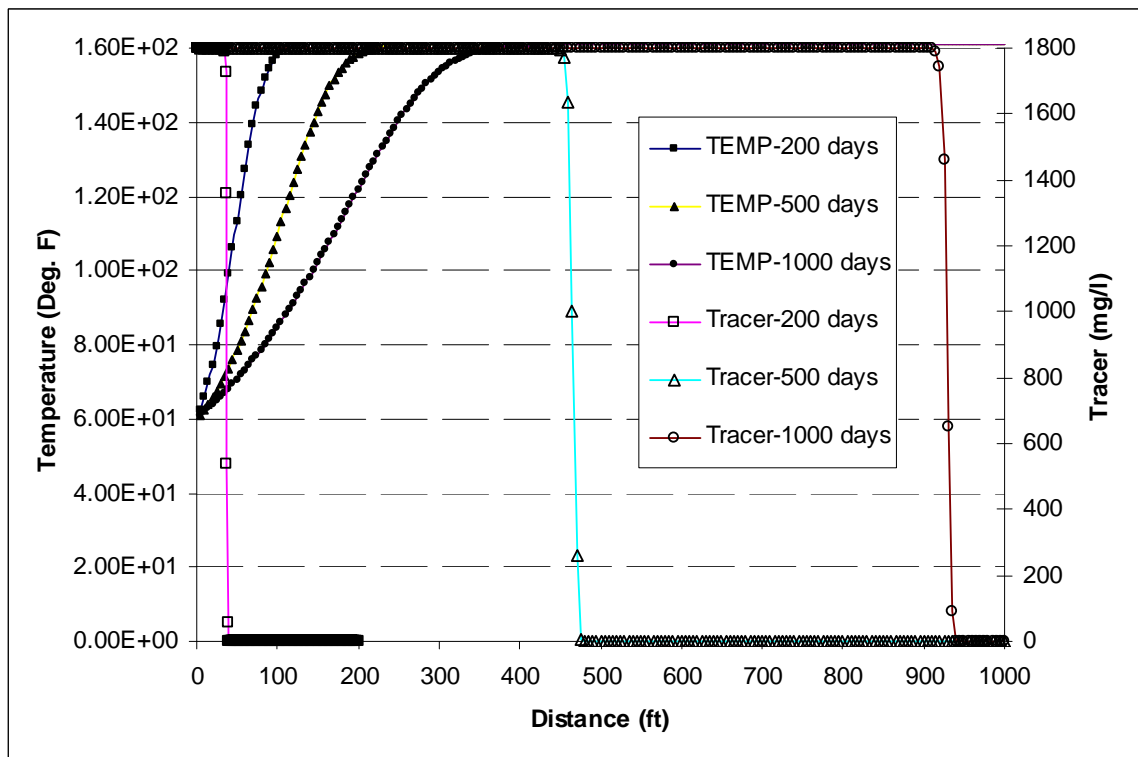


Figure 6.60 Delay in the temperature front with respect to the injection front at different times

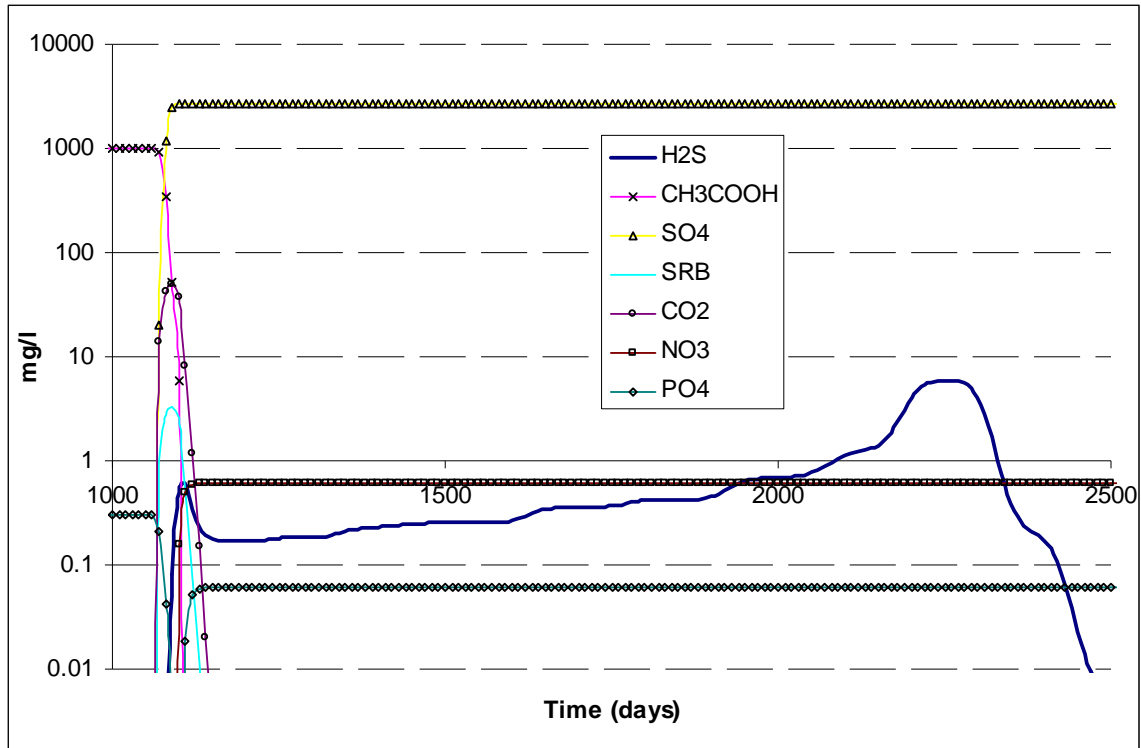


Figure 6.61 Concentration of all species in aqueous phase in the production well

6.10 Summary

We introduced the parameters which are needed to simulate the reservoir souring with UTCHEM. Then, explained the corresponding flags which are used to define the necessary parameters in INPUT file for the generation and transportation of hydrogen sulfide in the reservoir (sections 6.1-2). In section 6.3, the factors which control the activity of the SRB in a typical seawater injected reservoir were discussed. The corresponding flags which are input to switch between mixing, biofilm, TVS, and our model are explained in Section 6.4. Section 6.5 shows the results of simulation of reservoir souring for a case study which applies mixing model. In Section 6.6, the results of mixing, biofilm and TVS are reproduced to show the capability of our simulator. Section 6.7.1.1 shows the effective parameters which have a major role in generation and transportation of hydrogen sulfide. This section describes the propagation of temperature front with respect to the injection front both analytically and numerically for 1D and 3D

reservoirs. In addition, we investigated the effects of the variation of the properties of the reservoir and injection water on the profile and lag of the temperature front. Section 6.7.1.2 investigates the conditions for the vertical equilibrium in temperature front in seawater injected reservoirs. Section 6.7.2 shows the effect of dispersivity of the porous media on the distribution of the species and consequently the reservoir souring prediction. Effects of layering and vertical grid refinement on the predicted results of reservoir souring are given in Section 6.7.3. Investigation of the chemical and physical constraints on the hydrogen sulfide generation and transportation is reflected in Section 6.8. Section 6.9 gives an overall view of the variation of the mentioned constraints in the reservoir while traveling from injector to the producer. This observation provides a better understanding of the behavior of SRB and distribution of the species in the mixing zone developed between injection and formation waters.

Chapter 7

Field Application of the Developed Model and Simulator

Abstract

In this chapter, first we investigate the parameters which affect the reservoir souring prediction both in generation and transportation of hydrogen sulfide in porous media. We use the experimental design and response surface methodology to investigate the sensitivity of the reservoir souring to different variables using response surface analysis.

The second part of this chapter shows the capability of our simulator in prediction of the reservoir souring in real fields. The variation of the parameters in a typical seawater injected reservoir has been investigated. Using our model enables us to track the temperature propagation, electron acceptor, substrate, and nutrient concentrations and follow the produced hydrogen sulfide in the porous media. The field case studies will provide the criteria to categorize the soured and not soured reservoirs.

7.1 Introduction

In this chapter, we apply the experimental design concept to have a better interpretation of the previous study (Chapter 6) on the reservoir souring prediction. This approach helps integrate the effective parameters which control the onset of reservoir souring. This investigation can help to reach a guideline for the extreme conditions for a reservoir to be considered soured or not. After the experimental design investigation, two multi-layered reservoirs which resemble real fields are modeled and the results of reservoir souring are discussed.

7.2 Response Surface Methodology and Experimental Design

The basic concept of the response surface methodology and experimental design are given (Box et al., 2005). For this study, the main goal is the application of the methodology to optimize the objective function (lower hydrogen sulfide production) based on the response surface (Mason et al., 1989; Myers and Montgomery, 2002). Before starting this approach, we use our previous knowledge which shows the effective parameters that affect the generation and transportation of hydrogen sulfide in the seawater injected reservoirs. Among many parameters which can affect the complicated process of reservoir souring, we decided on four parameters which control the generation and transportation of hydrogen sulfide in porous media. The selected parameters and their range of variation are given in Table 7.1. For a fixed SRB type (Table 3.1), the temperature and nutrient concentrations control the generation term, while the adsorption and partitioning determine the arrival of hydrogen sulfide to the production well. For this study the reservoir characteristics and condition are given in Tables 6.5-6.7. In addition

we, assumed thermophilic SRB (Table 3.1) and the reservoir at 200°F. Further information regarding the model input parameters and run numbers are given in Appendix E.

Table 7.1 Parameters used for experimental design study

Parameters	Lower limit	Upper limit	Type
Reservoir Temperature (°F)	110	200	numeric
Nutrients (mg/l)	0.3	0.9	numeric
Partitioning (g/g)	3	4	numeric
Adsorption factor	0	2	numeric

7.2.1 Fitted Model Examination

To test whether the empirical model properly represents the true response surface, the method of residual analysis is used. The residual analysis is performed to check the normality assumptions of the residual between observed response variable and fitted response variable. The residual is plotted on normal probability plot, as shown in Figure 7.1. The straight line in the plot shows that the residuals are normally distributed and the response surface method can be used successfully for this analysis.

Design-Expert® Software
Log10(H2S)

Color points by value of
Log10(H2S):

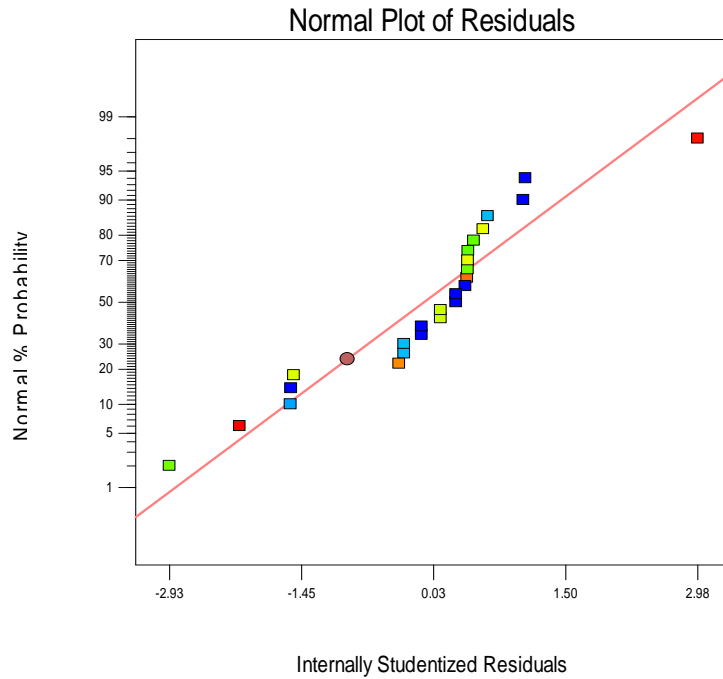


Figure 7.1 Normal probabilities of residuals

Figure 7.2 represents the effect of nutrients and temperature on generation of hydrogen sulfide. For this case study, the lower nutrient concentration (0.3 mg/l) and higher reservoir temperature (200 °F) generate less hydrogen sulfide while the higher nutrient concentrations (0.9 mg/l) and the optimum temperature of about 130 °F, produce maximum hydrogen sulfide (7 mg/l in aqueous phase).

Design-Expert® Software
 Original Scale
 H2S
 ● Design points above predicted value
 25
 0.01
 X1 = C: Temperature
 X2 = D: Nutrients
 Actual Factors
 A: Partition = 3.50
 B: Adsorption = 1.00

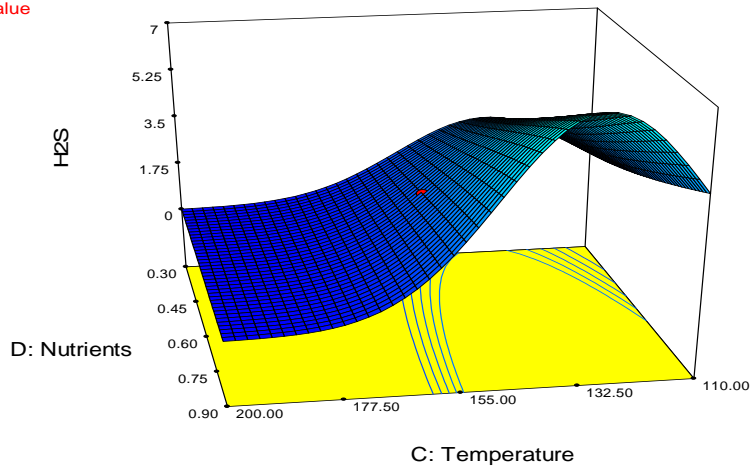


Figure 7.2 Effects of nutrients and temperature on the produced hydrogen sulfide

The effect of adsorption and partitioning on the concentration of the hydrogen sulfide in the produced water is shown in Figure 7.3. The adsorption can dramatically reduce the concentration of the produced hydrogen sulfide, while in the range of operation, the partitioning effect is not a an effective parameter.

Design-Expert® Software
 Original Scale
 H2S
 ● Design points above predicted value
 25
 0.01
 X1 = A: Partition
 X2 = B: Adsorption
 Actual Factors
 C: Temperature = 155.00
 D: Nutrients = 0.74

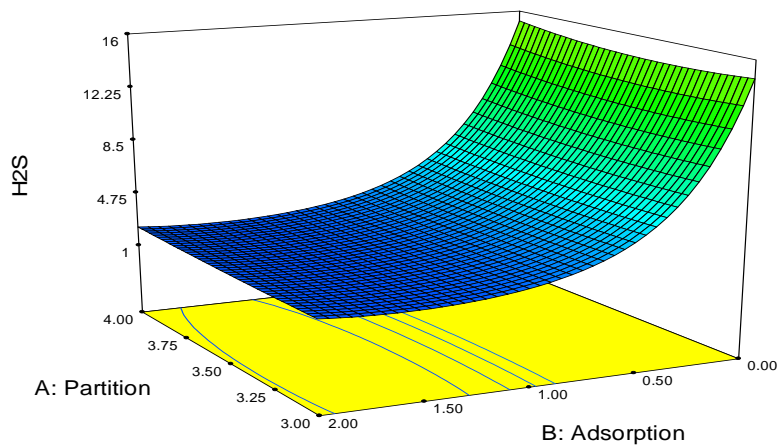


Figure 7.3 Effects of adsorption and partitioning on the produced hydrogen sulfide

Design-Expert® Software
Original Scale

H2S



X1 = A: Partition
X2 = C: Temperature

Actual Factors
B: Adsorption = 1.00
D: Nutrients = 0.74

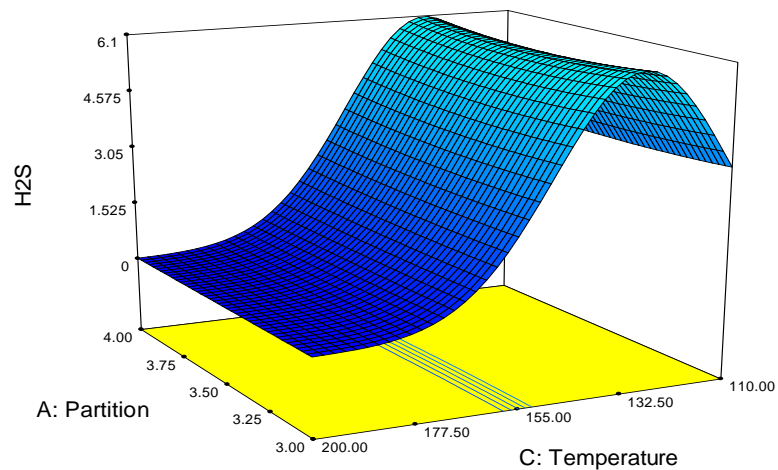


Figure 7.4 Effects of temperature and partitioning on the produced hydrogen sulfide

Effects of partitioning and temperature on the produced hydrogen sulfide are reflected in Figure 7.4. Temperature plays an important role while the partitioning effect is minimal.

Figures 7.5-7.7 show the effects of nutrient and partitioning, temperature and adsorption, and nutrient and adsorption respectively. Overall results show that to minimize hydrogen sulfide production in a specific reservoir, the lower nutrient, the higher adsorption, and even very high reservoir temperature or very low reservoir temperature are favorable. In application we do not have control over reservoir temperature and adsorption capacity. To reduce the reservoir souring, we need to reduce the available nutrients or any method which reduce the generation of hydrogen sulfide.

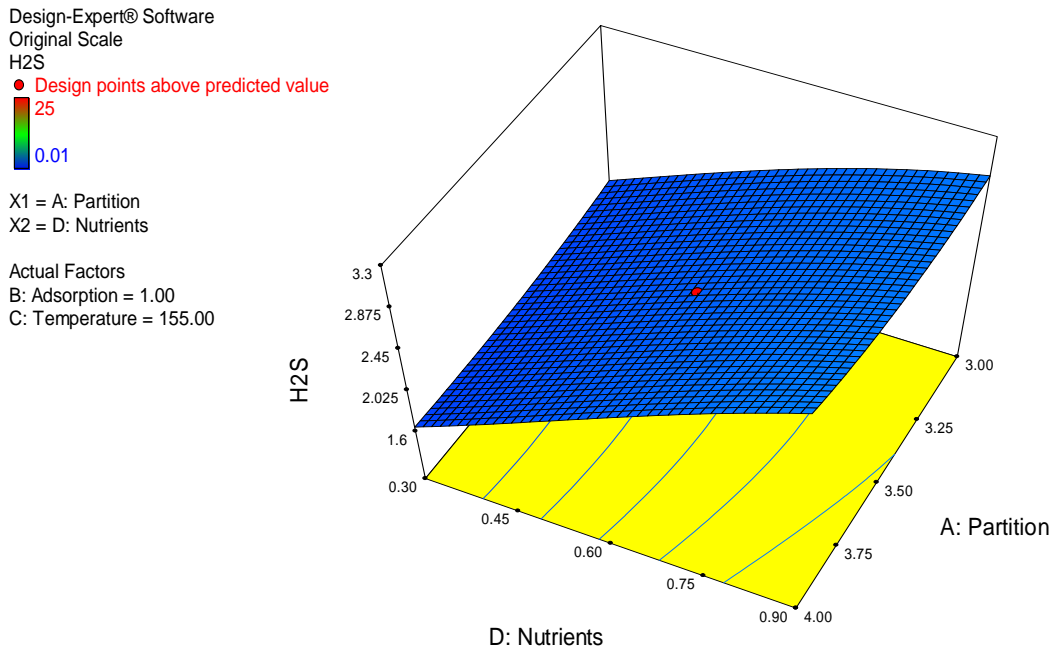


Figure 7.5 Effects of nutrients and partitioning on the produced hydrogen sulfide

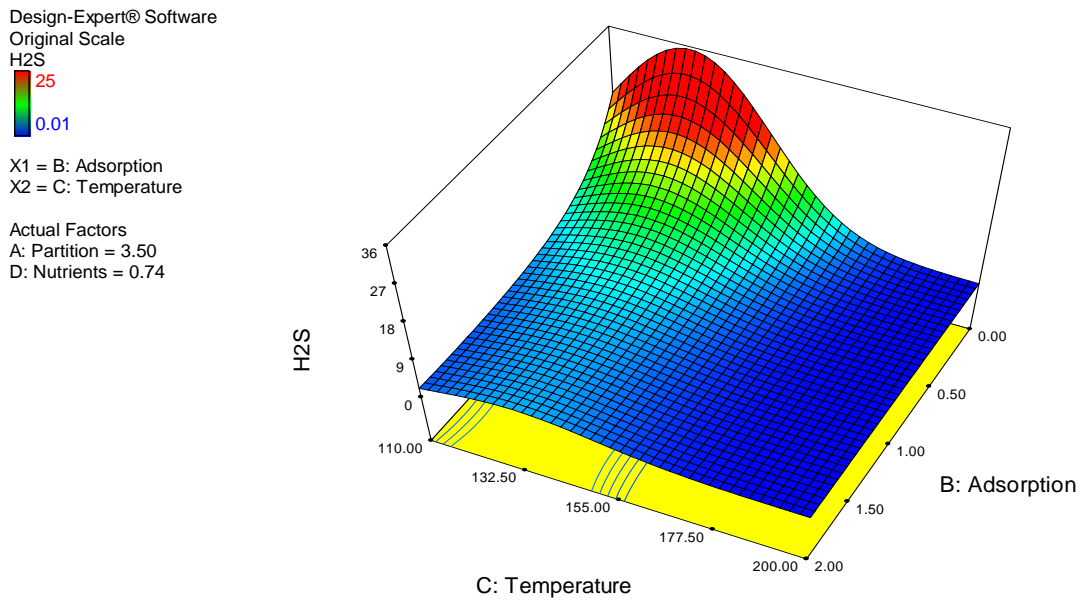


Figure 7.6 Effects of temperature and adsorption on the produced hydrogen sulfide

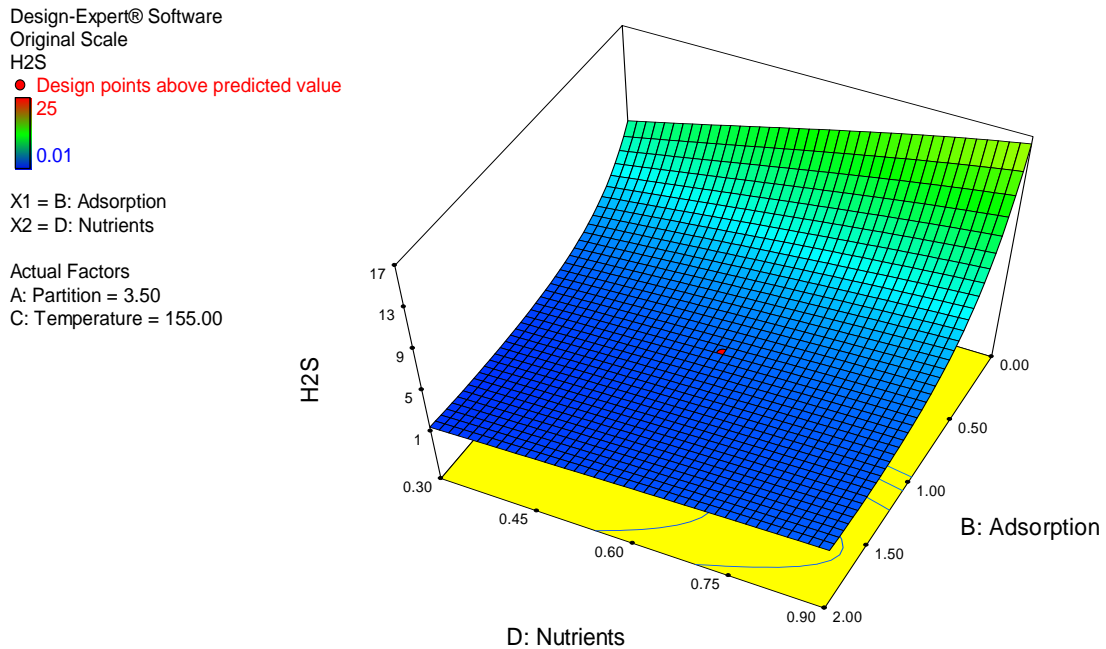


Figure 7.7 Effects of nutrients and adsorption on the produced hydrogen sulfide

7.3 Field Application of the Developed Model and Simulator

In this section, the capabilities of our model in prediction of the reservoir souring in 3D reservoirs are discussed. In the following sections, we describe two different cases. The first case is a quarter five spot reservoir with ten layers of varying properties. The second case is a reservoir with three layers with stochastic estimation of porosity and permeability. This case also consists of five injection and eight production wells. These two case studies show that UTCHEM is capable of handling a complicated case which maybe encountered in real fields.

7.3.1 Application of the Simulator for a Multi-layered reservoir

In this case study, a reservoir which consists of ten layers with variable porosity and permeability are simulated. The reservoir data, conditions and characteristics are given in Tables 7.2a-e. The UTCHEM INPUT file corresponding to this case is given in Appendix F.

Table 7.2a Reservoir characteristics

Layer #	L1	L2	L3	L4	L5	L6	L7	L8	L9	L10
Porosity	0.25	0.28	0.3	0.32	0.2	0.23	0.26	0.29	0.25	0.25
Perm-x, md	300	250	150	200	100	85	125	200	300	100
Perm-y, md	300	250	150	200	100	85	125	200	300	100
Perm-z, md	60	50	30	40	20	16	25	40	60	20

Table 7.2b Reservoir conditions

S_{wi}	S_{wr}	S_{or}	Water end point relative permeability	Oil end point relative permeability	Water relative permeability exponent	Oil relative permeability exponent
0.3	0.147	0.28	0.1377	0.9148	2.18	1.4

Table 7.2c Reservoir conditions (continued)

Initial Temperature (°F)	Initial Pressure (psia)	Reservoir Depth (ft)	Rock Compres. (1/psi)	Water Compres. (1/psi)	Oil Compres. (1/psi)	Water Vis. (cp)	Oil Vis. (cp)
160	3771	6200	5.2E-6	3E-6	5.65E-6	0.4	1.25

Table 7.2d Reservoir data for energy balance equation

Rock density (lb/ft ³)	Rock thermal conduct. (Btu(lb-°F) ⁻¹)	Rock heat capacity (Btu(lb-F) ⁻¹)	Water phase heat capacity (Btu(lb-°F) ⁻¹)	Oil phase heat capacity (Btu(lb-°F) ⁻¹)	Water density (psi/ft)	Oil density (psi/ft)
165.43	40	0.2117	1	0.5	0.4368	0.3462

Table 7.2e Reservoir simulation data

Injection well, constant rate (ft ³ /day)	Production well, constant pressure (psi)	N _x , Δx (ft)	N _y , Δy (ft)	Δz (ft)
4000	3771	30×20	10×30	8, 15, 27, 14, 20, 5, 9, 10, 14, 12

To show the profile of the concentration of the species involved in reservoir souring, 3D view representation of these variables are given in different times during simulation. Furthermore, a non-reacting water tracer is also introduced to the reservoir to follow the concentration profiles. This investigation shows that we have a tool to track all the species which may have a role in reservoir souring.

Figures 7.8-7.10 show the water tracer advancement in the reservoir after 3 months, 1 year, and 2 years, respectively.

The concentrations of the hydrogen sulfide, nitrate, phosphate and SRB in aqueous phase after 2 years of injecting sea water are also given in Figures 7.11-7.14, respectively.

The temperature distributions which play an important role on the biological activities are shown in Figures 7.15-7.17.

The sketched profiles show that after 2 years of water injection, the tracer (Figure 7.10) reached the production well. At the same time, Figure 7.11 shows that the plume of

produced hydrogen sulfide follows the tracer with a lag due to partitioning between phases. As expected, hydrogen sulfide generated in only mixing zone between injection and formation water. The plume of hydrogen sulfide followed the mixing zone with a delay due to retardation effect. Figures 7.12-7.14 show that the concentration of nitrate, phosphate and SRB, respectively. The concentration of nitrate (after 2 years, Figure 7.12) decrease continually from injection well to the injection front which is the reaction zone (it is assumed that nitrate is provided from injection water). Figure 7.13 shows that phosphate concentration ranges from its concentration in formation water to its minimum in injection front (it is assumed that phosphate is provided from formation water). As indicated in Figure 7.14, the maximum concentration of SRB occurs in injection front. Figures 7.15-7.17 represent the advancement of temperature front while injecting cold seawater to the same reservoir after 3 months, 1 year and 2 years, respectively. Comparing the water injection front (Figure 7.10) with the temperature advancement front (Figure 7.16) shows that the temperature front follows the injection front with a delay. For this case study, the temperature effect on the biological reactions will reduce as time passes but it may have strong effect at earlier time (SRB type is thermophilic, Table 3.1).

The overall results of the prediction of the reservoir souring onset are reflected in Figures 7.18 and 7.19. The water breakthrough (and tracer), which is shown in Figure 7.18 is about 0.45 PV. Figure 7.19 indicates the history of the produced hydrogen sulfide and other species involved in the biological reactions. The observed hydrogen sulfide has a delay with respect to water breakthrough which is due to retardation.

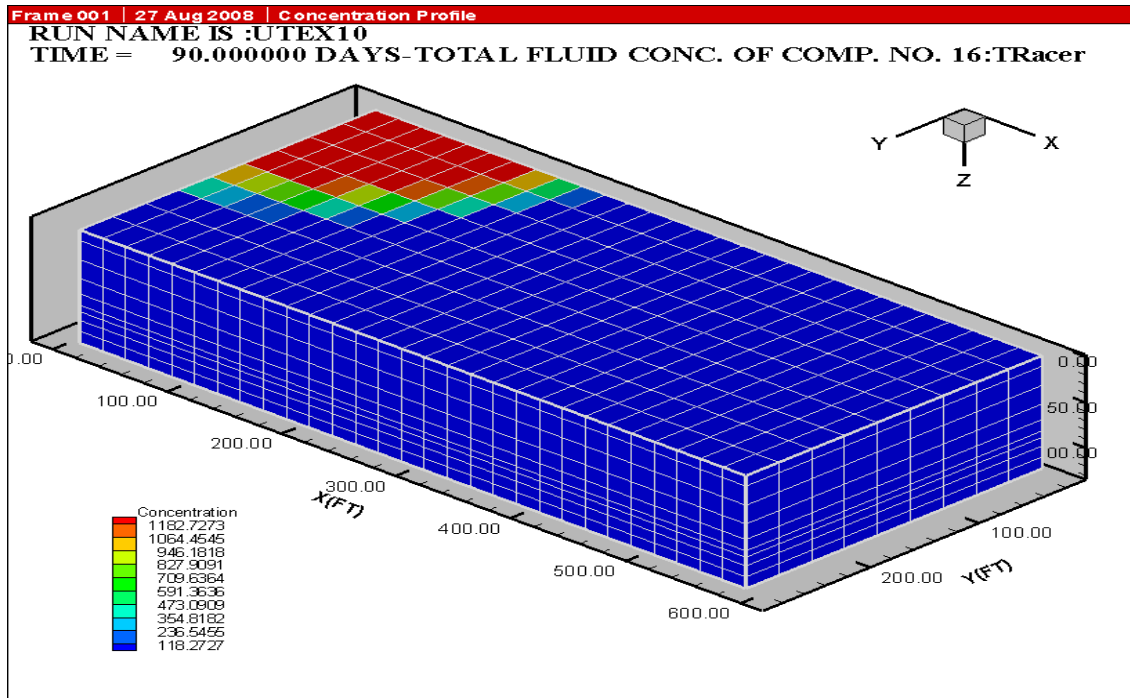


Figure 7.8 Profile of water tracer after 3 months of seawater injection

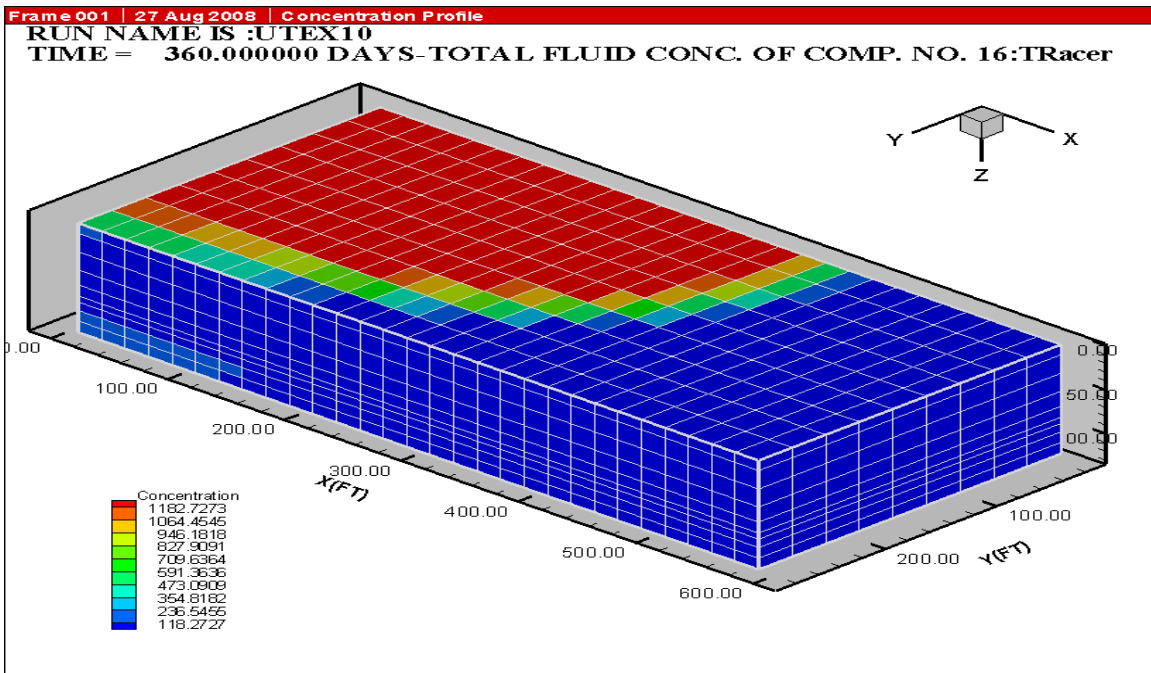


Figure 7.9 Profile of water tracer after 1 year of seawater injection

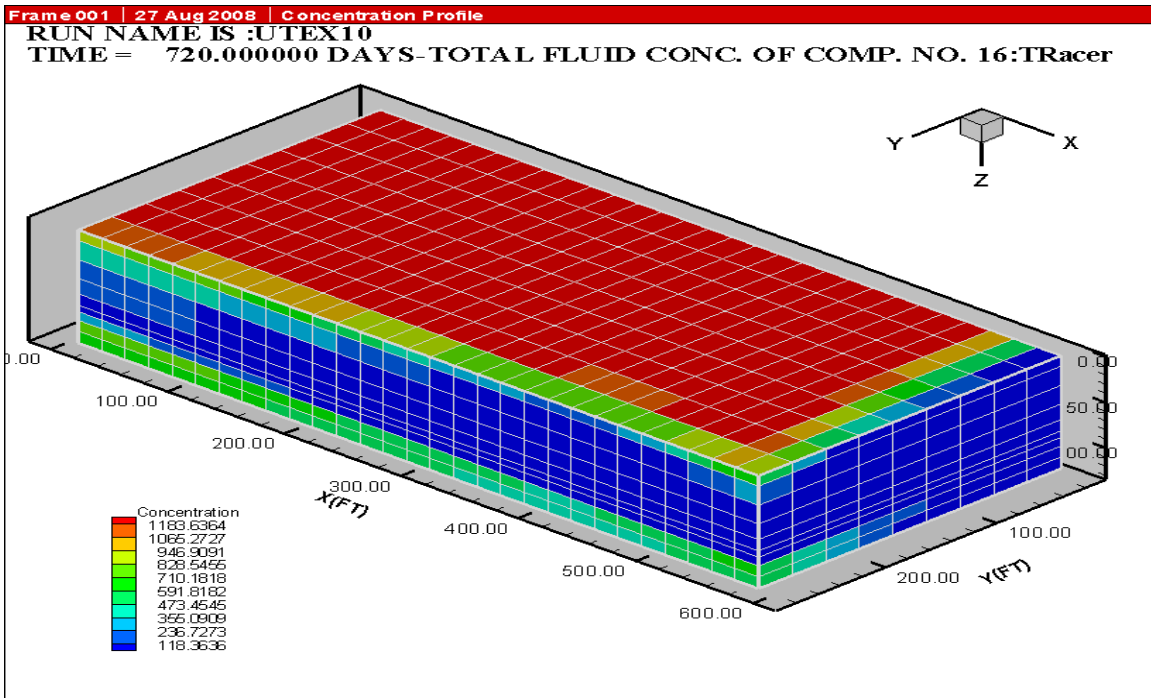


Figure 7.10 Profile of water tracer after 2 years of seawater injection

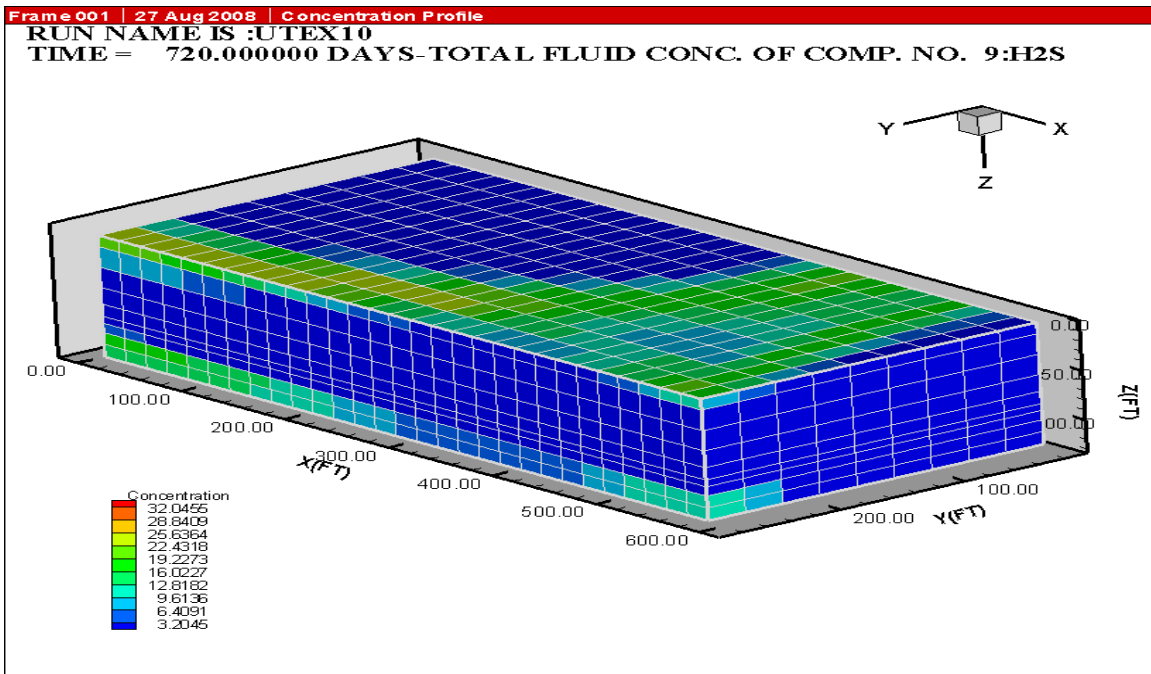


Figure 7.11 Profile of hydrogen sulfide after 2 years of seawater injection

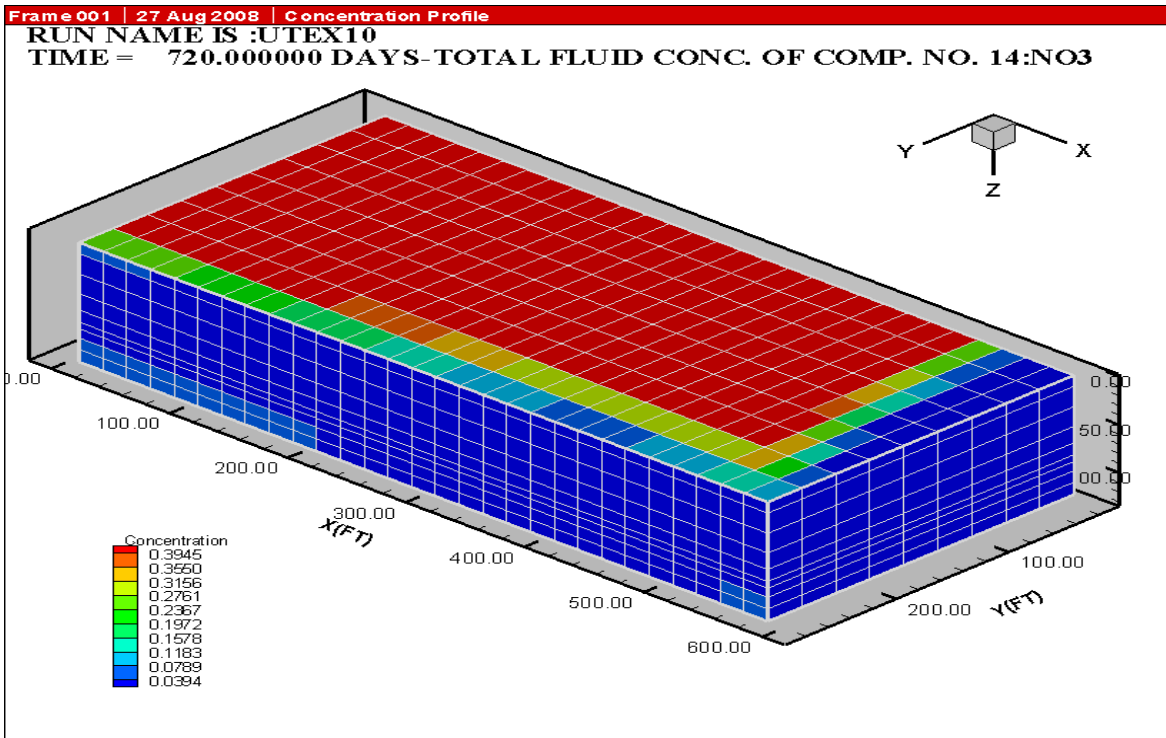


Figure 7.12 Profile of nitrate after 2 years of seawater injection

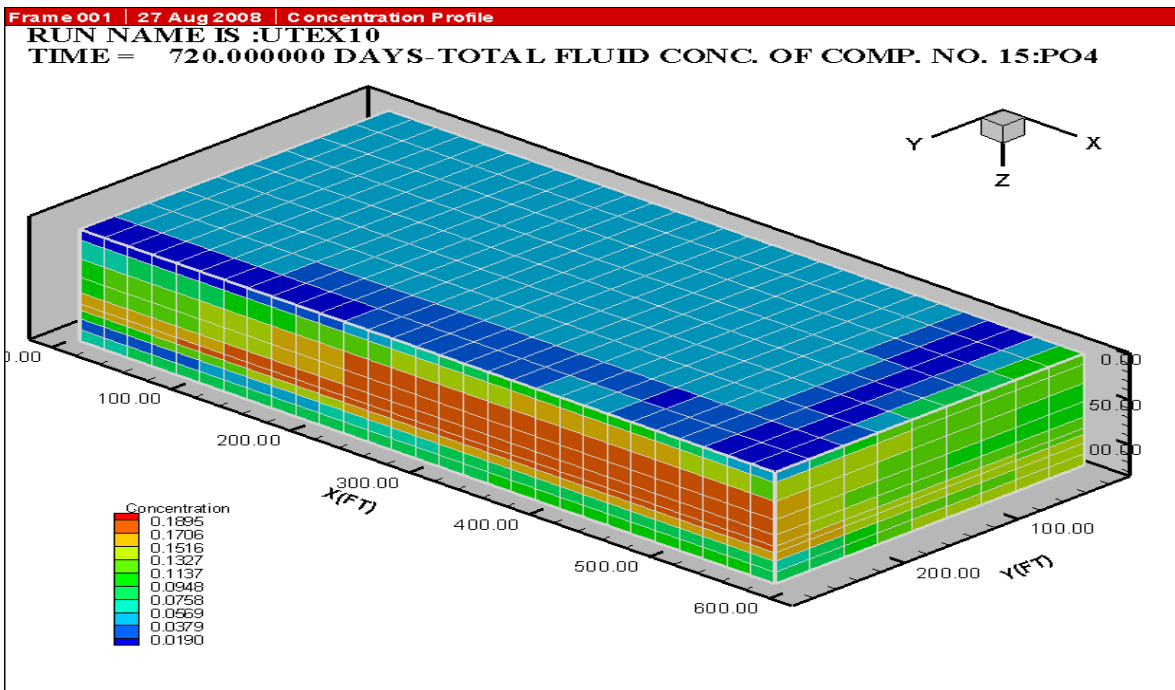


Figure 7.13 Profile of phosphate after 2 years of seawater injection

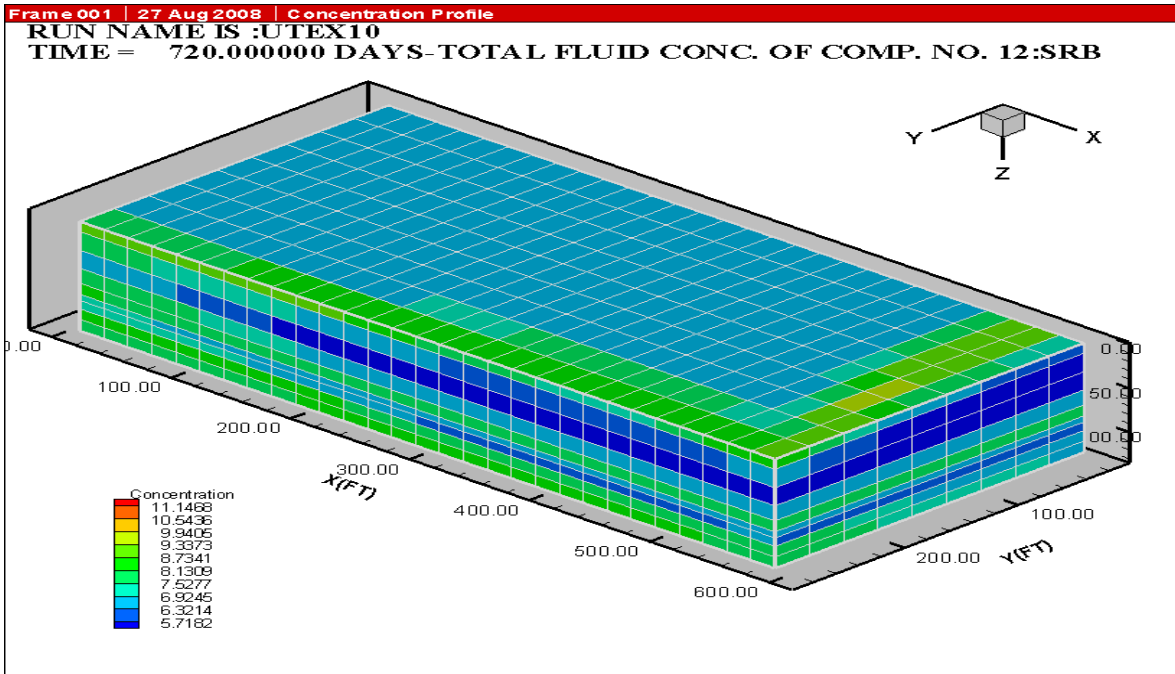


Figure 7.14 Profile of SRB after 2 years of seawater injection

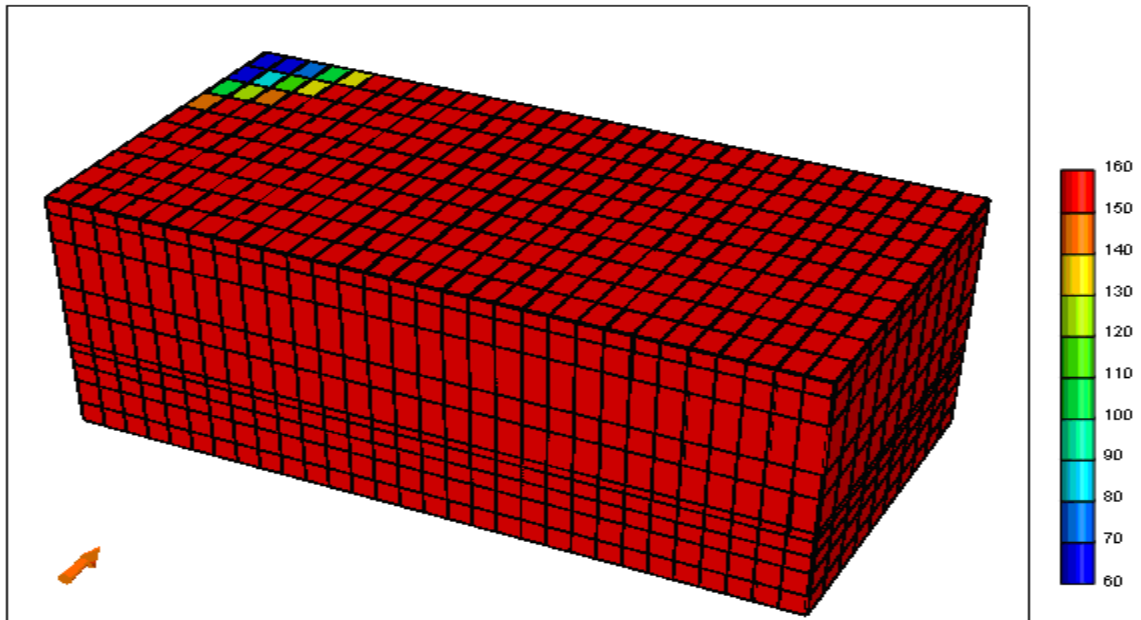


Figure 7.15 Temperature advancement after 3 months of seawater injection

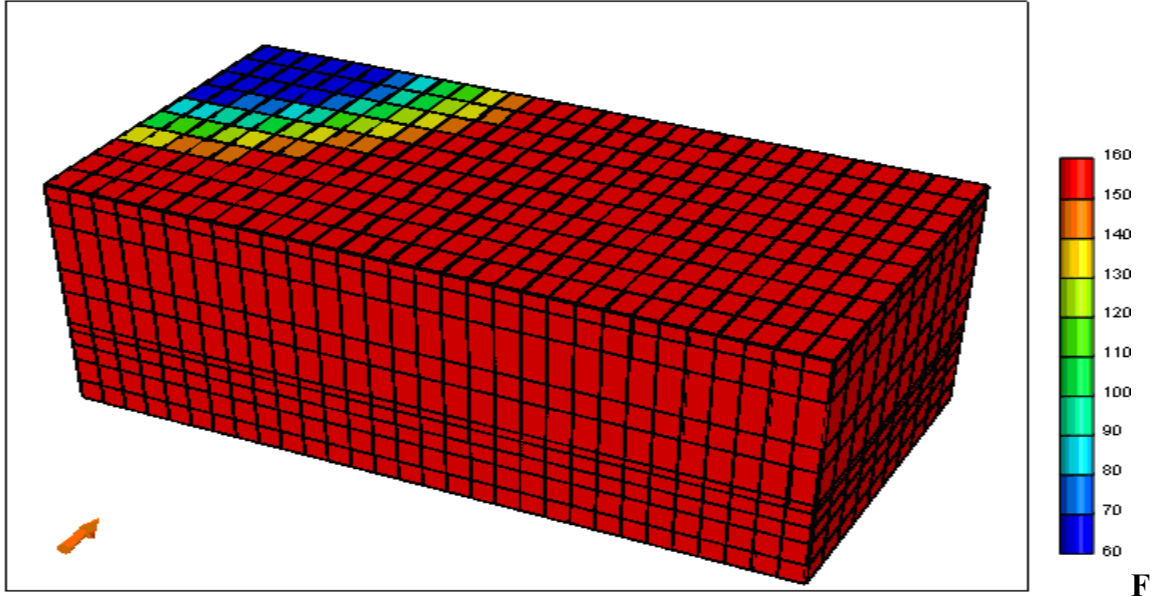


figure 7.16 Temperature advancement after 1 year of seawater injection

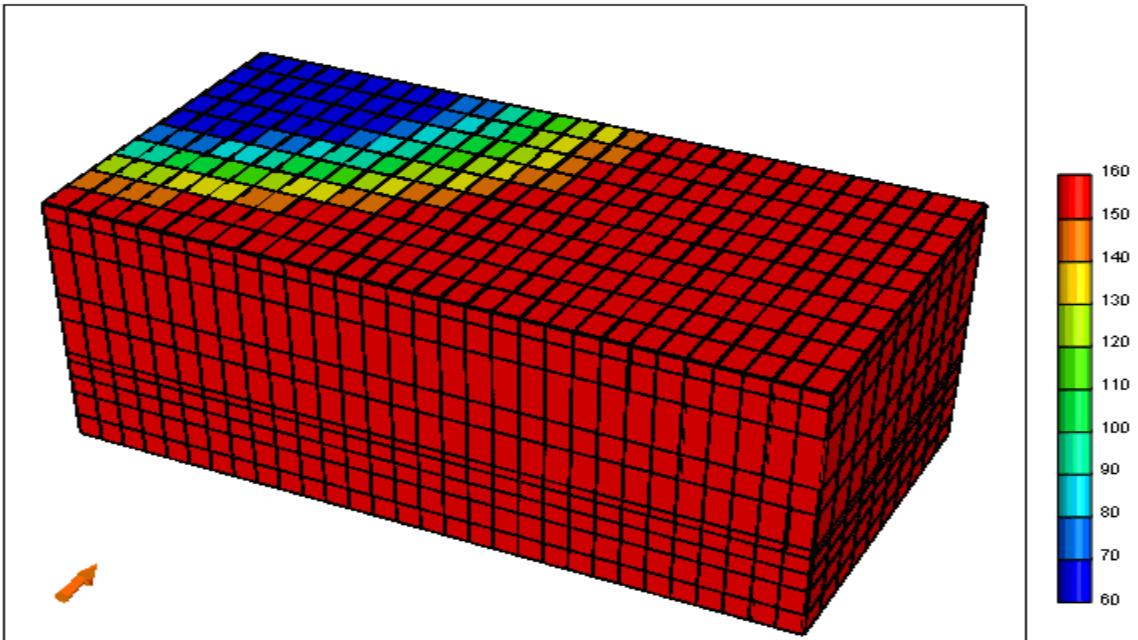


Figure 7.17 Temperature advancement after 2 years of seawater injection

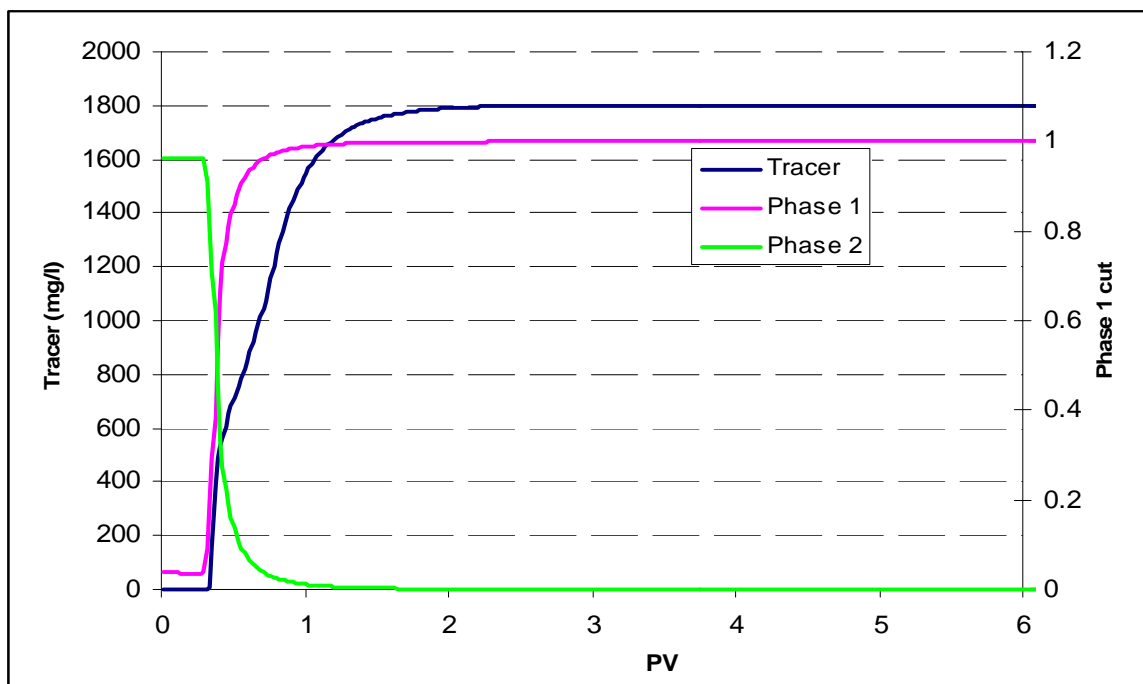


Figure 7.18 Water breakthrough vs. pore volume injected

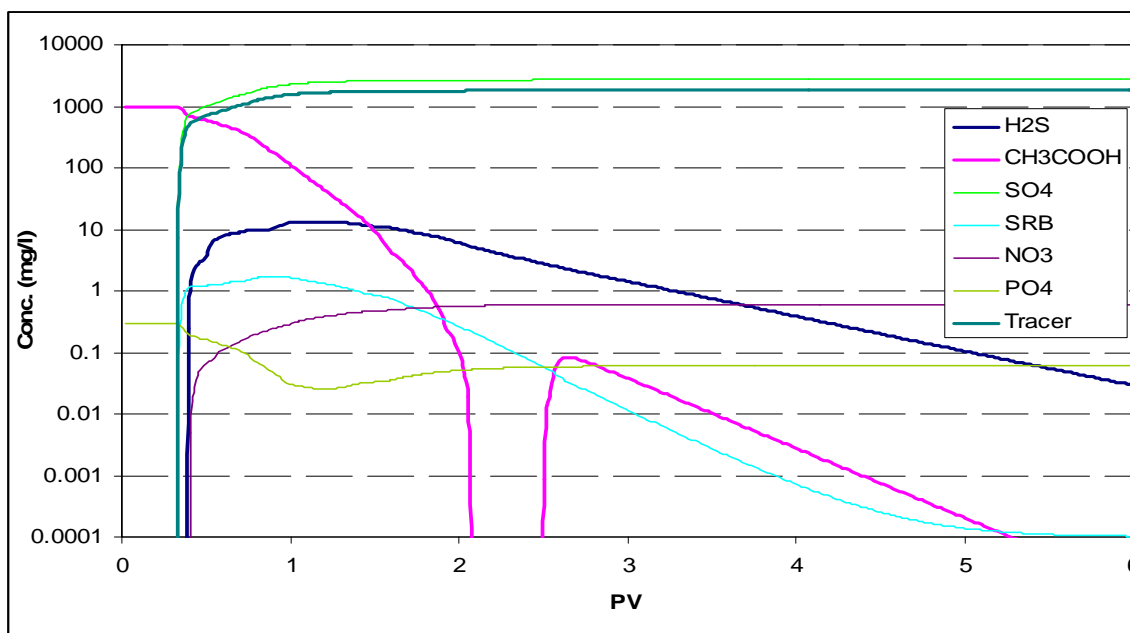


Figure 7.19 History of the produced hydrogen sulfide and other species involved in biological reactions

7.3.2 Application of the Simulator for a Multi-layered and Multi-well reservoir

In this case study, a reservoir which consists of three layers of varying properties and thirteen wells has been defined. The reservoir properties and conditions are given in Tables 7.3a-e. Figure 7.20 represents the location of the wells in the model where the circles represent the production wells, triangles represent the injection wells, and W_i represents the well number.

Table 7.3a Reservoir characteristics

Layer #	L1, L2, L3
Porosity	0.3
Perm-x, md	800-2300
Perm-y, md	Perm-y = Perm-x
Perm-z, md	Perm-z = 0.1 Perm-x

Table 7.3b Reservoir conditions

S_{WI}	S_{WR}	S_{OR}	K_{rw0}	K_{ro0}	Water relative permeability exponent	Oil relative permeability exponent
0.32-0.72	0.25	0.15	0.2	0.95	3	2

Table 7.3c Reservoir conditions (continued)

Initial Temperature (°F)	Initial Pressure (psia)	Reservoir Depth (ft)	Rock Compres. (1/psi)	Water Compres. (1/psi)	Oil Compres. (1/psi)	Water Vis. (cp)	Oil Vis. (cp)
160	1770	4150	0	0	0	0.46	40

Table 7.3d Reservoir data for energy balance equation

Rock density (lb/fr ³)	Rock thermal conduct. (Btu(lb-°F) ⁻¹)	Rock heat capacity (Btu(lb-F) ⁻¹)	Water phase heat capacity (Btu(lb-°F) ⁻¹)	Oil phase heat capacity (Btu(lb-°F) ⁻¹)	Water density (psi/ft)	Oil density (psi/ft)
165.43	40	0.2117	1	0.5	0.4368	0.3462

Table 7.3e Reservoir simulation data

Injection well, constant rate (ft ³ /day)	Production well, constant rate (ft ³ /day)	$N_x, \Delta x$ (ft)	$N_y, \Delta y$ (ft)	Δz (ft)
W3, 1967	W1, -679	19×32.8	19×32.8	10, 20, 10
W6, 2123	W2, -803			
W8, 2244	W4, -928			
W9, 1740	W5, -850			
W11, 1942	W7, -2088			
---	W10, -843			
---	W12, -611			
---	W13, -693			

The overall results of the prediction of hydrogen sulfide in the production wells are given in Figures 7.21 and 7.22. The results show that maximum concentration of the observed hydrogen sulfide in well number 7 occurs around 0.83 PV (the earlier breakthrough) and for well number 10 is about 1.55 PV (the late breakthrough) after injecting seawater. Figure 7.20 confirms that the earlier observed souring in well number 7 compared to other wells is due to the shortest distance between injectors and producers. Furthermore, well number 7 is surrounded by four injectors which cause higher production rates and consequently earlier breakthrough.

	1	2	3	4	5	6	7	8	9	10	11	12	13	14	15	16	17	18	19
1																			
2																			
3			W5 ○							W2 ○							W1 ○		
4																			
5																			
6																			
7							W6 △							W3 △					
8																			
9																			
10										W7 ○									
11	W10 ○																	W4 ○	
12																			
13																			
14							W11 △							W8 △					
15																			
16																			
17			W13 ○						W12 ○										
18																	W9 △		
19																			

Figure 7.20 Location of the injection and production wells in field case 2

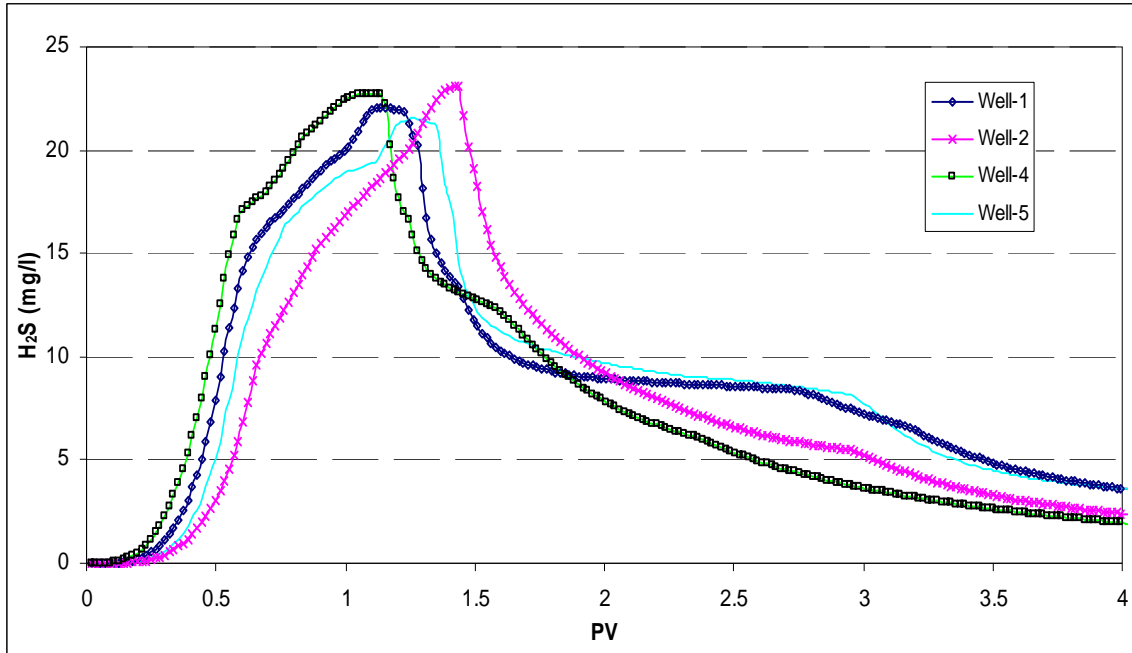


Figure 7.21 History of the produced hydrogen sulfide in wells 1, 2, 4, and 5

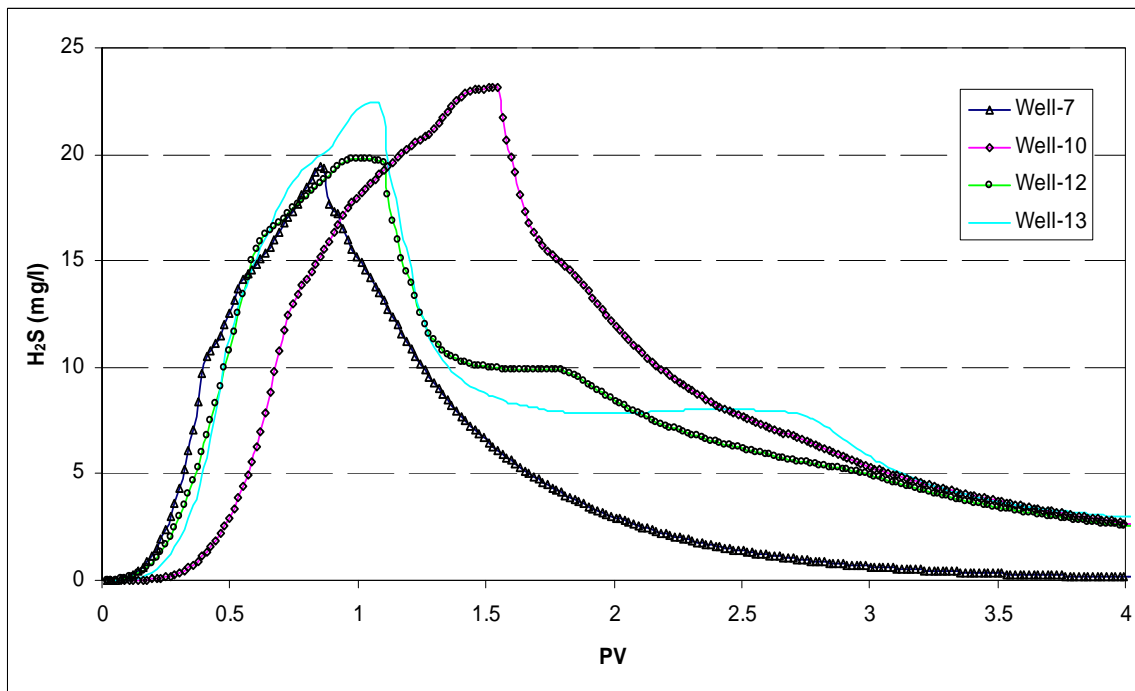


Figure 7.22 History of the produced hydrogen sulfide in wells 7, 10, 12, and 13

Figures 7.23-7.34 show the propagation of the essential physical and chemical variables which control the reservoir souring in this reservoir model. Figures 7.23-25 show the distribution of a water tracer after 1, 2 and 3 years of seawater injection. The tracer will distribute between injectors and producers while the corners of the reservoir remain untouched. Similar distribution can be observed for the temperature fronts as shown in Figures 7.26-28. Figure 7.29 shows the hydrogen sulfide distribution in the reservoir after 2 years of sea water injection. Hydrogen sulfide distribution shows that after 2 years (Figure 7.29) the mixing zone has passed the production wells (Figures 7.21 and 22). Thus, the maximum hydrogen sulfide concentration is not within the reservoir and as time passes the remaining concentration of hydrogen sulfide in the reservoir will decrease.

Distribution of the nitrate (from injected water) and phosphate (in formation water), after two years are shown in Figures 7.30 and 7.31, respectively. The concentrations in the corners for nitrate and phosphate are in reverse order, while distribution of nitrate from injection water (Figure 7.30) is less in corner points which is less affected by injection water. On the other hand, in the corners the distribution of phosphate in formation water remains unchanged at its initial concentration and decreases where fluid flow occurs. The SRB, which is produced within the reservoir, has a distribution (Figure 7.32) similar to phosphate (Figure 7.31). This observation also can be explained in terms of migration of the mixing zone and the unaffected corners. The distribution of sulfate (from injected water) and acetate (in formation) also are illustrated in Figure 7.33 and 7.34, respectively. As expected, the acetate distribution (Figure 7.34) shows higher concentration in unaffected regions, like corner points, while the

concentration decreases where fluid flow occurs. This conclusion is reversed for sulfate which is injected by seawater (Figure 7.33).

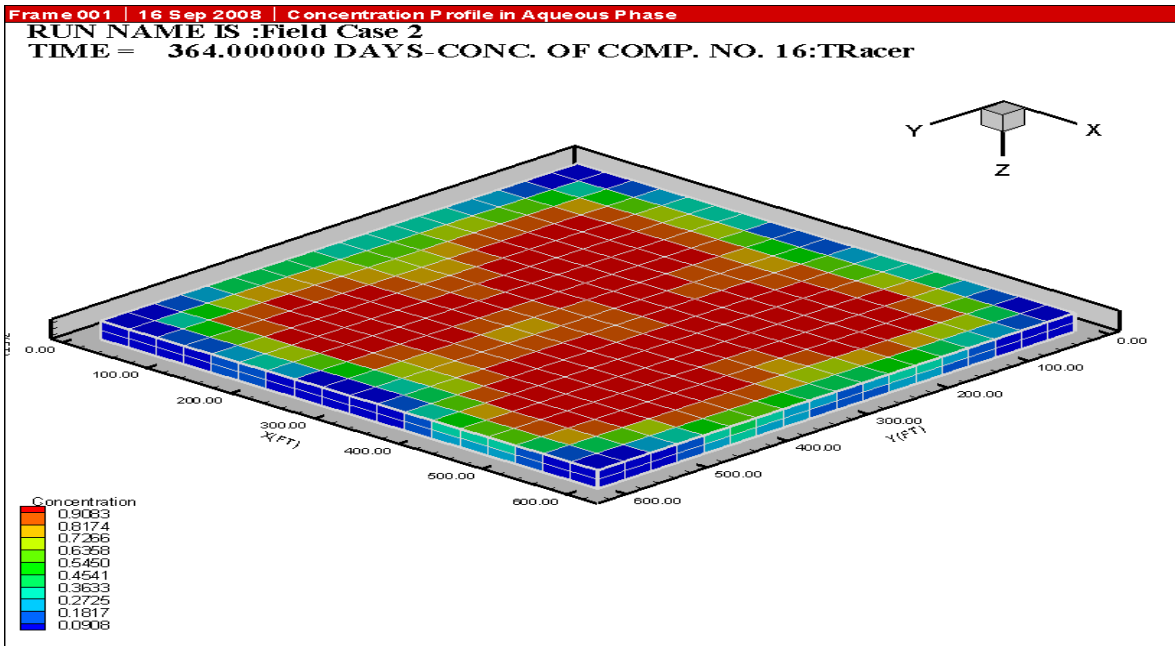


Figure 7.23 Tracer distribution after 1 year of water injection

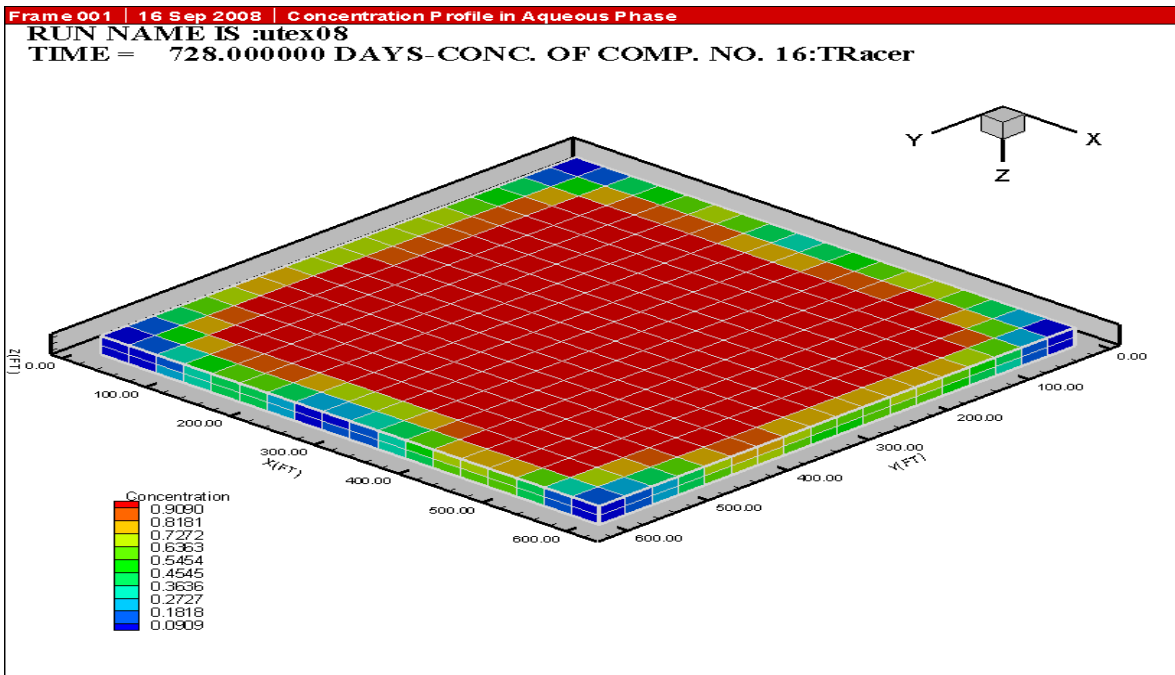


Figure 7.24 Tracer distribution after 2 years of water injection

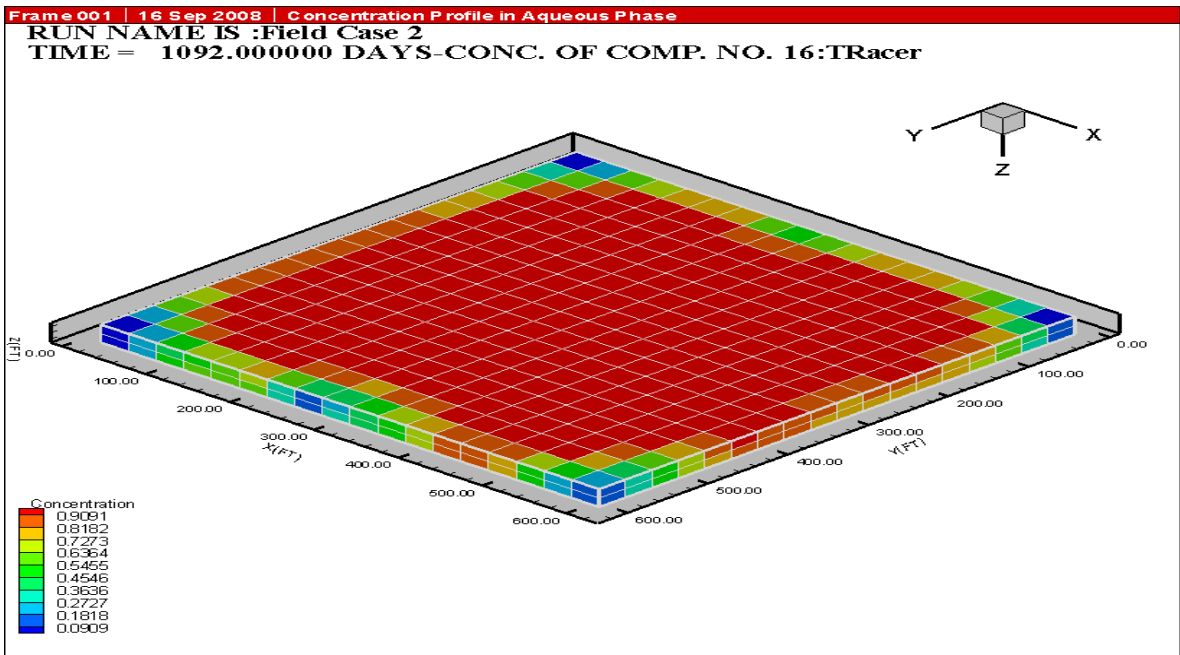


Figure 7.25 Tracer distribution after 3 years of water injection

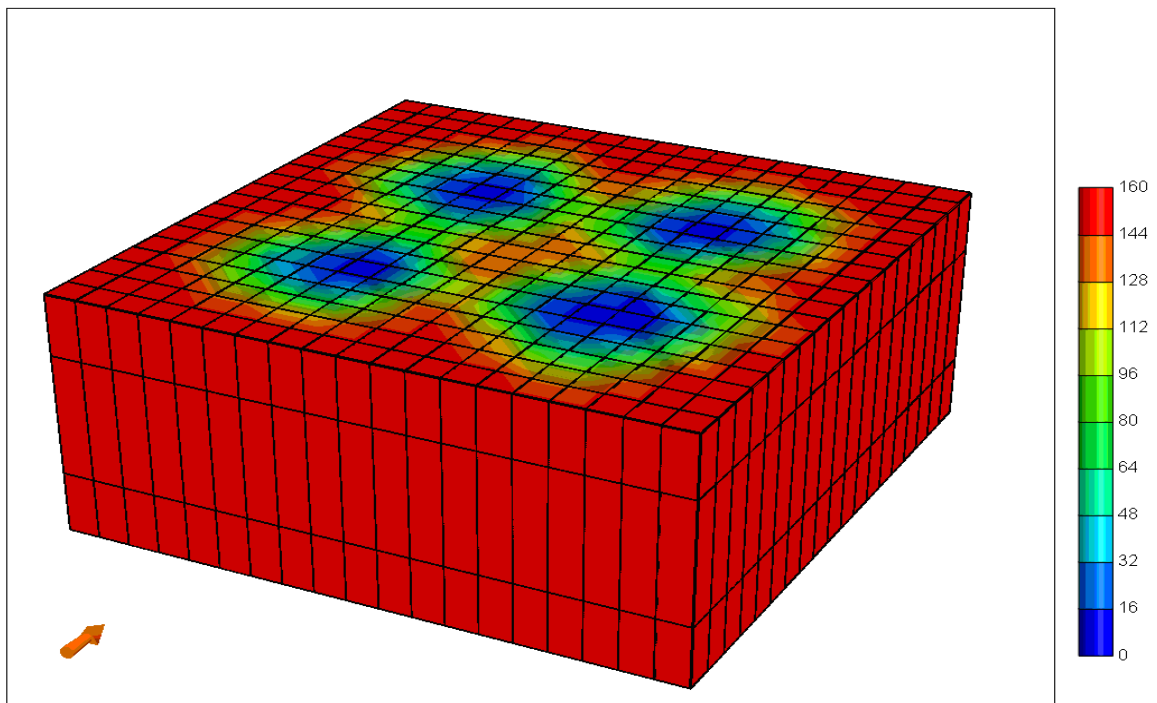


Figure 7.26 Temperature distribution after 1 year of water injection

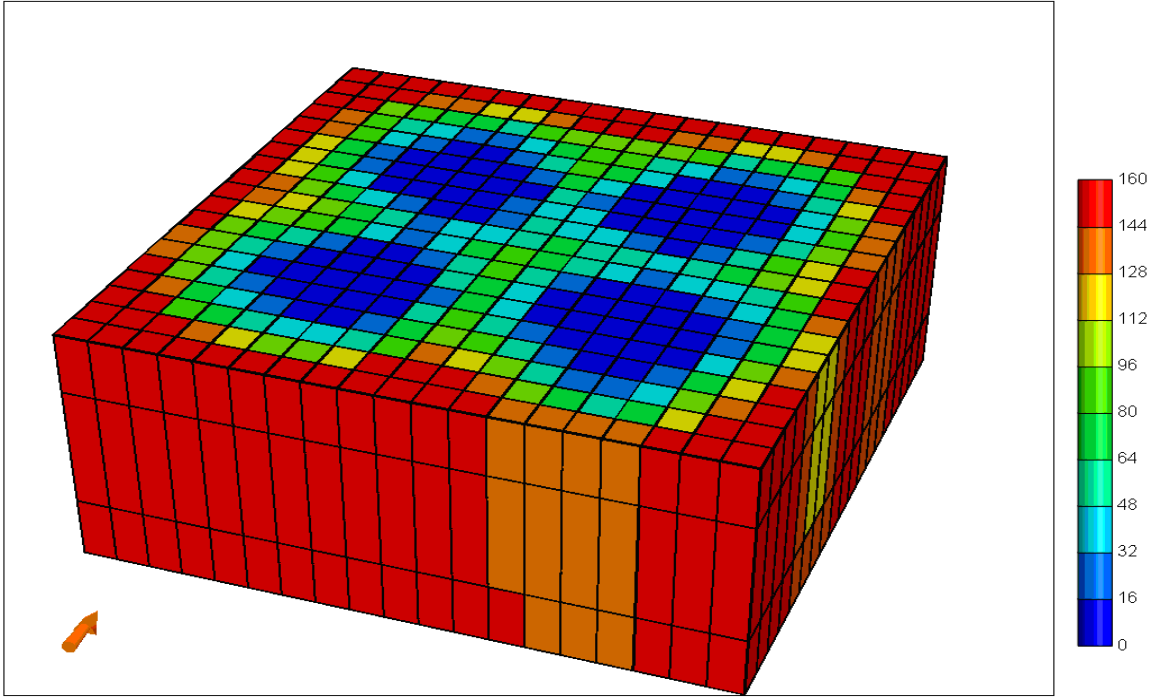


Figure 7.27 Temperature distribution after 2 years of water injection

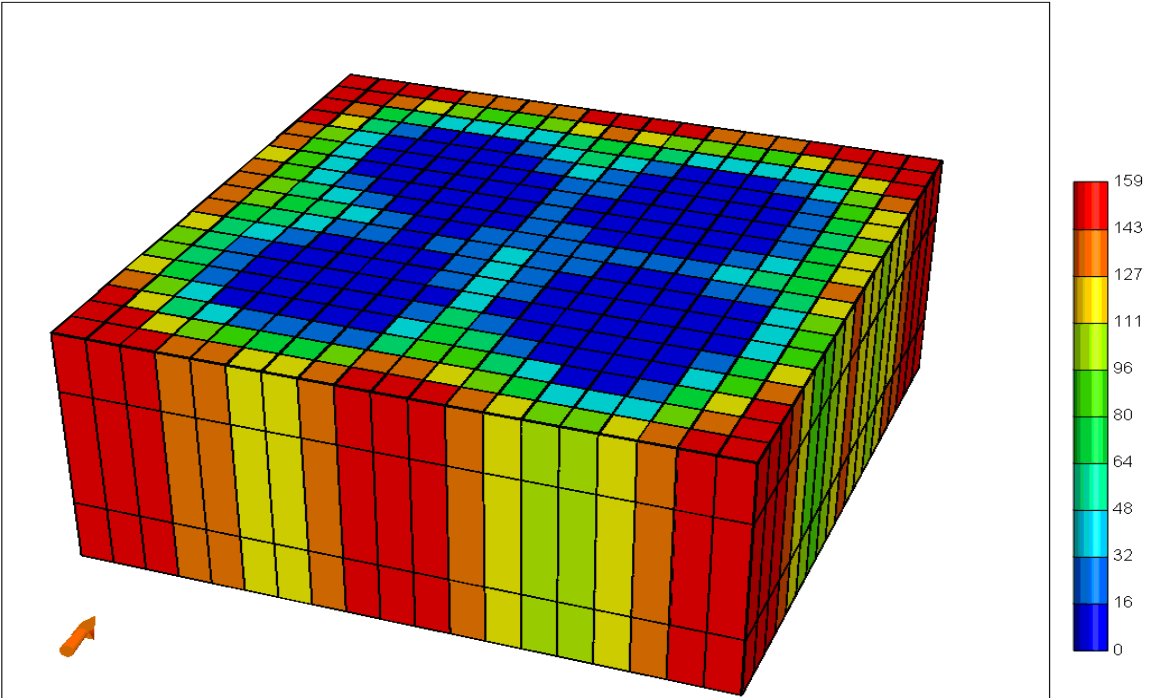


Figure 7.28 Temperature distribution after 3 years of water injection

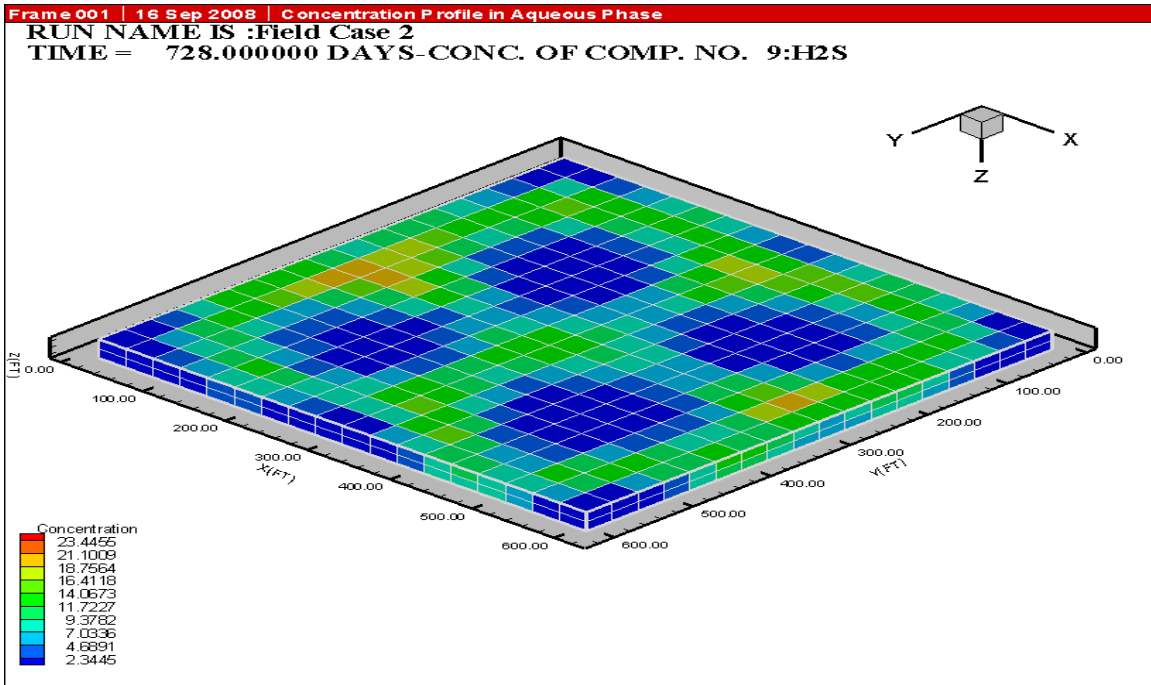


Figure 7.29 Hydrogen sulfide distribution after 2 years of water injection

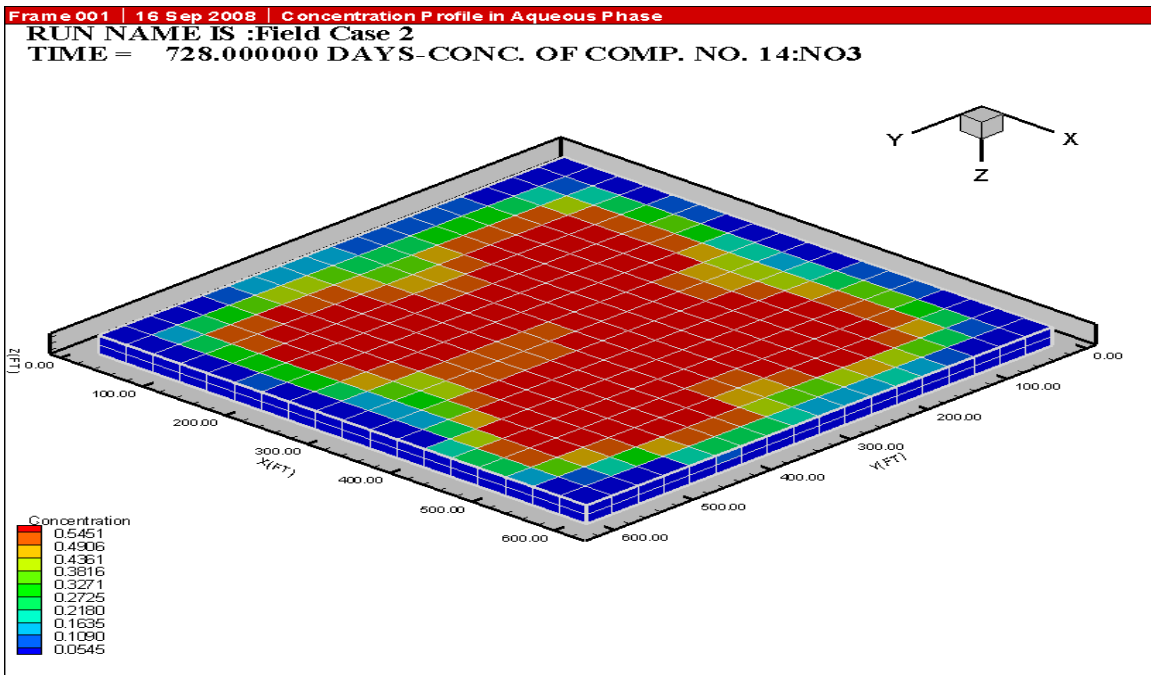


Figure 7.30 Nitrate distribution after 2 years of water injection

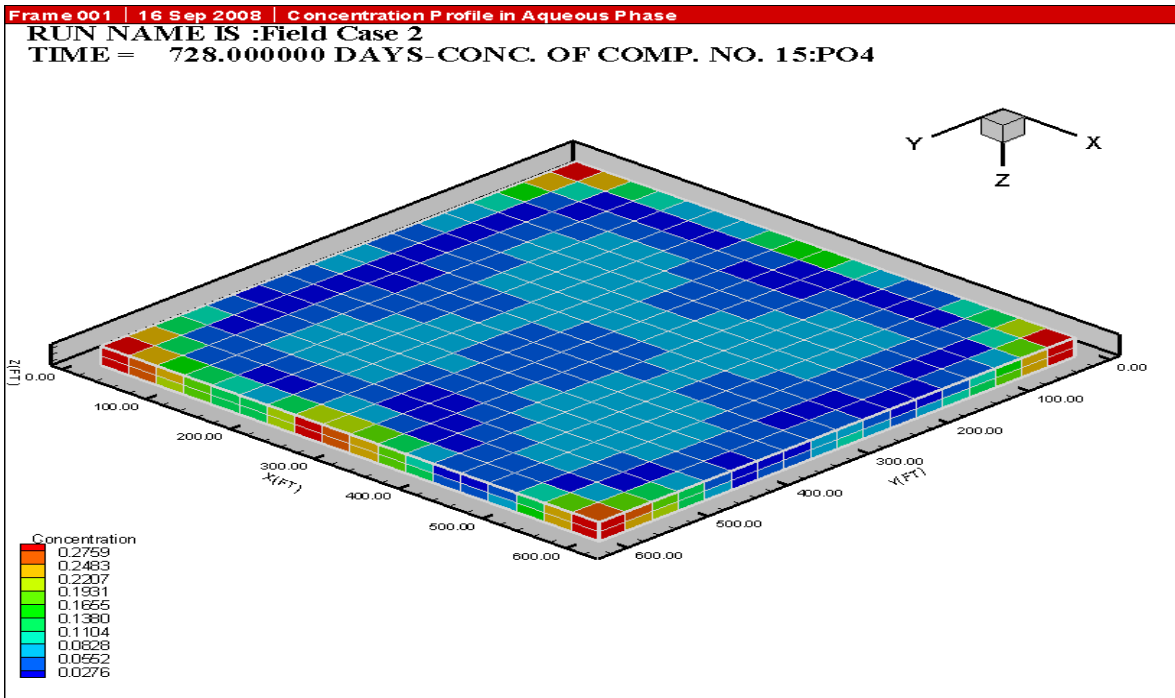


Figure 7.31 Phosphate distribution after 2 years of water injection

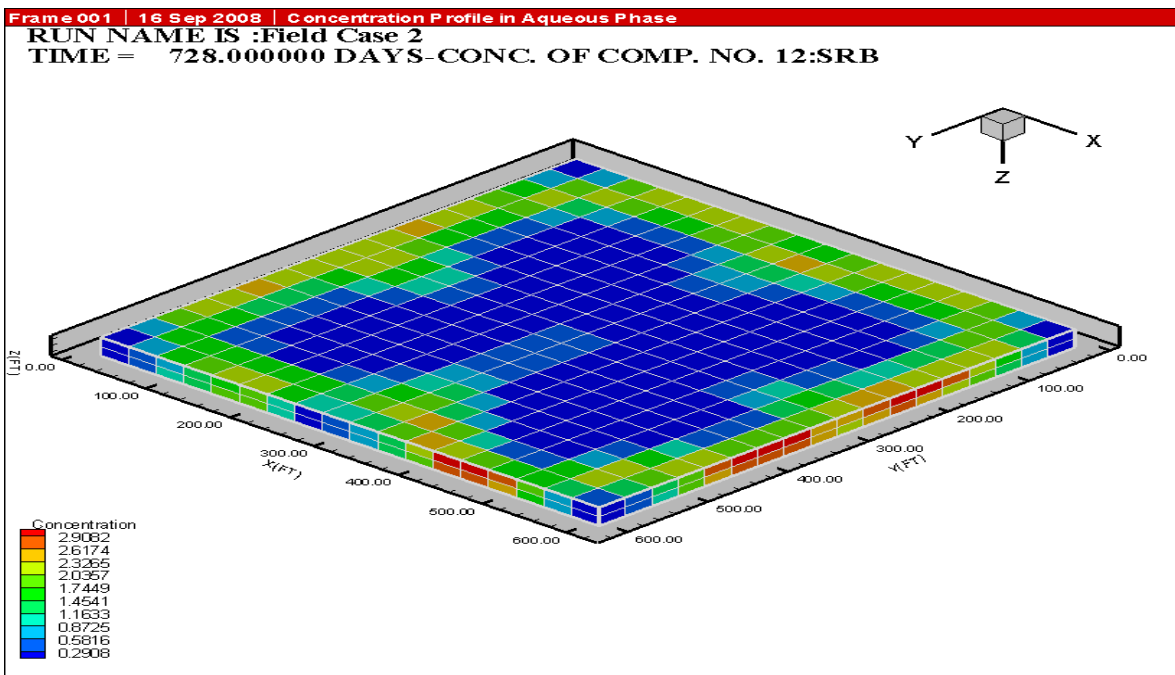


Figure 7.32 SRB distribution after 2 years of water injection

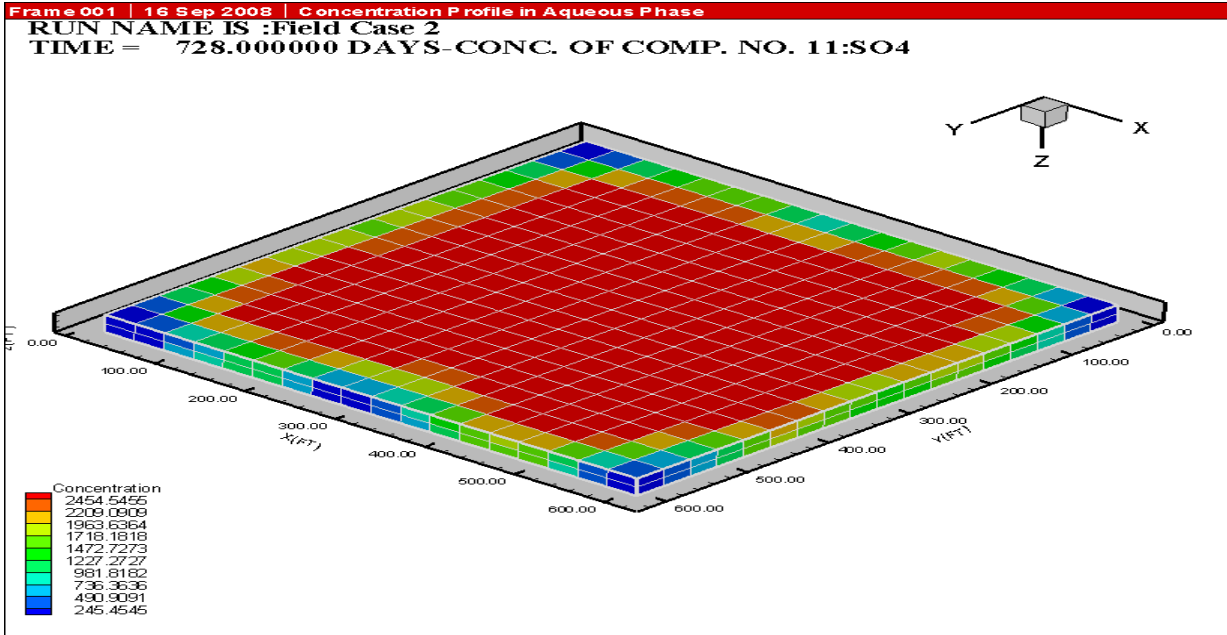


Figure 7.33 Sulfate distribution after 2 years of water injection

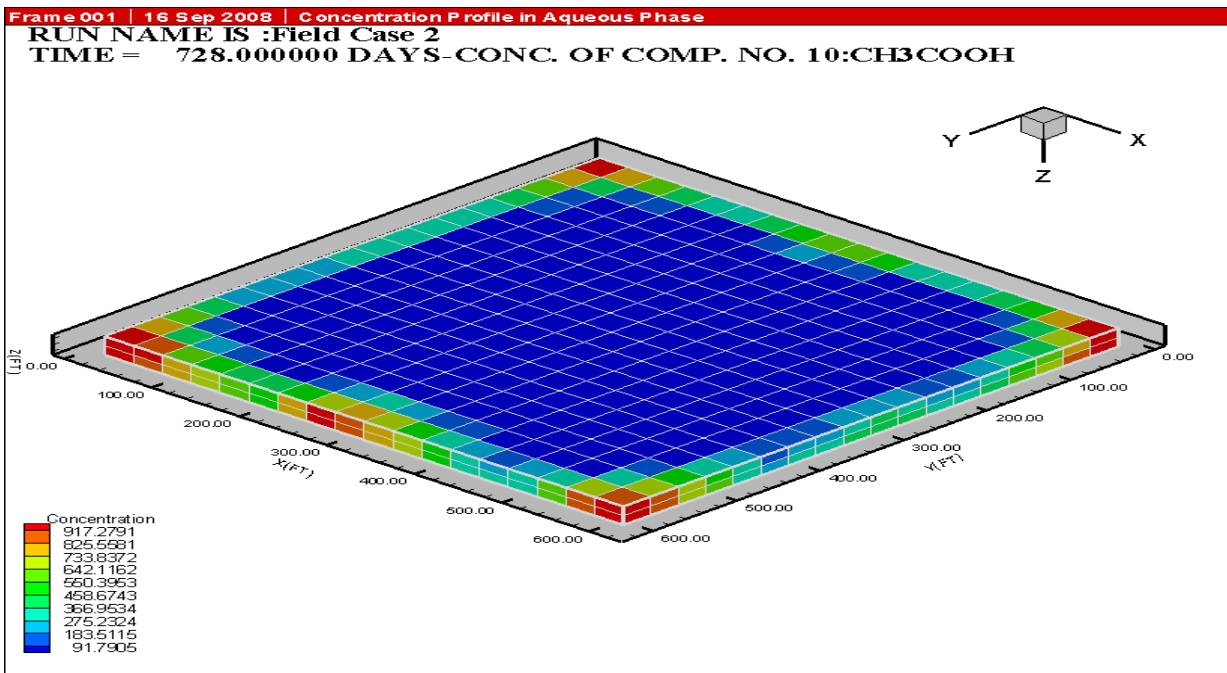


Figure 7.34 Acetate distribution after 2 years of water injection

7.3.3 Effects of grid refinement on the reservoir souring predictions in field case studies

As we explained in detail in section 6.7 the dispersivity of the media has an effective role on the profile of the predicted hydrogen sulfide in reservoirs. The numerical dispersion decreases by grid refinement, as a result the profiles of predicted hydrogen sulfide will change qualitatively and quantitatively (section 6.7).

Figures 7.35 and 7.36 show the profiles of hydrogen sulfide in the case study 2 in the previous section after grid refinement. In this simulation all reservoir properties and conditions remains the same except the gridblocks which are doubled in x, y and z directions. Comparing the profiles of hydrogen sulfide with Figures 7.21 and 7.22 show that the predicted results have changed both qualitatively and quantitatively. These results show that the peak in hydrogen sulfide has dropped while there is more delay in the predicted results. This behavior is more pronounced for wells 2 and 10. Where, the peak in the produced hydrogen sulfide for well 2 (Figure 7.21) has dropped from 23 to 18 mg/l (Figure 7.35) and its arrival has delayed from 0.25 to 0.4 pore volume. The same trends are true for other production wells.

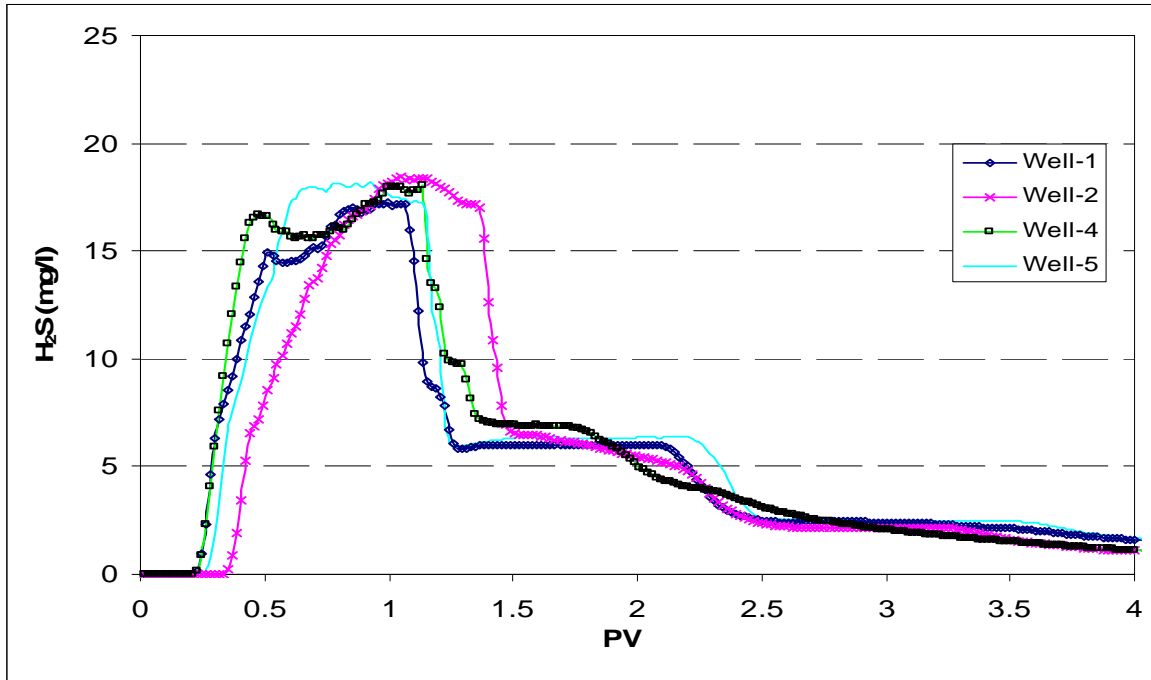


Figure 7.35 History of the produced hydrogen sulfide in wells 1, 2, 4, and 5

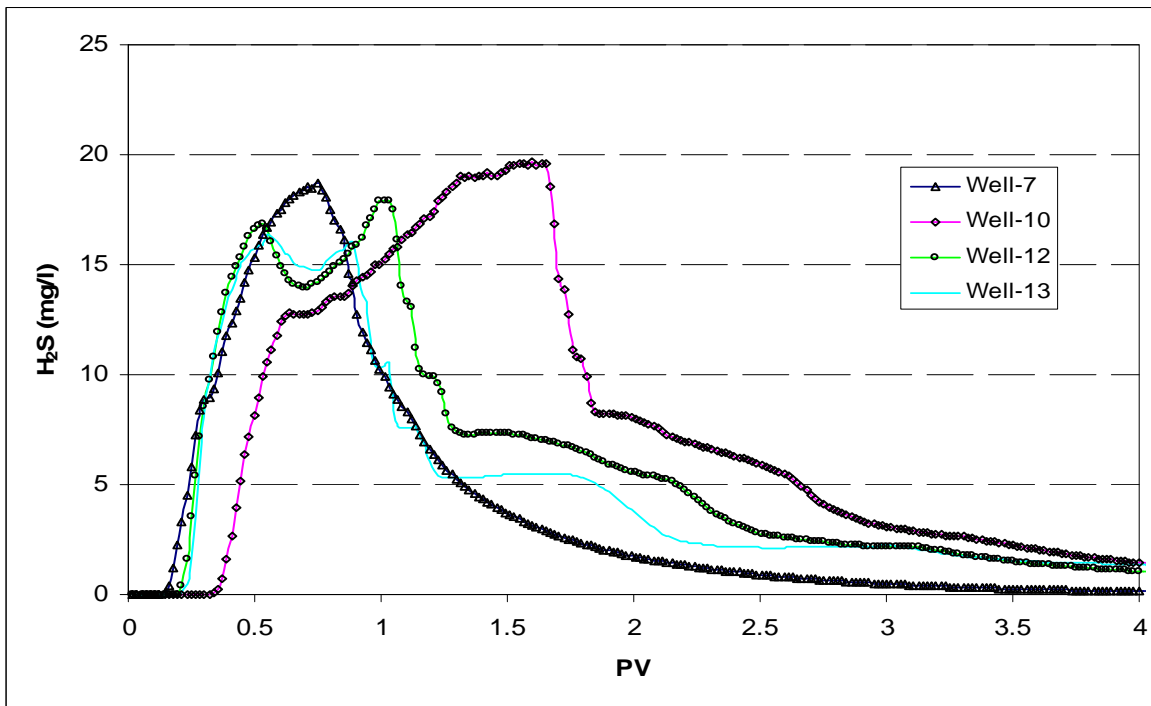


Figure 7.36 History of the produced hydrogen sulfide in wells 7, 10, 12, and 13

Chapter 8

Summary, Conclusions, and Recommendations for Future Work

8.1. Summary

We studied the reservoir souring phenomenon regarding the history, generation and its movement in the porous media. Then, we performed a critical review of the published papers on the modeling and simulation of the prediction of the reservoir souring onset in the seawater injected reservoirs. Simultaneously, we searched for the reservoir souring mechanisms, similar case studies and updated works in this area. Comparing the published models with the mechanisms of reservoir souring in porous media, we concluded that a more comprehensive model is needed. The comprehensive model should have the capabilities to encompass the parameters which have effective roles in the generation and transportation of the hydrogen sulfide in the porous media.

Among the parameters that affect the onset of reservoir souring and were disregarded by other models, there were the effects of temperature and available nutrients on generation of hydrogen sulfide. Some of the models included the effects of partitioning and adsorption on the transportation term and some did not. In addition to the mentioned parameters, most of the previously published models and simulators considered one-dimensional reservoirs. For a model to be applicable for a real reservoir case it needs to be three-dimensional.

Having knowledge of the mechanisms of generation and transportation of hydrogen sulfide in porous media and deficits in the previous models, we developed a new model which is more comprehensive. The developed model was implemented in The University of Texas Chemical Flooding Simulator (UTCHEM). UTCHEM has the features which allow it to be used for the prediction of the onset of souring in real fields.

8.2 Conclusions

1. A three-dimensional reservoir souring model was developed and implemented in a chemical flooding simulator.
2. The developed model has more capability with respect to the previous models (mixing, biofilm, and TVS) in modeling of the generation and transportation of hydrogen sulfide in the reservoir.
3. This model is capable of including the effect of temperature on the biogenic reactions, thus the production of H₂S by different SRB types can be identifiable.
4. The effect of the heterogeneity of the reservoir on the reservoir souring can be included.
5. Results of the extensive simulation show that the generation of hydrogen sulfide in a reservoir for a given SRB type, depends on the available nutrient and reservoir temperature. Other parameters like the concentration of sulfate in seawater, acetate in formation water, and temperature of injected water, for a typical reservoir can be constant.
6. The partitioning of H₂S between oil and water phases varies little from reservoir to reservoir while the adsorption capacities of different rocks can be variable. Thus, the adsorption capacity of a reservoir is critical in prediction of the delay in observed souring with respect to water breakthrough.

7. To reach the guidelines for screening of the reservoirs as the potent to be soured or not, a combination of data about the kind of SRB, available nutrient, reservoir temperature and the rock adsorption capacities are needed.
8. Our model can reproduce the behavior of the mixing, biofilm and TVS models.
9. Investigation of the mixing, biofilm and TVS models shows that each of them has some deficits in simulating the generation and transportation of hydrogen sulfide in the porous media. The mixing model cannot include the effect of nutrients and temperature on generation of hydrogen sulfide. The biofilm model cannot include the effect of temperature on generation of hydrogen sulfide and also it does not consider the partitioning effect on transport of hydrogen sulfide. The TVS model is based on the laboratory experimental data at specified conditions. It cannot include the effects of nutrients in generation of hydrogen sulfide. TVS also is not able to consider the adsorption and partitioning effects on transport of hydrogen sulfide in the reservoirs
10. In real fields, depending on the permeability of the porous media, SRB can attach to the rock surfaces or move with the bulk flow. Only our model can consider this behavior.
11. Prediction of reservoir souring in a real field needs a more comprehensive simulator that can include the effective variables in generation and transportation of hydrogen sulfide in the porous media. The enhanced simulator can include these parameters in addition to the heterogeneity of the media. To the best of our knowledge, UTCHEM is the most comprehensive simulator for field application of reservoir souring predictions.
12. Our simulator can be used to predict the onset of reservoir souring in real fields with different heterogeneities and variation in the physical and chemical variables.

8.2 Recommendations for Future Work

The most important step left in this work is the validation of the simulator with field data. Although we developed a model with many features, we tested the model with one set of field data which were used in testing of biofilm model. We also had access to worldwide data on reservoir souring. However, due to the lack of some essential parameters, they were useless validation. The most uncertain parameter in the prediction of reservoir souring is the adsorption capacity of the rocks. It is highly recommended that before any application of the simulator, the sorption capacity of reservoir rocks be determined.

With the increased interest in chemical flooding, there is a need to couple the geochemistry and biology option in UTCHEM. This feature enables us to predict the reservoir souring for the extreme cases when there are high concentration of alkaline (extreme changes in pH and salinity) and changes in redox potential of the medium. This feature is unique in reservoir simulation.

The reservoir souring process is not limited to the oil reservoirs, it could also happen at certain conditions in gas reservoirs, as well (Hitzman et al., 1997 and 1998; Worden et al., 1996; Koutsyn et al., 1998). The reservoir souring prediction model can be extended to the gas reservoirs. The developed model should be implemented in a compositional reservoir simulator with the capabilities of phase behavior to predict the exact onset of reservoir souring in oil below bubble point pressure.

In the enhanced oil recovery processes, which use gas injection, the presence of hydrogen sulfide is beneficial for the reduction of the minimum miscibility pressure (Shedid et al., 2004). It would be interesting to design the process to produce insitu hydrogen sulfide to help oil recovery.

The basic features which are needed for the simulation of the microbial enhanced oil recovery are included in the biological option of UTCHEM. It would be beneficial to

use the developed model for the non-isothermal process (Hitzman et al., 1994; Premuzic et al., 1999).

The application of the simulator can be extended to the subsurface remediation under non-isothermal conditions, too (Cassinis et al., 1998; Davidova et al., 2001).

The prevention of reservoir souring by controlling the nutrients concentrations and competing with other biological species are possible using our model (Hands et al., 2002; Sahm et al., 1999). There is a need to investigate the simulation of the process and validation of the results with laboratory and field data.

The application of our model should be extended to the simulation of the reservoir souring process for naturally fractured reservoirs. Then, the simulator should be validated with field data. Although we studied in detail the effects of numerical and physical dispersions on the final results of reservoir souring for 1D case (Chapter 6), investigation of these effects for 3D cases needs to be studied. Finally, the UTCHEM user's guide manual should be revised to include the reservoir souring option.

APPENDIX A

INPUT files for simulation of mixing, biofilm, TVS and UTCHEM models for prediction of reservoir souring

MIXING Model

HEAD file

```
Setup1
NX NY NZ N NWELL
26 1 8 15 2
NTW NTA
1 0
NO NPHASE
0 3
IDUAL NSUBV NSUBH
0 0 0
ITENS
0
```

INPUT file

```
CC*****
CC
CC BRIEF DESCRIPTION OF DATA SET : UTCHEM (VERSION 10.0)
CC
CC*****
CC
CC WATER FLOODING
CC
CC LENGTH (FT) : 2740 PROCESS : WATER FLOODING
CC THICKNESS (FT) : 26. INJ. PRESSURE (PSI) : 4121
CC WIDTH (FT) : 100. COORDINATES : CARTESIAN
CC POROSITY : 0.33 TEMP. VARI. NON ISOTHERMAL
CC GRID BLOCKS : 26x1x8
CC DATE : 06/13/2000
CC
CC*****
CC
CC*****
CC
CC RESERVOIR DESCRIPTION
CC
CC*****
CC
CC
*----RUNNO
UTEX10
CC
CC
*----HEADER
```

```

EXmix
Simulation of MIXING model (corresponding to Lightelm et al., 1991)
NONISOTHERMAL SIMULATION, UTCHEM VERSION 10.0
CC
CC SIMULATION FLAGS
*---- IMODE IMES IDISPC ICWM ICAP IREACT IBIO ICOORD ITREAC ITC IGAS
IENG IDUAL ITENS
      1   3   3       0   0   0       1   1   0   0   0   1
0      0
CC
CC NUMBER OF GRID BLOCKS AND FLAG SPECIFIES CONSTANT OR VARIABLE GRID
SIZE
*----NX   NY  NZ  IDXYZ  IUNIT
      26   1   1   2      0
CC
CC VARIABLE GRID BLOCK SIZE IN X
*----DX(I)
      54.000   154.000   154.000   154.000   154.000   154.000
154.000   154.000   138.400   138.400   238.400   288.400
288.400   288.400   288.400   238.400   156.500   156.500
156.500   156.500   156.500   156.500   156.500   156.500
163.500   63.500
CC
CC CONSTANT GRID BLOCK SIZE IN Y
*----DY
      100
CC
CC VARIABLE GRID BLOCK SIZE IN Y
*----DZ
      50
CC
CC TOTAL NO. OF COMPONENTS, NO. OF TRACERS, NO. OF GEL COMPONENTS
*----N   NO  NTW  NTA  NGC  NG  NOTH
      15   0   1   0   0   0   6
CC
CC
*--- SPNAME(I), I=1,N
WATER
OIL
SURF.
POLYMER
CHLORIDE
CALCIUM
ALCOHOL1
ALCOHOL2
H2S
CH3COOH
SO4
SRB
CO2
NO3
PO4
CC
CC FLAG INDICATING IF THE COMPONENT IS INCLUDED IN CALCULATIONS OR NOT
*----ICF(KC) FOR KC=1,N
      1   1  0  0  0  0  0  0  1  1  1  1  1  1  1  1
CC

```



```

CC*****
CC
CC   OUTPUT OPTIONS
CC
CC*****
CC
CC
CC FLAG TO WRITE TO SUMMARY, FLAG FOR PV OR DAYS FOR OUTPUT AND STOP THE
RUN
*----ICUMTM  ISTOP  IOUTGMS
      1          1    0
CC
CC FLAG INDICATING IF THE PROFILE OF KCTH COMPONENT SHOULD BE WRITTEN
*----IPRFLG(KC),KC=1,N
      1  1  0  0  0  0  0  0  1  1  1  1  1  1  1
CC
CC FLAG FOR PRES,SAT.,TOTAL CONC.,TRACER CONC.,CAP.,GEL, ALKALINE
PROFILES
*----IPPRES IPSAT IPCTOT IPBIO IPCAP IPGEL IPALK ITEMP IPOBS
      1      1      1      1      0      0      0      1      0
CC
CC FLAG FOR WRITING SEVERAL PROPERTIES
*----ICKL  IVIS IPER ICNM  ICSE IFOAM  IHYST  INONEQ
      1      1      1      0      0      0      0      0
CC
CC FLAG FOR WRITING SEVERAL PROPERTIES TO PROF)
*----IADS  IVEL  IRKF IPHSE
      0      0      0      0
CC
CC*****
CC
CC   RESERVOIR PROPERTIES
CC
CC*****
CC
CC
CC MAX. SIMULATION TIME ( PV)
*---- TMAX
      10
CC
CC ROCK COMPRESSIBILITY (1/PSI), STAND. PRESSURE(PSIA)
*----COMPR  PSTAND
      0.      1000.
CC
CC FLAGS INDICATING CONSTANT OR VARIABLE POROSITY, X,Y,AND Z
PERMEABILITY
*----IPOR1 IPERMX IPERMY IPERMZ  IMOD
      0      0      0      0      0
CC
CC   constant porosity for whole reservoir
*----PORC1
      0.30
CC
CC constant X-PERMEABILITY (MILIDARCY) for whole reservoir
*----PERMX
      200
CC

```

```

CC constant Y-PERMEABILITY (MILIDARCY) FOR whole reservoir
*----PERMY
      200
CC
CC constant  Z-PERMEABILITY (MILIDARCY) for whole reservoir
*----PERMZC (MILIDARCY)
      200
CC
CC FLAG FOR CONSTANT OR VARIABLE DEPTH, PRESSURE, WATER SATURATION
*----IDEPH  IPRESS  ISWI  ICWI
      0        0        0   -1
CC
CC VARIABLE DEPTH (FT)
*----D111
      6200
CC
CC CONSTANT PRESSURE (PSIA)
*----PRESS1
      3771.04
CC
CC CONSTANT INITIAL WATER SATURATION
*----SWI
      0.72
CC
CC CONSTANT CHLORIDE AND CALCIUM CONCENTRATIONS (MEQ/ML)
*----C50      C60
      0.627    .133
CC
CC*****
CC                                                                 *
CC   PHYSICAL PROPERTY DATA                                     *
CC                                                                 *
CC*****
CC
CC
CC OIL CONC. AT PLAIT POINT FOR TYPE II(+)AND TYPE II(-), CMC
*---- C2PLC  C2PRC  EPSME  IHAND
      0.      1.      .0001  0
CC
CC FLAG INDICATING TYPE OF PHASE BEHAVIOR PARAMETERS
*---- IFGHBN
      0
CC SLOPE AND INTERCEPT OF BINODAL CURVE AT ZERO, OPT., AND 2XOPT
SALINITY
CC FOR ALCOHOL 1
*----HBNS70 HBNC70 HBNS71 HBNC71 HBNS72 HBNC72
      0.      .030    0.      .030    0.0    .030
CC
CC SLOPE OF BINODAL WITH TEMP., SLOPE OF SALINITY WITH TEMP. (1/F)
*---- HBNT0      HBNT1      HBNT2      CSET(0.00415)
      0.00017  0.00017  0.00017  0.00415
CC SLOPE AND INTERCEPT OF BINODAL CURVE AT ZERO, OPT., AND 2XOPT
SALINITY
CC FOR ALCOHOL 2
*----HBNS80 HBNC80 HBNS81 HBNC81 HBNS82 HBNC82
      0.      0.      0.      0.      0.      0.
CC

```

```

CC LOWER AND UPPER EFFECTIVE SALINITY FOR ALCOHOL 1 AND ALCOHOL 2
*----CSEL7  CSEU7  CSEL8  CSEU8
      .65  .9  0.  0.
CC
CC THE CSE SLOPE PARAMETER FOR CALCIUM AND ALCOHOL 1 AND ALCOHOL 2
*----BETA6  BETA7  BETA8
      0.0  0.  0.
CC
CC FLAG FOR ALCOHOL PART. MODEL AND PARTITION COEFFICIENTS
*----IALC  OPSK70  OPSK7S  OPSK80  OPSK8S
      0  0.  0.  0.  0.
CC
CC NO. OF ITERATIONS, AND TOLERANCE
*----NALMAX  EPSALC
      20  .0001
CC
CC ALCOHOL 1 PARTITIONING PARAMETERS IF IALC=1
*----AKWC7  AKWS7  AKM7  AK7  PT7
      4.671  1.79  48.  35.31  .222
CC
CC ALCOHOL 2 PARTITIONING PARAMETERS IF IALC=1
*----AKWC8  AKWS8  AKM8  AK8  PT8
      0.  0.  0.  0.  0.
CC
CC
*---- IFT MODEL FLAG
      0
CC
CC INTERFACIAL TENSION PARAMETERS
*----G11  G12  G13  G21  G22  G23
      13.  -14.8  .007  13.2  -14.5  .010
CC
CC LOG10 OF OIL/WATER INTERFACIAL TENSION
*----XIFTW
      1.477
CC
CC FLAG TO ALLOW SOLUBILITY OF OIL IN WATER
*---- IMASS  ICOR
      0  0
CC
CC CAPILLARY DESATURATION PARAMETERS FOR PHASE 1, 2, AND 3
*----ITRAP  T11  T22  T33
      0  1865.  28665.46  364.2
CC
CC FLAG FOR DIRECTION OF REL. PERM. AND PC CURVES, HYSTERESIS
*---- IPERM
      0
CC
CC FLAG FOR CONSTANT OR VARIABLE REL. PERM. PARAMETERS
*----ISRW  IPRW  IEW
      0  0  0
CC
CC CONSTANT RES. SATURATION OF PHASES 1,2,AND 3 AT LOW CAPILLARY NO.
*----S1RWC  S2RWC  S3RWC
      .147  .28  .147
CC

```

```

CC CONSTANT ENDPOINT REL. PERM. OF PHASES 1,2,AND 3 AT LOW CAPILLARY
NO.
*----P1RW  P2RW    P3RW
      .13771  0.9148   .13771
CC
CC CONSTANT REL. PERM. EXPONENT OF PHASES 1,2,AND 3 AT LOW CAPILLARY
NO.
*----E1W    E2W  E3W
      2.1817  1.40475  2.1817
CC
CC WATER AND OIL VISCOSITY , VIS. AT REF.TEMPERATURE
*----VIS1  VIS2  TSTAND
      0.42   1.25  122.0
CC
CC VISCOSITY-TEMP PARAMETERS
*----BVI(1) BVI(2)
      0.0    0.0
CC
CC VISCOSITY PARAMETERS
*----ALPHA1 ALPHA2  ALPHA3  ALPHA4  ALPHA5
      0.0    0.0    0.0  0.000865  4.153
CC
CC PARAMETERS TO CALCULATE POLYMER VISCOSITY AT ZERO SHEAR RATE
*----AP1    AP2    AP3
      73.0    1006.0  10809.31
CC
CC PARAMETER TO COMPUTE CSEP,MIN. CSEP, AND SLOPE OF LOG VIS. VS. LOG
CSEP
*----BETAP CSE1  SSLOPE
      2.     .01   .0
CC
CC PARAMETER FOR SHEAR RATE DEPENDENCE OF POLYMER VISCOSITY
*----GAMMAC  GAMHF  POWN
      10.0    187.985  1.8429
CC
CC FLAG FOR POLYMER PARTITIONING, PERM. REDUCTION PARAMETERS
*----IPOLYM EPHI3 EPHI4 BRK  CRK
      1      1.    0.9  1000.  0.0186
CC
CC SPECIFIC WEIGHT FOR COMPONENTS 1,2,3,7,AND 8 , AND GRAVITY FLAG
*----DEN1  DEN2  den23  DEN3  DEN7 DEN8 IDEN
      .4368  .3462333  0.3462333  .433333  .346  0.  2
CC
CC FLAG FOR CHOICE OF UNITS ( 0:BOTTOMHOLE CONDITION , 1: STOCK TANK)
*----ISTB
      0
CC
CC COMPRESSIBILITY FOR VOL. OCCUPYING COMPONENTS 1,2,3,7,AND 8
*----COMPC(1) COMPC(2) COMPC(3) COMPC(7) COMPC(8)
      0.     0.     0.     0.     0.
CC
CC CONSTANT OR VARIABLE PC PARAM., WATER-WET OR OIL-WET PC CURVE FLAG
*----ICPC  IEPC  IOW
      0     0     0
CC
CC CAPILLARY PRESSURE PARAMETERS, CPC
*----CPC

```

```

9.
CC
CC CAPILLARY PRESSURE PARAMETERS, EPC
*---- EPC
    2.
CC
CC MOLECULAR DIFFUSIVITY OF KCTH COMPONENT IN PHASE 1 (D(KC),KC=1,N)
*----D(1) D(2)
    0.  0. 0. 0. 0. 0. 0. 0. 0. .000066 .000066 .000066 .000066 .000066
.000066 .000066
CC
CC MOLECULAR DIFFUSIVITY OF KCTH COMPONENT IN PHASE 2 (D(KC),KC=1,N)
*----D(1) D(2)
    0.  0. 0. 0. 0. 0. 0. 0. 0. .0000066 .0000066 .000066 .000066
.000066 .000066 .000066
CC
CC MOLECULAR DIFFUSIVITY OF KCTH COMPONENT IN PHASE 3 (D(KC),KC=1,N)
*----D(1) D(2)
    0.  0. 0. 0. 0. 0. 0. 0. 0. .000066 .000066 .000066 .000066 .000066
.000066 .000066
CC
CC LONGITUDINAL AND TRANSVERSE DISPERSIVITY OF PHASE 1
*----ALPHAL(1)  ALPHAT(1)
    22.0          0.4
CC
CC LONGITUDINAL AND TRANSVERSE DISPERSIVITY OF PHASE 2
*----ALPHAL(2)  ALPHAT(2)
    22.0          0.4
CC
CC LONGITUDINAL AND TRANSVERSE DISPERSIVITY OF PHASE 3
*----ALPHAL(3)  ALPHAT(3)
    22.0          0.4
CC
CC FLAG TO SPECIFY ORGANIC ADSORPTION CALCULATION
*----IADSO
    0
CC
CC SURFACTANT AND POLYMER ADSORPTION PARAMETERS
*----AD31  AD32  B3D   AD41  AD42  B4D  IADK,  IADS1,  FADS  refk
    2.2    .0 1000.  1.1   0.   100.   0    0    0    0
CC
CC PARAMETERS FOR CATION EXCHANGE OF CLAY AND SURFACTANT
*----QV    XKC   XKS   EQW
    0     0.   0.   804
CC
CC TRACER PARTITIONING COEFFICIENT
*---- TK(I)  , I=1,NTW+NTA
    3.5
CC
CC TRACER PARTITIONING COEFFICIENT SALINITY PARAMETER (1/MEQ/ML)
*---- TKS(I)  ,I=1 TO NTW  C5INI
    0         0
CC
CC TRACER PARTITIONING COEFFICIENT TEMP. DEPENDENT (1/F)
*---- TKT(I)  , I=1 TO NTW+NTA
    0
CC

```

```

CC RADIOACTIVE DECAY COEFFICIENT
*----- RDC(I)      , I=1, NTW+NTA
          0
CC
CC TRACER ADSORPTION PARAMETER
*----- RET(I)    , I=1, NTW+NTA
          0.0
CC
CC INITIAL TEMPERATURE
*---- TEMPI (F)
          160.0
CC
CC ROCK DENSITY, CONDUCTIVITY, HEAT CAPACITY
*----- DENS      CRTC   CVSPR   CVSPL(1) CVSPL(2) CVSPL(3)
          165.43    40.001  0.2117   1.000454  0.5000227  1.000454
CC
CC HEAT LOSS FLAG, ANALYTICAL SOLUTION
*----- IHLOS    IANAL
          1        0
CC
CC OVERBURDEN AND UNDERBURDEN ROCK THERMAL PROPERTIES
*---- TCONO    DENO    CVSPO    TCONU    DENU    CVSPU
          35.      165.43  0.2117  35.      165.43  0.2117
CC
CC*****
CC
CC          BIOLOGICAL DATA
CC
CC*****
CC
CC
CC BULK DENSITY
*----- DENBLK
          1.64
CC
CC MINIMUM CONCENTRATIONS, CONVERGENCE TOLERANCE, TYPE FOR TIME STEP
CONTROL
*----- CMIN      EPSBIO    IBTMIN    BVOLMAX
          0.001    0.00001  0         10
CC
CC CHEMICAL AND BIOLOGICAL, METABOLIC COMBINATIONS, FLAGS FOR
BIODEGRADATION KINETICS, POROSITY AND PERMEABILITY
*----- NBC      NMET     IBKIN     IBPP     ibtem
          7        1        1         0
CC
CC INITIAL AQUEOUS PHASE CONCENTRATIONS
*----- KC(I)      ITYPE(I)    CINIT(I)    RABIO(I)    NPABIO(I)
          9         1         0.         0.         0.
          10        1         1000.     0.         0.
          11        1         0.         0.         0.
          12        2         0.         0.         0.
          13        1         0.         0.         0.
          14        1         0.         0.         0.
          15        1         0.3       0.         0.
CC
CC BIOLOGICAL SPECIES PARAMETERS

```

```

*----- KC(I)   DENBIO(I)   RCOL(I)   TCOL(I)   COLNUM(I)   EDDOG(I)
EDDOGB(I) CBI(I)   CBIOMN(I)   ADSBIO(I)
          12      1           0.000615   0.000084   100       0
0          1000000   1000000   0
CC
CC METEBOLIC COMBINATION INFORMATION
*----- ISUB(I)   IEA(I)   IBS(I)   BRMAX(I)   BRMAXB(I)   YXS(I)   AKS(I)
AKA(I)   FEA(I)
          10      11      12      1      0           0.05   0.01
0.01     1.6
CC
CC COMPETITION, INHIBITION, PRODUCT GEN., NUTRIENT LIM., COMETEBOLISM
INFORMATION
*----- ISUB(I)   IEA(I)   IBS(I)   NCOMPS(I)   NIHB(I)   NPROD(I)
NNUT(I)   ICOMET(I)
          10      11      12      0      0           2      0
0
CC
CC PRODUCT GENERATION BY METABOLIC COMBINATION I
*----- ISUB(I)   IEA(I)   IBS(I)   IPR(I)   FPR(I)
          10      11      12      9      0.57
          10      11      12      13     0.73
CC
CC*****
CC
CC WELL DATA
CC
CC*****
CC
CC FLAG FOR PRESSURE CONST. BOUNDARIES
*----- IBOUND   IZONE
          0      0
CC
CC TOTAL NUMBER OF WELLS, WELL RADIUS FLAG, FLAG FOR TIME OR COURANT
NO.
*-----NWELL   IRO   ITIME   NWREL
          2      2      1      2
CC
CC WELL ID,LOCATIONS,AND FLAG FOR SPECIFYING WELL TYPE, WELL RADIUS,
SKIN
*-----IDW   IW   JW   IFLAG   RW   SWELL   IDIR   IFIRST   ILAST
IPRF
          1   1   1   1   .5   0.   3   1   1   0
CC
CC WELL NAME
*----- WELNAM
INJECTOR
CC
CC ICHEK MAX. AND MIN. ALLOWABLE BOTTOMHOLE PRESSURE AND RATE
*-----ICHEK   PWFMIN   PWFMAX   QTMIN   QTMAX
          1   0.0   5801.6   0.0   5615.
CC
CC WELL ID, LOCATION, AND FLAG FOR SPECIFYING WELL TYPE, WELL RADIUS,
SKIN
*-----IDW   IW   JW   IFLAG   RW   SWELL   IDIR   IFIRST   ILAST   IPRF
          2   26   1   2   .5   0.   3   1   1   0

```


0 0 0
ITENS
0

INPUT file

```
CC*****
CC
CC BRIEF DESCRIPTION OF DATA SET : UTCHEM (VERSION 10.0)
CC
CC*****
CC
CC WATER FLOODING
CC
CC LENGTH (FT) : 2740 PROCESS : WATER FLOODING
CC THICKNESS (FT) : 26. INJ. PRESSURE (PSI) : 4121
CC WIDTH (FT) : 100. COORDINATES : CARTESIAN
CC POROSITY : 0.33 TEMP. VARI. NON ISOTHERMAL
CC GRID BLOCKS : 26x1x8
CC DATE : 06/13/2000
CC
CC*****
CC
CC*****
CC
CC RESERVOIR DESCRIPTION
CC
CC*****
CC
CC
*----RUNNO
UTEX10
CC
CC
*----HEADER
EXTvs
Simulation of TVS model
NONISOTHERMAL SIMULATION, UTCHEM VERSION 10.0
CC
CC SIMULATION FLAGS
*---- IMODE IMES IDISPC ICWM ICAP IREACT IBIO ICOORD ITREAC ITC IGAS
IENG IDUAL ITENS
      1 3 3 0 0 0 1 1 0 0 0 1
0 0
CC
CC NUMBER OF GRID BLOCKS AND FLAG SPECIFIES CONSTANT OR VARIABLE GRID
SIZE
*----NX NY NZ IDXYZ IUNIT
      26 1 1 2 0
CC
CC VARIABLE GRID BLOCK SIZE IN X
*----DX(I)
      54.000 154.000 154.000 154.000 154.000 154.000
154.000 154.000 138.400 138.400 238.400 288.400
```

```

288.400    288.400    288.400    238.400    156.500    156.500
156.500    156.500    156.500    156.500    156.500    156.500
163.500    63.500
CC
CC CONSTANT GRID BLOCK SIZE IN Y
*-----DY
      100
CC
CC VARIABLE GRID BLOCK SIZE IN Y
*-----DZ
      50
CC
CC TOTAL NO. OF COMPONENTS, NO. OF TRACERS, NO. OF GEL COMPONENTS
*-----N    NO  NTW  NTA  NGC  NG  NOTH
      15   0   1   0   0   0   6
CC
CC
*---- SPNAME(I), I=1,N
WATER
OIL
SURF.
POLYMER
CHLORIDE
CALCIUM
ALCOHOL1
ALCOHOL2
H2S
CH3COOH
SO4
SRB
CO2
NO3
PO4
CC
CC FLAG INDICATING IF THE COMPONENT IS INCLUDED IN CALCULATIONS OR NOT
*-----ICF(KC) FOR KC=1,N
      1  1  0  0  0  0  0  0  1  1  1  1  1  1  1  1
CC
CC*****
CC
CC      OUTPUT OPTIONS
CC
CC*****
CC
CC
CC FLAG TO WRITE TO SUMMARY, FLAG FOR PV OR DAYS FOR OUTPUT AND STOP THE
RUN
*-----ICUMTM  ISTOP  IOUTGMS
      1          1      0
CC
CC FLAG INDICATING IF THE PROFILE OF KCTH COMPONENT SHOULD BE WRITTEN
*-----IPRFLG(KC), KC=1,N
      1  1  0  0  0  0  0  0  1  1  1  1  1  1  1  1
CC
CC FLAG FOR PRES, SAT., TOTAL CONC., TRACER CONC., CAP., GEL, ALKALINE
PROFILES
*-----IPPRES IPSAT IPCTOT IPBIO IPCAP IPGEL IPALK ITEMP IPOBS

```

```

      1      1      1      1      0      0      0      1      0
CC
CC FLAG FOR WRITING SEVERAL PROPERTIES
*---ICKL  IVIS  IPER  ICNM  ICSE  IFOAM  IHYST  INONEQ
      1      1      1      0      0      0      0      0
CC
CC FLAG FOR WRITING SEVERAL PROPERTIES TO PROF)
*---IADS  IVEL  IRKF  IPHSE
      0      0      0      0
CC
CC*****
CC
CC      RESERVOIR PROPERTIES
CC
CC*****
CC
CC
CC MAX. SIMULATION TIME ( PV)
*---- TMAX
      10
CC
CC ROCK COMPRESSIBILITY (1/PSI), STAND. PRESSURE(PSIA)
*----COMPR  PSTAND
      0.      1000.
CC
CC FLAGS INDICATING CONSTANT OR VARIABLE POROSITY, X,Y,AND Z
PERMEABILITY
*----IPOR1  IPERMX  IPERMY  IPERMZ  IMOD
      0      0      0      0      0
CC
CC constant porosity for whole reservoir
*----PORC1
      0.30
CC
CC constant X-PERMEABILITY (MILIDARCY) for whole reservoir
*----PERMX
      200
CC
CC constant Y-PERMEABILITY (MILIDARCY) FOR whole reservoir
*----PERMY
      200
CC
CC constant Z-PERMEABILITY (MILIDARCY) for whole reservoir
*----PERMZC (MILIDARCY)
      200
CC
CC FLAG FOR CONSTANT OR VARIABLE DEPTH, PRESSURE, WATER SATURATION
*----IDEPH  IPRESS  ISWI  ICWI
      0      0      0  -1
CC
CC VARIABLE DEPTH (FT)
*----D111
      6200
CC
CC CONSTANT PRESSURE (PSIA)
*----PRESS1
      3771.04

```

```

CC
CC CONSTANT INITIAL WATER SATURATION
*----SWI
      0.72
CC
CC CONSTANT CHLORIDE AND CALCIUM CONCENTRATIONS (MEQ/ML)
*----C50      C60
      0.627      .133
CC
CC*****
CC
CC          PHYSICAL PROPERTY DATA
CC
CC*****
The same as Mixing Model
CC
CC*****
CC
CC          BIOLOGICAL DATA
CC
CC*****
CC
CC          BULK DENSITY
*---- DENBLK
      1.64
CC
CC MINIMUM CONCENTRATIONS, CONVERGENCE TOLERANCE, TYPE FOR TIME STEP
CONTROL
*---- CMIN      EPSBIO      IBTMIN      BVOLMAX
      0.001      0.00001      0          10
CC
CC CHEMICAL AND BIOLOGICAL, METABOLIC COMBINATIOS, FLAGS FOR
BIODEGRADATION KINETICS, POROSITY AND PERMEABILITY
*---- NBC      NMET      IBKIN      IBPP      ibtem
      7      1      1      0      1
CC
CC
*---- tlob      tmxb      tupb
      50      98      108
CC
CC INITIAL AQUEOUS PHASE CONCENTRATIOS
*---- KC(I)      ITYPE(I)      CINIT(I)      RABIO(I)      NPABIO(I)
      9          1          0.          0.          0.
      10         1          1000.        0.          0.
      11         1          0.          0.          0.
      12         2          0.          0.          0.
      13         1          0.          0.          0.
      14         1          0.          0.          0.
      15         1          0.3         0.          0.
CC
CC BIOLOGICAL SPECIES PARAMETERS
*---- KC(I)      DENBIO(I)      RCOL(I)      TCOL(I)      COLNUM(I)      EDDOG(I)
EDDOGB(I)      CBI(I)      CBIOMN(I)      ADSBIO(I)

```

```

12      1      0.000615  0.000084  100      0
0      1000000  1000000  0
CC
CC METEBOLIC COMBINATION INFORMATION
*---- ISUB(I)  IEA(I)  IBS(I)  BRMAX(I)  BRMAXB(I)  YXS(I)  AKS(I)
AKA(I)  FEA(I)
      10      11      12      1      0      0.05  0.01
0.01    1.6
CC
CC COMPETITION, INHIBITION, PRODUCT GEN., NUTRIENT LIM., COMETEBOLISM
INFORMATION
*---- ISUB(I)  IEA(I)  IBS(I)  NCOMPS(I)  NIHB(I)  NPROD(I)
NNUT(I)  ICOMET(I)
      10      11      12      0      0      2      0
0
CC
CC PRODUCT GENERATION BY METABOLIC COMBINATION I
*---- ISUB(I)  IEA(I)  IBS(I)  IPR(I)  FPR(I)
      10      11      12      9      0.57
      10      11      12      13      0.73
CC
CC*****
CC
CC WELL DATA
CC
CC*****
CC
CC
CC FLAG FOR PRESSURE CONST. BOUNDARIES
*---- IBOUND  IZONE
      0      0
CC
CC TOTAL NUMBER OF WELLS, WELL RADIUS FLAG, FLAG FOR TIME OR COURANT
NO.
*----NWELL  IRO  ITIME  NWREL
      2      2      1      2
CC
CC WELL ID,LOCATIONS,AND FLAG FOR SPECIFYING WELL TYPE, WELL RADIUS,
SKIN
*----IDW  IW  JW  IFLAG  RW  SWELL  IDIR  IFIRST  ILAST
IPRF
      1  1  1  1  .5  0.  3  1  1  0
CC
CC WELL NAME
*---- WELNAM
INJECTOR
CC
CC ICHEK MAX. AND MIN. ALLOWABLE BOTTOMHOLE PRESSURE AND RATE
*----ICHEK  PWFMIN  PWFMAX  QTMIN  QTMAX
      1  0.0  5801.6  0.0  5615.
CC
CC WELL ID, LOCATION, AND FLAG FOR SPECIFYING WELL TYPE, WELL RADIUS,
SKIN
*----IDW  IW  JW  IFLAG  RW  SWELL  IDIR  IFIRST  ILAST  IPRF
      2  26  1  2  .5  0.  3  1  1  0
CC
CC WELL NAME

```

```

*----- WELNAM
PRODUCER
CC
CC MAX. AND MIN. ALLOWABLE BOTTOMHOLE PRESSURE AND RATE
*-----ICHEK PWFMIN PWFMAX QTMIN QTMAX
          0      0.0      5000.   0.0      50000.
CC
CC ID, INJ. RATE AND INJ. COMP. FOR RATE CONS. WELLS FOR EACH PHASE
(L=1,3)
*-----ID  QI(M,L)  C(M,KC,L)
          1      1000.0  1.0  0. 0. 0. 0. 0. 0. 0. 0. 0. 0. 0. 2700.  0.0001  0.0
0.6  0.06
          1      0.      0.  0. 0. 0. 0. 0. 0. 0. 0. 0. 0. 0. 0. 0. 0.
0.  0.
          1      0.      0.  0. 0. 0. 0. 0. 0. 0. 0. 0. 0. 0. 0. 0. 0.
0.  0.
CC
CC
*---- ID, INJ. TEMP (F)
          1      60.
CC
CC ID, BOTTOM HOLE PRESSURE FOR PRESSURE CONSTRAINT WELL (IFLAG=2 OR 3)
*-----ID  PWF
          2      3771.04
CC
CC CUM. INJ. TIME , AND INTERVALS (PV OR DAY) FOR WRITING TO OUTPUT
FILES
*-----TINJ  CUMPR1  CUMHI1  WRHPV  WRPRF  RSTC
          10      0.3      0.3      0.01  0.15  1.
CC
CC FOR IMES=2 ,THE INI. TIME STEP, CONC. TOLERANCE, MAX., MIN. TIME STEPS
*-----DT  DCLIM  DTMAX  DTMIN
          0.01  0.1  0.1  0.00001  .00001  .00001  .00001  .00001  .00001  .00001
.00001  .00001  .00001  .00001  .00001  .00001  .00001  0.1  0.001

```

••

BIOFILM Model

HEAD file

Setup1

NX NY NZ N NWELL
26 1 8 15 2
NTW NTA
1 0
NO NPHASE
0 3
IDUAL NSUBV NSUBH
0 0 0
ITENS
0

INPUT file

```
CC*****
CC
CC BRIEF DESCRIPTION OF DATA SET : UTCHEM (VERSION 10.0)
CC
CC*****
CC
CC WATER FLOODING
CC
CC LENGTH (FT) : 2740 PROCESS : WATER FLOODING
CC THICKNESS (FT) : 26. INJ. PRESSURE (PSI) : 4121
CC WIDTH (FT) : 100. COORDINATES : CARTESIAN
CC POROSITY : 0.33 TEMP. VARI. NON ISOTHERMAL
CC GRID BLOCKS : 26x1x8
CC DATE : 06/13/2000
CC
CC*****
CC
CC*****
CC
CC RESERVOIR DESCRIPTION
CC
CC*****
CC
CC
*----RUNNO
UTEX10
CC
CC
*----HEADER
EXbof
Simulation of BIOFILM model (corresponding to Sunde et al., 1993)
NONISOTHERMAL SIMULATION, UTCHEM VERSION 10.0
CC
CC SIMULATION FLAGS
```

```

*----- IMODE IMES IDISPC ICWM ICAP IREACT IBIO ICOORD ITREAC ITC IGAS
IENG IDUAL ITENS
      1  1  3      0  0  0      1  1  0  0  0  1
0      0
CC
CC NUMBER OF GRID BLOCKS AND FLAG SPECIFIES CONSTANT OR VARIABLE GRID
SIZE
*-----NX  NY  NZ  IDXYZ  IUNIT
      26  1  1  2      0
CC
CC VARIABLE GRID BLOCK SIZE IN X
*-----DX(I)
      54.000  154.000  154.000  154.000  154.000  154.000
154.000  154.000  138.400  138.400  138.400  138.400
138.400  138.400  138.400  138.400  156.500  156.500
156.500  156.500  156.500  156.500  156.500  156.500
163.500  63.500
CC
CC CONSTANT GRID BLOCK SIZE IN Y
*-----DY
      50
CC
CC VARIABLE GRID BLOCK SIZE IN Y
*-----DZ
      27
CC
CC TOTAL NO. OF COMPONENTS, NO. OF TRACERS, NO. OF GEL COMPONENTS
*-----N  NO  NTW  NTA  NGC  NG  NOTH
      15  0  2  0  0  0  5
CC
CC
*---- SPNAME(I), I=1,N
WATER
OIL
SURF.
POLYMER
CHLORIDE
CALCIUM
ALCOHOL1
ALCOHOL2
H2S
CH3COOH
SO4
SRB
CO2
NO3
PO4
CC
CC FLAG INDICATING IF THE COMPONENT IS INCLUDED IN CALCULATIONS OR NOT
*-----ICF(KC) FOR KC=1,N
      1  1  0  0  0  0  0  1  1  1  1  1  1  1
CC
CC*****
CC
CC OUTPUT OPTIONS
CC
CC*****

```



```

CC
CC
CC FLAG TO WRITE TO SUMMARY, FLAG FOR PV OR DAYS FOR OUTPUT AND STOP THE
RUN
*-----ICUMTM  ISTOP  IOUTGMS
      1      1      0
CC
CC FLAG INDICATING IF THE PROFILE OF KCTH COMPONENT SHOULD BE WRITTEN
*-----IPRFLG(KC),KC=1,N
      1  1  0  0  0  0  0  0  1  1  1  1  1  1  1  1
CC
CC FLAG FOR PRES,SAT.,TOTAL CONC.,TRACER CONC.,CAP.,GEL, ALKALINE
PROFILES
*-----IPPRES IPSAT IPCTOT IPBIO IPCAP IPGEL IPALK ITEMP IPOBS
      1      1      1      1      0      0      0      1      0
CC
CC FLAG FOR WRITING SEVERAL PROPERTIES
*---ICKL  IVIS  IPER  ICNM  ICSE  IFOAM  IHYST  INONEQ
      1      1      1      0      0      0      0      0
CC
CC FLAG FOR WRITING SEVERAL PROPERTIES TO PROF)
*---IADS  IVEL  IRKF  IPHSE
      0      0      0      0
CC
CC*****
CC RESERVOIR PROPERTIES *
CC *
CC*****
CC
CC
CC MAX. SIMULATION TIME ( PV)
*----- TMAX
      10
CC
CC ROCK COMPRESSIBILITY (1/PSI), STAND. PRESSURE(PSIA)
*-----COMPR  PSTAND
      0.      1000.
CC
CC FLAGS INDICATING CONSTANT OR VARIABLE POROSITY, X,Y,AND Z
PERMEABILITY
*-----IPOR1 IPERMX IPERMY IPERMZ  IMOD
      0      0      0      0      0
CC
CC constant porosity for whole reservoir
*-----PORC1
      0.30
CC
CC constant X-PERMEABILITY (MILIDARCY) for whole reservoir
*-----PERMX
      5000
CC
CC constant Y-PERMEABILITY (MILIDARCY) FOR whole reservoir
*-----PERMY
      5000
CC
CC constant Z-PERMEABILITY (MILIDARCY) for whole reservoir

```

```

*----PERMZC (MILIDARCY)
      5000
CC
CC FLAG FOR CONSTANT OR VARIABLE DEPTH, PRESSURE, WATER SATURATION
*----IDEPH  IPRESS  ISWI  ICWI
      0      0      0  -1
CC
CC VARIABLE DEPTH (FT)
*----D111
      6200
CC
CC CONSTANT PRESSURE (PSIA)
*----PRESS1
      3771.04
CC
CC CONSTANT INITIAL WATER SATURATION
*----SWI
      .85
CC
CC CONSTANT CHLORIDE AND CALCIUM CONCENTRATIONS (MEQ/ML)
*----C50      C60
      0.627      .133
CC
CC*****
CC
CC      PHYSICAL PROPERTY DATA
CC
CC*****

```

The same as Mixing Model

```

CC
CC*****
CC
CC      BIOLOGICAL DATA
CC
CC*****
CC
CC      BULK DENSITY
*----  DENBLK
      1.64
CC
CC MINIMUM CONCENTRATIONS, CONVERGENCE TOLERANCE, TYPE FOR TIME STEP
CONTROL
*----  CMIN      EPSBIO      IBTMIN  BVOLMAX
      0.001      0.00001      0      1
CC
CC CHEMICAL AND BIOLOGICAL, METABOLIC COMBINATIOS, FLAGS FOR
BIODEGRADATION KINETICS, POROSITY AND PERMEABILITY
*----  NBC      NMET      IBKIN  IBPP
      7      1      2      0
CC
CC INITIAL AQUEOUS PHASE CONCENTRATIOS
*----  KC(I)      ITYPE(I)      CINIT(I)      RABIO(I)      NPABIO(I)
      9      1      0.      0.      0.
      10      1      0.1      0.      0.

```

```

11          1          0.          0.          0
12          2          0.          0.          0.
13          1          0.          0.          0.
14          1          0.          0.          0.
15          1          0.3         0.          0.
CC
CC BIOLOGICAL SPECIES PARAMETERS
*----- KC(I)   DENBIO(I)   RCOL(I)   TCOL(I)   COLNUM(I)   EDDOG(I)
EDDOGB(I) CBI(I)   CBIOMN(I)  ADSBIO(I)
12          1          0.000615  0.000084  100          0
0          1000000  1000000  100000
CC
CC METEBOLIC COMBINATION INFORMATION
*----- ISUB(I)   IEA(I)   IBS(I)   BRMAX(I)   BRMAXB(I)   YXS(I)   AKS(I)
AKA(I)   FEA(I)
10          11          12          0.0012     0.0012     0.05
0.01      0.01      1.6
CC
CC COMPETITION, INHIBITION, PRODUCT GEN., NUTRIENT LIM., COMETEBOLISM
INFORMATION
*----- ISUB(I)   IEA(I)   IBS(I)   NCOMPS(I)   NIHB(I)   NPROD(I)
NNUT(I)  ICOMET(I)
10          11          12          0          0          2          0
0
CC
CC PRODUCT GENERATION BY METABOLIC COMBINATION I
*----- ISUB(I)   IEA(I)   IBS(I)   IPR(I)   FPR(I)
10          11          12          9          0.57
10          11          12          13         0.73
CC
CC*****
CC
CC WELL DATA
CC
CC*****
CC
CC FLAG FOR PRESSURE CONST. BOUNDARIES
*----- IBOUND  IZONE
0          0
CC
CC TOTAL NUMBER OF WELLS, WELL RADIUS FLAG, FLAG FOR TIME OR COURANT
NO.
*-----NWELL  IRO  ITIME  NWREL
2          2          0          2
CC
CC WELL ID,LOCATIONS,AND FLAG FOR SPECIFYING WELL TYPE, WELL RADIUS,
SKIN
*-----IDW  IW  JW  IFLAG  RW  SWELL  IDIR  IFIRST  ILAST
IPRF
1          1          1          1          .5  0.          3          1          1          0
CC
CC WELL NAME
*----- WELNAM
INJECTOR
CC
CC ICHEK MAX. AND MIN. ALLOWABLE BOTTOMHOLE PRESSURE AND RATE

```

```

*----ICHEK   PWFMIN   PWFMAX   QTMIN   QTMAX
      1       0.0     5801.6   0.0     5615.
CC
CC WELL ID, LOCATION, AND FLAG FOR SPECIFYING WELL TYPE, WELL RADIUS,
SKIN
*----IDW   IW    JW    IFLAG    RW      SWELL   IDIR   IFIRST   ILAST   IPRF
      2     26    1     2         .5      0.     3     1       1       0
CC
CC WELL NAME
*---- WELNAM
PRODUCER
CC
CC MAX. AND MIN. ALLOWABLE BOTTOMHOLE PRESSURE AND RATE
*----ICHEK   PWFMIN   PWFMAX   QTMIN   QTMAX
      0       0.0     5000.   0.0     50000.
CC
CC ID, INJ. RATE AND INJ. COMP. FOR RATE CONS. WELLS FOR EACH PHASE
(L=1,3)
*----ID   QI(M,L)  C(M,KC,L)
      1     4250.0  1.0  0. 0. 0. 0. 0. 0. 0. 0. 5.0 2700. 0.0001
0.0 0.6 0.06
      1     0.      0.  0. 0. 0. 0. 0. 0. 0. 0. 0. 0. 0. 0.
0. 0.
      1     0.      0.  0. 0. 0. 0. 0. 0. 0. 0. 0. 0. 0. 0.
0. 0.
CC
CC
*---- ID, INJ. TEMP (F)
      1     60.
CC
CC ID, BOTTOM HOLE PRESSURE FOR PRESSURE CONSTRAINT WELL (IFLAG=2 OR 3)
*----ID   PWF
      2     3771.04
CC
CC CUM. INJ. TIME , AND INTERVALS (PV OR DAY) FOR WRITING TO OUTPUT
FILES
*----TINJ   CUMPR1   CUMHI1   WRHPV   WRPRF   RSTC
      10     1       1       0.04   0.6     1.
CC
CC FOR IMES=2 ,THE INI. TIME STEP,CONC. TOLERANCE,MAX.,MIN. TIME STEPS
*----DT     DCLIM     DTMAX     DTMIN
      0.01    0.1  0.1   0.00001  .00001  .00001  .00001  .00001  .00001  .00001
.00001  .00001  .00001  .00001  .00001  .00001  .00001  .00001  0.1  0.001
YY

```

UTCHEM Model

HEAD file

```
Setup1
NX NY NZ N NWELL
26 1 8 15 2
NTW NTA
1 0
NO NPHASE
0 3
IDUAL NSUBV NSUBH
0 0 0
ITENS
0
```

INPUT file

```
CC*****
CC
CC BRIEF DESCRIPTION OF DATA SET : UTCHEM (VERSION 10.0)
CC
CC*****
CC
CC WATER FLOODING
CC
CC LENGTH (FT) : 2740 PROCESS : WATER FLOODING
CC THICKNESS (FT) : 26. INJ. PRESSURE (PSI) : 4121
CC WIDTH (FT) : 100. COORDINATES : CARTESIAN
CC POROSITY : 0.33 TEMP. VARI. NON ISOTHERMAL
CC GRID BLOCKS : 26x1x8
CC DATE : 06/13/2000
CC
CC*****
CC
CC*****
CC
CC RESERVOIR DESCRIPTION
CC
CC*****
CC
CC
*----RUNNO
UTEX10
CC
CC
*----HEADER
EXum
Simulation of reservoir souring using Developed Model
NONISOTHERMAL SIMULATION, UTCHEM VERSION 10.0
CC
CC SIMULATION FLAGS
```

```

*----- IMODE IMES IDISPC ICWM ICAP IREACT IBIO ICOORD ITREAC ITC IGAS
IENG IDUAL ITENS
      1 1 1 0 0 0 1 1 0 0 0 1
0      0
CC
CC NUMBER OF GRID BLOCKS AND FLAG SPECIFIES CONSTANT OR VARIABLE GRID
SIZE
*-----NX NY NZ IDXYZ IUNIT
      100 1 2 2 0
CC
CC VARIABLE GRID BLOCK SIZE IN X
*-----DX(I)
 25 25 25 25 25 25 25 25 25 25 25 25 25 25 25 25 25 25 25 25 25 25
25 25 25 25 25 25 25 25 25 25 25 25 25 25 25 25 25 25 25 25 25 25
25 25 25 25 25 25 25 25 25 25 25 25 25 25 25 25 25 25 25 25 25 25
25 25 25 25 25 25 25 25 25 25 25 25 25 25 25 25 25 25 25 25 25 25
25 25 25 25 25
CC
CC CONSTANT GRID BLOCK SIZE IN Y
*-----DY
      100
CC
CC VARIABLE GRID BLOCK SIZE IN Y
*-----DZ
      25 25
CC
CC TOTAL NO. OF COMPONENTS, NO. OF TRACERS, NO. OF GEL COMPONENTS
*-----N NO NTW NTA NGC NG NOTH
      16 0 1 0 0 0 7
CC
CC
*---- SPNAME(I), I=1,N
WATER
OIL
SURF.
POLYMER
CHLORIDE
CALCIUM
ALCOHOL1
ALCOHOL2
H2S
CH3COOH
SO4
SRB
CO2
NO3
PO4
TRacer
CC
CC FLAG INDICATING IF THE COMPONENT IS INCLUDED IN CALCULATIONS OR NOT
*-----ICF(KC) FOR KC=1,N
      1 1 0 0 0 0 0 1 1 1 1 1 1 1 1 1
CC
CC*****
CC
CC OUTPUT OPTIONS
CC

```

```

CC*****
CC
CC
CC FLAG TO WRITE TO SUMMARY, FLAG FOR PV OR DAYS FOR OUTPUT AND STOP THE
RUN
*----ICUMTM  ISTOP  IOUTGMS
      0      0      0
CC
CC FLAG INDICATING IF THE PROFILE OF KCTH COMPONENT SHOULD BE WRITTEN
*----IPRFLG(KC),KC=1,N
      1  1  0  0  0  0  0  0  1  1  1  1  1  1  1  1
CC
CC FLAG FOR PRES,SAT.,TOTAL CONC.,TRACER CONC.,CAP.,GEL, ALKALINE
PROFILES
*----IPPRES IPSAT IPCTOT IPBIO IPCAP IPGEL IPALK ITEMP IPOBS
      1      1      1      1      0      0      0      1      0
CC
CC FLAG FOR WRITING SEVERAL PROPERTIES
*---ICKL  IVIS  IPER  ICNM  ICSE  IFOAM  IHYST  INONEQ
      1      1      1      0      0      0      0      0
CC
CC FLAG FOR WRITING SEVERAL PROPERTIES TO PROF)
*---IADS  IVEL  IRKF  IPHSE
      0      0      0      0
CC
CC*****
CC
CC      RESERVOIR PROPERTIES
CC
CC*****
CC
CC
CC MAX. SIMULATION TIME ( PV)
*---- TMAX
      7500
CC
CC ROCK COMPRESSIBILITY (1/PSI), STAND. PRESSURE(PSIA)
*----COMPR  PSTAND
      0.      1000.
CC
CC FLAGS INDICATING CONSTANT OR VARIABLE POROSITY, X,Y,AND Z
PERMEABILITY
*----IPOR1 IPERMX IPERMY IPERMZ  IMOD
      1      1      1      1      0
CC
CC  constant porosity for whole reservoir
*----PORC1
      0.15  0.35
CC
CC constant X-PERMEABILITY (MILIDARCY) for whole reservoir
*----PERMX
      100  400
CC
CC constant Y-PERMEABILITY (MILIDARCY) FOR whole reservoir
*----PERMY
      100  400
CC

```

```

CC constant Z-PERMEABILITY (MILIDARCY) for whole reservoir
*----PERMZC (MILIDARCY)
      100  400
CC
CC FLAG FOR CONSTANT OR VARIABLE DEPTH, PRESSURE, WATER SATURATION
*----IDEPTH  IPRESS  ISWI  ICWI
      0      0      0  -1
CC
CC VARIABLE DEPTH (FT)
*----D111
      6200
CC
CC CONSTANT PRESSURE (PSIA)
*----PRESS1
      3771.04
CC
CC CONSTANT INITIAL WATER SATURATION
*----SWI
      0.72
CC
CC CONSTANT CHLORIDE AND CALCIUM CONCENTRATIONS (MEQ/ML)
*----C50      C60
      0.627      .133
CC
CC*****
CC
CC      PHYSICAL PROPERTY DATA
CC
CC*****
CC
CC
CC OIL CONC. AT PLAIT POINT FOR TYPE II(+)AND TYPE II(-), CMC
*---- C2PLC  C2PRC  EPSME  IHAND
      0.      1.      .0001  0
CC
CC FLAG INDICATING TYPE OF PHASE BEHAVIOR PARAMETERS
*---- IFGHBN
      0
CC SLOPE AND INTERCEPT OF BINODAL CURVE AT ZERO, OPT., AND 2XOPT
SALINITY
CC FOR ALCOHOL 1
*----HBNS70 HBNC70 HBNS71 HBNC71 HBNS72 HBNC72
      0.      .030  0.      .030  0.0  .030
CC
CC SLOPE OF BINODAL WITH TEMP., SLOPE OF SALINITY WITH TEMP. (1/F)
*---- HBNT0      HBNT1      HBNT2      CSET(0.00415)
      0.00017  0.00017  0.00017  0.00415
CC SLOPE AND INTERCEPT OF BINODAL CURVE AT ZERO, OPT., AND 2XOPT
SALINITY
CC FOR ALCOHOL 2
*----HBNS80 HBNC80 HBNS81 HBNC81 HBNS82 HBNC82
      0.      0.      0.      0.      0.      0.
CC
CC LOWER AND UPPER EFFECTIVE SALINITY FOR ALCOHOL 1 AND ALCOHOL 2
*----CSEL7  CSEU7  CSEL8  CSEU8
      .65  .9  0.      0.
CC

```



```

CC THE CSE SLOPE PARAMETER FOR CALCIUM AND ALCOHOL 1 AND ALCOHOL 2
*----BETA6  BETA7  BETA8
      0.0    0.    0.
CC
CC FLAG FOR ALCOHOL PART. MODEL AND PARTITION COEFFICIENTS
*----IALC  OPSK70  OPSK7S  OPSK80  OPSK8S
      0      0.    0.    0.    0.
CC
CC NO. OF ITERATIONS, AND TOLERANCE
*----NALMAX  EPSALC
      20      .0001
CC
CC ALCOHOL 1 PARTITIONING PARAMETERS IF IALC=1
*----AKWC7  AKWS7  AKM7  AK7    PT7
      4.671  1.79  48.   35.31  .222
CC
CC ALCOHOL 2 PARTITIONING PARAMETERS IF IALC=1
*----AKWC8  AKWS8  AKM8  AK8    PT8
      0.    0.    0.    0.    0.
CC
CC
*--- IFT MODEL FLAG
      0
CC
CC INTERFACIAL TENSION PARAMETERS
*----G11  G12    G13  G21  G22  G23
      13.  -14.8  .007  13.2  -14.5  .010
CC
CC LOG10 OF OIL/WATER INTERFACIAL TENSION
*----XIFTW
      1.477
CC
CC FLAG TO ALLOW SOLUBILITY OF OIL IN WATER
*---- IMASS  ICOR
      0      0
CC
CC CAPILLARY DESATURATION PARAMETERS FOR PHASE 1, 2, AND 3
*----ITRAP  T11    T22    T33
      0      1865.   28665.46  364.2
CC
CC FLAG FOR DIRECTION OF REL. PERM. AND PC CURVES, HYSTERESIS
*---- IPERM
      0
CC
CC FLAG FOR CONSTANT OR VARIABLE REL. PERM. PARAMETERS
*----ISRW  IPRW  IEW
      0      0      0
CC
CC CONSTANT RES. SATURATION OF PHASES 1,2,AND 3 AT LOW CAPILLARY NO.
*----S1RWC  S2RWC  S3RWC
      .147   .28   .147
CC
CC CONSTANT ENDPOINT REL. PERM. OF PHASES 1,2,AND 3 AT LOW CAPILLARY
NO.
*----P1RW  P2RW    P3RW
      .13771  0.9148  .13771
CC

```

```

CC CONSTANT REL. PERM. EXPONENT OF PHASES 1,2,AND 3 AT LOW CAPILLARY
NO.
*----E1W      E2W  E3W
      2.1817   1.40475  2.1817
CC
CC WATER AND OIL VISCOSITY , VIS. AT REF.TEMPERATURE
*----VIS1    VIS2    TSTAND
      1     1.25    122.0
CC
CC VISCOSITY-TEMP PARAMETERS
*----BVI(1)  BVI(2)
      0.0     0.0
CC
CC VISCOSITY PARAMETERS
*----ALPHA1 ALPHA2  ALPHA3  ALPHA4  ALPHA5
      0.0     0.0     0.0    0.000865  4.153
CC
CC PARAMETERS TO CALCULATE POLYMER VISCOSITY AT ZERO SHEAR RATE
*----AP1     AP2     AP3
      73.0    1006.0  10809.31
CC
CC PARAMETER TO COMPUTE CSEP,MIN. CSEP, AND SLOPE OF LOG VIS. VS. LOG
CSEP
*----BETAP  CSE1  SSLOPE
      2.     .01   .0
CC
CC PARAMETER FOR SHEAR RATE DEPENDENCE OF POLYMER VISCOSITY
*----GAMMAC  GAMHF  POWN
      10.0    187.985  1.8429
CC
CC FLAG FOR POLYMER PARTITIONING, PERM. REDUCTION PARAMETERS
*----IPOLYM  EPHI3  EPHI4  BRK    CRK
      1      1.     0.9   1000.  0.0186
CC
CC SPECIFIC WEIGHT FOR COMPONENTS 1,2,3,7,AND 8 , AND GRAVITY FLAG
*----DEN1    DEN2    den23    DEN3    DEN7  DEN8  IDEN
      .4368   .3462333  0.3462333  .433333  .346  0.   2
CC
CC FLAG FOR CHOICE OF UNITS ( 0:BOTTOMHOLE CONDITION , 1: STOCK TANK)
*-----ISTB
      0
CC
CC COMPRESSIBILITY FOR VOL. OCCUPYING COMPONENTS 1,2,3,7,AND 8
*----COMPC(1)  COMPC(2)  COMPC(3)  COMPC(7)  COMPC(8)
      0.        0.        0.        0.        0.
CC
CC CONSTANT OR VARIABLE PC PARAM., WATER-WET OR OIL-WET PC CURVE FLAG
*----ICPC     IEPC  IOW
      0        0     0
CC
CC CAPILLARY PRESSURE PARAMETERS, CPC
*----CPC
      9.
CC
CC CAPILLARY PRESSURE PARAMETERS, EPC
*---- EPC
      2.

```

```

CC
CC MOLECULAR DIFFUSIVITY OF KCTH COMPONENT IN PHASE 1 (D(KC),KC=1,N)
*----D(1) D(2)
      0.  0. 0. 0. 0. 0. 0. 0. 0. .00000066 .00000066 .00000066 .00000066
.00000066 .00000066 .00000066 0.00000066
CC
CC MOLECULAR DIFFUSIVITY OF KCTH COMPONENT IN PHASE 2 (D(KC),KC=1,N)
*----D(1) D(2)
      0.  0. 0. 0. 0. 0. 0. 0. 0. .00000066 .00000066 .00000066 .00000066
.00000066 .00000066 .00000066 0.00000066
CC
CC MOLECULAR DIFFUSIVITY OF KCTH COMPONENT IN PHASE 3 (D(KC),KC=1,N)
*----D(1) D(2)
      0.  0. 0. 0. 0. 0. 0. 0. 0. .00000066 .00000066 .00000066 .00000066
.00000066 .00000066 .00000066 0.00000066
CC
CC LONGITUDINAL AND TRANSVERSE DISPERSIVITY OF PHASE 1
*----ALPHAL(1)      ALPHAT(1)
      0.0           0.0
C
CC LONGITUDINAL AND TRANSVERSE DISPERSIVITY OF PHASE 2
*----ALPHAL(2)      ALPHAT(2)
      0.0           0.0
CC
CC LONGITUDINAL AND TRANSVERSE DISPERSIVITY OF PHASE 3
*----ALPHAL(3)      ALPHAT(3)
      0.0           0.0
CC
CC FLAG TO SPECIFY ORGANIC ADSORPTION CALCULATION
*----IADSO
      0
CC
CC SURFACTANT AND POLYMER ADSORPTION PARAMETERS
*----AD31  AD32  B3D   AD41  AD42  B4D  IADK,  IADS1,  FADS  refk
      2.2    .0  1000.  1.1   0.   100.   0     0     0     0
CC
CC PARAMETERS FOR CATION EXCHANGE OF CLAY AND SURFACTANT
*----QV      XKC   XKS   EQW
      0       0.   0.   804
CC
CC TRACER PARTITIONING COEFFICIENT
*---- TK(I)   , I=1,NTW+NTA
      0
CC
CC TRACER PARTITIONING COEFFICIENT SALINITY PARAMETER (1/MEQ/ML)
*---- TKS(I)   ,I=1 TO NTW   C5INI
      0         0
CC
CC TRACER PARTITIONING COEFFICIENT TEMP. DEPENDENT (1/F)
*---- TKT(I)   , I=1 TO NTW+NTA
      0
CC
CC RADIOACTIVE DECAY COEFFICIENT
*---- RDC(I)   , I=1, NTW+NTA
      0
CC
CC TRACER ADSORPTION PARAMETER

```

```

*----- RET(I) , I=1, NTW+NTA
          0.0
CC
CC INITIAL TEMPERATURE
*---- TEMPI (F)
          160.0
CC
CC ROCK DENSITY, CONDUCTIVITY, HEAT CAPACITY
*----- DENS      CRTC    CVSPR    CVSPL(1) CVSPL(2) CVSPL(3)
          165.43    40.001  0.2117  1.000454  0.5000227  1.000454
CC
CC HEAT LOSS FLAG, ANALYTICAL SOLUTION
*----- IHLOS  IANAL
          0      0
CC
CC*****
CC
CC          BIOLOGICAL DATA
CC
CC*****
CC
CC
CC    BULK DENSITY
*----- DENBLK
          1.64
CC
CC MINIMUM CONCENTRATIONS, CONVERGENCE TOLERANCE, TYPE FOR TIME STEP
CONTROL
*----- CMIN      EPSBIO    IBTMIN  BVOLMAX
          0.001    0.00001  0      10
CC
CC CHEMICAL AND BIOLOGICAL, METABOLIC COMBINATIONS, FLAGS FOR
BIODEGRADATION KINETICS, POROSITY AND PERMEABILITY
*----- NBC      NMET     IBKIN   IBPP   ibtem
          8      1      2      0     1
CC
CC
*----- tlob     tmxb     tupb
          100    145    170
CC
CC INITIAL AQUEOUS PHASE CONCENTRATIONS
*----- KC(I)      ITYPE(I)    CINIT(I)    RABIO(I)    NPABIO(I)
          9          1          0.          0.          0.
          10         1        1000.        0.          0.
          11         1          0.          0.          0.
          12         2          0.          0.          0.
          13         1          0.          0.          0.
          14         1          0.          0.          0.
          15         1         0.3          0.          0.
          16         1          0.          0.          0.
CC
CC BIOLOGICAL SPECIES PARAMETERS
*----- KC(I)    DENBIO(I)    RCOL(I)    TCOL(I)    COLNUM(I)    EDDOG(I)
EDDOGB(I)  CBI(I)    CBIOMN(I)  ADSBIO(I)
          12      1          0.000615  0.000084  100          0
0          1000000  1000000  0
CC

```

```

CC METEBOLIC COMBINATION INFORMATION
*---- ISUB(I) IEA(I) IBS(I) BRMAX(I) BRMAXB(I) YXS(I) AKS(I)
AKA(I) FEA(I)
      10      11      12      0.693      0      0.05      0.01
0.01      1.6
CC
CC COMPETITION, INHIBITION, PRODUCT GEN., NUTRIENT LIM., COMETEBOLISM
INFORMATION
*---- ISUB(I) IEA(I) IBS(I) NCOMPS(I) NIHB(I) NPROD(I)
NNUT(I) ICOMET(I)
      10      11      12      0      0      2      2
0
CC
CC PRODUCT GENERATION BY METABOLIC COMBINATION I
*---- ISUB(I) IEA(I) IBS(I) IPR(I) FPR(I)
      10      11      12      9      0.57
      10      11      12      13      0.73
CC
CC Nutrient effects
*---- ISUB(I) IEA(I) IBS(I) INUT(I) AKN(I)
FN(I)
      10      11      12      14      0.001
0.0068
      10      11      12      15      0.0001
0.00195
CC
CC*****
CC
CC WELL DATA
CC
CC*****
CC
CC FLAG FOR PRESSURE CONST. BOUNDARIES
*---- IBOUND IZONE
      0      0
CC
CC TOTAL NUMBER OF WELLS, WELL RADIUS FLAG, FLAG FOR TIME OR COURANT
NO.
*----NWELL IRO ITIME NWREL
      2      2      0      2
CC
CC WELL ID,LOCATIONS,AND FLAG FOR SPECIFYING WELL TYPE, WELL RADIUS,
SKIN
*----IDW IW JW IFLAG RW SWELL IDIR IFIRST ILAST
IPRF
      1      1      1      1      .5      0.      3      1      2      0
CC
CC WELL NAME
*---- WELNAM
INJECTOR
CC
CC ICHEK MAX. AND MIN. ALLOWABLE BOTTOMHOLE PRESSURE AND RATE
*----ICHEK PWFMIN PWFMAX QTMIN QTMAX
      1      0.0      5801.6      0.0      5615.
CC

```

```

CC WELL ID, LOCATION, AND FLAG FOR SPECIFYING WELL TYPE, WELL RADIUS,
SKIN
*-----IDW  IW   JW   IFLAG    RW    SWELL  IDIR  IFIRST   ILAST   IPRF
          2   100  1    2         .5     0.     3     1       2       0
CC
CC WELL NAME
*----- WELNAM
PRODUCER
CC
CC MAX. AND MIN. ALLOWABLE BOTTOMHOLE PRESSURE AND RATE
*-----ICHEK  PWFMIN  PWFMAX  QTMIN  QTMAX
          0     0.0    5000.   0.0    50000.
CC
CC ID, INJ. RATE AND INJ. COMP. FOR RATE CONS. WELLS FOR EACH PHASE
(L=1,3)
*-----ID  QI(M,L)  C(M,KC,L)
          1    1000.0  1.0  0. 0. 0. 0. 0. 0. 0. 0. 0. 0. 2700.  0.0001  0.0
0.6  0.06  1800
          1     0.     0.  0. 0. 0. 0. 0. 0. 0. 0. 0. 0. 0. 0. 0.
0.  0.  1800
          1     0.     0.  0. 0. 0. 0. 0. 0. 0. 0. 0. 0. 0. 0. 0.
0.  0.  1800
CC
CC
*---- ID, INJ. TEMP (F)
          1     60.
CC
CC ID, BOTTOM HOLE PRESSURE FOR PRESSURE CONSTRAINT WELL (IFLAG=2 OR 3)
*-----ID  PWF
          2     3771.04
CC
CC CUM. INJ. TIME , AND INTERVALS (PV OR DAY) FOR WRITING TO OUTPUT
FILES
*-----TINJ    CUMPR1    CUMHI1    WRHPV    WRPRF    RSTC
          7500     20     20     20     20     20
CC
CC FOR IMES=2 ,THE INI. TIME STEP, CONC. TOLERANCE, MAX., MIN. TIME STEPS
*-----DT    DCLIM    DTMAX    DTMIN
          1

```

ÿÿ

APPENDIX B

UTCHEM source codes with modification for reservoir souring purpose.

C

```
SUBROUTINE BIOREAD
USE MODULE1, ONLY :
& ZERO,ONE,ONEM,ONEM4,ONEM5,ONEM6,ONEM7,ONEM8,ONEM9
& ,
ONEM10,ONEM12,ONEP12,ONEM50,ONEP50,ONEM5M,PONEM,ONE199,PRCSN
& , PIE,F1P8
& , DNOILC,DENBIO
& , CTOT,C,CSE,S
& , CE
& , DT,CURANT,NXM1,NX,NY,NZ,NXNY,NBL,NBLW,N
& , POR,RKF
& , VIS,RPERM,PERMX,PERMY
& , PERMZ,QI,QB,Q,QT
& , CUMQI,CUMQP,PWF
& , DCO,WSOL,CNEM2,IMASS,ISOL,ICOR
& , SCHM,REY,SHER,DP
& , MMOM1,NO,LMO
& , SPNAME,PWFR,WELNAM
& , RUNNO
& , CUMI,CUMP,OIP,OP,TIME=>T,TINJ,WHPV
& , PRF,ICNT,IINJ,INEC,IRST
& , DCMAX,IDISPC,ICF,ICOORD,ITC,IUNIT
& , DUM1=>TWS1,DUM2=>TWS2,DUM3=>TWS3
& , DUM4=>TWS4,DP2=>TWS5
& , CB,BIOMIN
& , BIOCUM,EPSBIO,ADSBIO
& , AKA,AKN,AKS
& , BRMAX,BRMAXB
& , BSIHB,CBIOMN,CMIN,COLMAS
& , COLNUM,COLSA,DENBLK,ENDOG
& , ENDOGB,FEA,FN
& , FP,FPABIO,RABIO,RCOL
& , TCOL,VCOL,YXS,ICSUB
& , IDMET,IPABIO
& , IRABIO,NCOMPS,NIHB,NNUT
& , NPABIO,NPROD,NARTOT
& , IMSUB,IMEA,IMBS
& , IHB,IPR,INUT
& , IKCB,IBIOC
& , SBIOO,SBION,IBPP
```

```

& , IBKIN,IBNONB,NBC,NBS,NBCNOB,NBIOEQ,IRLIMCOUNT,NMET
& , NBCNAQ,IBIAQ,NAPTOT
& , BTMAX,BTMIN,BIOTIM,BIORME,EFMIN,DAMX,BTSAVG
& , IBTIM,IMAUTO,IMTVAR,NBTS
& , AKR,FRC,FRP
& , TC,ICOMET,IGROW
& , IRLIM
& , CINIT,CBI
& , RED,REDB
& , BVOLMX
C -- ali --
& , IBTEM,IENG
& , TLOB,TMXB,TUPB
C
C -----
C PURPOSE: READ AND ECHO THE INPUT DATA FOR THE
BIODEGRADATION
C OPTION (IBIO=1)
C -----
C
C IMPLICIT DOUBLE PRECISION (A-H,O-Z)
C INTEGER, ALLOCATABLE :: ICOUNT(:)
C DOUBLE PRECISION, ALLOCATABLE:: REDI(:)
C INTEGER, ALLOCATABLE:: IRCT(:)
C -- ali --
C DOUBLE PRECISION, ALLOCATABLE:: TLOB(:)
C DOUBLE PRECISION, ALLOCATABLE:: TMXB(:)
C DOUBLE PRECISION, ALLOCATABLE:: TUPB(:)
C
WRITE (2,230)
READ (5,225)
READ (5,220)
READ (5,*) DENBLK
WRITE (2,298) DENBLK
READ (5,220)
READ (5,*) CMIN,EPSBIO,IBTIM,BVOLMX
WRITE (2,301) CMIN,EPSBIO,IBTIM,BVOLMX
IF(IBTIM.EQ.0) THEN
WRITE (2,*) "IBTIM = 0; NO BIO. TIME STEP CONTROL"
WRITE (2,*) "BIO. EQUATIONS WILL BE SOLVED AT EVERY TIME STEP"
ELSE IF (IBTIM.EQ.1) THEN
WRITE (2,*) "IBTIM = 1; MANUAL BIO. TIME STEP CONTROL"
WRITE (2,*) "SMALLEST BIO. TIME STEP IS BTMIN"
WRITE(2,*)
READ (5,220)
READ (5,*) BTMIN

```



```

WRITE (2,290) BTMIN
ELSE
WRITE (2,*) "IBTIM = 2; AUTOMATIC BIO. TIME STEP CONTROL ",
+ "SELECTED."
WRITE (2,*) "BIO. TIME STEP CONTROLLER WILL KEEP OPERATOR ",
+ "SPLITTING ERROR LESS THAN BIORME"
WRITE(2,*)
READ (5,220)
READ (5,*) BIORME,BTMAX
WRITE (2,291) BIORME,BTMAX
ENDIF
READ (5,220)
READ (5,*) NBC,NMET,IBKIN,IBPP,IBTEM
WRITE (2,299)
WRITE (2,310) NBC,NMET,IBKIN,IBPP,IBTEM
C STOP AND PRINT WARNING IF IMASS = 2 (NON-EQUILIBRIUM MASS
TRANSFER)
C AND IBPP = 1.
IF (IBPP.EQ.1.AND.IMASS.EQ.2) THEN
WRITE (2,*) 'CANNOT USE BIO PERMEABILITY REDUCTION'
WRITE (2,*) 'MODEL WITH NON-EQUILIBRIUM MASS TRANSFER'
STOP
ENDIF
BIOTIM = 0.0
C
C WRITE WARNING MESSAGE TO ECHO AND STOP IF IMET>1 FOR IBKIN=3
C
IF (IBKIN.EQ.3.AND.NMET.GT.1) THEN
WRITE (2,*)
WRITE (2,*) 'THE INSTANTANEOUS KINETICS OPTION IS',
+ ' ONLY AVAILABLE FOR A SINGLE SUBSTRATE, ELECTRON'
WRITE(2,*)'ACCEPTOR, AND BIOLOGICAL SPECIES COMPRISING A',
+ ' SINGLE METABOLIC COMBINATION.'
STOP
ENDIF
C
C WRITE TYPE OF KINETICS TO ECHO IN WORDS
C
WRITE(2,*) 'BIODEGRADATION KINETICS OPTION:'
IF (IBKIN.EQ.0) THEN
WRITE (2,*) ' NO BIODEGRADATION CALCULATIONS'
IMAUTO = 0
ELSEIF (IBKIN.EQ.1) THEN
WRITE(2,*) ' MONOD KINETICS WITH MASS TRANSFER'
IMAUTO = 0
ELSEIF (IBKIN.EQ.2) THEN

```

```

WRITE(2,*) ' MONOD KINETICS - NO MASS TRANSFER'
  IMAUTO = 0
ELSEIF (IBKIN.EQ.3) THEN
  WRITE(2,*) ' INSTANTANEOUS KINETICS'
  IMAUTO = 0
ELSE
  WRITE(2,*) ' MONOD KINETICS WITH AUTOMATIC SELECTION OF
MASS ',
  WRITE(2,*) ' MONOD KINETICS WITH AUTOMATIC SELECTION OF
MASS '
+ ,
+ 'TRANSFER/NO MASS TRANSFER'
  READ (5,220)
  READ (5,*) IMTVAR
  IF (IMTVAR.EQ.1) THEN
    READ (5,220)
    READ (5,*) DAMX
    WRITE(2,*) 'BASED ON DAMKOHLER NUMBER'
    WRITE (2,292) IMTVAR,DAMX
  ELSE
    READ (5,220)
    READ (5,*) EFMIN
    WRITE(2,*) 'BASED ON EFFECTIVENESS FACTOR'
    WRITE (2,293) IMTVAR,EFMIN
  ENDIF
  IBKIN = 1
  IMAUTO = 1
ENDIF
IF (IBPP.EQ.0) THEN
  WRITE (2,*)
  WRITE(2,*) 'NO BIOMASS EFFECT ON POROSITY OR PERMEABILITY'
ELSE
  WRITE (2,*)
  WRITE(2,*) 'BIOMASS GROWTH AFFECTS POROSITY AND
PERMEABILITY'
ENDIF
  WRITE(2,*)
  WRITE(2,*) 'NUMBER OF BIODEGRADATION SPECIES = ',NBC
  WRITE(2,*) 'NUMBER OF METABOLIC COMBINATIONS = ',NMET
C -- ali --
C
  ALLOCATE(TLOB(NMET))
  ALLOCATE(TMXB(NMET))
  ALLOCATE(TUPB(NMET))
  TLOB(1:NMET)=0.0
  TMXB(1:NMET)=0.0

```

```

TUPB(1:NMET)=0.0
C
C
IF(IBTEM.EQ.1.AND.IENG.EQ.1) THEN
WRITE(2,*) " "
WRITE(2,*) " Bioreactions are temp. dependent"
WRITE(2,*) " TLOB(IMET), TMXB(IMET), TUPB(IMET) "
READ(5,220)
DO 81 IMET=1,NMET
READ(5,*) TLOB(IMET), TMXB(IMET), TUPB(IMET)
WRITE(2,*) TLOB(IMET), TMXB(IMET), TUPB(IMET)
WRITE(2,*) " "
81 CONTINUE
ELSE
WRITE(2,*)
WRITE(2,*) " IBMET=0 , Bioactions are not temp. dependent"
WRITE(2,*) " "
ENDIF
C-----
ALLOCATE(NPABIO(NBC),IRABIO(NBC),IBIOC(N))
NPABIO(1:NBC)=0
IRABIO(1:NBC)=0
IBIOC(1:N)=0
ALLOCATE(RABIO(NBC))
RABIO(1:NBC)=0.0
ALLOCATE(IKCB(NBC))
ALLOCATE(ICOUNT(MAX(NBC,NMET)))
ICOUNT(1:MAX(NBC,NMET))=0
C
C-----
C INITIAL CONCENTRATIONS AND SPECIES IDENTIFICATION
C
NBCNOB = 0
NBS = 0
NARTOT = 0
NBTS = 0
BTS AVG = 0.
READ (5,220)
ISKIP = 8+NO
NBCNAQ = 0
NAPTOT = 0
DO 90 I = 1,NBC
READ (5,*) KC,ITYPE,TEMP1,TEMP2,ITEMP3
IF (KC.LE.ISKIP) NBCNAQ = NBCNAQ+1
IF (ITYPE.EQ.1) THEN
NBCNOB = NBCNOB+1

```

```

    INDEX = NBC+1-NBCNOB
ELSE
    NBS = NBS+1
    INDEX = NBS
ENDIF
ICOUNT(INDEX) = ITYPE
IBIOC(KC) = INDEX
IKCB(INDEX) = KC
CINIT(KC) = TEMP1
RABIO(INDEX) = TEMP2
NPABIO(INDEX) = ITEMP3
IF (NPABIO(INDEX).NE.0) THEN
    NAPTOT = NAPTOT+1
ENDIF
IF(RABIO(INDEX).GT.0.) THEN
    NARTOT = NARTOT+1
    IRABIO(NARTOT) = KC
ENDIF
90 CONTINUE
CC-----
    CALL ALLOC_BIO
    ALLOCATE(REDI(NBS))
    REDI(1:NBS)=0.0
    ALLOCATE(IRCT(NMET))
    IRCT(1:NMET)=0
    IBNONB = NBS+1
    IBIAQ = IBNONB+NBCNAQ
C
C ARRANGE BIO INDEXES IN ORDER OF INCREASING UTCHEM
C COMPONENT NUMBER FOR EASE OF PRINTING.  EXCEPT: INDEXES
C OF BIOLOGICAL SPECIES WILL ALWAYS BE OUT OF ORDER UNLESS
C ENTERED IN ORDER BY THE USER
C
    NBCM1 = NBC-1
    DO 650 I = IBNONB,NBCM1
    DO 650 J = I,NBCM1
        IF (IKCB(J).GT.IKCB(J+1)) THEN
            IBIOC(IKCB(J)) = J+1
            ITEST = IKCB(J)
            IKCB(J) = IKCB(J+1)
            RABTMP = RABIO(J)
            NPATMP = NPABIO(J)
            RABIO(J) = RABIO(J+1)
            NPABIO(J) = NPABIO(J+1)
            IBIOC(IKCB(J+1)) = J
            IKCB(J+1) = ITEST

```

```

        RABIO(J+1) = RABTMP
        NPABIO(J+1) = NPATMP
    ENDIF
650 CONTINUE
    IF(NBS.NE.1) THEN
        NBSM1=NBS-1
        DO 640 I=1,NBSM1
        DO 640 J=I,NBSM1
            IF (IKCB(J).GT.IKCB(J+1)) THEN
                IBIOC(IKCB(J))=J+1
                ITEST = IKCB(J)
                IKCB(J)=IKCB(J+1)
                RABTMP=RABIO(J)
                NPATMP=NPABIO(J)
                RABIO(J)=RABIO(J+1)
                NPABIO(J)=NPABIO(J+1)
                IBIOC(IKCB(J+1))=J
                IKCB(J+1)=ITEST
                RABIO(J+1)=RABTMP
                NPABIO(J+1)=NPATMP
            ENDIF
        640 CONTINUE
    ENDIF
C
C CONVERT INDICES OF ABIOTIC PRODUCTS FROM UTCHEM INDICES TO
BIO INDICES
C
    IF (NARTOT.GT.0) THEN
        DO 660 I=1,NARTOT
            IRABIO(I)=IBIOC(IRABIO(I))
        660 CONTINUE
    ENDIF
    WRITE (2,*) 'INDEXES OF UTCHEM SPECIES IN BIO ROUTINES'
    WRITE (2,*)
    WRITE(2,355)
    DO 96 I=1,NBC
        WRITE(2,356) IKCB(I),I
    96 CONTINUE
    WRITE (2,359)
    DO 45 I=1,NBC
        WRITE (2,370) IKCB(I),ICOUNT(I),CINIT(IKCB(I)),
+ RABIO(I),NPABIO(I),
+ SPNAME(IKCB(I))
    45 CONTINUE
    WRITE (2,*)
    IF(NBCNAQ.GT.0) THEN

```

```

        WRITE(2,*) 'WARNING! INITIAL AQUEOUS PHASE CONCENTRATIONS',
+   ' SPECIFIED FOR COMPONENTS < 8 + NO HAVE BEEN IGNORED.'
        WRITE(2,*)
    ENDIF
C
C INITIALIZE METABOLIC COMB. IDENTIFIER TO 0 FOR ALL
COMBINATIONS
C
    DO 65 I=1,NBC
    DO 65 J=1,NBC
    DO 65 L=1,NBC
        IDMET(I,J,L)=0
65 CONTINUE
C
    DO 80 IMET = 1,NMET
        BRMAX(IMET) = 0.
        BRMAXB(IMET) = 0.
        NCOMPS(IMET) = 0
        YXS(IMET) = 0.
        AKS(IMET) = 0.
        AKA(IMET) = 0.
        FEA(IMET) = 0.
        NIHB(IMET) = 0
        NPROD(IMET) = 0
        NNUT(IMET) = 0
        IGROW(IMET) = 0
        TC(IMET) = 0.
        FRP(IMET) = 0.
        FRC(IMET) = 0.
        ICOMET(IMET) = 0
        DO 82 J = 1,NBCNOB
            FP(IMET,J) = 0.
            FN(IMET,J) = 0.
            BSIHB(IMET,J)=0.
            ICSUB(IMET,J)=0
82 CONTINUE
80 CONTINUE
    DO 85 I=1,NBS
        AKR(I) = 0.
        CBI(I) = 0.
        CBIOMN(I) = 0.
        IRLIM(I) = 0
        REDI(I) = 0.
        ADSBIO(I)=0.
85 CONTINUE
C

```

```

C PROPERTIES OF EACH BIOLOGICAL SPECIES
C
  READ (5,220)
  DO 700 I=1,NBS
C   LINE 3.6.10:
KC,DENBIO,RCOL,TCOL,COLNUM,ENDOG,ENDOGB,CBI,CBIOMN,ADSBIO
  READ (5,*) KC,TEMP1,TEMP2,TEMP3,TEMP4,
+ TEMP5,TEMP6,TEMP7,TEMP8, TEMP9
  IF (TEMP7.LT.TEMP8) THEN
    WRITE (2,*) 'CHECK CBI & CBIOMN.'
    WRITE (2,*) 'CBI CANNOT BE LESS THAN CBIOMN.'
    STOP
  ENDIF
  INDEX = IBIOC(KC)
  DENBIO(INDEX)=TEMP1
  RCOL(INDEX)=TEMP2
  TCOL(INDEX)=TEMP3
  COLNUM(INDEX)=TEMP4
  ENDOG(INDEX)=TEMP5
  ENDOGB(INDEX)=TEMP6
  CBI(INDEX)=TEMP7
  CBIOMN(INDEX)=TEMP8
  ADSBIO(INDEX)=TEMP9
700 CONTINUE
  WRITE (2,321)
  WRITE (2,329)
  WRITE (2,330) (IKCB(I),DENBIO(I),
+ RCOL(I),TCOL(I),COLNUM(I),
+ ENDOG(I),ENDOGB(I),CBI(I),CBIOMN(I),ADSBIO(I),I=1,NBS)
C
C CONVERT BIOMASS DENSITY FROM G/CC TO MG/L
C
  DO 600 I = 1,NBS
    DENBIO(I) = DENBIO(I)*1000000.
600 CONTINUE
C
C METABOLIC COMBINATION INFORMATION
C
  READ (5,220)
  DO 130 IMET=1,NMET
C   LINE 3.6.11: ISUB,IEA,IBS,BRMAX,BRMAXB,YXS,AKS,AKA,FEA
C   ISUB: STORED AS IMSUB
C   IEA: STORED AS IMEA
C   IBS: STORED AS IMBS
    READ (5,*) J,K,L,BRMAX(IMET),BRMAXB(IMET),YXS(IMET),
+ AKS(IMET),AKA(IMET),FEA(IMET)

```

```

    IMSUB(IMET)=IBIOC(J)
    IMEA(IMET)=IBIOC(K)
    IMBS(IMET)=IBIOC(L)
    IDMET(IBIOC(J),IBIOC(K),IBIOC(L))=IMET
130 CONTINUE
    WRITE (2,322)
    WRITE (2,319)
    DO 140 IMET = 1,NMET
        WRITE (2,320) IKCB(IMSUB(IMET)),IKCB(IMEA(IMET)),
+ IKCB(IMBS(IMET)),
+ BRMAX(IMET),BRMAXB(IMET),YXS(IMET),AKS(IMET),
+ AKA(IMET),FEA(IMET)
140 CONTINUE
C
C FLAGS FOR COMPETITION, INHIBITION, PRODUCT GENERATION,
NUTRIENTS,
C COMETABOLISM.
C
    READ (5,220)
    DO 143 I=1,NMET
C LINE 3.6.12: ISUB,IEA,IBS,NCOMPS,NIHB,NPROD,NNUT,ICOMET
    READ (5,*) J,K,L,ITEMP1,ITEMP2,ITEMP3,ITEMP4,ITEMP5
    IMET=IDMET(IBIOC(J),IBIOC(K),IBIOC(L))
C
C PRINT WARNING IF METABOLIC COMBINATION IS INVALID
C
    IF(IMET.EQ.0) THEN
        WRITE(2,*)
        WRITE(2,*) 'PROGRAM STOPPED.'
        WRITE(2,*) 'CHECK METABOLIC COMBINATIONS IN THE METABOLIC',
+ ' FLAGS SECTION'
        STOP
    ENDIF
    NCOMPS(IMET)=ITEMP1
    NIHB(IMET)=ITEMP2
    NPROD(IMET)=ITEMP3
    NNUT(IMET)=ITEMP4
    ICOMET(IMET)=ITEMP5
143 CONTINUE
    WRITE (2,323)
    WRITE (2,324)
    DO 145 IMET = 1,NMET
        WRITE (2,325) IKCB(IMSUB(IMET)),IKCB(IMEA(IMET)),
+ IKCB(IMBS(IMET)),
+ NCOMPS(IMET),NIHB(IMET),NPROD(IMET),
+ NNUT(IMET),ICOMET(IMET)

```



```

145 CONTINUE
C
C NO COMPETITION, INHIBITION, NUTRIENTS,ETC. ALLOWED FOR IBKIN=3
C
  IF(IBKIN.EQ.3) THEN
    KSUM=NCOMPS(1)+NIHB(1)+NPROD(1)+NNUT(1)+ICOMET(1)
    IF (KSUM.GT.0) THEN
      WRITE (2,*)
      WRITE (2,*) 'SUBSTRATE COMPETITION, INHIBITION, PRODUCT',
+ ' GENERATION, NUTRIENT LIMITATIONS OR COMETABOLIC'
      WRITE (2,*) ' REACTION KINETICS ARE NOT ALLOWED FOR',
+ ' INSTANTANEOUS KINETICS'
      STOP
    ENDIF
  ENDIF
C
C SUBSTRATE COMPETITION PARAMETERS
C
  ITOT = 0
  DO 72 IMET = 1,NMET
    ITOT = ITOT+NCOMPS(IMET)
72 CONTINUE
  IF(ITOT.NE.0) THEN
C
C REMINDER ABOUT ORDER OF INFO. IN THIS SECTION.
C
    WRITE(2,*)
    WRITE(2,*) '!!!REMINDER - METABOLIC COMBINATIONS FOR',
+ ' SUBSTRATE COMPETITION ENTERED IN THE SECTION BELOW'
    WRITE(2,*) 'MUST BE LISTED IN THE SAME ORDER AS IN',
+ ' THE METABOLIC COMBINATION MONOD PARAM. SECTION ABOVE'
    WRITE(2,*)
    WRITE(2,*) 'ALSO - COMPETING SUBSTRATES MUST BE
BIODEGRADED',
+ ' BY THE SAME '
    WRITE(2,*) 'BIOLOGICAL SPECIES USING THE SAME ELECTRON',
+ ' ACCEPTOR.'
    DO 77 IMET=1,NMET
      ICOUNT(IMET)=0
77 CONTINUE
C NOTE: MUST BE ENTERED IN SAME ORDER AS METABOLIC
COMBINATION INFO.
    READ (5,220)
    DO 100 I=1,NMET
      IF(NCOMPS(I).NE.0) THEN
C LINE 3.6.13: ISUB,IEA,IBS,ICSUB

```

```

      READ (5,*) J,K,L,(ICOUNT(M),M=1,NCOMPS(I))
      IMET=IDMET(IBIOC(J),IBIOC(K),IBIOC(L))
C
C PRINT WARNING IF METABOLIC COMBINATION IS INVALID
C
      IF(IMET.EQ.0) THEN
        WRITE(2,*)
        WRITE(2,*) 'PROGRAM STOPPED.'
        WRITE(2,*) 'CHECK METABOLIC COMBINATIONS'
+      , 'IN THE SUBSTRATE',
+      ' COMPETITION SECTION'
        STOP
      ENDIF
      DO 98 INUM=1,NCOMPS(IMET)
        INDEX = IBIOC(ICOUNT(INUM))
        IF (INDEX.LE.NBS) THEN
          WRITE (2,*) 'I THINK WE SHOULD STOP HERE.'
          WRITE (2,*) 'ICSUB MUST BE A CHEMICAL COMPONENT.'
          WRITE (2,*) 'RIGHT?'
          STOP
        ENDIF
C      ICSUB(IMET,INUM)=IBIOC(ICOUNT(INUM))
      ICSUB(IMET,INUM) = INDEX
98      CONTINUE
      ENDIF
100     CONTINUE
      WRITE (2,351)
      WRITE (2,349)
      DO 120 IMET=1,NMET
        IF (NCOMPS(IMET).NE.0) THEN
          WRITE (2,350) IKCB(IMSUB(IMET)),IKCB(IMEA(IMET)),
+          IKCB(IMBS(IMET)),
+          (IKCB(ICSUB(IMET,INUM)),INUM=1,NCOMPS(IMET))
        ENDIF
120     CONTINUE
      ENDIF
C
C INHIBITION CONSTANTS
C
      ITOT = 0
      DO 70 IMET = 1,NMET
        ITOT = ITOT+NIHB(IMET)
70     CONTINUE
      IF(ITOT.NE.0) THEN
        DO 75 IMET=1,NMET
          ICOUNT(IMET)=0

```

```

75  CONTINUE
    READ (5,220)
    DO 76 I=1,ITOT
C   LINE 3.6.14: ISUB,IEA,IBS,IHB,BSIHB
    READ (5,*) J,K,L,M,TEMP
    IMET=IDMET(IBIOC(J),IBIOC(K),IBIOC(L))
C
C   PRINT WARNING IF METABOLIC COMBINATION IS INVALID
C
    IF(IMET.EQ.0) THEN
        WRITE(2,*)
        WRITE(2,*) 'PROGRAM STOPPED.'
        WRITE(2,*) 'CHECK METABOLIC COMBINATIONS'
+       , ' IN THE INHIBITION',
+   ' SECTION'
        STOP
    ENDIF
    INDEX = IBIOC(M)
    IF (INDEX.LE.NBS) THEN
        WRITE (2,*) 'I THINK WE SHOULD STOP HERE.'
        WRITE (2,*) 'IHB MUST BE A CHEMICAL COMPONENT.'
        WRITE (2,*) 'RIGHT?'
        STOP
    ENDIF
    ICOUNT(IMET)=ICOUNT(IMET)+1
    IHB(IMET,ICOUNT(IMET)) = INDEX
    BSIHB(IMET,ICOUNT(IMET))=TEMP
76  CONTINUE
    WRITE (2,345)
    WRITE (2,339)
    DO 110 IMET=1,NMET
        IF (NIHB(IMET).NE.0) THEN
            DO 109 I=1,NIHB(IMET)
                WRITE (2,340) IKCB(IMSUB(IMET)),IKCB(IMEA(IMET)),
+                IKCB(IMBS(IMET)),IKCB(IHB(IMET,I)),BSIHB(IMET,I)
109          CONTINUE
            ENDIF
110  CONTINUE
        ENDIF
C
C   PRODUCT GENERATION
C
    ITOTB = 0
    ITOTA = 0
    DO 163 IMET=1,NMET
        ITOTB = ITOTB+NPROD(IMET)

```

```

163 CONTINUE
    DO 164 I=1,NBC
        ITOTA = ITOTA+NPABIO(I)
164 CONTINUE
    IF(ITOTB.NE.0.OR.ITOTA.NE.0) THEN
        DO 162 IMET=1,NMET
            ICOUNT(IMET)=0
162 CONTINUE
        IF(ITOTB.NE.0) THEN
C
C READ INFORMATION FOR PRODUCTS OF BIOLOGICAL REACTIONS
C
            READ (5,220)
            DO 167 I=1,ITOTB
C LINE 3.6.15: ISUB,IEA,IBS,IPR,FPR
C FPR: STORED AS FP
                READ (5,*) J,K,L,M,TEMP
                IMET=IDMET(IBIOC(J),IBIOC(K),IBIOC(L))
C
C CHECK VALIDITY OF METABOLIC COMBINATION
C
                IF(IMET.EQ.0) THEN
                    WRITE(2,*)
                    WRITE(2,*) 'CHECK METABOLIC COMBINATIONS'
&                , ' IN THE SECTION ABOVE'
                    STOP
                ENDIF
                INDEX = IBIOC(M)
                IF (INDEX.LE.NBS) THEN
                    WRITE (2,*) 'I THINK WE SHOULD STOP HERE.'
                    WRITE (2,*) 'IPR MUST BE A CHEMICAL COMPONENT.'
                    WRITE (2,*) 'RIGHT?'
                    STOP
                ENDIF
                ICOUNT(IMET)=ICOUNT(IMET)+1
                IPR(IMET,ICOUNT(IMET)) = INDEX
                FP(IMET,ICOUNT(IMET))=TEMP
167 CONTINUE
                WRITE (2,365)
                WRITE (2,369)
                DO 170 IMET=1,NMET
                    IF (NPROD(IMET).NE.0) THEN
                        DO 169 I=1,NPROD(IMET)
                            WRITE (2,380) IKCB(IMSUB(IMET)),IKCB(IMEA(IMET)),
+                            IKCB(IMBS(IMET)),IKCB(IPR(IMET,I)),
+                            FP(IMET,I)

```

```

169     CONTINUE
        ENDIF
170     CONTINUE
        ENDIF
        IF(ITOTA.NE.0) THEN
C
C READ INFORMATION FOR PRODUCTS OF ABIOTIC REACTIONS
C
        READ (5,220)
        DO 165 I=1,NBC
            ICOUNT(I)=0
165     CONTINUE
            DO 166 I=1,ITOTA
C LINE 3.6.16: ISUB,IPR,FPR
C IPR: STORED AS IPABIO
C FPR: STORED AS FPABIO
                READ (5,*) J,K,TEMP
                INDEX = IBIOC(J)
                IF (INDEX.LE.NBS) THEN
                    WRITE (2,*) 'I THINK WE SHOULD STOP HERE.'
                    WRITE (2,*) 'ISUB MUST BE A CHEMICAL COMPONENT.'
                    WRITE (2,*) 'RIGHT?'
                    STOP
                ENDIF
                INDECIES = IBIOC(K)
                IF (INDECIES.LE.NBS) THEN
                    WRITE (2,*) 'IPR IS A CHEMICAL COMPONENT.'
                ELSE
                    WRITE (2,*) 'IPR IS A BIOLOGICAL COMPONENT.'
                ENDIF
C             ICOUNT(IBIOC(J))=ICOUNT(IBIOC(J))+1
C             ICOUNT(INDEX)=ICOUNT(INDEX)+1
C             IPABIO(IBIOC(J),ICOUNT(IBIOC(J)))=IBIOC(K)
C             IPABIO(INDEX,ICOUNT(INDEX)) = INDECIES
C             FPABIO(IBIOC(J),ICOUNT(IBIOC(J)))=TEMP
C             FPABIO(INDEX,ICOUNT(INDEX))=TEMP
166     CONTINUE
            WRITE (2,366)
            WRITE (2,367)
            DO 175 I=1,NBC
                IF(NPABIO(I).NE.0) THEN
                    DO 176 J=1,NPABIO(I)
                        WRITE (2,368) IKCB(I),IKCB(IPABIO(I,J)),FPABIO(I,J)
176                 CONTINUE
                    ENDIF
175     CONTINUE

```

```

        ENDIF
    ENDIF
C
C NUTRIENT LIMITATIONS
C
    ITOT = 0
    DO 440 IMET = 1,NMET
        ITOT = ITOT+NNUT(IMET)
440 CONTINUE
    IF(ITOT.NE.0) THEN
        DO 441 IMET = 1,NMET
            ICOUNT(IMET) = 0
441 CONTINUE
            READ (5,220)
            DO 445 I = 1,ITOT
C LINE 3.6.17: ISUB,IEA,IBS,INUT,AKN,FN
                READ (5,*) J,K,L,M,TEMP1,TEMP2
                IMET = IDMET(IBIOC(J),IBIOC(K),IBIOC(L))
C
C PRINT WARNING IF METABOLIC COMBINATION IS INVALID
C
                IF (IMET.EQ.0) THEN
                    WRITE(2,*)
                    WRITE(2,*) 'PROGRAM STOPPED.'
                    WRITE(2,*) 'CHECK METABOLIC COMBINATIONS IN THE NUTRIENT'
+
+           ' LIMITATIONS SECTION'
                    STOP
                ENDIF
                INDEX = IBIOC(M)
                IF (INDEX.LE.NBS) THEN
                    WRITE (2,*) 'I THINK WE SHOULD STOP HERE.'
                    WRITE (2,*) 'INUT MUST BE A CHEMICAL COMPONENT.'
                    WRITE (2,*) 'RIGHT?'
                    STOP
                ENDIF
                ICOUNT(IMET)=ICOUNT(IMET)+1
                INUT(IMET,ICOUNT(IMET)) = INDEX
                AKN(IMET,ICOUNT(IMET))=TEMP1
                FN(IMET,ICOUNT(IMET))=TEMP2
445 CONTINUE
                WRITE (2,385)
                WRITE (2,379)
                DO 430 IMET = 1,NMET
                    IF (NNUT(IMET).NE.0) THEN
                        DO 447 I = 1,NNUT(IMET)

```

```

        WRITE (2,340) IKCB(IMSUB(IMET)),IKCB(IMEA(IMET)),
+       IKCB(IMBS(IMET)),IKCB(INUT(IMET,I)),
+       AKN(IMET,I),FN(IMET,I)
447     CONTINUE
        ENDIF
430     CONTINUE
        ENDIF
C
C DETERMINE WHETHER ANY COMETABOLIC REACTION DATA MUST BE
READ.
C
        ITOT = 0
        DO 530 IMET = 1,NMET
            ITOT = ITOT+ICOMET(IMET)
530     CONTINUE
        IF (ITOT.NE.0) THEN
C
C READ TRANSFORMATION CAPACITY DATA.
C
            IRLIMCOUNT = 0
            READ (5,220)
            DO 535 I=1,ITOT
C LINE 3.6.18: ISUB,IEA,IBS,TC,IRLIM
C IRLIM: STORED AS IRCT AS WELL AS IRLIM
                READ (5,*) J,K,L,TEMP,ITEMP
                IMET = IDMET(IBIOC(J),IBIOC(K),IBIOC(L))
C
C PRINT WARNING IF METABOLIC COMBINATION IS INVALID
C
                IF (IMET.EQ.0) THEN
                    WRITE(2,*)
                    WRITE(2,*) 'PROGRAM STOPPED.'
                    WRITE(2,*) 'CHECK METABOLIC COMBINATIONS IN'
+                   ', THE COMETABOLIC'
+                   ', TRANSFORMATION CAPACITY SECTION'
                    STOP
                ENDIF
                TC(IMET) = TEMP
                IRCT(IMET) = ITEMP
                IF (IRLIM(IMBS(IMET)).EQ.0) THEN
                    IRLIM(IMBS(IMET)) = ITEMP
                    IRLIMCOUNT = IRLIMCOUNT+1
                ENDIF
535     CONTINUE
            WRITE (2,391)
            WRITE (2,389)

```

```

DO 540 IMET = 1,NMET
  IF (ICOMET(IMET).NE.0) THEN
    WRITE (2,390) IKCB(IMSUB(IMET)),IKCB(IMEA(IMET)),
+   IKCB(IMBS(IMET)),TC(IMET),IRCT(IMET)
    ENDIF
540  CONTINUE
C
C PRINT WARNING IF A TRANSFORMATION CAPACITY IS SPECIFIED BUT
C CBIOMN IS >0.
C
DO 544 I = 1,NBS
  ICOUNT(I) = 0
544  CONTINUE
DO 543 IMET = 1,NMET
  IF (ICOUNT(IMBS(IMET)).LE.0) THEN
    IF (CBIOMN(IMBS(IMET)).GT.ZERO
&   .AND.ICOMET(IMET).EQ.1) THEN
      WRITE(2,*)
      WRITE(2,*) 'WARNING!'
      WRITE(2,393) SPNAME(IKCB((IMBS(IMET))))
      ICOUNT(IMBS(IMET))=ICOUNT(IMBS(IMET))+1
    ENDIF
  ENDIF
543  CONTINUE
C
C READ NADH LIMITATION PARAMETERS
C
NRLIM = 0
DO 547 I = 1,NMET
  NRLIM = NRLIM+IRCT(I)
547  CONTINUE
IF (NRLIM.NE.0) THEN
  DO 532 I=1,NMET
    ICOUNT(I) = 0
532  CONTINUE
  READ (5,220)
  DO 533 I=1,NRLIM
C LINE 3.6.19: ISUB,IEA,IBS,IGROW,REDI,AKR,FRP,FRC
  READ (5,*) J,K,L,M,TEMP1,TEMP2,TEMP3,TEMP4
  IMET = IDMET(IBIOC(J),IBIOC(K),IBIOC(L))
C
C PRINT WARNING IF METABOLIC COMBINATION IS INVALID
C
IF(IMET.EQ.0) THEN
  WRITE(2,*)
  WRITE(2,*) 'PROGRAM STOPPED.'

```



```

        WRITE(2,*) 'CHECK METABOLIC COMBINATIONS IN THE NADH',
+   ' LIMITATIONS SECTION'
        STOP
        ENDIF
        REDI(IBIOC(L)) = TEMP1
        AKR(IBIOC(L)) = TEMP2
        FRC(IMET) = TEMP4
        JMET = IDMET(IBIOC(M),IBIOC(K),IBIOC(L))
        IF(JMET.EQ.0) THEN
            WRITE(2,*)
            WRITE(2,*) 'PROGRAM STOPPED.'
            WRITE(2,*) 'CHECK METABOLIC COMBINATIONS IN THE NADH',
+   ' LIMITATIONS SECTION'
            STOP
            ENDIF
            ICOUNT(IMET) = JMET
            IGROW(JMET) = IBIOC(M)
            FRP(JMET) = TEMP3
533    CONTINUE
        WRITE (2,392)
        WRITE (2,394)
        DO 550 IMET=1,NMET
            IF (IRCT(IMET).NE.0) THEN
                WRITE (2,395) IKCB(IMSUB(IMET)),IKCB(IMEA(IMET)),
+   IKCB(IMBS(IMET)),IKCB(IGROW(ICOUNT(IMET))),
+   REDI(IMBS(IMET)),AKR(IMBS(IMET)),FRP(ICOUNT(IMET)),
+   FRC(IMET)
            ENDIF
550    CONTINUE
        ENDIF
    ENDIF
C
C CALCULATE THE NUMBER OF EQUATIONS TO BE SOLVED BY THE
C ODE SOLVER, INCLUDING THE NUMBER OF EQUATIONS DUE TO NADH
C LIMITATIONS:
C
C MAP NAPL COMPONENT DENSITIES INTO DENBIO FOR USE IN
C CONVERSION FROM VOLUME FRACTION TO MG/L UNITS IN
C BIODEGRADATION
C SUBROUTINES
C
C IF IKCB > 8+NO, DENBIO = 0
C IF IKCB <= 8+NO, DENBIO IS IN GM/CC UNIT.
C OTHERS HAVE MG/L UNIT.
C 1 GM/CC = 0.433 PSI/FT
C 2.309 GM/CC = 1 PSI/FT

```

```

IF(IUNIT.EQ.0) THEN
  DO 1236 I=IBNONB,NBC
    DENBIO(I)=DNOILC(IKCB(I))*2.309
1236 CONTINUE
  ELSE
    DO 1238 I=IBNONB,NBC
      DENBIO(I)=DNOILC(IKCB(I))
1238 CONTINUE
  ENDIF
C
C CALCULATE MICROCOLONY PARAMETERS
C
  DO 30 I=1,NBS
    COLSA(I) = PIE*RCOL(I)**2.
    VCOL(I) = COLSA(I)*TCOL(I)
    COLMAS(I) = DENBIO(I)*VCOL(I)*0.001
C    [MG] = [MG/L] *[CM3] *0.001 [L/CM3]
  30 CONTINUE
C
C CALCULATE THE BIOFILM MASS CONCENTRATION AT EACH GRID
BLOCK AND
C READ IN THE INITIAL COMPONENT CONCENTRATIONS.
C
  DO 40 I = 1,NBL
    DO 20 J=1,NBS
      CB(I,J,J) = (CBI(J)*DENBLK*COLMAS(J)*1000.)/
+      (COLNUM(J)*POR(I))
C CB: [MG/L(PORE)]
C NUMERATOR
C CBI: [# OF CELLS/G(ROCK)]
C DENBLK: [G(ROCK)/CM3(BULK)]
C COLMAS: [MG/COLONY]
C 1000 [CM3(PORE)/L(PORE)]
C DENOMINATOR
C COLNUM: [# OF CELLS/COLONY]
C POR: [CM3(PORE)/CM3(BULK)]
C CB IS IN [MG/L].
C
C CALCULATE BIOMN IN TERMS OF A MASS CONCENTRATION
C
  BIOMIN(I,J) = (CBIOMN(J)*DENBLK*COLMAS(J)*1000.)/
+      (COLNUM(J)*POR(I))
C
C INITIALIZE THE NADH CONCENTRATION IN ALL GRID BLOCKS.
C
  RED(I,J) = REDI(J)

```

```

        REDB(I,J,J) = REDI(J)
20  CONTINUE
40  CONTINUE
C
C  INITIALIZE THE MASS BALANCE VARIABLE BIOCUM
C
        DO 610 I = 1,NBC
            BIOCUM(I) = 0.0
610  CONTINUE
C  CALCULATE D50 FROM CARMEN-KOZENY CORRELATION IN CM
        ONEP3 = 1000.
        DO 620 I = 1,NBL
            DP2(I) = 300*PERMX(I)/ONEP3*(1-POR(I))**2/POR(I)**3
            DP(I) = 0.0001*SQRT(DP2(I))
620  CONTINUE
        WRITE (2,360)
C
220  FORMAT (//)
225  FORMAT (//////)
230  FORMAT (//*****'
+ //BIOLOGICAL DATA://
+ 'AVERAGE PART. DIAM, BULK DENS., MIN. CONC., ODE CONV. TOL./')
298  FORMAT (1X,1X,'DENBLK= ',T10,E15.5/)
301  FORMAT (1X,'CMIN = ',T10,E15.5/1X
&           , 'EPSBIO = ',T10,E15.5/
+ 1X,'IBTIM = ',T14,I2/1X
+   , 'BVOLMX = ',T10,E15.5)
290  FORMAT (1X,'BTMIN = ',T10,E15.5/
)
291  FORMAT (1X,'BIORME = ',T10,E15.5/1X,'BTMAX = ',T10,E15.5/)
292  FORMAT (/3X,'IMTVAR = ',I2/3X,'DAMX = ',T10,E12.5/)
293  FORMAT (/3X,'IMTVAR = ',I2/3X,'EFMIN = ',T10,E12.5/)
299  FORMAT(/"NUMBER OF COMPONENTS PARTICIPATING IN BIO RXNS',
+ ' NUMBER OF METABOLIC COMBINATIONS, TYPE OF BIO KINETICS'/)
310  FORMAT(1X,'NBC= ',T10,I3/1X,'NMET= ',T10,I3/1X,'IBKIN= ',
+ T10,I3/1X,'IBPP= ',T10,I3/1X,'IBTEM= ',T10,I3/)
319  FORMAT (1X,/3X,'ISUB',2X,'IEA',2X,'IBS',T22,'BRMAX',T33,
+ 'BRMAXB',T49,'YXS',T60,'AKS',T71,'AKA',T82,'FEA'/)
320  FORMAT (1X,(T2,3I5,6(3X,E9.3)))
321  FORMAT(/"BIOLOGICAL SPECIES PROPERTIES")
322  FORMAT(/"METABOLIC COMBINATION MONOD PARAMETERS")
323  FORMAT(/"METABOLIC COMBINATION KINETICS FLAGS")
324  FORMAT (1X,/3X,'ISUB',2X,'IEA',2X,'IBS',T20,'NCOMPS',T28,
+ 'NIHB',T36,'NPROD',T44,'NNUT',T52,'ICOMET'/)
325  FORMAT (1X,(T2,3I5,T19,I4,T27,I4,T35,I4,T43,I4,T51,I4))
329  FORMAT (1X,/T4,'KC',T13,'DENBIO',T24,'RCOL',T36,'TCOL',T48,
+ 'COLNUM',T59,'ENDOG',T72,'ENDOGB',T83,'CBI',

```

```

+ T94,'CBIOMN',T104,'ADSBIO'/)
330 FORMAT (1X,(T2,I5,9(3X,E9.3)))
339 FORMAT (1X,/T5,'ISUB',T10,'IEA',T15,'IBS',T20,'IHB',
+ T30,'BSIHB'/)
340 FORMAT (1X,(T3,4I5,3X,2(E9.3,8X)))
345 FORMAT(/'INHIBITING SPECIES AND INHIBITION CONSTANTS')
349 FORMAT (1X,/T4,'ISUB',T9,'IEA',T14,'IBS',T19,
+ 10X,'COMPONENT NUMBERS OF COMPETITIVE SUBSTRATES'/)
350 FORMAT (1X,(T2,3I5,10X,10I5))
351 FORMAT(/'COMPETING SUBSTRATES')
352 FORMAT (1X,'NBC= ',T20,I3/1X,'NBCNOB= ',T20,I3/
+ 1X,'IBNONB= ',T20,I3/)
355 FORMAT (1X,'UTCHEM COMPONENT INDEX',T35,'BIOD. COMP. INDEX'/)
356 FORMAT(1X,T14,I3,T40,I3)
359 FORMAT (1X,/'UTCHEM INDEX OF BIODEGRADATION COMPONENTS,
+ COMPONENT TYPE, INITIAL CONC. AND ABIOTIC REACTION
CONSTANT:'
+ //'COMPONENT NO.',T15,'ITYPE',T23,'INITIAL CONC.',T40,
+ '1ST ORDER RXN CONST.',T64,'NO. OF ABIOTIC PRODUCTS',
+ T92,'NAME'/)
365 FORMAT ('BIODEGRADATION PRODUCTS AND STOICH. RATIO')
366 FORMAT ('ABIOTIC PRODUCTS')
367 FORMAT (1X,/T5,' KC ',T10,'IPR',T15,'FPABIO'/)
368 FORMAT (1X,T6,I2,T10,I2,T14,E9.3)
370 FORMAT (1X,T5,I2,T15,I3,T24,D9.3,T44,D9.3,T72,I2,T92,A8)
369 FORMAT (1X,/T5,'ISUB',T10,'IEA',T15,'IBS',T20,'IPR',T29,'FP'/)
379 FORMAT (1X,/T5,'ISUB',T10,'IEA',T15,'IBS',T20,
+ 'INUT',T29,'AKN',T43,'FN'/)
380 FORMAT (1X,(T3,4I5,3X,2(E9.3,3X)))
385 FORMAT ('NUTRIENT LIMITATION PARAMETERS')
389 FORMAT (1X,/T5,'ISUB',T10,'IEA',T15,'IBS',T25,
+ 'TC',T33,'IRLIM'/)
390 FORMAT (1X,(T3,3I5,3X,E9.3,3X,I3))
391 FORMAT ('COMETABOLISM PARAMETERS')
392 FORMAT ('NADH LIMITATION PARAMETERS')
393 FORMAT (' A TRANSFORMATION CAPACITY IS SPECIFIED',
+ ' FOR BIOMASS ',A8,/' BUT CBIOMN IS > 0. MODEL MAY PRODUCE',
+ ' INCORRECT RESULTS'/
+ ' BECAUSE BIOMASS IS NOT ALLOWED TO DIE OFF')
394 FORMAT (1X,/T5,'ISUB',T10,'IEA',T15,'IBS',T20,'IGROW',T29,'REDI',
+ T40,'AKR',T53,'FRP',T65,'FRC'/)
395 FORMAT (1X,T2,4I5,4(3X,E9.3))
360 FORMAT (1X,/'END OF BIOLOGICAL DATA'/'
+ '*****'/)
RETURN

```

END

C

```
SUBROUTINE F(N,T,Y,YDOT)
USE MODULE1, ONLY:
& ZERO,ONE,ONEM,ONEM4,ONEM5,ONEM6,ONEM7,ONEM8,ONEM9
& ,
ONEM10,ONEM12,ONEP12,ONEM50,ONEP50,ONEM5M,PONEM,ONE199,PRCSN
& , PIE,F1P8
& , DNOILC,DENBIO
& , CTOT,C,CSE,S
& , CE
& , SCHM,REY,SHER,DP
& , IXYZ
& , CB,BIOMIN
& , BIOCUM,EPSBIO,ADSBIO
& , AKA,AKN,AKS
& , BRMAX,BRMAXB
& , BSIHB,CBIOMN,CMIN,COLMAS
& , COLNUM,COLSA,DENBLK,ENDOG
& , ENDOGB,FEA,FN
& , FP,FPABIO,RABIO,RCOL
& , TCOL,VCOL,YXS,ICSUB
& , IDMET,IPABIO
& , IRABIO,NCOMPS,NIHB,NNUT
& , NPABIO,NPROD,NARTOT
& , IMSUB,IMEA,IMBS
& , IHB,IPR,INUT
& , IKCB,IBIOC
& , SUBMAX,EAMAX,RMTMAX,CEXIT
& , BMTC,SC
& , IBKIN,IBNONB,NBC,NBS,NBCNOB,NBIOEQ,IRLIMCOUNT,NMET
& , NBCNAQ,IBIAQ,NAPTOT
& , AKR,FRC,FRP
& , TC,ICOMET,IGROW
& , IRLIM
& , SBIOO,SBION,IBPP
& , DCF,DCBF
& , CF,CBF
& , DREDF,DREDBF
& , REDF,REDBF
& , BVOLMX
& , TEM
& , TLOB,TMXB,TUPB
```

```

C
C -----
C PURPOSE: CALCULATE VALUES OF THE DERIVATIVES FOR
C FOR THE BIODEGRADATION OPTION
C -----
C
C IMPLICIT DOUBLE PRECISION (A-H,O-Z)
C DIMENSION Y(*),YDOT(*)
C
C
C
C PHASE BEHAVIOR OF TYPE II(-)
C
C IF (S(IXYZ,1).NE.ZERO) THEN
C   STERM = S(IXYZ,1)
C ELSE
C   STERM = S(IXYZ,3)
C ENDIF
C
C CALCULATION OF MASS TRANSFER TERMS AND ENDOGENEOUS DECAY
C TERMS
C FOR THE BIOMASS. EACH SUBSTRATE AND ELECTRON ACCEPTOR
C DIFFUSES
C INTO THE BIOMASS WHETHER IT REACTS BIOLOGICALLY IN THAT
C BIOMASS OR
C NOT.
C
C SUBMAX = 0.
C EAMAX = 0.
C RMTMAX = 0.
C
C READ VALUES OF Y INTO C'S WHICH ARE USED IN SUBROUTINE
C CALCULATIONS.
C ALSO, INITIALIZE DC AND DCB, THE DERIVATIVE FUNCTION ARRAYS.
C
C ICOUNT = 0
C DO 540 I = IBNONB,NBC
C   ICOUNT = ICOUNT+1
C   CF(I) = Y(ICOUNT)
C   DCF(I) = 0.
C   IF(IBKIN.NE.1) GOTO 540
C DO 541 J = 1,NBS
C   ICOUNT = ICOUNT+1
C   CBF(I,J) = Y(ICOUNT)
C   DCBF(I,J) = 0.
541 CONTINUE

```

```

540 CONTINUE
    DO 550 I = 1,NBS
        ICOUNT = ICOUNT+1
        CF(I) = Y(ICOUNT)
        DCF(I) = 0.
        ICOUNT = ICOUNT+1
        CBF(I,I) = Y(ICOUNT)
        DCBF(I,I) = 0.
550 CONTINUE
    IF (IRLIMCOUNT.EQ.0) GOTO 555
    DO 551 I = 1,NBS
        IF(IRLIM(I).EQ.0) GOTO 551
        ICOUNT = ICOUNT+1
        REDF(I) = Y(ICOUNT)
        DREDF(I) = 0.
        ICOUNT = ICOUNT+1
        REDBF(I,I) = Y(ICOUNT)
        DREDBF(I,I) = 0.
551 CONTINUE
555 CONTINUE
C
C CALCULATE MAXIMUM SUBSRATE AND ELECTRON ACCEPTOR
CONCENTRATIONS
C TO DETERMINE WHETHER OR NOT TO EXIT SDRIV2.
C
    DO 560 IMET = 1,NMET
        SUBMAX = MAX(SUBMAX,CF(IMSUB(IMET)))
560 CONTINUE
    DO 570 IMET = 1,NMET
        EAMAX = MAX(EAMAX,CF(IMEA(IMET)))
570 CONTINUE
C
C ABIOTIC REACTIONS
C
    IF (NARTOT.EQ.0) GOTO 17
    DO 15 I = 1,NARTOT
        DCF(IRABIO(I)) = DCF(IRABIO(I))-RABIO(IRABIO(I))*
+ CF(IRABIO(I))
        DO 14 K=1,NBS
            DCBF(IRABIO(I),K) = DCBF(IRABIO(I),K)-
+ RABIO(IRABIO(I))*CBF(IRABIO(I),K)
14 CONTINUE
    IF(NPABIO(IRABIO(I)).EQ.0) GOTO 15
C PRODUCT GENERATION FROM ABIOTIC REACTIONS
    DO 16 J=1,NPABIO(IRABIO(I))
        DCF(IPABIO(IRABIO(I),J)) = DCF(IPABIO(IRABIO(I),J)) +

```

```

+   RABIO(IRABIO(I))*CF(IRABIO(I))*FPABIO(IRABIO(I),J)
DO 18 K=1,NBS
  DCBF(IPABIO(IRABIO(I),J),K) =
+   DCBF(IPABIO(IRABIO(I),J),K) + RABIO(IRABIO(I))*
+   CBF(IRABIO(I),K)*FPABIO(IRABIO(I),J)
18  CONTINUE
16  CONTINUE
15  CONTINUE
17  CONTINUE
C
C MASS TRANSFER CALCULATIONS
C
  DO 10 J = 1,NBS
C
C SKIP MASS TRANSFER INTO BIOMASS WHEN NO ATTACHED BIOMASS
EXISTS
C FOR THAT BIOLOGICAL SPECIES.
C
  IF (CBF(J,J).LE.ZERO) GOTO 9
C
C SKIP MASS TRANSFER IF THE IBKIN=2 (NO MASS TRANSFER OPTION)
C
  IF (IBKIN.EQ.2) GOTO 8
C
  DO 20 I = IBNONB,NBC
    AKMASS = COLSA(J)*BMTC(I)*CBF(J,J)*0.001/(COLMAS(J))
    DCF(I) = DCF(I)-AKMASS*(CF(I)-CBF(I,J))
    AKMASSB = COLSA(J)*BMTC(I)/(VCOL(J))
    DCBF(I,J) = DCBF(I,J)+AKMASSB*(CF(I)-CBF(I,J))
    RMTMAX = MAX(RMTMAX,DCBF(I,J))
19  CONTINUE
20  CONTINUE
C
C CALCULATE DECAY OF BOTH FREE-FLOATING AND ATTACHED
BIOMASS
C
  8  CONTINUE
    DCBF(J,J) = DCBF(J,J)-ENDOGB(J)*CBF(J,J)
  9  CONTINUE
    IF (CF(J).LE.ZERO) GOTO 10
    DCF(J) = DCF(J)-ENDOG(J)*CF(J)
10  CONTINUE
C
C
C BULK LIQUID BIODEGRADATION
C

```



```

C
C CALCULATE BIODEGRADATION TERMS FOR EACH COMBINATION OF
SUBSTRATE,
C ELECTRON ACCEPTOR, AND BIOLOGICAL SPECIES.
C
  DO 40 IMET=1,NMET
C -- ali --
C
  IF(TEM(IXYZ).GE.TLOB(IMET).AND.TEM(IXYZ).LE.TUPB(IMET)) THEN
    TFACTB=1
  ELSE
    TFACTB=0
  END If
C
  BRMX=BRMAX(IMET)*TFACTB
  BRMXB=BRMAXB(IMET)*TFACTB
CCCCC
C  BRMAX(IMET) ----- > BRMX
c  BRMAXB(IMET) ----- > BRMXB
C
C SKIP CALCULATION OF BULK PHASE BIODEGRADATION IF NO BULK
PHASE
C BIODEGRADATION OCCURS FOR THIS METABOLIC COMBINATION.
C
  IF (BRMX.LE.ZERO.OR.CF(IMBS(IMET)).LE.ZERO) GOTO 75
C
C THE BIOLOGICAL RATE CONSTANTS AND THE ELECTRON ACCEPTOR
HALF-
C SATURATION COEFFICIENTS MUST BE READ INTO VARIABLES HERE SO
THAT THEY
C DO NOT CHANGE WITH EACH LOOP SINCE THEY ARE MODIFIED BY
INHIBITION
C TERMS.
C
  RBIOM = BRMX
  AKSC = AKS(IMET)
C
C CALCULATE MODIFIED HALF-SATURATION CONSTANTS FOR EACH
COMBINATION OF
C SUBSTRATE, ELECTRON ACCEPTOR AND BIOLOGICAL SPECIES FOR
WHICH THERE
C IS SUBSTRATE COMPETITION.
C
  IF (NCOMPS(IMET).EQ.0) GOTO 65
  COMPKS = 0.
  DO 60 INUM = 1,NCOMPS(IMET)

```

```

        COMPKS = COMPKS+CF(ICSUB(IMET,INUM))/
&      AKS(IDMET(ICSUB(IMET,INUM),IMEA(IMET),IMBS(IMET)))
60  CONTINUE
    AKSC = AKSC*(1+COMPKS)
C
C  MODIFY MAXIMUM SUBSTRATE UTILIZATION RATE IF INHIBITED BY
THE
C  SUBSTRATE OR ELECTRON ACCEPTOR (BULK LIQUID PHASE).
C
65  IF (NIHB(IMET).EQ.0) GOTO 72
    DO 92 I = 1,NIHB(IMET)
        IF (CF(IHB(IMET,I)).LE.ZERO) GOTO 93
        RBIOM = RBIOM*BSIHB(IMET,I)/
&      (BSIHB(IMET,I)+CF(IHB(IMET,I)))
93  CONTINUE
92  CONTINUE
72  CONTINUE
C
C  MODIFY MAXIMUM SUBSTRATE UTILIZATION RATE IF LIMITED BY
C  NUTRIENTS
C
    IF (NNUT(IMET).EQ.0) GOTO 305
    DO 301 I = 1,NNUT(IMET)
        RBIOM = RBIOM*CF(INUT(IMET,I))/(AKN(IMET,I)+
+      CF(INUT(IMET,I)))
301  CONTINUE
305  CONTINUE
C
C  MODIFY MAXIMUM SUBSTRATE UTILIZATION RATE IF LIMITED BY
C  NADH
C
    IF (IRLIM(IMBS(IMET)).EQ.0) GOTO 320
        RBIOM = RBIOM*REDF(IMBS(IMET))/(AKR(IMBS(IMET))+
+      REDF(IMBS(IMET)))
320  CONTINUE
C
C  CALCULATE MONOD/INHIBITION PORTION OF KINETIC EXPRESSION
C
    RMONOD = RBIOM*CF(IMBS(IMET))*
+      CF(IMSUB(IMET))/(AKSC+CF(IMSUB(IMET)))*
+      CF(IMEA(IMET))/(AKA(IMET)+CF(IMEA(IMET)))
C
C  CALCULATE THE DERIVATIVES FOR THIS METABOLIC COMBINATION
C
    DCBIO = RMONOD/YXS(IMET)
    DCF(IMSUB(IMET)) = DCF(IMSUB(IMET))-DCBIO

```

```

      DCF(IMEA(IMET)) = DCF(IMEA(IMET))-DCBIO*FEA(IMET)
C
C SKIP BIOLOGICAL GROWTH IF THIS METABOLIC COMBINATION IS A
C COMETABOLISM REACTION.
C TAKE CARE OF THE SURFACTANT SOLUTION
      IF (ICOMET(IMET).EQ.1) GOTO 321
      DCF(IMBS(IMET)) = DCF(IMBS(IMET))+RMONOD
+    *(1-SBIOO(IXYZ)/(BVOLMX*STERM))
321  CONTINUE
C
C SUBTRACT BIOLOGICAL ACTIVITY LOST DUE TO COMETABOLIC
REACTIONS
C IF THIS METABOLIC COMBINATION IS A COMETABOLIC REACTION:
C
      IF (ICOMET(IMET).EQ.0) GOTO 340
      DCF(IMBS(IMET)) = DCF(IMBS(IMET))-(ONE/TC(IMET))*DCBIO
C
C CONSUME NADH IF THIS IS A COMETABOLIC REACTION AND NADH
LIMITATIONS
C ARE CONSIDERED:
C
      IF (IRLIM(IMBS(IMET)).EQ.0) GOTO 340
C LIMIT INTRACELLULAR NADH CONCENTRATION TO 0.01 INTIAL.
      IF (REDF(IMBS(IMET)).LE.0.000005) GOTO 340
      DREDF(IMBS(IMET)) = DREDF(IMBS(IMET))-FRC(IMET)*DCBIO
+    /CF(IMBS(IMET))
340  CONTINUE
C
C PRODUCE NADH IF THIS METABOLIC COMBINATION IS A GROWTH
SUBSTRATE FOR
C A COMETABOLIC REACTION AND NADH LIMITATIONS ARE
CONSIDERED:
C
C LIMIT INTRACELLULAR NADH CONCENTRATION TO 30% OF CELL BY
MASS.
      IF (REDF(IMBS(IMET)).GE.0.0029) GOTO 341
      IF (IGROW(IMET).EQ.IMSUB(IMET).AND.
+    IRLIM(IMBS(IMET)).EQ.1) THEN
      DREDF(IMBS(IMET)) = DREDF(IMBS(IMET))+FRP(IMET)*DCBIO
+    /CF(IMBS(IMET))
      ENDIF
341  CONTINUE
C
C PRODUCT GENERATION
C
      IF (NPROD(IMET).EQ.0) GOTO 311

```

```

        DO 73 I = 1,NPROD(IMET)
          DCF(IPR(IMET,I)) = DCF(IPR(IMET,I))+DCBIO*FP(IMET,I)
73    CONTINUE
C
C NUTRIENT CONSUMPTION
C
311  IF (NNUT(IMET).EQ.0) GOTO 75
      DO 312 I = 1,NNUT(IMET)
        DCF(INUT(IMET,I)) = DCF(INUT(IMET,I))-DCBIO*FN(IMET,I)
312  CONTINUE
C
C
C ATTACHED BIOMASS BIODEGRADATION WITH MASS TRANSFER
C
C
C SKIP CALCULATION OF BIOMASS PHASE BIODEGRADATION IF NO
C BIODEGRADATION OCCURS FOR THIS METABOLIC COMBINATION.
C
75    IF (BRMXB.LE.ZERO.OR.
      +   CBF(IMBS(IMET),IMBS(IMET)).LE.ZERO) GOTO 50
C
C SKIP CALCULATION OF BIOMASS PHASE BIODEGRADATION IF NO
C BIOFILM
C IS PRESENT AT THIS GRID NODE.
C
      IF (IBKIN.EQ.2) GOTO 1000
C
C THE BIOLOGICAL RATE CONSTANTS AND THE ELECTRON ACCEPTOR
C HALF-
C SATURATION COEFFICIENTS MUST BE READ INTO VARIABLES HERE SO
C THAT THEY
C DO NOT CHANGE WITH EACH LOOP SINCE THEY ARE MODIFIED BY
C INHIBITION
C TERMS.
C
      RBIOMB = BRMXB
      AKSC = AKS(IMET)
C
C CALCULATE MODIFIED HALF-SATURATION CONSTANTS FOR EACH
C COMBINATION OF
C SUBSTRATE, ELECTRON ACCEPTOR AND BIOLOGICAL SPECIES FOR
C WHICH THERE
C IS SUBSTRATE COMPETITION.
C
      IF (NCOMPS(IMET).EQ.0) GOTO 66
      COMPKS = 0.

```

```

DO 67 INUM = 1, NCOMPS(IMET)
  COMPKS = COMPKS + CBF(ICSUB(IMET, INUM), IMBS(IMET)) /
+   AKS(IDMET(ICSUB(IMET, INUM), IMEA(IMET), IMBS(IMET)))
67  CONTINUE
  AKSC = AKSC * (1 + COMPKS)
C
C  MODIFY MAXIMUM SUBSTRATE UTILIZATION RATE IF INHIBITED BY
THE
C  SUBSTRATE OR ELECTRON ACCEPTOR (BIOMASS PHASE).
C
66  IF (NIHB(IMET).EQ.0) GOTO 90
  DO 94 I = 1, NIHB(IMET)
  IF (CBF(IHB(IMET, I), IMBS(IMET))).LE.ZERO) GOTO 97
  RBIOMB = RBIOMB * BSIHB(IMET, I) /
+   (BSIHB(IMET, I) + CBF(IHB(IMET, I), IMBS(IMET)))
97  CONTINUE
94  CONTINUE
90  CONTINUE
C
C  MODIFY MAXIMUM SUBSTRATE UTILIZATION RATE IF INHIBITED BY
C  NUTRIENTS
C
  IF (NNUT(IMET).EQ.0) GOTO 310
  DO 309 I = 1, NNUT(IMET)
  IF (AKN(IMET, I).LE.ZERO) GOTO 308
  RBIOMB = RBIOMB * CBF(INUT(IMET, I), IMBS(IMET)) /
+   (AKN(IMET, I) + CBF(INUT(IMET, I), IMBS(IMET)))
308  CONTINUE
309  CONTINUE
310  CONTINUE
C
C  MODIFY MAXIMUM SUBSTRATE UTILIZATION RATE IF LIMITED BY
C  NADH
C
  IF (IRLIM(IMBS(IMET)).EQ.0) GOTO 330
  RBIOMB = RBIOMB * REDBF(IMBS(IMET), IMBS(IMET)) /
+   (AKR(IMBS(IMET)) + REDBF(IMBS(IMET), IMBS(IMET)))
330  CONTINUE
C
C  CALCULATE THE MONOD/INHIBITION PORTION OF THE KINETIC
EXPRESSION
C
  RMONOD = RBIOMB * CBF(IMSUB(IMET), IMBS(IMET)) /
+   (AKSC + CBF(IMSUB(IMET), IMBS(IMET))) *
+   CBF(IMEA(IMET), IMBS(IMET)) /
+   (AKA(IMET) + CBF(IMEA(IMET), IMBS(IMET)))

```

```

C
C CALCULATE THE DERIVATIVE TERM VALUES FOR THIS METABOLIC
COMBINATION
C
    DCBIOB = RMONOD*DENBIO(IMBS(IMET))/YXS(IMET)
    DCBF(IMSUB(IMET),IMBS(IMET)) =
+   DCBF(IMSUB(IMET),IMBS(IMET))-DCBIOB
    DCBF(IMEA(IMET),IMBS(IMET)) =
+   DCBF(IMEA(IMET),IMBS(IMET))-DCBIOB*FEA(IMET)
C
C SKIP BIOLOGICAL GROWTH IF THIS IS A COMETABOLIC REACTION.
C
    IF (ICOMET(IMET).EQ.1) GOTO 331
    DCBF(IMBS(IMET),IMBS(IMET)) = DCBF(IMBS(IMET),IMBS(IMET))+
+   RMONOD*CBF(IMBS(IMET),IMBS(IMET))
+   *(1-SBIOO(IXYZ)/(BVOLMX*STERM))
331  CONTINUE
C
C SUBTRACT BIOLOGICAL ACTIVITY LOST DUE TO COMETABOLIC
REACTIONS
C IF THIS METABOLIC COMBINATION IS A COMETABOLIC REACTION:
C
    IF (ICOMET(IMET).EQ.0) GOTO 350
    DCBF(IMBS(IMET),IMBS(IMET)) = DCBF(IMBS(IMET),IMBS(IMET))-
+   (ONE/TC(IMET))*RMONOD*CBF(IMBS(IMET),IMBS(IMET))/YXS(IMET)
C
C CONSUME NADH IF THIS IS A COMETABOLIC REACTION AND NADH
LIMITATIONS
C ARE CONSIDERED:
C
    IF (IRLIM(IMBS(IMET)).EQ.0) GOTO 350
C LIMIT INTRACELLULAR NADH CONCENTRATION TO 0.01 INTIAL.
    IF (REDBF(IMBS(IMET),IMBS(IMET)).LE.0.000005) GOTO 350
    DREDBF(IMBS(IMET),IMBS(IMET)) = DREDBF(IMBS(IMET),IMBS(IMET))-
+   FRC(IMET)*RMONOD/YXS(IMET)
350  CONTINUE
C
C PRODUCE NADH IF THIS METABOLIC COMBINATION IS A GROWTH
SUBSTRATE FOR
C A COMETABOLIC REACTION AND NADH LIMITATIONS ARE
CONSIDERED:
C
C LIMIT INTRACELLULAR NADH CONCENTRATION TO 30% OF CELL BY
MASS.
    IF (REDBF(IMBS(IMET),IMBS(IMET)).GE.0.0029) GOTO 351
    IF (IGROW(IMET).EQ.IMSUB(IMET).AND.

```

```

+   IRLIM(IMBS(IMET)).EQ.1) THEN
+     DREDBF(IMBS(IMET),IMBS(IMET)) =
+     DREDBF(IMBS(IMET),IMBS(IMET))+RMONOD*FRP(IMET)
+     /YXS(IMET)
  ENDIF
351 CONTINUE
C
C PRODUCT GENERATION
C
  IF (NPROD(IMET).EQ.0) GOTO 313
  DO 77 I = 1,NPROD(IMET)
    DCBF(IPR(IMET,I),IMBS(IMET)) = DCBF(IPR(IMET,I),IMBS(IMET))+
+    DCBIOB*FP(IMET,I)
77  CONTINUE
C
C NUTRIENT CONSUMPTION
C
313  IF (NNUT(IMET).EQ.0) GOTO 50
    DO 314 I = 1,NNUT(IMET)
      DCBF(INUT(IMET,I),IMBS(IMET)) =
+    DCBF(INUT(IMET,I),IMBS(IMET))-DCBIOB*FN(IMET,I)
314  CONTINUE
      GOTO 50
1000 CONTINUE
C
C
C ATTACHED BIOMASS BIODEGRADATION - NO MASS TRANSFER
C
C
C THIS SECTION FOR BIODEGRADATION BY ATTACHED BIOMASS WHEN
THERE IS
C NO MASS TRANSFER RESISTANCE
C
C THE BIOLOGICAL RATE CONSTANTS AND THE ELECTRON ACCEPTOR
HALF-
C SATURATION COEFFICIENTS MUST BE READ INTO VARIABLES HERE SO
THAT THEY
C DO NOT CHANGE WITH EACH LOOP SINCE THEY ARE MODIFIED BY
INHIBITION
C TERMS.
C
  RBIOMB = BRMXB
  AKSC = AKS(IMET)
C
C CALCULATE MODIFIED HALF-SATURATION CONSTANTS FOR EACH
COMBINATION OF

```

```

C SUBSTRATE, ELECTRON ACCEPTOR AND BIOLOGICAL SPECIES FOR
WHICH THERE
C IS SUBSTRATE COMPETITION.
C
  IF (NCOMPS(IMET).EQ.0) GOTO 1066
  COMPKS = 0.
  DO 1067 INUM = 1,NCOMPS(IMET)
    COMPKS = COMPKS+CF(ICSUB(IMET,INUM))/
    &   AKS(IDMET(ICSUB(IMET,INUM),IMEA(IMET),IMBS(IMET))))
1067  CONTINUE
    AKSC = AKSC*(1+COMPKS)
C
C MODIFY MAXIMUM SUBSTRATE UTILIZATION RATE IF INHIBITED BY
THE
C SUBSTRATE OR ELECTRON ACCEPTOR (BIOMASS PHASE).
C
1066  IF (NIHB(IMET).EQ.0) GOTO 1090
      DO 1094 I = 1,NIHB(IMET)
        IF (CF(IHB(IMET,I)).LE.ZERO) GOTO 1097
        RBIOMB = RBIOMB*BSIHB(IMET,I)/
        &   (BSIHB(IMET,I)+CF(IHB(IMET,I)))
1097  CONTINUE
1094  CONTINUE
1090  CONTINUE
C
C MODIFY MAXIMUM SUBSTRATE UTILIZATION RATE IF INHIBITED BY
C NUTRIENTS
C
  IF (NNUT(IMET).EQ.0) GOTO 1310
  DO 1309 I = 1,NNUT(IMET)
    RBIOMB = RBIOMB*CF(INUT(IMET,I))/(AKN(IMET,I)+
  +   CF(INUT(IMET,I)))
1309  CONTINUE
1310  CONTINUE
C
C MODIFY MAXIMUM SUBSTRATE UTILIZATION RATE IF LIMITED BY
C NADH
C
  IF (IRLIM(IMBS(IMET)).EQ.0) GOTO 1330
  RBIOMB = RBIOMB*REDBF(IMBS(IMET),IMBS(IMET))/
  +   (AKR(IMBS(IMET))+REDBF(IMBS(IMET),IMBS(IMET)))
1330  CONTINUE
C
C CALCULATE THE MONOD/INHIBITION PORTION OF THE KINETIC
EXPRESSION
C

```



```

    RMONOD = RBIOMB*CBF(IMBS(IMET),IMBS(IMET))*
+   C F(IMSUB(IMET))/(AKSC+CF(IMSUB(IMET)))*
&   CF(IMEA(IMET))/(AKA(IMET)+CF(IMEA(IMET)))
C
C CALCULATE THE DERIVATIVE TERM VALUES FOR THIS METABOLIC
COMBINATION
C
    DCBIOB = RMONOD/YXS(IMET)
    DCF(IMSUB(IMET)) = DCF(IMSUB(IMET))-DCBIOB
    DCF(IMEA(IMET)) = DCF(IMEA(IMET))-DCBIOB*FEA(IMET)
C
C SKIP BIOLOGICAL GROWTH IF THIS IS A COMETABOLIC REACTION.
C
    IF(ICOMET(IMET).EQ.1) GOTO 1331
    DCBF(IMBS(IMET),IMBS(IMET)) = DCBF(IMBS(IMET),IMBS(IMET))+
+   RMONOD
+   *(1-SBIOO(IXYZ)/(BVOLMX*STERM))
C
1331  CONTINUE
C
C SUBTRACT BIOLOGICAL ACTIVITY LOST DUE TO COMETABOLIC
REACTIONS
C IF THIS METABOLIC COMBINATION IS A COMETABOLIC REACTION:
C
    IF (ICOMET(IMET).EQ.0) GOTO 1350
    DCBF(IMBS(IMET),IMBS(IMET)) = DCBF(IMBS(IMET),IMBS(IMET))-
+   (ONE/TC(IMET))*DCBIOB
C
C CONSUME NADH IF THIS IS A COMETABOLIC REACTION AND NADH
LIMITATIONS
C ARE CONSIDERED:
C
    IF(IRLIM(IMBS(IMET)).EQ.0) GOTO 1350
C LIMIT INTRACELLULAR NADH CONCENTRATION TO 0.01 INITIAL.
    IF(REDBF(IMBS(IMET),IMBS(IMET)).LE.0.000005) GOTO 1350
    DREDBF(IMBS(IMET),IMBS(IMET)) =
+   DREDBF(IMBS(IMET),IMBS(IMET))-FRC(IMET)*DCBIOB
+   /CBF(IMBS(IMET),IMBS(IMET))
1350  CONTINUE
C
C PRODUCE NADH IF THIS METABOLIC COMBINATION IS A GROWTH
SUBSTRATE FOR
C A COMETABOLIC REACTION AND NADH LIMITATIONS ARE
CONSIDERED:
C

```

C LIMIT INTRACELLULAR NADH CONCENTRATION TO 30% OF CELL BY MASS.

```
      IF(REDBF(IMBS(IMET),IMBS(IMET)).GE.0.0029) GOTO 1351
      IF (IGROW(IMET).EQ.IMSUB(IMET).AND.
+   IRLIM(IMBS(IMET)).EQ.1) THEN
      DREDBF(IMBS(IMET),IMBS(IMET)) =
+   DREDBF(IMBS(IMET),IMBS(IMET))+FRP(IMET)*DCBIOB
+   /CBF(IMBS(IMET),IMBS(IMET))
      ENDIF
1351  CONTINUE
```

C
C PRODUCT GENERATION
C

```
      IF (NPROD(IMET).EQ.0) GOTO 1313
      DO 1077 I = 1,NPROD(IMET)
      DCF(IPR(IMET,I)) = DCF(IPR(IMET,I))+DCBIOB*FP(IMET,I)
1077  CONTINUE
```

C
C NUTRIENT CONSUMPTION
C

```
1313  IF (NNUT(IMET).EQ.0) GOTO 50
      DO 1314 I = 1,NNUT(IMET)
      DCF(INUT(IMET,I)) = DCF(INUT(IMET,I))-DCBIOB*FN(IMET,I)
1314  CONTINUE
```

C
C READ DERIVATIVE VALUES INTO YDOT AND RETURN TO SDRIV2
C

```
50    CONTINUE
40    CONTINUE
100   CONTINUE
```

C

```
      ICOUNT = 0
      DO 110 I = IBNONB,NBC
      ICOUNT = ICOUNT+1
      YDOT(ICOUNT) = DCF(I)
      IF(IBKIN.NE.1) GOTO 110
      DO 111 J = 1,NBS
      ICOUNT = ICOUNT+1
      YDOT(ICOUNT) = DCBF(I,J)
111   CONTINUE
110   CONTINUE
      DO 115 I = 1,NBS
      ICOUNT = ICOUNT+1
      YDOT(ICOUNT) = DCF(I)
      ICOUNT = ICOUNT+1
      YDOT(ICOUNT) = DCBF(I,I)
```

```
115 CONTINUE
    IF (IRLIMCOUNT.EQ.0) GOTO 117
    DO 116 I = 1,NBS
        IF(IRLIM(I).EQ.0) GOTO 116
        ICOUNT = ICOUNT+1
        YDOT(ICOUNT) = DREDF(I)
        ICOUNT = ICOUNT+1
        YDOT(ICOUNT) = DREDBF(I,I)
116 CONTINUE
117 CONTINUE
    RETURN
    END
```

APPENDIX C

Parameters used for simulation of the reservoir souring

The reservoir conditions and characteristics which are used in the simulations were adjusted to the published results from the corresponding models. However, for the sake of the similarity between the aqueous phase velocities, we defined different reservoir for mixing and biofilm models accordingly. For simulation of the TVS model the same reservoir size and conditions as for the mixing model was used.

Table C1 Reservoir conditions and characteristics

Model	Temp.(°F)	Press. (psi)	Porosity (%)	Perm.(md)	Length (ft)
Mixing	140	3771	30	250	4515
Biofilm	140	3771	30	5000	3700

Table C2 Injected seawater properties

Model	CH ₃ COOH(mg/l)	All other components	Injection rate (ft ³ /day)
Mixing	The same as original paper (Ligthelm et al., 1991)	The same as original paper (Ligthelm et al., 1991)	1000.0
Biofilm	10.00(mg/l)	The same as original paper (Sunde et al., 1993)	4250.0

Table C3 Retardation factor used in the models

Model	Adsorption		Partitioning	
	Original paper	UTCHEM	Original paper	UTCHEM
Mixing	0	0	3.5	3.5
Biofilm	Not specified	4.0	0	0
TVS	Not specified	0	Not specified	0

Table C4 Biological species used in UTCHEM model (Sunde et al., 1992).

Biological species	Initial temp. of activation (°F)	Temp. of max. activation(°F)	Upper limit temp. of activation(°F)
SRB-Mesophiles	50	95	109
SRB-Thermophiles	100	145	170
SRB-Hyperthermophiles	163	203	219

Mixing model (Ligthelm et al., 1991):

Table C5 Flow parameters

Pore velocity	4×10^{-6} m/s
Dispersivity	22 m
Residual oil saturation	28

Table C6 Data on bacterial reaction kinetics

Initial fatty acids concentration in formation water	0.02 kmole/m ³
Initial sulfate concentration in injected seawater	0.03 kmole/m ³
Time constant for bacteria growth rate	1-30 days
Partitioning, (mole conc. in oil phase)/(mole conc. in water phase)	20

Biofilm model (Sunde and Thorstenson, 1993):

Table C7 Initial concentration data

SRB in seawater	0.0001 (mg/l)
SO ₄	2700.0 (mg/l)
POC (part. Org. C)	0.01 (mg/l)
NO ₃	0.6 (mg/l)
PO ₄	0.06 (mg/l)
CH ₃ COOH in formation water	1000.0 (mg/l)
PO ₄	0.3 (mg/l)

Table C8 Reservoir characteristic data

Darcy velocity	1.6 (m/day)
Porosity	0.3
Length of reservoir	1125.0 (m)

Table C9 SRB/Nutrient data

Bacterial growth rate	1.0 (dbl/day)
K _C half saturation constant	0.01 (mg/l)
K _N half saturation constant	0.001 (mg/l)
K _P half saturation constant	0.0001 (mg/l)
K _{SO4} half saturation constant	0.01 (mg/l)

TVS model (Eden et al., 1993):

The slope of the middle line in the trilinear approximation of sulfate reduction is calculated using statistical techniques. The slope, β , is a function of pressure, P in atmosphere and temperature, T in °C as defined in the following equation:

$$\beta = 0.6134P - 10.67T_0 - 0.07048PT_0 + 1.476T_0^2 + 0.001015PT_0^2 - 0.0249T_0^3$$

where $\frac{T_0 - 20}{50 - 20} = \frac{T - T_L}{T_U - T_L}$

where β must be set to zero whenever the pressure is so large as to give a negative β or whenever T lies outside the region between T_L and T_U .

In this formulation β , T_L , and T_U stand for the rate of sulfate consumption, lower, and upper limits of temperature for the activation of SRB, respectively.

APPENDIX D

Table D1 Reservoir conditions and characteristics

T(°F)	P (psi)	ϕ (%)	ΔX (ft)	ΔY (ft)	ΔZ (ft)
86*	3771	33-34	8*54, 8*38.4, 8*56.5	82.02	4*3.25, 2*3.5, 2*3.0

* Injection water at 60°F

Table D2 Reservoir conditions and characteristics (continued)

α_l, α_v	K_x	K_y	K_z	Sor	Swr	Swi
(ft)	(mDarcy)	(mDarcy)	(mDarcy)			
0, 0	5600 - 11700	$K_y = K_x$	4200 - 9900	0.25	0.147	0.147

Table D3 Well constraints

Well 1, Injector	Well 2, Producer
4121	3771

Table D4 Thermal properties of rock and fluids in the reservoir (abbreviation is given below)

DENSE	CRTC	CVSPR	CVSPL(1)	CVSPL(2)	CVSPL(3)
165.43	40	0.2117	1	0.5	1
TCONO	DENO	CVSPO	TCONU	DENDU	CVSPU
35	165.43	0.2117	35	165.43	0.2117

DENS = Reservoir density (lb/ft³)

CRTC = Reservoir thermal conductivity (Btu (day-ft-°F)-1)

CVSPR = Reservoir rock heat capacity (Btu (lb-°F)-1)

CVSPL(L)= Phase L heat capacity (Btu (lb-°F)-1)

APPENDIX E

Parameters, run number and responses used in experimental design.

Table E1 The run number, parameters, and responses used in experimental design

Run #	Partitioning	Adsorption Coefficient	Temperature (°F)	Nutrients (mg/l)	H ₂ S in produced aqueous phase (mg/l)
1	3.5	1	155	0.6	2.4
2	3.5	2	110	0.3	1.1
3	3	2	200	0.3	0.01
4	4	0	200	0.3	0.035
5	4	1	200	0.9	0.01
6	4	2	110	0.9	2.7
7	4	0	155	0.9	22
8	3	2	110	0.9	3.05
9	3	0	200	0.3	0.042
10	3	2	200	0.6	0.01
11	3	0	200	0.9	0.042
12	4	2	110	0.3	1.05
13	3	2	200	0.6	0.01
14	3.5	0	110	0.9	25
15	3.5	2	200	0.9	0.01
16	4	2	200	0.3	0.01
17	3	2	155	0.3	1.22
18	3	2	110	0.3	1.22
19	4	0	110	0.3	8.7
20	3.5	1	155	0.6	2.4
21	3	0	110	0.3	10.7
22	3	0	200	0.9	0.042
23	3	1	200	0.3	0.01
24	3	2	110	0.9	3
25	3.5	2	200	0.9	0.01

APPENDIX F

UTCHEM input files for field case 1 and 2.

Field case 1:

```
CC*****
CC
CC BRIEF DESCRIPTION OF DATA SET : UTCHEM (VERSION 10.0)
CC
CC*****
CC WATER FLOODING
CC
CC LENGTH (FT) : 2740 PROCESS : WATER FLOODING
CC THICKNESS (FT) : 26. INJ. PRESSURE (PSI) : 4121
CC WIDTH (FT) : 100. COORDINATES : CARTESIAN
CC POROSITY : 0.33 TEMP. VARI. NON ISOTHERMAL
CC GRID BLOCKS : 26x1x8
CC DATE : 06/13/2000
CC
CC*****
CC
CC*****
CC RESERVOIR DESCRIPTION
CC
CC*****
CC
CC
*----RUNNO
UTEX10
CC
CC
*----HEADER
EXf1
Field case 1
NONISOTHERMAL SIMULATION, UTCHEM VERSION 10.0
CC
CC SIMULATION FLAGS
*---- IMODE IMES IDISPC ICWM ICAP IREACT IBIO ICOORD ITREAC ITC IGAS
IENG IDUAL ITENS
      1 1 3 0 0 0 1 1 0 0 0 1
0 0
CC
CC NUMBER OF GRID BLOCKS AND FLAG SPECIFIES CONSTANT OR VARIABLE GRID
SIZE
*----NX NY NZ IDXYZ IUNIT
      30 10 10 2 0
CC
CC VARIABLE GRID BLOCK SIZE IN X
*----DX(I)
      30*20
CC
CC CONSTANT GRID BLOCK SIZE IN Y
```

```

*----DY
      10*30
CC
CC VARIABLE GRID BLOCK SIZE IN Y
*----DZ
      8 15 27 14 20 5 9 10 14 12
CC
CC TOTAL NO. OF COMPONENTS, NO. OF TRACERS, NO. OF GEL COMPONENTS
*----N  NO  NTW  NTA  NGC  NG  NOTH
      16  0   1   0   0   0   7
CC
CC
*--- SPNAME(I),I=1,N
WATER
OIL
SURF.
POLYMER
CHLORIDE
CALCIUM
ALCOHOL1
ALCOHOL2
H2S
CH3COOH
SO4
SRB
CO2
NO3
PO4
TRacer
CC
CC FLAG INDICATING IF THE COMPONENT IS INCLUDED IN CALCULATIONS OR NOT
*----ICF(KC) FOR KC=1,N
      1 1 0 0 0 0 0 0 1 1 1 1 1 1 1 1
CC
CC*****
CC
CC OUTPUT OPTIONS
CC
CC*****
CC
CC
CC FLAG TO WRITE TO SUMMARY, FLAG FOR PV OR DAYS FOR OUTPUT AND STOP THE
RUN
*----ICUMTM  ISTOP  IOUTGMS
      0         0     0
CC
CC FLAG INDICATING IF THE PROFILE OF KCTH COMPONENT SHOULD BE WRITTEN
*----IPRFLG(KC),KC=1,N
      1 1 0 0 0 0 0 0 1 1 1 1 1 1 1 1
CC
CC FLAG FOR PRES,SAT.,TOTAL CONC.,TRACER CONC.,CAP.,GEL, ALKALINE
PROFILES
*----IPPRES IPSAT IPCTOT IPBIO IPCAP IPGEL IPALK ITEMP IPOBS
      1     1     1     1     0     0     0     1     0
CC
CC FLAG FOR WRITING SEVERAL PROPERTIES
*---ICKL  IVIS  IPER  ICNM  ICSE  IFOAM  IHYST  INONEQ

```

```

      1      1      1      0      0      0      0      0
CC
CC FLAG FOR WRITING SEVERAL PROPERTIES TO PROF)
*---IADS  IVEL  IRKF  IPHSE
      0      1      0      0
CC
CC*****
CC
CC      RESERVOIR PROPERTIES
CC
CC*****
CC
CC
CC MAX. SIMULATION TIME ( PV)
*---- TMAX
      10000
CC
CC ROCK COMPRESSIBILITY (1/PSI), STAND. PRESSURE(PSIA)
*----COMPR  PSTAND
      5.2e-6      2842
CC
CC FLAGS INDICATING CONSTANT OR VARIABLE POROSITY, X,Y,AND Z
PERMEABILITY
*----IPOR1  IPERMX  IPERMY  IPERMZ  IMOD
      1      1      3      3      0
CC
CC      constant porosity for whole reservoir
*----PORC1
      0.25      0.28      0.3      0.32      0.20      0.23      0.26      0.29      0.25      0.25
CC
CC constant X-PERMEABILITY (MILIDARCY) for whole reservoir
*----PERMX
      300  250  150  200  100  85  125  200  300  100
CC
CC constant Y-PERMEABILITY (MILIDARCY) FOR whole reservoir
*----Facy
      1
CC
CC constant Z-PERMEABILITY (MILIDARCY) for whole reservoir
*----Factz
      0.2
CC
CC FLAG FOR CONSTANT OR VARIABLE DEPTH, PRESSURE, WATER SATURATION
*----IDEPH  IPRESS  ISWI  ICWI
      0      0      0      -1
CC
CC VARIABLE DEPTH (FT)
*----D111
      6200
CC
CC CONSTANT PRESSURE (PSIA)
*----PRESS1
      3771.
CC
CC CONSTANT INITIAL WATER SATURATION
*----SWI
      0.3

```

```

CC
CC CONSTANT CHLORIDE AND CALCIUM CONCENTRATIONS (MEQ/ML)
*----C50      C60
      0.627      .133
CC
CC*****
CC
CC      PHYSICAL PROPERTY DATA
CC
CC*****
CC
CC OIL CONC. AT PLAIT POINT FOR TYPE II(+)AND TYPE II(-), CMC
*---- C2PLC   C2PRC   EPSME   IHAND
      0.       1.       .0001   0
CC
CC FLAG INDICATING TYPE OF PHASE BEHAVIOR PARAMETERS
*---- IFGHBN
      0
CC SLOPE AND INTERCEPT OF BINODAL CURVE AT ZERO, OPT., AND 2XOPT
SALINITY
CC FOR ALCOHOL 1
*----HBNS70 HBNC70 HBNS71 HBNC71 HBNS72 HBNC72
      0.       .030    0.       .030    0.0     .030
CC
CC SLOPE OF BINODAL WITH TEMP., SLOPE OF SALINITY WITH TEMP. (1/F)
*---- HBNT0     HBNT1     HBNT2     CSET(0.00415)
      0.00017  0.00017  0.00017  0.00415
CC SLOPE AND INTERCEPT OF BINODAL CURVE AT ZERO, OPT., AND 2XOPT
SALINITY
CC FOR ALCOHOL 2
*----HBNS80 HBNC80 HBNS81 HBNC81 HBNS82 HBNC82
      0.       0.       0.       0.       0.       0.
CC
CC LOWER AND UPPER EFFECTIVE SALINITY FOR ALCOHOL 1 AND ALCOHOL 2
*----CSEL7  CSEU7  CSEL8  CSEU8
      .65   .9    0.     0.
CC
CC THE CSE SLOPE PARAMETER FOR CALCIUM AND ALCOHOL 1 AND ALCOHOL 2
*----BETA6  BETA7  BETA8
      0.0   0.    0.
CC
CC FLAG FOR ALCOHOL PART. MODEL AND PARTITION COEFFICIENTS
*----IALC  OPSK70  OPSK7S  OPSK80  OPSK8S
      0     0.     0.     0.     0.
CC
CC NO. OF ITERATIONS, AND TOLERANCE
*----NALMAX  EPSALC
      20     .0001
CC
CC ALCOHOL 1 PARTITIONING PARAMETERS IF IALC=1
*----AKWC7  AKWS7  AKM7  AK7     PT7
      4.671  1.79  48.  35.31  .222
CC
CC ALCOHOL 2 PARTITIONING PARAMETERS IF IALC=1
*----AKWC8  AKWS8  AKM8  AK8     PT8
      0.     0.     0.     0.     0.

```

```

CC
CC
*--- IFT MODEL FLAG
    0
CC
CC INTERFACIAL TENSION PARAMETERS
*----G11  G12    G13   G21   G22   G23
      13.  -14.8   .007  13.2   -14.5  .010
CC
CC LOG10 OF OIL/WATER INTERFACIAL TENSION
*----XIFTW
      1.477
CC
CC FLAG TO ALLOW SOLUBILITY OF OIL IN WATER
*---- IMASS  ICOR
      0      0
CC
CC CAPILLARY DESATURATION PARAMETERS FOR PHASE 1, 2, AND 3
*----ITRAP  T11      T22      T33
      0      1865.    28665.46   364.2
CC
CC FLAG FOR DIRECTION OF REL. PERM. AND PC CURVES, HYSTERESIS
*---- IPERM
      0
CC
CC FLAG FOR CONSTANT OR VARIABLE REL. PERM. PARAMETERS
*----ISRW  IPRW  IEW
      0      0      0
CC
CC CONSTANT RES. SATURATION OF PHASES 1,2,AND 3 AT LOW CAPILLARY NO.
*----S1RWC  S2RWC  S3RWC
      0.147   0.28   0.147
CC
CC CONSTANT ENDPOINT REL. PERM. OF PHASES 1,2,AND 3 AT LOW CAPILLARY
NO.
*----P1RW   P2RW   P3RW
      0.13771  0.9148  .13771
CC
CC CONSTANT REL. PERM. EXPONENT OF PHASES 1,2,AND 3 AT LOW CAPILLARY
NO.
*----E1W    E2W    E3W
      2.1817   1.40475  2.1817
CC
CC WATER AND OIL VISCOSITY , VIS. AT REF.TEMPERATURE
*----VIS1  VIS2  TSTAND
      0.42   1.25  122.0
CC
CC VISCOSITY-TEMP PARAMETERS
*----BVI(1)  BVI(2)
      0.0     0.0
CC
CC VISCOSITY PARAMETERS
*----ALPHA1 ALPHA2  ALPHA3  ALPHA4  ALPHA5
      0.0     0.0     0.0     0.000865  4.153
CC
CC PARAMETERS TO CALCULATE POLYMER VISCOSITY AT ZERO SHEAR RATE
*----AP1     AP2     AP3

```

```

73.0      1006.0   10809.31
CC
CC PARAMETER TO COMPUTE CSEP,MIN. CSEP, AND SLOPE OF LOG VIS. VS. LOG
CSEP
*----BETAP CSE1  SSLOPE
      2.      .01   .0
CC
CC PARAMETER FOR SHEAR RATE DEPENDENCE OF POLYMER VISCOSITY
*----GAMMAC  GAMHF  POWN
      10.0     187.985   1.8429
CC
CC FLAG FOR POLYMER PARTITIONING, PERM. REDUCTION PARAMETERS
*----IPOLYM EPHI3 EPHI4 BRK   CRK
      1       1.     0.9   1000.  0.0186
CC
CC SPECIFIC WEIGHT FOR COMPONENTS 1,2,3,7,AND 8 , AND GRAVITY FLAG
*----DEN1     DEN2     den23     DEN3     DEN7 DEN8 IDEN
      .4368   .3462333  0.3462333 .433333  .346  0.  2
CC
CC FLAG FOR CHOICE OF UNITS ( 0:BOTTOMHOLE CONDITION , 1: STOCK TANK)
*-----ISTB
      0
CC
CC COMPRESSIBILITY FOR VOL. OCCUPYING COMPONENTS 1,2,3,7,AND 8
*----COMPC(1)  COMPC(2)  COMPC(3)  COMPC(7)  COMPC(8)
      3E-6     5.65E-6     0         0         0
CC
CC CONSTANT OR VARIABLE PC PARAM., WATER-WET OR OIL-WET PC CURVE FLAG
*----ICPC  IEPC  IOW
      0       0   0
CC
CC CAPILLARY PRESSURE PARAMETERS, CPC
*----CPC
      9.
CC
CC CAPILLARY PRESSURE PARAMETERS, EPC
*---- EPC
      2.
CC
CC MOLECULAR DIFFUSIVITY OF KCTH COMPONENT IN PHASE 1 (D(KC),KC=1,N)
*----D(1) D(2)
      0.     0.  0.  0.  0.  0.  0.  0.  0.  .00000066 .00000066 .00000066 .00000066
      .00000066 .00000066 .00000066 0.00000066
CC
CC MOLECULAR DIFFUSIVITY OF KCTH COMPONENT IN PHASE 2 (D(KC),KC=1,N)
*----D(1) D(2)
      0.     0.  0.  0.  0.  0.  0.  0.  0.  .00000066 .00000066 .00000066 .00000066
      .00000066 .00000066 .00000066 0.00000066
CC
CC MOLECULAR DIFFUSIVITY OF KCTH COMPONENT IN PHASE 3 (D(KC),KC=1,N)
*----D(1) D(2)
      0.     0.  0.  0.  0.  0.  0.  0.  0.  .00000066 .00000066 .00000066 .00000066
      .00000066 .00000066 .00000066 0.00000066
CC
CC LONGITUDINAL AND TRANSVERSE DISPERSIVITY OF PHASE 1
*----ALPHAL(1)      ALPHAT(1)
      0.0           0.0

```

```

CC
CC LONGITUDINAL AND TRANSVERSE DISPERSIVITY OF PHASE 2
*----ALPHAL(2)      ALPHAT(2)
      0.0           0.0
CC
CC LONGITUDINAL AND TRANSVERSE DISPERSIVITY OF PHASE 3
*----ALPHAL(3)      ALPHAT(3)
      0.0           0.0
CC
CC FLAG TO SPECIFY ORGANIC ADSORPTION CALCULATION
*----IADSO
      0
CC
CC SURFACTANT AND POLYMER ADSORPTION PARAMETERS
*----AD31  AD32  B3D   AD41  AD42  B4D  IADK, IADS1, FADS  refk
      2.2    .0 1000.  1.1   0.   100.   0     0     0   0
CC
CC PARAMETERS FOR CATION EXCHANGE OF CLAY AND SURFACTANT
*----QV      XKC   XKS   EQW
      0       0.   0.   804
CC
CC TRACER PARTITIONING COEFFICIENT
*---- TK(I)   , I=1,NTW+NTA
      3.5
CC
CC TRACER PARTITIONING COEFFICIENT SALINITY PARAMETER (1/MEQ/ML)
*---- TKS(I)   ,I=1 TO NTW   C5INI
      0         0
CC
CC TRACER PARTITIONING COEFFICIENT TEMP. DEPENDENT (1/F)
*----  TKT(I)   , I=1 TO NTW+NTA
      0
CC
CC RADIOACTIVE DECAY COEFFICIENT
*---- RDC(I)   , I=1, NTW+NTA
      0
CC
CC TRACER ADSORPTION PARAMETER
*----  RET(I)   , I=1, NTW+NTA
      0.01
CC
CC INITIAL TEMPERATURE
*---- TEMPI (F)
      160.0
CC
CC ROCK DENSITY, CONDUCTIVITY, HEAT CAPACITY
*---- DENS      CRTC  CVSPR  CVSPL(1)  CVSPL(2)  CVSPL(3)
      165.43    40.001  0.2117  1.000454  0.5000227  1.000454
CC
CC HEAT LOSS FLAG, ANALYTICAL SOLUTION
*---- IHLOS  IANAL
      0       0
CC
CC*****
CC
CC          BIOLOGICAL DATA
CC

```

```

CC*****
CC
CC
CC   BULK DENSITY
*---- DENBLK
      1.64
CC
CC MINIMUM CONCENTRATIONS, CONVERGENCE TOLERANCE, TYPE FOR TIME STEP
CONTROL
*---- CMIN      EPSBIO      IBTMIN      BVOLMAX
      0.001      0.00001      0          10
CC
CC CHEMICAL AND BIOLOGICAL, METABOLIC COMBINATIONS, FLAGS FOR
BIODEGRADATION KINETICS, POROSITY AND PERMEABILITY
*---- NBC      NMET      IBKIN      IBPP      ibtem
      8         1         2         0         1
CC
CC
*---- TLOB      TMXB      TUPB
      100       145       170
CC
CC INITIAL AQUEOUS PHASE CONCENTRATIONS
*---- KC(I)      ITYPE(I)      CINIT(I)      RABIO(I)      NPABIO(I)
      9          1          0.          0.          0.
      10         1          1000.       0.          0.
      11         1          0.          0.          0.
      12         2          0.          0.          0.
      13         1          0.          0.          0.
      14         1          0.          0.          0.
      15         1          0.3         0.          0.
      16         1          0.          0.          0.
CC
CC BIOLOGICAL SPECIES PARAMETERS
*---- KC(I)      DENBIO(I)      RCOL(I)      TCOL(I)      COLNUM(I)      EDDOG(I)
EDDOGB(I) CBI(I) CBIOMN(I) ADSBIO(I)
      12         1          0.000615    0.000084    100          0
0          1000000    1000000    0
CC
CC METABOLIC COMBINATION INFORMATION
*---- ISUB(I)   IEA(I)   IBS(I)   BRMAX(I)   BRMAXB(I)   YXS(I)   AKS(I)
AKA(I) FEA(I)
      10        11        12        0.693     0          0.05    0.01
0.01    1.6
CC
CC COMPETITION, INHIBITION, PRODUCT GEN., NUTRIENT LIM., COMETEBOLISM
INFORMATION
*---- ISUB(I)   IEA(I)   IBS(I)   NCOMPS(I)   NIHB(I)   NPROD(I)
NNUT(I) ICOMET(I)
      10        11        12        0          0          2          2
0
CC
CC PRODUCT GENERATION BY METABOLIC COMBINATION I
*---- ISUB(I)   IEA(I)   IBS(I)   IPR(I)   FPR(I)
      10        11        12        9        0.57
      10        11        12        13       0.73
CC
CC   Nutrient effects

```



```

    1      0.      0.  0.  0.  0.  0.  0.  0.  0.  0.  0.  0.  0.  0.
0.  0.  1800
    1      0.      0.  0.  0.  0.  0.  0.  0.  0.  0.  0.  0.  0.  0.
0.  0.  1800
CC
CC
*---- ID, INJ. TEMP (F)
    1      60.0
CC
CC ID, BOTTOM HOLE PRESSURE FOR PRESSURE CONSTRAINT WELL (IFLAG=2 OR 3)
*-----ID   PWF
    2      3771.0
CC
CC CUM. INJ. TIME , AND INTERVALS (PV OR DAY) FOR WRITING TO OUTPUT
FILES
*-----TINJ   CUMPR1   CUMHI1   WRHPV   WRPRF   RSTC
    10000     30       30       30       30       30
CC
CC FOR IMES=2 ,THE INI. TIME STEP,CONC. TOLERANCE,MAX.,MIN. TIME STEPS
*-----DT     DCLIM     DTMAX     DTMIN
    1

```

ÿÿ

Field case 2:

```

CC*****
CC
CC   BRIEF DESCRIPTION OF DATA SET : UTCHEM (VERSION 10.0)
CC
CC*****
CC
CC   WATERFLOOD (PILOTW), 19X19X3
CC
CC   PROCESS : WATERFLOODING
CC
CC   COORDINATES : CARTESIAN
CC
CC   GRID BLOCKS : 19X19X3
CC   DATE : 06/16/2000
CC
CC*****
CC
CC*****
CC
CC   PART1 : RESERVOIR DESCRIPTION
CC
CC*****
CC
CC
*----RUN
utex08
CC
CC
*----HEADER
utex08
3-d WATERFLOOD TEST for UTCHEM 10.0
stochastic permeability and porosity
CC
CC SIMULATION FLAGS
*---- IMODE IMES IDISPC ICWM ICAP IREACT ibio ICOORD ITREAC ITC IGAS
IENG idual itens
      1   1   1   0   0   0   1   1   0   0   0
1     0   0
CC
CC NUMBER OF GRID BLOCKS AND FLAG SPECIFIES CONSTANT OR VARIABLE GRID
SIZE
*----NX   NY   NZ   IDXYZ   IUNIT
      19   19   3   2       0
CC
CC   CONSTANT GRID BLOCK SIZE IN X--DIRECTION (FT)
*----DX(I), I=1,NX
      32.8 32.8 32.8 32.8 32.8 32.8 32.8 32.8 32.8 32.8 32.8 32.8 32.8
32.8 32.8 32.8 32.8 32.8 32.8
CC
CC   CONSTANT GRID BLOCK SIZE IN Y--DIRECTION (FT)
*----DY(J), J=1,NY
      32.8 32.8 32.8 32.8 32.8 32.8 32.8 32.8 32.8 32.8 32.8 32.8
32.8 32.8 32.8 32.8 32.8 32.8
CC

```

```

CC VARIABLE GRID BLOCK SIZE IN Z--DIRECTION (FT)
*----DZ(K), K=1,NZ
      10.  20.  10.
CC
CC TOTAL NO. OF COMPONENTS, NO. OF TRACERS,NO. OF GEL COMPONENTS
*----N   no   NTW  NTA  ngc  NG  noth
      16   0   1   0   0   0   7
CC
CC
*--- SPNAME(I), I=1,N
WATER
OIL
SURF.
POLYMER
CHLORIDE
CALCIUM
ALCOHOL1
ALCOHOL2
H2S
CH3COOH
SO4
SRB
CO2
NO3
PO4
TRacer
CC
CC FLAG INDICATING IF THE COMPONENT IS INCLUDED IN CALCULATIONS OR NOT
*----ICF(KC) FOR KC=1,N
      1  1  0  0  0  0  0  0  1  1  1  1  1  1  1  1
CC
CC*****
CC
CC   PART2 : OUTPUT OPTIONS
CC
CC*****
CC
CC
CC FLAG FOR PV OR DAYS
*----ICUMTM  ISTOP  IOUTGMS
      0      0      0
CC
CC FLAG INDICATING IF THE PROFILE OF KCTH COMPONENT SHOULD BE WRITTEN
*----IPRFLG(KC),KC=1,N
      1  1  0  0  0  0  0  0  1  1  1  1  1  1  1  1
CC
CC FLAG FOR PRES,SAT.,TOTAL CONC.,TRACER CONC.,CAP.,GEL, ALKALINE
PROFILES
*----IPPRES  IPSAT  IPCTOT  IPBIO  IPCAP  IPGEL  IPALK  IPTEMP  IPOBS
      1      1      1      1      0      0      0      1      0
CC
CC FLAG FOR WRITING SEVERAL PROPERTIES
*----ICKL  IVIS  IPER  ICNM  ICSE  IFOAM  IHYST  INONEQ
      1      1      1      0      0      0      0      0
CC
CC FLAG FOR WRITING SEVERAL PROPERTIES TO PROF
*----IADS  IVEL  IRKF  IPHSE

```

```

      0      1      0      0
CC
CC*****
CC
CC      PART3 : RESERVOIR PROPERTIES
CC
CC*****

```

As reflected in Tables 7.3a-e

```

CC*****
CC
CC      PART4 : PHYSICAL PROPERTY DATA
CC
CC*****

```

The same as case 1.

```

CC*****
CC
CC      BIOLOGICAL DATA
CC
CC*****

```

The same as case 2.

```

CC
CC*****
CC
CC      PART5 : WELL DATA
CC
CC*****
CC
CC      FLAG FOR WELL
CC      IBOUNDARY      IZONE
      0              0
CC
CC TOTAL NUMBER OF WELLS, WELL RADIUS FLAG, FLAG FOR TIME OR COURANT
NO.
*----NWELL      IRO      ITIME      nwrel
      13          2          0          13
CC
CC WELL ID,LOCATIONS,AND FLAG FOR SPECIFYING WELL TYPE, WELL RADIUS,
SKIN
*----IDW      IW      JW      IFLAG      RW      SWELL      IDIR      IFIRST      ILAST
IPRF
      1      17      3          4          .49      0.          3          1          3          0
CC
CC WELL NAME
*---- WELNAM
A1
CC
CC MAX. AND MIN. ALLOWABLE BOTTOMHOLE PRESSURE AND RATE
*----ICHEK      PWFMIN      PWFMAX      QTMIN      QTMAX
      0          0.0      3700.      0.0      7100.

```

```

CC
CC WELL ID,LOCATIONS,AND FLAG FOR SPECIFYING WELL TYPE, WELL RADIUS,
SKIN
*----IDW   IW     JW     IFLAG   RW     SWELL  IDIR   IFIRST  ILAST
IPRF
      2     10     3       4       .49   0.     3       1       3       0
CC
CC WELL NAME
*---- WELNAM
A2
CC
CC MAX. AND MIN. ALLOWABLE BOTTOMHOLE PRESSURE AND RATE
*----ICHEK PWFMIN  PWFMAX  QTMIN  QTMAX
      0       0.0    3700.   0.0    7100.
CC
CC WELL ID,LOCATIONS,AND FLAG FOR SPECIFYING WELL TYPE, WELL RADIUS,
SKIN
*----IDW   IW     JW     IFLAG   RW     SWELL  IDIR   IFIRST  ILAST  IPRF
      3     14     7       1       .49   0.     3       1       3       0
CC
CC WELL NAME
*---- WELNAM
A3
CC
CC MAX. AND MIN. ALLOWABLE BOTTOMHOLE PRESSURE AND RATE
*----ICHEK PWFMIN  PWFMAX  QTMIN  QTMAX
      0       0.0    3700.   0.0    7100.
CC
CC WELL ID,LOCATIONS,AND FLAG FOR SPECIFYING WELL TYPE, WELL RADIUS,
SKIN
*----IDW   IW     JW     IFLAG   RW     SWELL  IDIR   IFIRST  ILAST  IPRF
      4     18     11      4       .49   0.     3       1       3       0
CC
CC WELL NAME
*---- WELNAM
A4
CC
CC MAX. AND MIN. ALLOWABLE BOTTOMHOLE PRESSURE AND RATE
*----ICHEK PWFMIN  PWFMAX  QTMIN  QTMAX
      0       0.0    3700.   0.0    7100.
CC
CC WELL ID,LOCATIONS,AND FLAG FOR SPECIFYING WELL TYPE, WELL RADIUS,
SKIN
*----IDW   IW     JW     IFLAG   RW     SWELL  IDIR   IFIRST  ILAST  IPRF
      5     3      3       4       .49   0.     3       1       3       0
CC
CC WELL NAME
*---- WELNAM
A5
CC
CC MAX. AND MIN. ALLOWABLE BOTTOMHOLE PRESSURE AND RATE
*----ICHEK PWFMIN  PWFMAX  QTMIN  QTMAX
      0       0.0    3700.   0.0    7100.
CC
CC WELL ID,LOCATIONS,AND FLAG FOR SPECIFYING WELL TYPE, WELL RADIUS,
SKIN

```

```

*-----IDW   IW     JW     IFLAG   RW   SWELL  IDIR   IFIRST  ILAST  IPRF
      6     7     7       1     .49   0.     3     1     3     0
CC
CC WELL NAME
*----- WELNAM
A6
CC
CC MAX. AND MIN. ALLOWABLE BOTTOMHOLE PRESSURE AND RATE
*-----ICHEK PWFMIN   PWFMAX  QTMIN   QTMAX
      0       0.0    3700.   0.0    7100.
CC
CC WELL ID,LOCATIONS,AND FLAG FOR SPECIFYING WELL TYPE, WELL RADIUS,
SKIN
*-----IDW   IW     JW     IFLAG   RW   SWELL  IDIR   IFIRST  ILAST  IPRF
      7     10    10     4     .49   0.     3     1     3     0
CC
CC WELL NAME
*----- WELNAM
A7
CC
CC MAX. AND MIN. ALLOWABLE BOTTOMHOLE PRESSURE AND RATE
*-----ICHEK PWFMIN   PWFMAX  QTMIN   QTMAX
      0       0.0    3700.   0.0    7100.
CC
CC WELL ID,LOCATIONS,AND FLAG FOR SPECIFYING WELL TYPE, WELL RADIUS,
SKIN
*-----IDW   IW     JW     IFLAG   RW   SWELL  IDIR   IFIRST  ILAST  IPRF
      8     14    14     1     .49   0.     3     1     3     0
CC
CC WELL NAME
*----- WELNAM
A8
CC
CC MAX. AND MIN. ALLOWABLE BOTTOMHOLE PRESSURE AND RATE
*-----ICHEK PWFMIN   PWFMAX  QTMIN   QTMAX
      0       0.0    3700.   0.0    7100.
CC
CC WELL ID,LOCATIONS,AND FLAG FOR SPECIFYING WELL TYPE, WELL RADIUS,
SKIN
*-----IDW   IW     JW     IFLAG   RW   SWELL  IDIR   IFIRST  ILAST
IPRF
      9     16    18     2     .49   0.     3     1     3     0
CC
CC WELL NAME
*----- WELNAM
A9
CC
CC MAX. AND MIN. ALLOWABLE BOTTOMHOLE PRESSURE AND RATE
*-----ICHEK PWFMIN   PWFMAX  QTMIN   QTMAX
      0       0.0    3700.   0.0    7100.
CC
CC WELL ID,LOCATIONS,AND FLAG FOR SPECIFYING WELL TYPE, WELL RADIUS,
SKIN
*-----IDW   IW     JW     IFLAG   RW   SWELL  IDIR   IFIRST  ILAST  IPRF
      10    2     11     4     .49   0.     3     1     3     0
CC
CC WELL NAME

```

```

*----- WELNAM
A10
CC
CC MAX. AND MIN. ALLOWABLE BOTTOMHOLE PRESSURE AND RATE
*-----ICHEK  PWFMIN  PWFMAX  QTMIN  QTMAX
           0         0.0    3700.   0.0    7100.
CC
CC WELL ID,LOCATIONS,AND FLAG FOR SPECIFYING WELL TYPE, WELL RADIUS,
SKIN
*-----IDW   IW      JW      IFLAG   RW    SWELL  IDIR   IFIRST  ILAST  IPRF
           11     7      14      1      .49   0.     3     1      3     0
CC
CC WELL NAME
*----- WELNAM
A11
CC
CC MAX. AND MIN. ALLOWABLE BOTTOMHOLE PRESSURE AND RATE
*-----ICHEK  PWFMIN  PWFMAX  QTMIN  QTMAX
           0         0.0    3700.   0.0    7100.
CC
CC WELL ID,LOCATIONS,AND FLAG FOR SPECIFYING WELL TYPE, WELL RADIUS,
SKIN
*-----IDW   IW      JW      IFLAG   RW    SWELL  IDIR   IFIRST  ILAST
IPRF
           12     9      17      4      .49   0.     3     1      3     0
CC
CC WELL NAME
*----- WELNAM
A12
CC
CC MAX. AND MIN. ALLOWABLE BOTTOMHOLE PRESSURE AND RATE
*-----ICHEK  PWFMIN  PWFMAX  QTMIN  QTMAX
           0         0.0    3700.   0.0    7100.
CC
CC WELL ID,LOCATIONS,AND FLAG FOR SPECIFYING WELL TYPE, WELL RADIUS,
SKIN
*-----IDW   IW      JW      IFLAG   RW    SWELL  IDIR   IFIRST  ILAST  IPRF
           13     3      17      4      .49   0.     3     1      3     0
CC
CC WELL NAME
*----- WELNAM
A13
CC
CC MAX. AND MIN. ALLOWABLE BOTTOMHOLE PRESSURE AND RATE
*-----ICHEK  PWFMIN  PWFMAX  QTMIN  QTMAX
           0         0.0    3700.   0.0    7100.
CC
CC ID, PRODUCING RATE FOR RATE CONSTRAINT WELL (IFLAG=4)
*-----ID   QT
           1  -679.19
CC
CC ID, PRODUCING RATE FOR RATE CONSTRAINT WELL (IFLAG=4)
*-----ID   QT
           2  -803.88
CC
CC ID,INJ. RATE AND INJ. COMP. FOR RATE CONS. WELLS FOR EACH PHASE
(L=1,3)

```



```

*-----ID  QI(M,L)  C(M,KC,L)
      3 1967.44  1.0  0. 0. 0. 0. 0. 0. 0. 0. 0. 0. 2700.  0.0001  0.0
0.6  0.06  1800
      3    0.    0. 0. 0. 0.    0.    0. 0 0 0 0 0 0 0 0 0 0
      3    0.    0. 0. 0. 0.    0.    0. 0 0 0 0 0 0 0 0 0 0
CC
CC
*---- ID, INJ. TEMP (F)
      1    60.0
CC
CC ID, PRODUCING RATE FOR RATE CONSTRAINT WELL (IFLAG=4)
*-----ID  QT
      4 -928.32
CC
CC ID, PRODUCING RATE FOR RATE CONSTRAINT WELL (IFLAG=4)
*-----ID  QT
      5 -850.24
CC
CC ID, INJ. RATE AND INJ. COMP. FOR RATE CONS. WELLS FOR EACH PHASE
(L=1,3)
*-----ID  QI(M,L)  C(M,KC,L)
      6 2123.77  1.0  0. 0. 0. 0. 0. 0. 0. 0. 0. 0. 2700.  0.0001  0.0  0.6
0.06  1800
      6    0.    0. 0. 0. 0.    0.    0. 0 0 0 0 0 0 0 0 0 0
      6    0.    0. 0. 0. 0.    0.    0. 0 0 0 0 0 0 0 0 0 0
CC
CC
*---- ID, INJ. TEMP (F)
      1    60.0
CC
CC ID, PRODUCING RATE FOR RATE CONSTRAINT WELL (IFLAG=4)
*-----ID  QT
      7 -2088.94
CC
CC ID, INJ. RATE AND INJ. COMP. FOR RATE CONS. WELLS FOR EACH PHASE
(L=1,3)
*-----ID  QI(M,L)  C(M,KC,L)
      8 2244.66  1.0  0. 0. 0. 0. 0. 0. 0. 0. 0. 0. 2700.  0.0001  0.0  0.6
0.06  1800
      8    0.    0. 0. 0. 0.    0.    0. 0 0 0 0 0 0 0 0 0 0
      8    0.    0. 0. 0. 0.    0.    0. 0 0 0 0 0 0 0 0 0 0
CC
CC
*---- ID, INJ. TEMP (F)
      1    60.0
CC
CC ID, PRODUCING RATE FOR RATE CONSTRAINT WELL (IFLAG=4)
*-----ID  PWF
      9 1740.
CC
CC ID, PRODUCING RATE FOR RATE CONSTRAINT WELL (IFLAG=4)
*-----ID  QT
      10 -843.90
CC
CC ID, INJ. RATE AND INJ. COMP. FOR RATE CONS. WELLS FOR EACH PHASE
(L=1,3)
*-----ID  QI(M,L)  C(M,KC,L)

```

```

11 1942.17 1.0 0. 0. 0. 0. 0. 0. 0. 0. 0. 0. 2700. 0.0001 0.0 0.6
0.06 1800
11 0. 0. 0. 0. 0. 0. 0. 0. 0 0 0 0 0 0 0 0 0 0
11 0. 0. 0. 0. 0. 0. 0. 0. 0 0 0 0 0 0 0 0 0 0
CC
CC
*---- ID, INJ. TEMP (F)
      1    60.0
CC
CC ID, PRODUCING RATE FOR RATE CONSTRAINT WELL (IFLAG=4)
*-----ID  QT
      12   -611.97
CC
CC ID, PRODUCING RATE FOR RATE CONSTRAINT WELL (IFLAG=4)
*-----ID  QT
      13   -693.95
CC
CC CUM. INJ. TIME , AND INTERVALS (PV OR DAY) FOR ERITING TO OUTPUT
FILES
*-----TINJ  CUMPR1  CUMHI1  WRHPV  WRPRF  RSTC
      5000    26.0    26.0    10.0    26.0    551.0
CC
CC FOR IMES=2 ,THE INI. TIME STEP,CONC. TOLERANCE,MAX.,MIN. TIME STEPS
*-----DT    DCLIM  DTMAX  DTMIN
      0.1

```

Nomenclature

This nomenclature was reproduced from the UTCHEM user manual.

A	aqueous phase electron acceptor concentration (ML^{-3})
\bar{A}	electron acceptor concentration in attached biomass (ML^{-3})
A_1, A_2	retardation factor
a_T	microgram/gram rock
b	endogenous decay coefficient (T^{-1})
C	Constant, or carbon element
C_κ	overall concentration of species κ in the mobile phases, L^3/L^3
C_κ°	compressibility of species κ , $(ML^{-1}t^{-2})^{-1}$
\hat{C}_κ	adsorbed concentration of species κ , L^3/L^3 PV
\tilde{C}_κ	overall concentration of species κ in the mobile and stationary phases, L^3/L^3 PV
$C_{\kappa\ell}$	concentration of species κ in phase ℓ , L^3/L^3
$C_{p\ell}$	constant pressure heat capacity of phase ℓ , $QT^{-1}M^{-1}$
C_r	rock compressibility, $(ML^{-1}t^{-2})^{-1}$
C_s	substrate concentration (mg/L)
C_t	total compressibility, $(ML^{-1}t^{-2})^{-1}$
\bar{C}_T	average adsorbed concentration
$C_{T\ell}$	flowing concentration in phase ℓ
$C_{v\ell}$	phase heat capacity at constant volume
C_{vs}	rock heat capacity
D	dispersion coefficient
D_{HW}	thermal mass of the solid
$\bar{\bar{D}}_{\kappa\ell}$	dispersion flux of species κ in phase ℓ
$\bar{\bar{K}}_{\kappa\ell}$	dispersion coefficient tensor of species κ in phase ℓ , L^2t^{-1}
D_s	ratio of adsorbed concentration to flowing concentration
E	mass of electron acceptor consumed per mass of substrate biodegraded
f	intra biomass concentration
h	depth, L
K	partitioning coefficient
K_A	electron acceptor half-saturation coefficient (ML^{-3})
K_{abio}	first-order reaction rate coefficient (for abiotic decay reactions, T^{-1})
K_H^{ow}	partitioning coefficient
K_N	limiting nutrient half-saturation coefficient concentration (ML^{-3})
K_p	nutrient half saturation (mg/l)

K_S	substrate half saturation coefficient (mg/l)
K_{SO_4}	sulfate half saturation coefficient (mg/l)
$k_{r\ell}$	relative permeability of phase ℓ
M_{T1}	volumetric heat capacity of phase 1 (water phase) $u_1 =$ velocity of phase 1 (water phase)
M_{TS}	volumetric heat capacity of solids
m_C	mass of cells in a single micro colony
M_W	molecular weight of water
M_O	molecular weight of oil
N	concentration of a limiting nutrient (ML^{-3})
n_{CV}	total number of volume occupying species (water, oil, surfactant, air)
n_p	number of phases
P_1	pressure of phase 1, water
$P_{c\ell 1}$	capillary pressure between the given phase and phase 1, Lt^2/m
P_R	reference phase pressure (1 atm)
P_{R0}	reference pressure (1 atm)
q_H	enthalpy source term per bulk volume
Q_L	heat loss to overburden and under burden, formation or soil
Q_κ	source/sink for species κ per bulk volume, L^3t^{-1}/L^3
RET	retardation due to adsorption
R_κ	total source/sink species κ , $ML^{-3}t^{-1}$
$r_{\kappa\ell}$	reaction rate for species κ in phase ℓ , $ML^{-3}t^{-1}$
$r_{\kappa S}$	reaction rate for species κ in solid phase, $mL^{-3}t^{-1}$
r_S	rate of substrate utilization, $ML^{-3}t^{-1}$
S	aqueous phase substrate concentration, ML^{-3}
\bar{S}	substrate concentration in attached biomass, ML^{-3}
S_ℓ	saturation of phase ℓ
S_o	oil saturation
SRB	sulfur reducing bacteria
S_w	water saturation
t	time, T
T	reservoir temperature
T_L	lower temperature limit, $^{\circ}C$
T_U	upper temperature limit, $^{\circ}C$
\rightarrow	Darcy flux of phase ℓ , Lt^{-1}
u_ℓ	
$u_{\ell i}, u_{\ell j}$	components of Darcy flux of phase ℓ in i and j direction, respectively, Lt^{-1}
V_C	volume of a single micro colony, L^3
v_{HW}	velocity of cold front

X	aqueous phase (unattached) biomass concentration, ML^{-3}
\bar{X}	attached biomass concentration; mass of attached cells per volume of aqueous phase, ML^{-3}
X_a	front location of injected water
Y	yield coefficient, mass of cells produced per mass of substrate biodegraded

Greek Symbols

α_{Ll}, α_{Tl}	longitudinal and transverse dispersivity of phases, respectively, L
β	surface area of a single micro colony, L^2
γ_l	specific weight of phase l , $ML^{-2}t^{-2}$
δ_{ij}	interfacial tension between phases l , and l' , Mt^2
κ	mass transfer coefficient (in biological reactions), LT^{-1}
κ	component number (in general mass and energy balance)
l	phase number
λ_T	thermal conductivity, $Qt^{-1}T^{-1}L$
$\lambda_{r,C}$	relative mobility of component C in phase l
λ_{rrC}	total relative mobility
μ	specific growth rate (1/day)
μ_l	viscosity of phase l
μ_{max}	maximum specific growth rate, t^{-1}
ϕ	porosity
ρ_κ	density of pure component κ at reference phase pressure, ML^{-3}
ρ_l	Density of phase l
ρ_o	density of oil, ML^{-3}
ρ_r	rock density
ρ_s	rock density
ρ_w	density of water, ML^{-3}
ρ_X	biomass density, mass of cells per volume of biomass, ML^{-3}
τ	tortuosity factor with definition of being a value > 1
$^{\circ}C$	degree of Centigrade
$^{\circ}F$	degree of Fahrenheit

References

- Al-Humaidan, A.Y., and Nasr-El-Din, H. A., "Optimization of Hydrogen Sulfide Scavengers Used During Well Stimulation," Paper SPE 50765 presented at the 1999 SPE International Symposium Oilfield Chemistry held in Houston, Texas, February 16-19, 1999.
- Al-Rasheedi, S., Kalli, C., Thrasher, D., and Al-Qabandi, S., "Prediction and Evaluation of the Impact of Reservoir Souring in North Kuwait, A Case Study," Paper SPE 53164 presented at the 1999 SPE Middle East Oil Show held in Bahrain, February 20-23, 1999.
- Amy, M. P., and Eilin, A. V., "Hydrogen Sulfide Forecasting Under PWIR (Produced Water Reinjection)," Paper SPE presented at the SPE International Conference on Health, Safety, and Environment in Oil and Gas Exploration and Production held in Stavangaer, Norway, June 26-28, 2000.
- Barton, L., L., "Sulfate Reducing Bacteria," Plenum Press, New York, 1995.
- Box, G. E. P., Hunter, J. S., and Hunter, W. G., Statistics for Experimenters: Design, Innovation, and Discovery, 2nd Edition, John Wiley & Sons, New Jersey, 2005.
- Burger, E. D., Jenneman, G. E., Vedvik, A., Bache, Ø., Jensen, T. B., and Soerensen, "A Mechanistic Model To Evaluate Reservoir Souring in Ekofisk Field," Paper SPE 93297-MS, presented at the SPE International Symposium on Oil Field Chemistry held in Houston, TX, February 2-4, 2005.
- Cavallaro, A. N., Gracia Martinez, M. E., Osters, H., Panarello, H., Cordero, R. R., "Oilfield Reservoir Souring During Waterflooding: A Case With Low Sulfate Concentration in Formation and Injection Waters," Paper SPE 92959 presented at the 2005 SPE International Symposium on Oilfield Chemistry held in Houston, Texas, February 2-4, 2005.
- Cord-Rudish, R., Kleinitz, W., and Widdel, F., "Sulfate-Reducing Bacteria and Their Activities in Oil Production," Paper SPE 13554, Journal of Petroleum Technology, January, 1987.
- Cassinis, R. B., Farone, W. A., and Portwood, J. H., "Microbial Water Treatment: An Alternative Treatment to Manage Sulfate Reducing Bacteria (SRB) Activity, Corrosion, Scale, Oxygen, and Oil Carry-Over at Wilmington Oil Field – Wilmington, CA," Paper SPE 49152 presented at the 1998 SPE Annual Technical Conference and Exhibition held in New Orleans, Louisiana, September 27-30, 1998.
- Chang, M. M., Chung, F. T. H., Bryant, R. S., Gao, H. W., and Burchfield, T. E., "Modeling and Laboratory Investigation of Microbial Transport Phenomena in Porous Media," Paper SPE 22845 presented at the 1991 66th Annual Technical Conference and Exhibition of the Society of Petroleum Engineers held in Dallas, Texas, October 6-9, 1991.

- Chen, B., Cunningham, A., Ewing, R., Peralta, R., and Visser, E., "Two-Dimensional Modeling of Microscale Transport and Biotransformation in Porous Media," *Numerical Methods for Partial Differential Equations*, 10, 65-83, 1994.
- Chen, C. I., Reinsel, M. A., and Mueller, R. F., "Kinetic Investigation of Microbial Souring in Porous Media Using Microbial Consortia from Oil Reservoirs," *Biotechnology and Bioengineering*, 44, 263-269, 1994.
- Cochrane, W. J., Jones, P. S., Sanders, P. F., Holt, D. M., and Mosley, M. J., "Studies on the Thermophilic Sulfate-Reducing Bacteria from a Souring North Sea Oil Field," Paper SPE 18368 presented at the 1988 SPE European Petroleum Conference, London, UK, 16-19 October, 1988.
- Davidova, I., Hicks, M. S., and Sufilita, J. M., "The Influence of Nitrate on Microbial Processes in Oil Industry Production Waters," *Journal of Industrial Microbiology & Biotechnology*, 27, 80-86, 2001.
- de Blanc, C. P., McKinney, D. C., Speitel Jr., G. E., Sepehrnoori, K., and Delshad, M., "A 3D NAPL Flow and Biodegradation Model," Proceedings of the Specialty Conference held in conjunction with the ASCE National Convention, Washington, D.C., November 12-14, 1996.
- Delshad, M., Pope, G. A., and Sepehrnoori, K., "A Compositional Simulator for Modeling Surfactant Enhanced Aquifer Remediation, 1 Formulation," *Journal of Contaminant Hydrology*, 23, 303-327, 1996.
- Delshad, M., Kazuhiro A., Pope A. G., and Sepehrnoori, K., "Simulation of Chemical and Microbial Enhanced Oil Recovery Methods," Paper SPE 75237, Thirteenth Symposium on Improved Oil Recovery held in Tulsa, Oklahoma, April 13-17, 2000.
- Dinning, A. J., Arctander, V. E., "World Wide Information on Reservoir Souring and Risks Associated with Produced Water Re-injection (PWRI)," Norwegian Oil Industry Association (OLF), January 2005.
- Drever, J. I., "The Geochemistry of Natural Waters," Prentice Hall, 1982.
- Eckford, R. E. and Fedorak, P. M., "Planktonic Nitrate-Reducing Bacteria and Sulfate-Reducing Bacteria in Some Western Canadian Oil Field Waters," *Journal of Industrial Microbiology & Biotechnology*, 29, 83-92, 2002.
- Eden, B., Laycock, P. J., and Fielder, M., "Oilfield Reservoir Souring," OTH 92 385, HSE Books, 1993.
- Evans, R., "Factors Influencing Sulphide Scale Generation Associated with Waterflood Induced Reservoir Souring," Paper SPE 68337 presented at the 2001 3rd SPE International Symposium on Oilfield Scale held in Aberdeen, UK, 30-31 January, 2001.
- Fanchi, R., "Multidimensional Numerical Dispersion," Society of Petroleum Engineers of AIME, February, 1983.

- Frazer, L. C., and Bolling, J. D., "Hydrogen Sulfide Forecasting Techniques for the Kuparuk River Field," Paper SPE presented at the International Arctic Technology Conference held in Anchorage, Alaska, May 29-31, 1991.
- Greene, E. A., Nemati, M., Jenneman, G. E., and Voordouw, G., "Nitrite Reductase Activity of Sulphate-Reducing Bacteria Prevents Their Inhibition by Nitrate-Reducing, Sulphide-Oxidizing Bacteria," *Environmental Microbiology* 5(7), 607-617, 2003.
- Hands, N., Oz, B., Roberts, B., Davis, P., Minchau, M., "Advances in Prediction and Management of Elemental Sulfur Deposition Associated with Sour Gas Production from Fractured Carbonate reservoirs," Paper SPE presented at the Annual Technical Conference and Exhibition held in San Antonio, Texas, September 29 – October 2, 2002.
- Herbert, B. N., Gilbert, P. D., Stockdale, H., and Watkinson, R. J., "Factors Controlling the Activity of Sulphate-Reducing Bacteria in Reservoirs During Water Injection," Paper SPE 13978/1 presented at the SPE meeting, Richardson, Texas, 1985.
- Hitzman, D. O. and Sperl, G. T., "A New Microbial Technology for Enhanced Oil Recovery and Sulfide Prevention and Reduction," Paper SPE/DOE 27752 presented at the SPE/DOE Ninth Symposium on Improved Oil Recovery held in Tulsa, Oklahoma, April 17-20, 1994.
- Hitzman, D. O., and Dennis, D. M., "New Technology for Prevention of Sour Oil and Gas," Paper SPE 37908 presented at the SPE/EPA Exploration and Production Environmental Conference held in Dallas, Texas, March 3-5, 1997.
- Hitzman, D. O., and Dennis, D. M., "Sulfide Removal and Prevention in Gas Wells," SPE Reservoir Evaluation and Engineering, 367-371, August 1998.
- Hydrogen Sulfide, University Park Press, Baltimore, 1979.
- Kalpakci, B., and Magri, N. F., "Mitigation of Reservoir Souring – Design Process," Paper SPE 28947, presented at the SPE International Symposium on Oil Field Chemistry held in San Antonio, TX, February 14-17, 1995.
- Khatib, Z. I., and Salanitro, P. J., "Reservoir Souring: Analysis of Surveys and Experience in Sour Waterfloods," Paper SPE 38795, presented in the SPE annual Technical Conference and Exhibition Held in San Antonio, Texas, October 5-8, 1997.
- Kleikemper, J., Schroth, M. H., Sigler, W. V., Schmucki, M., Bernasconi, S. M., Zeyer, J., "Activity and Diversity of Sulfate-Reducing Bacteria in a Petroleum Hydrorabon-Contaminated Aquifer," *Applied and Environmental Microbiology* , 68, 1516-1523, April 2002.
- Koutsyn, P. V., Gendel, G. L., "New Strategy of Controlling Risks in Development of Oil & Gas Fields with Hydrogen Sulfide," Paper SPE, presented at the Fourth International Conference on Health, Safety & Environment in Oil and Gas Exploration and Production (HSE), Caracas, Venezuela, June 7-10, 1998.

- Kuijvenhoven, C., Bostock, A., Chappell, D., Noirot, J. C., Khan, A., "Use of Nitrate to Mitigate Reservoir Souring in Bonga Deepwater Development Offshore Nigeria," Paper SPE 92795, presented at the SPE International Symposium on Oilfield Chemistry held in Houston, Texas, February 2-4, 2005.
- Lake, W. L., Hirasaki, G. J., "Taylor's Dispersion in Stratified Porous Media," Society of Petroleum Engineers of AIME, August 1981.
- Larry, L. W., *Enhanced Oil Recovery*, Prentice-Hall, Inc., 1989.
- Lappin-Scott, H. M., Bass, C. J., Mcalpine, K., Sanders, P. F., "Survival Mechanisms of Hydrogen Sulphide-Producing Bacteria Isolated from Extreme Environments and their Role in Corrosion," *International Biodeterioration & Biodegradation*, 34, 305-319, 1994.
- Lauwerier, H. A., "The Transport of Heat in an Oil Layer Caused by the Injection of Hot Fluid," *Applied Science Research*, Martinus Nijhoff publisher, The Hague, 5, 145-150, 1995.
- Leu, J. Y., McGovern-Traa, C. P., Porter, A. J. R., Hamilton, W. A., "The Same Species of Sulphate-Reducing Desulfomicrobium Occur in Different Oil Field Environments in the North Sea," *Letters in Applied Microbiology*, 29, 246-252, 1999.
- Ligthelm, D. J., de Boer, R. B., and Brint, J. F., and Schulte, "Reservoir Souring: An Analytical Model for H₂S Generation and Transportation in an Oil Reservoir Owing to Bacteria Activity," paper SPE 25197 presented at the Offshore Europe Conference held in Aberdeen, September 3-6, 1991.
- Liu, J., Pope G. A., and Sepehrnoori, K., "A High-resolution Finite-difference Scheme for Nonuniform grids," *Applied Mathematical Modeling*, 19, March, 1993.
- Liu, J., Delshad, M., Pope G. A., and Sepehrnoori, K., "Application of Higher-Order Flux-Limited Methods in Compositional Simulation," *Transport in Porous Media*, 16, 1, 1994.
- Londry, K. L. and Suflita, J. M., "Use of Nitrate to Control Sulfide Generation by Sulfate-Reducing Bacteria Associated with Oily Waste," *Journal of Industrial Microbiology & Biotechnology*, 22, 582-589, 1999.
- Mahadevan, J., Lake, L. W., and Johns, R. T., "Estimation of True Dispersivity in Field-Scale Permeable Media," *Journal of Society of Petroleum Engineers*, September, 2003.
- Mali, P. V., Khanra, A., Sagar, P. K., Meshram, P. N., Singh, R. K., and Johari, A., "Strategies to Mitigate Corrosion Caused Due to H₂S in Wells and Well Fluid Lines of Mumbai Offshore, India," Paper SPE 81457 presented at the SPE 13th Middle East Oil Show & Conference held in Bahrain, April 5-8, 2003.
- Marsland, S. D., Dawe, R. A., Kelsall, G. H., "Inorganic Chemical Souring of Oil Reservoirs," Paper SPE 18480, presented at the SPE International Symposium on Oilfield Chemistry held in Houston, Texas, February 8-10, 1989.

- Mason, R. L., Gunts, R. F., and Hess, J. L., *Statistical Design and Analysis of Experiments with Applications to Engineering and Science*, John Wiley & Sons, New York, 1989.
- Maxwell, S., and Spark, I., "Souring of Reservoirs by Bacterial Activity During Seawater Flooding" Paper SPE 93231, presented at the SPE International Symposium on Oilfield Chemistry held in Houston, Texas, February 2-4, 2005.
- Molz, F. J., Widdowson, M.A., and Benefield, L. D., "Simulation of Microbial Growth Dynamics Coupled to Nutrient and Oxygen Transport in Porous Media," *Water Resources Research*, 22, No.8, 1207-1216, August 1986.
- Mueller, R. F., and Nielsen, P. H., "Characterization of Thermophilic Consortia from Two Souring Oil Reservoirs," *Applied and Environmental Microbiology*, 3083-2087, September 1996.
- Myers, R. H., and Montgomery, D. C., *Response Surface: Process and Product Optimization Using Designed Experiments*, 2nd Edition, John Wiley & Sons, New Jersey, 2002.
- Nemati, M., Jenneman, G. E., and Voordouw, G., "Mechanistic Study of Microbial Control of Hydrogen Sulfide Production in Oil Reservoirs," *Biotechnology and Bioengineering*, 74, 424-434, 2001.
- Nemati, M., Mazutinec, T. J., Jenneman, G. E., and Voordouw, G., "Control of Biogenic H₂S Production with Nitrite and Molybdate," *Journal of Industrial Microbiology & Biotechnology*, 26, 350-355, 2001.
- Okabe, S., and Characklis, W. G., "Effects of Temperature and Phosphorous Concentration on Microbial Sulfate Reduction by *Desulfovibrio Desulfuricans*," *Biotechnology and Bioengineering*, 39, 1031-1042, 1992.
- Okabe, S., Nielsen, P. H., and Characklis, W. G., "Factors Affecting Microbial Sulfate Reduction by *Desulfovibrio Desulfuricans* in Continuous Culture: Limiting Nutrients and Sulfide Concentration," *Biotechnology and Bioengineering*, 40, 725-734, 1992.
- Platenkamp, R. J., "Temperature Distribution Around Water Injectors: Effects on Injection Performance," Paper SPE 13746 presented at the SPE Middle East Oil Technical Conference and Exhibition held in Bahrain, March 11-14, 1985.
- Premuzic, E. T. and Lin, M. S., "Induced biochemical conversions of heavy crude oils," *Journal of Petroleum Science and Engineering*, 22, 171-180, 1999.
- Reis, M. A., Almeida, J. S., Lemos, P. C., Carrondo, M., J., T., "Effect of Hydrogen Sulfide on Growth of Sulfate Reducing Bacteria," *Biotechnology and Bioengineering*, 40, 593-600, 1992.
- Rosnes, J. T., Graue, A., and Lien T., "Activity of Sulfate-Reducing Bacteria Under Simulated Reservoir Conditions," Paper SPE 19429, May 1991.
- Sahm, K., MacGregor, B. J., Jørgensen, B. B., Stahl, A., "Sulphate Reduction and Vertical Distribution of Sulphate-Reducing Bacteria Quantified by rRNA Slot-

- blot Hybridization in a Coastal Marine Sediment,” *Environmental Microbiology*, 1, 65-74, 1999.
- Sarkar, A. K., Georgiou, G., and Sharma, M. M., “Transport of Bacteria in Porous Media: I. An Experimental Investigation,” *Biotechnology and Bioengineering*, 44, 489-497, 1994.
- Sarkar, A. K., Georgiou, G., and Sharma, M. M., “Transport of Bacteria in Porous Media: II. A Model for Convective Transport and Growth,” *Biotechnology and Bioengineering*, 44, 499-508, 1994.
- Sawyer, C. N. and McCarthy, P. L., “Chemistry for Environmental Engineering,” Third Edition, McGraw-Hill Company, New York, 1978.
- Seto, C. J., and Beliveau, D. A., “Reservoir Souring in the Caroline Field,” Paper SPE 59778, presented at SPE/CERI Gas Technology Symposium held in Calgary, Alberta Canada, April 3-5, 2000.
- Shedid, S. A., and Abed, A. A., “Simulation Investigation of the Feasibility of Simultaneous Hydrogen Sulfide-Water Injection to Improve oil recovery,” Paper SPE 88503, presented at the Asia Pacific Oil and Gas Conference and Exhibition held in Perth, Australia, October 18-20, 2004.
- Sunde, E., Beeder, J., Nilsen, R. K., and Torsvik, T., “Aerobic Microbial Enhanced Oil Recovery for Offshore Use,” Paper SPE 24204 presented at the SPE/DOE Eighth Symposium on Enhanced Oil Recovery held in Tulsa, Oklahoma, April 22-24, 1992.
- Sunde, E., Thorstenson, T., Torsvik, T., Vagg, J. E., and Espedal, M. S., “Field-Related Mathematical Model to Predict and Reduce Reservoir Souring,” Paper SPE 25197 presented at the SPE International Symposium on Oilfield Chemistry held in New Orleans, LA, March 2-5, 1993.
- Tuttle, R. N., “What Is a Sour Environment?,” *Journal of Petroleum Technology*, 260-262, March, 1990.
- Tyrie, J. J., and Ljosland, E., “Predicted Increase in Gullfaks H₂S Production Associated With Injected Sea Water,” Paper SPE 26700 presented at the SPE Annual Technical Conference and Exhibition held in Houston, Texas, October 3-6, 1993.
- UTCHEM, “UTCHEM Technical Documentation for UTCHEM – 9.0,” Reservoir Engineering Research Program Center for Petroleum and Geosystems Engineering at The University of Texas at Austin, 2000.
- Vik, E. A., and Dinning, A. J., World Wide Information on Reservoir Souring and Risks Associated with Produced Water Re-Injection (PWRI), Phase one report Norwegian Oil Industry Association (OLF), 2005.
- Vinsome, P. K., and Westerveld, J., “A Simple Method for Predicting Cap and Base Rock heat Losses in Thermal Reservoir Simulators,” *Journal of Canadian Technology*, 87-90, July-September, 1980.
- Walter John, V., ”Essentials of Geochemistry,” Jones and Bartlett Publications, 2005.

- Wanner, O., and Cunningham, A. B., "Modeling Biofilm Accumulation and Mass Transport in a Porous Medium Under High Substrate Loading," *Biotechnology and Bioengineering*, 47, 703-712, 1995.
- Wilson, D. R., "Hydrogen Sulfide Scavengers: Recent Experience in a Major North Sea Field," Paper SPE 36943, presented in the SPE European Petroleum Conference held in Milan, Italy, October 22-24, 1998.
- Worden, R. H., and Smally, P. C., "H₂S-Producing Reactions in Deep Carbonate Gas Reservoirs: Khuff Formation, Abu Dhabi," *Journal of Chemical Geology*, 133, 157-171, 1996.
- Zhang, X., Knapp, R.M., and McInerney, M. J., "A Mathematical Model for Microbially Enhanced Oil Recovery Process," Paper SPE/DOE 24202 presented at the SPE/DOE Eighth Symposium on Enhanced Oil Recovery in Tulsa, Oklahoma, April 22-24, 1992.
- Zou, H., "Quantitative Geochemistry," Imperial college press, 2007.

VITA

Mohammad Ali Farhadinia was born in Shiraz, Iran, on June 23, 1969, the last son of Abdolkarim Farhadinia and Kokab Roshan. He received his Bachelor's degree in Petrochemical engineering from The Petroleum University of Technology, Ahvaz, Iran in March 1993, and Master of Science in Chemical engineering from University of Tehran, Iran in August 1995. He worked for six years as a chemical engineer in Research Institute of Petroleum Industry, Iran, on several projects related to oil, gas and petrochemical industries. In January 2004, he entered the graduate school of The University of Texas at Austin to pursue his PhD degree in petroleum engineering. Mr. Farhadinia has published several papers in journals and international conferences.

Permanent Address: No. 45, Hakimi Street, Mollasadra Street, Shiraz, Iran

This dissertation was typed by the author.